

# Topological holography: Towards a unification of Landau and beyond-Landau physics

Heidar Moradi,<sup>a,b,c</sup> Seyed Farough Moosavian,<sup>d</sup> and Apoorv Tiwari<sup>e</sup>

*a Physics and Astronomy, Division of Natural Sciences, University of Kent, Canterbury CT2 7NZ, United Kingdom*

*b Department of Applied Mathematics and Theoretical Physics, Centre for Mathematical Sciences, Wilberforce Road, Cambridge CB3 0WA, United Kingdom*

*c The Cavendish Laboratory, Department of Physics, 19 J J Thomson Avenue, Cambridge CB3 0HE, United Kingdom*

*d Department of Physics, McGill University, Ernest Rutherford Physics Building, 3600 Rue University, Montréal, QC H3A 2T8, Canada*

*e Department of Physics, KTH Royal Institute of Technology, Stockholm, 106 91 Sweden*

## Abstract

We outline a holographic\* framework that attempts to unify Landau and beyond-Landau paradigms of quantum phases and phase transitions. Leveraging a modern understanding of symmetries as topological defects/operators, the framework uses a topological order to organize the space of quantum systems with a global symmetry in one lower dimension. The global symmetry naturally serves as an input for the topological order. In particular, we holographically construct a *String Operator Algebra* (SOA) which is the building block of symmetric quantum systems with a given symmetry  $G$  in one lower dimension. This exposes a vast web of dualities which act on the space of  $G$ -symmetric quantum systems. The SOA facilitates the classification of gapped phases as well as their corresponding order parameters and fundamental excitations, while dualities help to navigate and predict various corners of phase diagrams and analytically compute universality classes of phase transitions. A novelty of the approach is that it treats conventional Landau and unconventional topological phase transitions on an equal footing, thereby providing a holographic unification of these seemingly-disparate domains of understanding. We uncover a new feature of gapped phases and their multi-critical points, which we dub *fusion structure*, that encodes information about which phases and transitions can be dual to each other. Furthermore, we discover that self-dual systems typically possess emergent non-invertible, i.e., beyond group-like symmetries. We apply these ideas to  $1+1d$  quantum spin chains with finite Abelian group symmetry, using topologically-ordered systems in  $2+1d$ . We predict the phase diagrams of various concrete spin models, and analytically compute the full conformal spectra of non-trivial quantum phase transitions, which we then verify numerically.

\* Not to be confused with the holographic principle in contexts such as the AdS/CFT Correspondence.

# Contents

<b>1</b>	<b>Introduction</b>	<b>2</b>
<b>2</b>	<b>Symmetry structures as topological operators</b>	<b>8</b>
2.1	Symmetries are topological	8
2.2	Building blocks of symmetric local operators	12
<b>3</b>	<b>Topological holography: Framework</b>	<b>14</b>
3.1	Symmetries of topologically-ordered phases	14
3.2	Boundary Hilbert space from the bulk theory	16
3.3	Mapping to generalized spin-chains	19
3.4	Gapped boundaries as gapped phases	22
3.5	From bulk symmetries to boundary dualities	25
3.6	Action of dualities on Hamiltonians	28
3.7	Action of dualities on non-symmetric theories	30
3.8	Emergence of non-invertible symmetries	31
<b>4</b>	<b>Topological holography: Application</b>	<b>32</b>
4.1	Gapped phases and web of dualities	33
4.2	Gapless phases, phase transitions, and critical points	37
4.3	Conformal spectroscopy from dualities	39
4.4	Duality: a gauging perspective	42
<b>5</b>	<b>Examples</b>	<b>44</b>
5.1	$\mathbb{Z}_2$ symmetric quantum spin chains	44
5.2	$\mathbb{Z}_N$ symmetric quantum spin chains	50
5.3	$\mathbb{Z}_2 \times \mathbb{Z}_2$ symmetric quantum spin chains	55
5.4	$\mathbb{Z}_3 \times \mathbb{Z}_3$ symmetric quantum spin chains	76
5.5	$\mathbb{Z}_2 \times \mathbb{Z}_4$ symmetric quantum spin chains	86
5.6	$\mathbb{Z}_2 \times \mathbb{Z}_2 \times \mathbb{Z}_2$ symmetric quantum spin chains	89
<b>6</b>	<b>Summary and future directions</b>	<b>93</b>
<b>A</b>	<b>From G-topological orders to G-symmetric quantum spin chains</b>	<b>95</b>
<b>B</b>	<b>Computation of duality groups</b>	<b>101</b>
<b>C</b>	<b>From Wen plaquette model to <math>\mathbb{Z}_N</math>-symmetric spin chains</b>	<b>107</b>
<b>D</b>	<b>Symmetry-twisted boundary conditions</b>	<b>115</b>
<b>E</b>	<b>Simplicial calculus</b>	<b>118</b>
<b>F</b>	<b>Group structure of the web of dualities</b>	<b>125</b>
<b>G</b>	<b>Conformal spectra of various phase transitions</b>	<b>128</b>

# 1 Introduction

Condensed-matter physics is the study of phases of matter and phase transitions between them. A fundamental endeavor of condensed-matter theory is to develop a framework within which possible phases of matter can be classified and characterized. Historically, the most successful framework in this regard has been the so-called *Landau theory* [1–3] within which symmetry and its spontaneous-breaking patterns play a key role. The Landau-Ginzburg-Wilson mean field theory provides a formalism capable of describing many aspects of conventional phases based on the existence of local order parameters. Corresponding quantum phase transitions occur between ordered and disordered phases where the symmetry of the ground state of the ordered phase is necessarily a subgroup of that of the disordered phase. Typical examples of such transitions are the  $\mathbb{Z}_2$  and  $U(1)$  symmetry breaking Ising and XY transitions, respectively [4].

The last four decades have seen a rapidly growing understanding of quantum phases and phase transitions that lie beyond Landau’s framework. Among these, an important class are so-called topological phases of matter, which are equivalence classes of locally indistinguishable gapped quantum systems (more precisely quantum liquids [5]) that are distinguished by their global or topological properties. Topological phases fall into two broad categories known as topologically ordered and symmetry protected topological (SPT) phases of matter respectively. The fractional quantum Hall phase [6–8] is a well-known example of the former category. Such phases have highly entangled liquid-like ground states which evade conventional ordering at zero temperature. They are instead distinguished by their patterns of long range entanglement [9–12] which manifest in fractionalized (anyonic) excitations with topological correlations [13–16]. A defining property of topologically ordered systems is the existence of ground state degeneracy when put on a topologically non-trivial manifold [17–19]. The multiplet of ground states form projective representations of the mapping class (modular) group of the spatial manifold, which can serve as a diagnostic of the phase [20–23]. A paradigmatic example of a topologically ordered system is the deconfined phase of the  $\mathbb{Z}_2$  gauge theory [24–27], which is expected to be realized in frustrated magnets [28–31] and play a crucial role in the physics of high temperature superconductors [32–37]. This is the simplest example of a general class of topological orders known as topological finite group gauge theories [38–40].

On the other hand, SPTs—as the name suggests—realize global symmetries in topologically distinct ways which is manifest in their bulk topological response to background symmetry gauge fields [41, 42] and in the appearance of anomalous quantum systems on their boundary [43–49]. These phases are trivial if symmetry is explicitly broken. The earliest and perhaps best known examples of SPTs are free fermion topological insulators and superconductors [50–53], which are classified using K-theory in what is known as the ten-fold way classification [54–56]. Interactions can alter the non-interacting classification [57–60]. The interacting classification of fermionic topological phases is formulated in terms of intricate mathematical structures such as super-group cohomology [61, 62] and cobordism theory [63, 64]. On the other hand, since bosons generically condense into the

lowest energy level, interactions are necessary to stabilize many-body gapped bosonic systems. In  $1 + 1d$ , bosonic SPTs are classified by projective representations of the symmetry group [65–67], which can be generalized to higher dimensions using the cohomology of groups [42]. The low-energy properties of topological phases of matter are expected to be described by topological quantum field theories.

Within the Landau paradigm, second-order or continuous quantum phase transitions occur between two phases such that the symmetry preserved by the (partially) ordered phase is necessarily a subgroup of the symmetry preserved by the disordered phase. It is now known that various kinds of non-Landau transitions may occur in quantum systems. These could happen if the phases on either side of the transition are themselves beyond the Landau classification scheme [68–71] or if the symmetry group on one side of the transition is not a subgroup of the symmetry on the other side. The former kind of transitions can be realized for instance between topological phases or between topological and non-topological phases of matter. The latter are known as deconfined quantum critical (DQC) transitions [72, 73]. Such transitions take place when defects or the disorder parameters of the broken symmetry on one side of the transition host the order parameter of the symmetry which is broken on the other side of the transition [74]. While the phases on either side of such a transition are captured by Landau’s classification scheme, the transition itself is beyond Landau. A prototypical example of the deconfined transition is realized between the valence bond solid and antiferromagnetic Neel state in a spin-rotation-symmetric spin model on a square lattice. The valence bond solid state breaks spatial four-fold rotation symmetry while the Neel state breaks spin-rotation symmetry. From a modern perspective, such transitions are understood to be realized in quantum systems that have mixed anomalies between internal and spatial symmetries, i.e., Lieb-Schultz-Mattis constraints [75–80].

As mentioned above, symmetry plays a very important role in organizing our understanding about the kinds of gapped phases and phases transitions realized in quantum systems. Despite its long and illustrious history, the understanding of symmetries in quantum matter is very much an evolving subject. In fact, there have been numerous developments over the past decade, that have led to new perspectives on the question: *what are global symmetries of quantum systems?* [81–83]. Conventionally, a global symmetry is defined via a collection of operators which (i) act on all of space, (ii) commute with the Hamiltonian and (iii) satisfy group-like fusion/composition rules. Mathematically, such symmetries are described by groups. Operators charged under such a symmetry are zero-dimensional (point-like) and transform in representations of the symmetry group. The low-energy description of quantum systems are usually formulated in terms of Euclidean quantum field theories, which possess emergent spacetime rotation symmetry in addition to other global symmetries. Within the low-energy description, there is no preferred time direction and hence no natural notion of all of space. The symmetry operators may therefore be defined on any codimension-1 (i.e.,  $\#$  of spacetime dimensions  $-1$ ) hypersurface in spacetime. The condition of commutativity with the Hamiltonian generalizes to ‘commutativity’ with the stress tensor—this amounts to the general property that *symmetry operators are topological*. This perspective begets the generalization that any topological subsector (subalgebra) of operators in a quantum system embodies a generalized symmetry structure. The topological operators within a theory need not be limited to codimension-1 operators that satisfy fusion rules representative of a group. Instead, in general, the set of topological operators may have higher codimensions [81] and satisfy fusion rules that vastly generalize the notion

of groups [82–101]. Furthermore, global symmetries may have ’t Hooft anomalies, which put strong non-perturbative constraints on the low energy phases/ground states realizable within the quantum system. Collectively, the mathematical framework that describes topological operators and therefore generalized symmetries in quantum field theory is that of higher fusion categories [100].

This modern perspective of global symmetries provides a number of insights applicable to the program of classifying and characterizing quantum matter. For instance, Landau’s symmetry breaking paradigm can be expanded to incorporate breaking of generalized symmetries [81, 102, 103]. In particular, a so-called  $p$ -form symmetry corresponding to a finite Abelian group  $G$  contains co-dimension- $(p + 1)$  topological operators that act on  $p$ -dimensional charged objects which transform in non-trivial representations of  $G$ . A system with spontaneously-broken 0-form  $G$  symmetry has a ground state degeneracy of  $|G|$  on a connected spatial manifold. Similarly, a system with spontaneously broken 1-form  $G$  symmetry has a ground state degeneracy of  $b_1^{|G|}$  where  $b_1$  is the number of independent non-contractible loops (1st Betti number) of the spatial manifold. This is the well-known topological ground-state degeneracy in topologically-ordered systems related to anyonic excitations. For this reason, it has been noted [102, 104] that 1-form symmetry breaking is closely related to topological order. Recently, these ideas have been used to propose a partial incorporation of topological order into Landau’s classification scheme [103]. Technically, SPT phases do not fit into the Landau paradigm as there are no spontaneously symmetry-breaking (even for generalized symmetries).

In this paper, we describe a different approach towards the unification of Landau and beyond-Landau paradigms. Our approach exploits the topological nature of global symmetries to decouple the global-symmetry features of a symmetric quantum system from its local physics. The symmetry operators and their action on charged operators can be holographically encapsulated in a topologically-ordered system that lives in one higher dimension. Independently, related ideas have recently appeared in the literature under the name of symmetry TFTs [105–110]. The action of symmetry operators on charged operators is encoded in the braiding of topological defects (e.g., anyons in  $2 + 1$  dimensions) of the topologically-ordered system. From this point of view, different phases such as Landau symmetry-breaking phases, SPTs as well as (Abelian) topologically-ordered phases all arise on the same footing, i.e, as gapped boundaries of a topological order in one higher dimension. Furthermore, the bulk topological order can be thought of as a theoretical gadget that allows one to conveniently discover numerous non-perturbative statements about the space of symmetric quantum systems. These include classification of gapped phases, order parameters of each phase as well as non-trivial dualities that act on the space of theories. The dualities descend from the internal symmetries of the bulk topological order and reveals rich hidden structures of the space of theories. We develop tools to exploit these dualities to constrain and construct the phase diagram and compute its various features efficiently through a study of the associated topological order. In order to provide concrete realizations that exemplify the utility of this approach in the simplest physically-relevant setting, we restrict ourselves to the study of  $1 + 1d$  quantum systems with finite Abelian group symmetry. Ideas related to using topological orders in one higher dimension to study symmetric quantum systems have appeared in a number of recent works [92, 94, 105–109, 111–118]. The present work provides a complimentary approach to these past works. Our work contextualizes the notion of symmetry TFTs/topological holography to concrete lattice models that are fairly

standard in quantum magnetism and lays out a detailed and practical framework to use such abstract notions to study the generically complex phase diagrams of these models.

## Summary of results

In this work, we detail a holographic approach that uses a topological order to systematically study the global symmetry aspects of quantum systems in one lower dimension. The framework is sufficiently general and can be applied to the study of symmetric quantum systems in general spacetime dimensions. In order to illustrate the construction in a simple and explicit setting, in this work we restrict ourselves to anomaly-free  $1 + 1d$  quantum systems with finite Abelian group symmetry (or equivalently,  $2 + 1d$  topological orders corresponding to Dijkgraaf-Witten theories with finite Abelian groups  $G$ ). The paper is organized into three main parts. Below we summarize the main results and contributions of each of these parts.

**Framework of topological holography:** In Section 2, we review the concept of (higher-form) symmetries as topological operators/defects. In Section 3, we describe the framework of topological holography. In particular, we review the symmetries of a  $2 + 1d$  Abelian  $G$  topological order. These comprise of two parts—(i) 1-form symmetries  $\mathcal{A} \simeq G \times G$  corresponding to anyonic Wilson lines, and (ii) 0-form symmetries  $\mathcal{G}[G]$  corresponding to permutation of anyons that preserve the topological correlations of the anyons. We show that the algebra of  $G$ -symmetric operators of  $1 + 1d$  theories, which we denote as the String Operator Algebra  $\text{SOA}[G]$ , can be constructed from the bulk 1-form symmetries of the higher dimensional topological order. We consider representations of these algebras on generalized spin chains. Using the SOA, we parameterize the space of  $G$ -symmetric (spin-chain) Hamiltonians. Furthermore, we show that the bulk 0-form symmetries act as dualities on the space of  $1 + 1d$   $G$ -symmetric theories, mapping between different symmetric Hamiltonians. The duality group  $\mathcal{G}[G]$  is in general non-Abelian and very large even for small finite Abelian groups  $G$ . For example, in the case of  $G = \mathbb{Z}_2^4$ , there are almost 350 million dualities.

We develop a detailed bulk-boundary dictionary for topological holography. Amongst other things, this holographic realization allows us to classify gapped phases of  $G$ -symmetric theories and construct fixed-point spin-chain Hamiltonians for each phase. From the point of view of topological order, each gapped phase is related to the condensation of a subset of anyons  $\mathcal{L}$ . From the condensation of anyons, we construct spin-chain order parameters for each gapped phase. We also argue how non-Abelian and sometimes non-invertible symmetries can emerge at self-dual regions in the space of symmetric models.

**Applying topological holography:** In Section 4, we outline how topological holography might be applied to study the space of symmetric quantum systems. In particular, the existence of dualities, the classification of gapped phases and the transformations under dualities can be used to strongly constrain and sometimes construct phase diagrams of concrete models. We derive several powerful and general results, useful in the study of phase diagrams of concrete Hamiltonian models. A summary of some of these results are

1. Properties such as a Hamiltonian  $H$  being gapped, gapless, critical, or at a first-order transition is preserved under duality transformations.

2. The action of the bulk 0-form symmetry group  $\mathcal{G}[\mathbf{G}]$  on the set of gapped phases gives rise to a vast **web of dualities** encoded in a graph whose vertices are gapped phases and edges are dualities.
3. Each gapped phase  $\mathcal{L}$  is characterized by a pair  $(\mathbf{H}_{\mathcal{L}}, \psi_{\mathcal{L}})$ , corresponding to a spontaneous symmetry-breaking down to a subgroup  $\mathbf{H}_{\mathcal{L}} \subset \mathbf{G}$  together with an SPT twist  $\psi_{\mathcal{L}} \in H^2(\mathbf{H}_{\mathcal{L}}, \mathbf{U}(1))$ . We show how the data  $(\mathbf{H}_{\mathcal{L}}, \psi_{\mathcal{L}})$  can be extracted from the anyons in  $\mathcal{L}$ .
4. *Obstruction to duality (gapped)*: Each gapped phase is characterized by a **fusion structure** corresponding to the algebra of condensed order parameters. There cannot exist dualities between two gapped phases  $\mathcal{L}$  and  $\mathcal{L}'$  unless they have isomorphic fusion structures. The web of dualities splits into connected components, one for each type of fusion structure.
5. *Emergent symmetries*: If a Hamiltonian  $H$  is self-dual under a subgroup  $\mathcal{S}$  of dualities  $\mathcal{G}[\mathbf{G}]$ , then this implies that it has new emergent symmetries. These are sometimes generalized non-invertible symmetries, in particular when they descend from bulk electric-magnetic 0-form symmetries.
6. *Implication of self-duality*: Given a Hamiltonian  $H$  self-dual under a subgroup  $\mathcal{S}$ , we give criteria to determine when the self-duality is an obstruction to  $H$  being in a gapped phase. In such a situation, the Hamiltonian  $H$  must be either at a phase transition or in a gapless phase.
7. *Multi-criticality*: Given a critical point  $\mathcal{C}$  self-dual under subgroup  $\mathcal{S}$  of dualities  $\mathcal{G}[\mathbf{G}]$ , we show how to determine the lower bound on the degree of multi-criticality of  $\mathcal{C}$ .
8. *Obstruction to duality (critical)*: critical points are characterized by a set of fusion structures corresponding to the gapped phases attached to them. Two critical points  $\mathcal{C}$  and  $\mathcal{C}'$  cannot be dual to each other unless their fusion structures are the same. This implies the decomposition of the space of  $\mathbf{G}$ -symmetric critical points into blocks labeled by fusion structures. Dualities can only act within each block.

Using these results, one can significantly constrain and potentially determine the phase diagrams of spin-chain models with very simple calculations. Topological holography is especially powerful for symmetry groups  $\mathbf{G}$  that have large duality groups  $\mathcal{G}[\mathbf{G}]$  and few possible fusion structures.

One of our most powerful applications of topological holography is to determine the complete conformal spectra of non-trivial critical points. This we achieve by lifting dualities from Hamiltonians (spatial) to the level of partition functions (spacetime). Given a (generalized symmetry-twisted) thermal partition function  $\mathcal{Z}_{\mathbf{g}, \mathbf{h}}$ , the partition function of a dual theory is given by

$$\mathcal{Z}_{\mathbf{g}^{\vee}, \mathbf{h}^{\vee}} = \frac{1}{|\mathbf{G}|} \sum_{\mathbf{g}, \mathbf{h} \in \mathbf{G}} \eta(\mathbf{g}, \mathbf{h}, \mathbf{g}^{\vee}, \mathbf{h}^{\vee}) \mathcal{Z}_{\mathbf{g}, \mathbf{h}}. \quad (1.1)$$

We find an explicit formula for the phases  $\eta(\mathbf{g}, \mathbf{h}, \mathbf{g}^{\vee}, \mathbf{h}^{\vee})$  in terms of dualities. Physically, these factors are related to topological partition functions of certain SPT phases living on duality domain-walls in the bulk. Finally, we give an interpretation of these dualities from the perspective of gauging global symmetries.



**Study of spin chains using topological holography:** In Section 5, we illustrate the theory developed in prior sections for specific examples of  $G$ .

First, we discuss the simplest example  $G = \mathbb{Z}_2$ . Next, we briefly discuss the  $G = \mathbb{Z}_N$  example, where topological holography is not very powerful due to multiple fusion structures and a small duality group. Next, we move on to examples where topological holography is very powerful such as  $G = \mathbb{Z}_2 \times \mathbb{Z}_2$ , and  $G = \mathbb{Z}_3 \times \mathbb{Z}_3$ . In particular, using topological holography we classify possible gapped phases, their associated set of condensed bulk anyons, the duality group, and the corresponding web of dualities. We then construct explicit spin-chain representations of the  $\text{SOA}[G]$  algebras. For each gapped phase, we construct fixed-point Hamiltonians. From the set of condensed anyons, we determine the corresponding spin-chain order parameters for each gapped phase, and from the set of confined anyons, we determine the fundamental spin-chain excitations.

To further exemplify our approach, we define so-called minimal Hamiltonians which are a linear combinations of fixed-point Hamiltonians and study their phase diagrams. These give us a rich set of models with rich phase diagrams containing all gapped phases and many non-trivial phase transitions. Using the general results mentioned above, we map out phase diagrams, identifying gapped regions, critical points/lines/surfaces, first-order transitions, etc. It turns out that these phase diagrams are surprisingly geometrical as we determine using dualities. Using Density Matrix Renormalization Group (DMRG) method and the order parameters provided by topological holography, we numerically verify the predicted phase diagrams. By computing entanglement entropy numerically, we confirm the predicted central charges along various points and critical lines.

For many non-trivial critical points, we explicitly compute the full conformal spectra using analytical methods from topological holography. The only extra input are the partition functions of simple order-disorder transitions such as the  $c = \frac{1}{2}$  Ising CFT. From this, we compute the spectrum of several interesting “*Landau-forbidden*” transitions such as *topological phase transitions* with no symmetry breaking between SPT phases, *topological spontaneous symmetry-breaking transitions* between a non-trivial SPT phase and a symmetry-broken phase, and *topological deconfined transitions*. From the action of global symmetry  $G$  on primary fields, we highlight the difference between topological spontaneous symmetry-breaking transitions and conventional Landau-allowed spontaneous symmetry-breaking transitions. Our approach makes explicit the relation between symmetry-enriched CFTs [119] and SPT invariants. Using Exact Diagonalization techniques, we numerically confirm these analytical predictions of conformal spectra.

More details about construction of generalized spins chain from holographic perspective, duality groups, symmetry-twisted boundary conditions, conformal spectra of various transitions, and some relevant background material are collected in the appendices. A simple and concrete realization of topological holography in an exactly-solvable lattice model is given in Appendix C.

**Note:** The idea that anyons and anyonic symmetries are related to global symmetries and dualities in one lower dimension has been discussed in [120] and also more thoroughly in [121] (see chapter 7 and section 7.5.5 of [122]). Furthermore, a relation between TQFTs in  $d+1$ -dimensions and generalized Kramers-Wannier dualities in  $d$ -dimensions was stated as an on-going work (see section 7.6 of [122]). This old unfinished work was revisited by



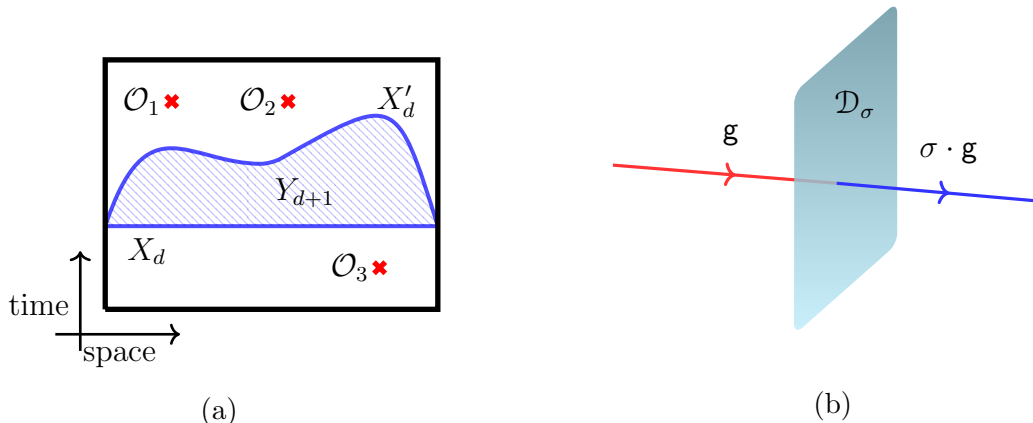


Figure 1: a) Symmetry operators are topological  $\mathcal{U}_g[X_d] = \mathcal{U}_g[X'_d]$ . This is due to the conserved current  $d\star j = 0$  implying  $\int_{Y_{d+1}} d\star j = \int_{X_d} \star j - \int_{X'_d} \star j = 0$ , where  $Y_{d+1}$  is a manifold bounded by  $X_d$  and  $X'_d$ . b) When both 0-form (here a surface) and 1-form (here a line) symmetries are present, the 0-form symmetry can act on the 1-form symmetry to form a higher mathematical structure called a 2-group.

us recently which the current paper (and other on-going works) is a result of. During the preparation of this paper, we became aware of several works [92, 94, 105–108, 112–118] that appeared in the recent past which contain related insights. While this paper some conceptual overlap with this literature, we believe that it is a good complement to the ongoing progress in the field and contains many new insights.

## 2 Symmetry structures as topological operators

The concept of symmetry plays a fundamental role in this work. Therefore, we start with a brief overview of what we mean by symmetries in generic quantum systems. We then explain how symmetries can be used to decompose the space of local operators.

### 2.1 Symmetries are topological

A quantum system is typically defined by a Hamiltonian acting on a Hilbert space which admits a tensor product decomposition into local (on-site) Hilbert spaces. Likewise, the Hamiltonian admits a decomposition into a sum of local terms each of which acts on the corresponding local Hilbert space. Global symmetry operators act on all of space and are required to commute with the Hamiltonian. They typically satisfy a group composition law, however in certain quantum systems they can satisfy a more general mathematical structure such as a fusion algebra which is not isomorphic to any group [83, 88–101]. For this paper, it is instructive to review the concept of symmetry from a modern perspective.

When a quantum system is described by a Euclidean quantum field theory, there is no preferred spatial hypersurface therefore the symmetry operators may be defined on any

codimension-1 surface embedded in spacetime. Consequently, the condition of commutativity with the Hamiltonian generalizes to commutativity with the energy-momentum tensor which implies topological invariance of the symmetry operators. More precisely, any correlation function or observable of a quantum field theory is invariant under smooth (topological) deformations of the support of the symmetry operators of the theory. A well-known example is a  $d + 1$ -dimensional quantum field theory invariant under a global  $U(1)$  symmetry. Noether's theorem mandates the existence of a conserved 1-form current  $j$ , satisfying the conservation law  $d\star j \sim \partial_\mu j^\mu = 0$ , associated to this symmetry. The global symmetry operators take the form

$$\mathcal{U}_{\mathbf{g}}[X_d] := \exp \left\{ i\mathbf{g} \int_{X_d} \star j \right\}, \quad (2.1)$$

where  $\mathbf{g} \in \mathbb{R}/2\pi\mathbb{Z} \simeq U(1)$ ,  $X_d$  is a given  $d$ -dimensional hypersurface embedded in the  $d + 1$ -dimensional spacetime. The exponent is often called the Noether charge and is the generator of infinitesimal symmetry transformations. These operators satisfy the  $U(1)$  group composition rule

$$\mathcal{U}_{\mathbf{g}}[X_d] \times \mathcal{U}_{\mathbf{g}'}[X_d] = \mathcal{U}_{\mathbf{g}+\mathbf{g}'}[X_d]. \quad (2.2)$$

Additionally, as a consequence of current conservation ( $d\star j = 0$ ), these operators can be moved around freely within correlation functions as long as they don't pierce any local operator  $\mathcal{O}_i$  that carries a non-trivial  $U(1)$  charge i.e.

$$\left\langle \mathcal{U}_{\mathbf{g}}[X_d] \prod_i \mathcal{O}_i(x_i) \right\rangle = \left\langle \mathcal{U}_{\mathbf{g}}[X'_d] \prod_i \mathcal{O}_i(x_i) \right\rangle, \quad (2.3)$$

when there exists a closed  $d + 1$ -dimensional region which does not contain any of the points  $x_i$  and whose boundary is the union of  $X_d$  and  $X'_d$  (see Figure 1a). This means that symmetry operators in a quantum theory are topological. We emphasize that even for non-topological systems, the symmetry structure is always topological.

An alternative way of seeing why symmetry operators are topological is to note that they, by definition, commute with the Hamiltonian and hence are conserved under time-evolution. They can therefore be deformed freely inside the partition function without any obstruction from the Hamiltonian. This point of view applies to finite symmetries as well, where there are no conserved Noether currents. More generally, similar to the  $U(1)$  case, gauge invariance of the background gauge field for a finite group implies topological invariance of the discrete symmetry structure (see Fig. 3).

Ordinary global symmetries like  $\mathcal{U}_{\mathbf{g}}[X_d]$  naturally act on 0-dimensional operators. In particular local operators that are *charged* under these symmetries transform under a representation  $\alpha$  of the corresponding symmetry group  $G$  if passed through the hypersurface  $X_d$ . Let  $X_d$  wrap a point  $x$ . Since the symmetry operators are topological, we can deform  $X_d$ , and in particular, we can shrink it. As a result of shrinking the surface, we have

$$\mathcal{U}_{\mathbf{g}}[X_d] \mathcal{O}_\alpha(x) = R_\alpha(\mathbf{g}) \mathcal{O}_\alpha(x), \quad (2.4)$$

where  $R_\alpha(\mathbf{g})$  is the representation matrix of  $G$  (see Figure 2a). If  $X_d$  is a time-slice and  $x \in X_d$ , then

$$\mathcal{U}_{\mathbf{g}}[X_d] \mathcal{O}_\alpha(x) \mathcal{U}_{\mathbf{g}}^\dagger[X_d] = R_\alpha(\mathbf{g}) \mathcal{O}_\alpha(x), \quad (2.5)$$

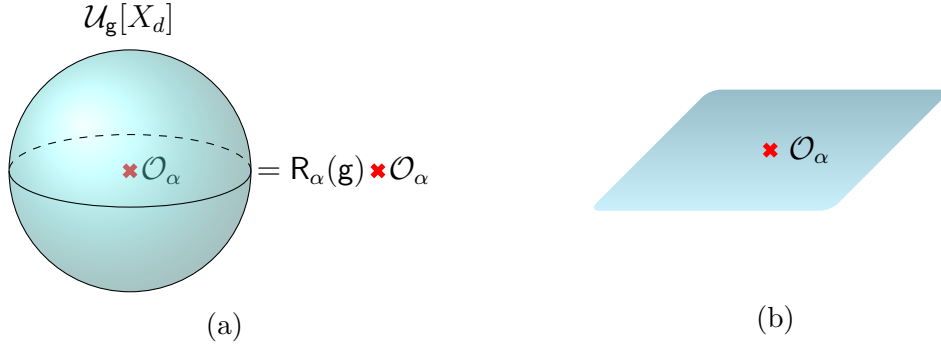


Figure 2: **(a)** A (0-form) global symmetry is associated with a  $d$ -dimensional surface  $X_d$  in a  $d + 1$ -dimensional spacetime. A 0-dimensional (local) operator will transform under some representation  $\alpha$  when crossing this hypersurface. If  $X_d$  wraps around the point  $x$ , then by shrinking the surface  $\mathcal{U}_g[X_d]\mathcal{O}_\alpha(x) = R_\alpha(g)\mathcal{O}_\alpha(x)$ . **(b)** If  $X_d$  is a time-slice associated with a Hilbert space then we have  $\mathcal{U}_g[X_d]\mathcal{O}_\alpha(x) = R_\alpha(g)\mathcal{O}_\alpha(x)\mathcal{U}_g[X_d]$ , which is the standard transformation law in a Hilbert space.

which is the standard way symmetries act on operators at the level of the Hilbert space of theory (see Figure 2b). Since these ordinary symmetries act on 0-dimensional operators, they are sometimes called 0-form symmetries and the corresponding symmetry operators are supported on a  $d$ -dimensional (or codimension-1<sup>1</sup>) manifolds  $X_d$  in the ambient  $d + 1$ -dimensional spacetime. We will call manifolds associated with symmetries, operators or defects interchangeably. More precisely these are referred to as operators when the surface is spacelike and defects otherwise.

As mentioned, this is not restricted to continuous symmetries. Similarly, discrete symmetries can also be associated with manifolds  $X_d$ . A well-known example in this regard is a global  $\mathbb{Z}_2$  operator in spin-1/2 systems defined as  $\prod_i \sigma_i^x$  and the product runs over the spin sites. In Euclidean field theory, a suitably chosen collection of symmetry operators can be used to simulate a given  $\mathbb{Z}_2$  background connection. Invariance of the background connection under  $\mathbb{Z}_2$  gauge transformations translates to topological invariance of the symmetry operators.

Recent years have seen various important generalizations of symmetry structures in quantum systems. One of these is the notion of generalized global symmetries which are symmetry structures under which extended objects are charged [81]. More specifically, in a  $d + 1$ -dimensional spacetime, there can exist  $d + 1 - q - 1 = d - q$  dimensional symmetry defects  $\mathcal{U}_g[X_{d-q}]$  which act on operators  $\mathcal{O}[\Sigma_q]$  supported on  $q$ -dimensional submanifolds  $\Sigma_q$ . Again, the symmetry operators  $\mathcal{U}_g[X_{d-q}]$  are topological and can be freely deformed within correlation functions, although the charged operators  $\mathcal{O}[\Sigma_q]$  need not be topological. Equations similar to (2.4) and (2.5) still hold in this case [81]. For example

$$\mathcal{U}_g[X_{d-q}]\mathcal{O}_\alpha[\Sigma_q] = R_\alpha(g)^{\text{Link}[X_{d-q}, \Sigma_q]} \mathcal{O}_\alpha[\Sigma_q], \quad (2.6)$$

<sup>1</sup>In this work, we often use the standard terminology codimension. A codimension- $p$  submanifold in a  $d + 1$ -dimensional spacetime has  $d + 1 - p$  spacetime dimensions.

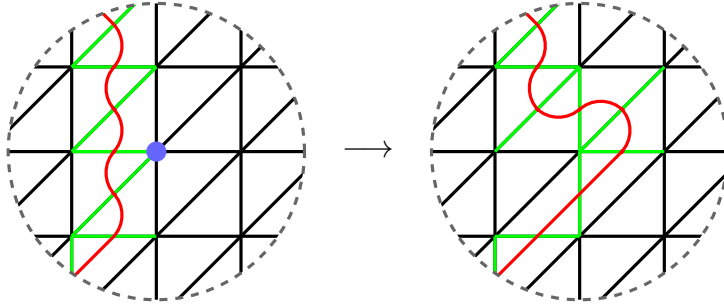


Figure 3: A gauge field corresponding to a finite Abelian group can be defined on a triangulated spacetime and is equivalent to collection of symmetry defects. Gauge transformations implement topological re-configurations of the symmetry defects. The figure illustrates a  $\mathbb{Z}_2$  gauge field  $A$ . The edges (1-simplices) in green and black have  $A_{ij} = 1$  and 0 respectively. Equivalently, this gauge field configuration can be described by a single symmetry defect denoted in red. A gauge transformation  $\phi_i = 1$  on a single site (in blue) and 0 everywhere else transforms the gauge field and correspondingly topologically deforms the symmetry defect.

where  $\text{Link}[X_{d-q}, \Sigma_q]$  is the linking number between the two manifolds. And if both  $X_{d-q}$  and  $\Sigma_q$  are in a time-slice, we find the usual Hilbert space action of symmetry

$$\mathcal{U}_{\mathbf{g}}[X_{d-q}] \mathcal{O}_{\alpha}[\Sigma_q] \mathcal{U}_{\mathbf{g}}^{-1}[X_{d-q}] = R_{\alpha}(\mathbf{g})^{\text{Intersect}[X_{d-q}, \Sigma_q]} \mathcal{O}_{\alpha}[\Sigma_q], \quad (2.7)$$

where  $\text{Intersect}[X_{d-q}, \Sigma_q]$  is the intersection number. Such symmetries are called  $q$ -form symmetries, where  $q = 0$  corresponds to what is conventionally known as global symmetry. Continuous  $q$ -form symmetries also lead to conservation laws similar to  $\mathbf{d} \star j = 0$ , but now conservation of  $q$ -dimensional charges. Note that if both operators  $\mathcal{U}_{\mathbf{g}}[X_{d-q}]$  and  $\mathcal{O}_{\alpha}[\Sigma_q]$  are topological, this implies that both are higher-form symmetry generators. A non-trivial  $R_{\alpha}$  in (2.6) and (2.7) gives rise to higher-form 't Hooft anomalies, as it serves as an obstruction to gauging both of these higher form symmetries together [81]. Regarding the application of these types of symmetries, we notice that extended objects can commonly emerge in condensed matter systems, despite the microscopic theory only having point-like degrees of freedom. Examples include Wilson operators in gauge-theoretic descriptions of spin systems and vortices in superfluids and superconductors.

When multiple higher-form symmetries are present simultaneously, one might wonder which mathematical structure they form together. Interestingly, it turns out that 0-form symmetries  $\mathcal{U}[X_d]$  can act on 1-form (or higher-form) symmetries  $\mathcal{U}[Y_{d-1}]$  when  $Y_{d-1}$  pierces through  $X_d$  as in Figure 1b. This leads to a mathematical structure called a 2-group (and more generally to  $n$ -groups) [82, 84–87]. Such a situation is common in topologically-ordered systems in  $2+1d$  and they will play the key role in this paper. The above mentioned notion of non-invertible symmetries can also be thought of within this framework [83, 88–101]. We notice that systems with these types of generalized symmetries can be accommodated into the framework presented here for symmetries with group-like structure. Other new notions of symmetry exist which for now is outside of the conceptual framework of this paper. For example subsystem symmetries, which play an important role in fracton topological order and can give rise to unusual phenomena like IR-UV mixing [123].

Let us briefly say few words about anomalies associated to global symmetries, i.e., 't Hooft anomalies. Certain symmetric quantum systems might have quantum anomalies which, being an renormalization group invariant property [124], strongly constrain their dynamics. If a system has a quantum anomaly in the microscopic/ultraviolet description, its low-energy/infra-red description can only realize phases which saturate the anomaly. Concretely, for a given quantum system, anomalies can be diagnosed by lack of gauge invariance of the gauged partition function or equivalently by the lack of topological invariance of a certain network of symmetry operators. Two condensed matter contexts where quantum anomalies arise are (i) the surface of symmetry-protected topological (SPT) phases [43, 47, 125] and (ii) in low-energy descriptions of quantum systems with Lieb-Schultz-Mattis constraints [78–80, 126].

Since the concept of symmetry is inherently topological in any quantum system, it is natural to ask whether the symmetry aspects of a theory can be studied and understood using a purely topological theory? In this paper, we are particularly interested in studying  $1 + 1d$  quantum systems with a finite Abelian global symmetry group  $G$ . The fundamental theorem of finite Abelian groups determines the structure of such groups: any finite Abelian group is isomorphic to a direct product of cyclic groups whose orders are powers of primes<sup>2</sup>

$$G = \prod_a \mathbb{Z}_{N_a}, \quad n_a = p_a^{k_a} \quad (2.8)$$

where  $N_a$ s and  $k_a$ s are positive integers and  $p_a$ s are (not necessarily distinct) prime numbers. It turns out that systems with such symmetry groups can be analyzed as the boundary of an auxiliary  $2 + 1d$  topologically ordered system, described by a topological gauge theory with gauge group  $G$ . As we will illustrate in detail, such theories encode all the physically-important features related to the global symmetry of the lower dimensional theory. This will give us powerful tools to study phase diagrams and phase transitions of  $1 + 1d$   $G$ -symmetric theories. The restriction of dimension and group structure is merely done to illustrate the power of this construction in a simple setting. We expect these concepts to naturally generalize to higher dimensions. We leave such explorations for future work.

## 2.2 Building blocks of symmetric local operators

To establish some notation, we will briefly study the space of linear operators acting on a Hilbert space. Consider a Hilbert space which admits a local tensor product decomposition  $\mathcal{H} = \otimes_i \mathcal{H}_i$  and the corresponding space of linear operators  $\mathcal{L}(\mathcal{H}) = \otimes_i \mathcal{L}(\mathcal{H}_i)$ . A (usual 0-form) symmetry acts on local operators  $\mathcal{O}_i \in \mathcal{L}(\mathcal{H}_i)$  as  $\mathcal{O}_i \rightarrow \mathcal{U}_g \mathcal{O}_i \mathcal{U}_g^\dagger$  and we assume that the operator  $\mathcal{U}_g$  has the following tensor product decomposition

$$\mathcal{U}_g = \bigotimes_i \mathcal{O}_{g,i}, \quad (2.9)$$

with the property  $\mathcal{O}_{g_1,i} \mathcal{O}_{g_2,i} = \mathcal{O}_{g_1 g_2,i}$ . In other words, we assume that the system has an on-site symmetry. Since the space of local operators is a representation space for the symmetry, we can decompose it into irreducible representations as

$$\mathcal{L}(\mathcal{H}_i) = \bigoplus_{\alpha \in \text{Rep}(G)} n_{\alpha,i} \mathcal{L}_{\alpha,i}, \quad (2.10)$$

---

<sup>2</sup>See section 2.1 of [127] for detailed discussion of this result.

where  $\text{Rep}(\mathbf{G})$  is the set of irreducible representations of the symmetry group  $\mathbf{G}$  and  $n_{\alpha,i}$  is the multiplicity of the representation  $\alpha$  at the site  $i$ . For simplicity of notation, we will suppress the multiplicity of a representation. The irreducible local operators  $\mathcal{O}_{\alpha,i} \in \mathcal{L}_{\alpha,i}$  have well-defined *charges* under the action of the symmetry group  $\mathbf{G}$

$$\mathcal{U}_{\mathbf{g}} \mathcal{O}_{\alpha,i} \mathcal{U}_{\mathbf{g}}^\dagger = \mathbf{R}_\alpha(\mathbf{g}) \cdot \mathcal{O}_{\alpha,i}, \quad (2.11)$$

where  $\mathbf{R}_\alpha(\mathbf{g})$  is the matrix representation of the group element  $\mathbf{g}$  in the representation  $\alpha$ . This relation is nothing but (2.5). This implies the following local operator identity

$$\mathcal{O}_{\mathbf{g},i} \mathcal{O}_{\alpha,i} \mathcal{O}_{\mathbf{g},i}^\dagger = \mathbf{R}_\alpha(\mathbf{g}) \cdot \mathcal{O}_{\alpha,i}. \quad (2.12)$$

The set of operators  $\{\mathcal{O}_{\mathbf{g},i}, \mathcal{O}_{\alpha,i}\}$  for  $\mathbf{g} \in \mathbf{G}$  and  $\alpha \in \text{Rep}(\mathbf{G})$ , are the building blocks of all other local operators and in particular the subalgebra of  $\mathbf{G}$ -symmetric operators. For example, for a finite Abelian group  $\mathbf{G}$ , a symmetric operator with finite support<sup>3</sup> takes the form

$$\mathcal{K} = \mathcal{O}_{\alpha_1,i_1} \mathcal{O}_{\mathbf{g}_1,i_1} \dots \mathcal{O}_{\alpha_n,i_n} \mathcal{O}_{\mathbf{g}_n,i_n}, \quad (2.13)$$

with the constraint that the product of local representations  $\alpha_{i_k}$  over  $k$  is the trivial representation in  $\text{Rep}(\mathbf{G})$ .

As the simplest example, for  $\mathbf{G} = \mathbb{Z}_2 = \{0, 1\}$ , we have two non-trivial representations  $\text{Rep}(\mathbb{Z}_2) = \{0, 1\}$  given by  $\mathbf{R}_{\alpha=0}(\mathbf{g}) = 1$  and  $\mathbf{R}_{\alpha=1}(\mathbf{g}) = (-1)^{\mathbf{g}}$ . The two corresponding local operators  $\mathcal{O}_{\mathbf{g},i} = (\sigma_i^x)^{\mathbf{g}}$  and  $\mathcal{O}_{\alpha,i} = (\sigma_i^z)^\alpha$  satisfy

$$\mathcal{U}_{\mathbf{g}} \sigma_i^x \mathcal{U}_{\mathbf{g}}^\dagger = \sigma_i^x, \quad \mathcal{U}_{\mathbf{g}} \sigma_i^z \mathcal{U}_{\mathbf{g}}^\dagger = (-1)^{\mathbf{g}} \sigma_i^z, \quad (2.14)$$

where the symmetry operator is given by  $\mathcal{U}_{\mathbf{g}} = (\prod_i \sigma_i^x)^{\mathbf{g}}$  and  $\sigma^x$  and  $\sigma^z$  denote the standard Pauli matrices.

For  $\mathbf{G} = \mathbb{Z}_N = \{0, 1, \dots, N-1\}$ , we have the representations  $\text{Rep}(\mathbb{Z}_N) = \{0, 1, \dots, N-1\}$  given by  $\mathbf{R}_\alpha(\mathbf{g}) = e^{\frac{2\pi i}{N} \alpha \mathbf{g}}$  and the operators  $\mathcal{O}_{\mathbf{g}} = X^{\mathbf{g}}$  and  $\mathcal{O}_\alpha = Z^\alpha$ , satisfying

$$\mathcal{U}_{\mathbf{g}} X_i^{\mathbf{g}} \mathcal{U}_{\mathbf{g}}^\dagger = X_i^{\mathbf{g}}, \quad \mathcal{U}_{\mathbf{g}} Z_i^\alpha \mathcal{U}_{\mathbf{g}}^\dagger = e^{\frac{2\pi i}{N} \alpha \mathbf{g}} Z_i^\alpha, \quad (2.15)$$

where the symmetry operator is given by  $\mathcal{U}_{\mathbf{g}} = (\prod_i X_i)^{\mathbf{g}}$ . Here  $X$  and  $Z$  are the  $\mathbb{Z}_N$  generalization of Pauli matrices satisfying the algebra

$$X^{\mathbf{g}} Z^\alpha = e^{\frac{2\pi i}{N} \alpha \mathbf{g}} Z^\alpha X^{\mathbf{g}}. \quad (2.16)$$

In this work, we are mostly interested in finite Abelian groups of the form  $\mathbf{G} = \mathbb{Z}_{N_1} \times \dots \times \mathbb{Z}_{N_n}$ . For this group, the general formula for representation  $\mathbf{R}_\alpha(\cdot)$  is given by

$$\mathbf{R}_\alpha(\mathbf{g}) = \exp \left( 2\pi i \sum_{a=1}^n \frac{\alpha_a \mathbf{g}_a}{N_a} \right), \quad (\mathbf{g}_a, \alpha_a) \in \mathbb{Z}_{N_a} \times \text{Rep}(\mathbb{Z}_{N_a}). \quad (2.17)$$

---

<sup>3</sup>Here by finite support, we mean that the set  $\{i_1, \dots, i_n\}$  which labels the local sites is a finite set.

### 3 Topological holography: Framework

As discussed in the previous section, symmetry operators are topological in nature. Therefore, we can pose the following question: can symmetry-related aspects of a  $1 + 1d$  theory be described by a topologically-ordered system in one higher dimension? If so, which topological order would be a candidate? One way to think about this is the following: 0-form symmetry in  $1 + 1d$  are given by a collection of line-like operators, therefore which  $2 + 1d$  topological orders have a (subset of) similar line-like topological operators? Such topological line operators are in fact ubiquitous in  $2 + 1d$  topological orders and correspond to anyonic excitation in the topological phase. From the perspective of symmetry, each Abelian anyon generates a 1-form global symmetry. In other words, in order to describe a  $G$ -symmetric  $1 + 1d$  theory we need to look at theories in  $2 + 1d$  with 1-form  $G$ -symmetries. This is exactly the case for topological gauge theories with gauge group  $G$ <sup>4</sup>. This is somewhat reminiscent of the AdS/CFT correspondence, where the gauge symmetry of the bulk gravitational theory, is dual to the global symmetry of the theory at its boundary<sup>5</sup> [130]. Therefore the reason gauge symmetry in the bulk becomes global (0-form) symmetry of the boundary originates from the 1-form symmetry of the bulk and the 0-form symmetry of the boundary being the same. Note that this reasoning does not straightforwardly generalize to non-Abelian groups since 1-form symmetries cannot be non-Abelian.

In the following sections we will describe the (higher) symmetries of topological gauge theories with finite Abelian gauge group  $G$ . We then describe the space of  $1 + 1d$  theories that can be realized at its boundary. Since this construction attempts to understand  $1 + 1d$  theories from a topological theory in higher dimensions, we call it *Topological Holography*<sup>6</sup>.

#### 3.1 Symmetries of topologically-ordered phases

Topological gauge theories, also known as Dijkgraaf-Witten theories [38] or Quantum Double models  $\mathcal{D}(G)$  [27] have two types of topological operators or symmetries that play a role in our construction. First, they are equipped with a set of line operators  $\mathcal{W}_d[\gamma]$  supported on any curve  $\gamma$  and are labeled by  $d = (g, \alpha)$ , where  $g \in G$  and  $\alpha \in \text{Rep}(G)$  correspond to the magnetic and electric charge of the line operator, respectively. These are often called Wilson lines. From the point of view of topological order, the end-points of these line operators correspond to anyonic excitations. The set of labels  $(g, \alpha)$  (or equivalently the set of line operators) form a group, denoted by  $\mathcal{A}$ , where the group multiplication is given by the fusion of quasiparticles (anyons). In the case of Abelian theories that we are considering in this paper, the fusion is simply given by  $\mathcal{W}_{d_1}[\gamma] \times \mathcal{W}_{d_2}[\gamma] = \mathcal{W}_{d_1+d_2}[\gamma]$  or

---

<sup>4</sup>More precisely,  $2 + 1d$  topological gauge theories with gauge group  $G$  always have a non-anomalous 1-form symmetry subgroup  $G$ .

<sup>5</sup>Recently, this has been modified to a more refined statement: the global symmetry of the boundary theory is actually dual to what has been dubbed as a long-range gauge symmetry of the bulk theory [128, 129].

<sup>6</sup>This should not be confused with the notion of topological holography in the context of topological string theory [131–135].



written graphically

$$\begin{array}{c} (g_1, \alpha_1) \quad (g_2, \alpha_2) \\ \text{---} \times \text{---} \\ \text{---} \end{array} = \begin{array}{c} (g_1 + g_2, \alpha_1 + \alpha_2) \\ \text{---} \\ \text{---} \end{array} . \quad (3.1)$$

When acting on a Hilbert space conjugation is defined as  $\mathcal{W}_d^\dagger[\gamma] = \mathcal{W}_{-d}[\gamma]$ , making them unitary. The anyonic charge  $d$  is defined with respect to the orientation of  $\gamma$ , changing the orientation flips the charge  $\mathcal{W}_d[\gamma] = \mathcal{W}_{-d}[\bar{\gamma}]$ , where  $\bar{\gamma}$  is  $\gamma$  with opposite orientation. These line operators are topological, i.e., they can be freely deformed. Therefore in the language of higher-symmetries, we can think of the group of line operators/anyonic excitations  $\mathcal{A}$ , as the group of 1-form symmetries of a topologically ordered system (see Figure 4a).

The second type of topological operators or symmetries in a  $2 + 1d$  topologically-ordered phase are  $\mathcal{D}_\sigma[\Sigma]$  for any oriented surface  $\Sigma$ , labeled by a group element  $\sigma \in \mathcal{G}[\mathbf{G}]$ . In the literature on topologically-order phases, the symmetries in  $\mathcal{G}[\mathbf{G}]$  are known as *anyonic symmetries* since they permute all anyons without changing their fusion rules or braiding phases [136–140]. We will define them more precisely in Section 3.5. We note that  $\mathcal{G}[\mathbf{G}]$  can be non-Abelian even if  $\mathbf{G}$  is Abelian. In this paper we will see that  $\mathcal{G}[\mathbf{G}]$  can contain hundreds of millions of elements, even for extremely simple groups like  $\mathbf{G} = (\mathbb{Z}_2)^4$  (see Appendix B). Again the element  $\sigma$  is defined relative to the orientation of  $\Sigma$ . Here an orientation of  $\Sigma$  is given by its normal vector. Flipping the direction of the normal vector inverses the group element:  $\mathcal{D}_\sigma[\Sigma] = \mathcal{D}_{\sigma^{-1}}[\bar{\Sigma}]$ , where  $\bar{\Sigma}$  is  $\Sigma$  with opposite normal vector. On the other hand, conjugation is defined as usual, i.e.  $\mathcal{D}_\sigma^\dagger[\Sigma] = \mathcal{D}_{\sigma^{-1}}[\Sigma]$ . Since they are the same dimension as a spatial time-slice, they correspond to conventional (0-form) symmetries of the topological phase. These surfaces also have a fusion product on a fixed oriented surface  $\Sigma$ ,  $\mathcal{D}_{\sigma_1}[\Sigma] \times \mathcal{D}_{\sigma_2}[\Sigma] = \mathcal{D}_{\sigma_1\sigma_2}[\Sigma]$ . This can be represented graphically as

$$\text{Diagram illustrating the composition of two diffeomorphisms. On the left, two overlapping parallelograms represent the domains } \mathcal{D}_{\sigma_1} \text{ and } \mathcal{D}_{\sigma_2}. \text{ An arrow points to a single parallelogram on the right, representing the domain } \mathcal{D}_{\sigma_1 \sigma_2}.$$

$$(3.2)$$

Note that since  $\mathcal{G}[\mathbf{G}]$  can be non-Abelian, this product must be defined with a convention relative to the choice of orientation/normal direction. Such a choice can always be made for  $d$  dimensional manifolds in  $d + 1$ -dimensional spacetimes, which is why 0-form symmetries can be non-Abelian. However, such a choice is not possible for 1- or higher-form symmetries and they must therefore always be Abelian<sup>7</sup>. The 0-form symmetry operators  $\mathcal{D}_\sigma[\Sigma]$  act on the 1-form symmetry operators  $\mathcal{W}_d[\gamma]$  by permuting their charges

$$d = (\mathbf{g}, \alpha) \longmapsto \sigma \cdot (\mathbf{g}, \alpha) \in \mathcal{A}, \quad \sigma \in \mathcal{G}[\mathbb{G}], \quad (3.3)$$

whenever the curve  $\gamma$  penetrates the surface  $\Sigma$  as in Figure 6a. Together, the 0-form group  $\mathcal{G}[\mathcal{G}]$  and 1-form group  $\mathcal{A}$  form a mathematical structure called a 2-group [82, 84–87].

In the following, we will elaborate more on these two types of topological operators and what kind of structures they holographically induce on a theory living at the  $1+1d$  spacetime

<sup>7</sup>If  $q$ -form symmetries are invertible and thus form a group (like the anyons in this paper), they must form an Abelian group. If we do not demand invertibility, then they can form a commutative fusion category. This is the case for 1-form symmetries of topologically-ordered phases with non-Abelian anyons.



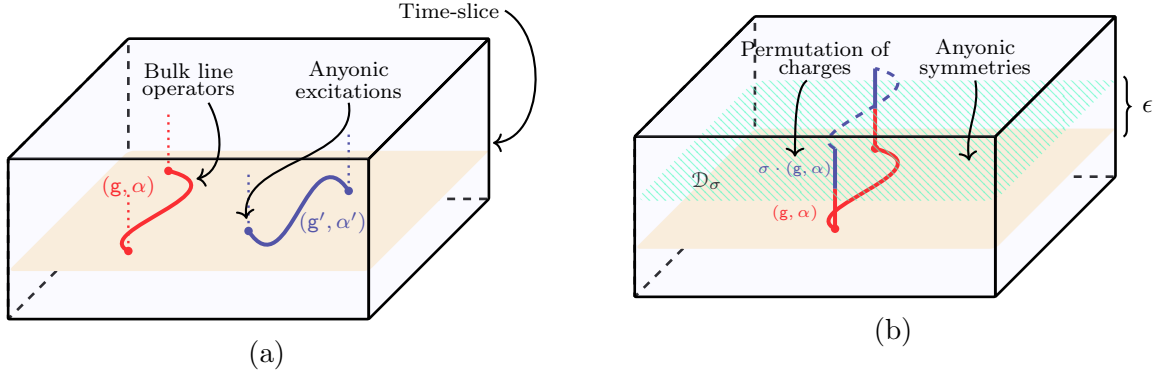


Figure 4: Illustration of the 2+1 dimensional spacetime of a topological gauge theory. The orange surface is a time-slice associated with a Hilbert space. **(a)** The theory has topological line operators labeled by  $d = (\mathbf{g}, \alpha)$ . The set of these operators are  $\mathcal{A}$ , is the group of 1-form symmetries. In a topological phase, open line operators create anyonic excitations at the end-points of the line. Under time evolution, these end-point evolve into world-lines (dotted lines). **(b)** Surface operators associated to global (0-form) symmetries of the theory  $\sigma \in \mathcal{G}[\mathbf{G}]$ . When the surface corresponding to the symmetry  $\mathcal{D}_\sigma$  is put on the time-slice it acts on the Hilbert space as a conventional symmetry operator, transforming the charges  $(\mathbf{g}, \alpha)$  to  $\sigma \cdot (\mathbf{g}, \alpha) \in \mathcal{A}$  with isomorphic operator algebras.

for 1-form symmetries where the charged line is itself topological. Interestingly, this can be thought of as 1-form 't Hooft anomalies. Since each line consists of an electric and a magnetic component, labeled by  $\alpha$  and  $\mathbf{g}$ , respectively, they are not true lines but rather ribbons. We can represent the twisting of such ribbons by another local rule

$$\text{Twisted ribbon} = e^{i\theta_{(\mathbf{g}, \alpha)}} \text{Straight ribbon} \quad (3.6)$$

The phase  $e^{i\theta_{(\mathbf{g}, \alpha)}}$  is sometimes called a topological spin, as it is gained when an anyon rotates  $2\pi$  around itself (as the above graphic encodes). By a version of the spin-statistics theorem, this phase also corresponds to self-statistics which is gained by exchanging two identical anyons. From these two pieces of data, we can form the so-called  $S$  and  $T$  matrices

$$S_{dd'} = \frac{1}{\sqrt{|\mathcal{A}|}} e^{i\theta_{dd'}}, \quad T_{dd'} = e^{i\theta_d} \delta_{dd'}, \quad (3.7)$$

which form a representation of  $\text{SL}(2, \mathbb{Z})$  and essentially describe all the data about a topological phase we need here. For the finite group gauge theories we consider in this paper, these phases are given by

$$e^{i\theta_{dd'}} = R_\alpha(\mathbf{g}') R_{\alpha'}(\mathbf{g}), \quad e^{i\theta_d} = R_\alpha(\mathbf{g}), \quad (3.8)$$

where  $d = (\mathbf{g}, \alpha)$  and  $d' = (\mathbf{g}', \alpha')$  (compare with Section 2.2) and  $R_\alpha(\mathbf{g})$  for a general finite Abelian group of the form (2.8) is defined in (2.17).

The operators  $S_d(a, b)$ , defined in (3.4), generate a local operator algebra on the boundary that we will call the String Operator Algebra

$$\mathbb{SOA}[\mathbf{G}] \equiv \left\langle S_d(a, b) \mid \forall d \in \mathcal{A} \text{ and } \forall a, b \right\rangle. \quad (3.9)$$

From this, we can see that all non-contractible line operators that wrap around the cylinder commute with all boundary operators since they intersect at even number of points with pairwise opposite orientations



$$(3.10)$$

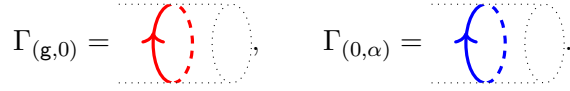
Line operators corresponding to a non-contractible curve  $\gamma$  will be denoted as

$$\Gamma_d \equiv \mathcal{W}_d[\gamma]. \quad (3.11)$$

The commutativity of such operators with an string operator can be stated as


$$\Gamma_d S_{d'}(a, b) = S_{d'}(a, b) \Gamma_d, \quad (3.12)$$

for all  $d, d', a$  and  $b$ . In particular, we have pure electric and magnetic non-contractible lines



$$\Gamma_{(\mathbf{g},0)} = \text{red dashed line with loop}, \quad \Gamma_{(0,\alpha)} = \text{blue dashed line with loop}. \quad (3.13)$$

Note that  $\Gamma_d \in \mathbb{SOA}[\mathbf{G}]$  since they are products of boundary operators  $S_d(a, b)$ , which can be depicted as follows



$$(3.14)$$

The bulk topological order has a topological ground-state degeneracy labeled by the eigenvalues of  $\Gamma_d$

$$\Gamma_d |d'\rangle = R_{\alpha'}(\mathbf{g}) R_{\alpha}(\mathbf{g}') |d'\rangle, \quad (3.15)$$

where  $|d'\rangle = |(\mathbf{g}', \alpha')\rangle$  denotes the topologically-degenerate ground states. Note that the eigenvalue in (3.15) is exactly the  $S$ -matrix (3.7) up to normalization, or in other words the mutual braiding statistics between two anyons. Since  $\Gamma_d$  commutes with operators in  $\mathbb{SOA}[\mathbf{G}]$ , the Hilbert space  $\mathcal{H}$  generated out of boundary operators  $S_d(a, b)$  decomposes into super-selection sectors labeled by line operators or anyons  $d'$

$$\mathcal{H} = \bigoplus_{d'=(\mathbf{g}', \alpha')} \mathcal{H}_{d'}. \quad (3.16)$$

The Hilbert space  $\mathcal{H}$  is a representation space of  $\mathbb{SOA}[\mathbf{G}]$  (see Appendix A for a more detailed construction). These super-selection sectors cannot be connected with any operator in  $\mathbb{SOA}[\mathbf{G}]$ . Since boundary operators commute with  $\Gamma_d$ , we can decompose

$$\mathbb{SOA}[\mathbf{G}] = \bigoplus_{d' \in \mathcal{A}} \mathbb{SOA}_{d'}[\mathbf{G}], \quad (3.17)$$

The bulk topological order has additional operators corresponding to semi-infinite lines ending on the boundary

From (3.5), we see that the following simple algebraic relations hold

This implies that  $\mathcal{Y}_d$  operators shift the eigenvalues of the  $\Gamma$ s

and thereby connect super-selection sectors

The reason  $\mathcal{Y}_d$  can connect super-selection sectors is that it does not belong to  $\text{SOA}[\mathcal{G}]$ . As mentioned earlier, on the boundary  $\Gamma_d$  becomes 0-form symmetries (see Figure 6a) and the String Operator Algebra consists of operators not charged under this symmetry. However,  $\mathcal{Y}_d$  corresponds to a charged local operator on the boundary. For example

It then follows from these considerations that any state  $|d'\rangle \in \mathcal{H}_{d'}$  can be constructed from some state  $|(0,0)\rangle \in \mathcal{H}_{(0,0)}$  in the trivial sector using (3.20)

### 3.3 Mapping to generalized spin-chains

In this section, we map the boundary Hilbert space constructed in the previous section to the language of (generalized) spin-chains. In particular, we would like to connect to the standard notation of operators and symmetries discussed in Section 2.2. The subset of the non-contractible operators

form a group isomorphic to  $G \subset \mathcal{A}$  (see equation (3.1)). This has the following important implications for the  $1+1d$  quantum spin chain on the boundary

- Since operators  $\mathcal{U}_{\mathbf{g}} \equiv \Gamma_{(\mathbf{g},0)}$  commute with all boundary operators, we can identify it with global symmetries of the boundary.

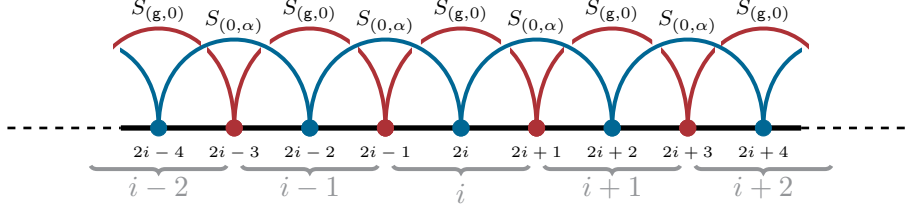


Figure 5: Regularization of the boundary such that magnetic lines  $S_{(\mathbf{g},0)}$  can only end on odd sites while electric lines  $S_{(0,\alpha)}$  can only end on even sites. Alternatively, this can be thought of as the boundary of a topological gauge theory with alternating topological (gapped) boundary conditions corresponding to the condensation of magnetic and electric lines. With such boundary conditions, electric and magnetic lines are allowed to end on certain segments of the boundary and remain gauge-invariant. These new non-contractible line operators correspond to relative homology cycles and become our boundary operators.

- Conversely, since the operators  $\mathcal{U}_{\mathbf{g}}$  commute with all the operators in  $\text{SOA}[\mathbf{G}]$ , the string operator algebra corresponds to the algebra of  $\mathbf{G}$ -symmetric operators of the boundary theory.

One might wonder about the other non-contractible operators

$$\mathcal{T}_{\alpha} \equiv \Gamma_{(0,\alpha)} = \text{blue dashed loop with arrow}, \quad (3.25)$$

A natural question is that what do these correspond to in the spin-chain language? A clear way to see what these operators become in the spin-chain language is to decompose the Hilbert space into eigenspaces of  $\mathcal{T}_{\alpha}$  only, but not of  $\mathcal{U}_{\mathbf{g}}$  (unlike (3.16) and (3.17))

$$\mathcal{H} = \bigoplus_{\mathbf{g}' \in \mathbf{G}} \mathcal{H}_{\mathbf{g}'}, \quad \text{SOA}[\mathbf{G}] = \bigoplus_{\mathbf{g}' \in \mathbf{G}} \text{SOA}_{\mathbf{g}'}[\mathbf{G}]. \quad (3.26)$$

Within each sector  $\mathcal{H}_{\mathbf{g}'}$ , these operators are diagonalized and equal to a complex phase  $\mathcal{T}_{\alpha}|_{\mathbf{g}'} = R_{\alpha}(\mathbf{g}')\mathbb{I}$  (see equation (3.15)). To make connection with a lattice spin-chain, we introduce a UV regularization such that the boundary is a 1D lattice and  $S_{(\mathbf{g},0)}(a,b)$  can only end on odd sites, while  $S_{(0,\alpha)}(a,b)$  end on even sites (see Figure 5). This regularization removes certain ambiguities related to the ribbon structure of the line operators. For simplicity, we will use this notation for the boundary operators

$$\begin{aligned} A_i[\mathbf{g}] &= \bigoplus_{\mathbf{g}' \in \mathbf{G}} A_i^{(\mathbf{g}')}[\mathbf{g}] \equiv S_{(\mathbf{g},0)}(2i-1, 2i+1), \\ B_{i,i+1}[\alpha] &= \bigoplus_{\mathbf{g}' \in \mathbf{G}} B_{i,i+1}^{(\mathbf{g}')}[\alpha] \equiv S_{(0,\alpha)}(2i, 2i+2), \end{aligned} \quad (3.27)$$

where we have decomposed the boundary operators into the blocks within sectors in (3.26). We can now make the identifications<sup>11</sup>

$$A_i^{(\mathbf{g}')}[\mathbf{g}] = \mathcal{O}_{\mathbf{g},i} \quad B_{i,i+1}^{(\mathbf{g}')}[\alpha] = \mathcal{O}_{\alpha,i} \mathcal{O}_{-\alpha,i+1}, \quad (3.28)$$

where  $\mathcal{O}_{\mathbf{g}}$  and  $\mathcal{O}_{\alpha}$  were defined in Section 2.2. This is true since the operators satisfy the same algebra as can be explicitly checked (for a more careful approach see Appendix A). Furthermore, these relations translate to (see (3.14))

$$\begin{aligned} \Gamma_{(\mathbf{g},0)} &= \prod_i S_{(\mathbf{g},0)}(2i, 2i+2) \quad \longrightarrow \quad \mathcal{U}_{\mathbf{g}} = \bigotimes_i \mathcal{O}_{\mathbf{g},i} \\ \Gamma_{(0,\alpha)} &= \prod_i S_{(0,\alpha)}(2i+1, 2i+3) \quad \longrightarrow \quad \mathcal{T}_{\alpha} \equiv \bigotimes_i \mathcal{O}_{\alpha,i} \mathcal{O}_{-\alpha,i+1} \end{aligned} \quad (3.29)$$

Since we are on a semi-infinite cylinder and using the fact that  $\mathcal{O}_{\alpha,i} \mathcal{O}_{-\alpha,i}$  is the identity operator, the last operator reduces to  $\mathcal{T}_{\alpha} = \mathcal{O}_{\alpha,1} \mathcal{O}_{-\alpha,L+1}$  which must be equal to  $R_{\alpha}(\mathbf{g}')\mathbb{I}$  in this sector. This can be achieved if we demand

$$\mathcal{O}_{\alpha,L+1} \equiv R_{\alpha}(\mathbf{g}') \mathcal{O}_{\alpha,1}. \quad (3.30)$$

In other words, if we construct Hamiltonians out of operators  $A$  and  $B$ , then each sector of (3.26) is the Hilbert space of a  $\mathbf{G}$ -symmetric spin-chain with symmetry-twisted boundary condition labeled by an element  $\mathbf{g}' \in \mathbf{G}$ . Thus the operator (3.25) measures the twisted boundary condition of a given spin-chain. From a  $1+1d$  spacetime point of view, it corresponds to having inserted a symmetry operator  $\mathcal{U}_{\mathbf{g}'}[\gamma]$  along the time direction which causes a twisted boundary condition and can be detected by  $\mathcal{T}_{\alpha}$ .

Using elements of  $\mathbb{SOA}[\mathbf{G}]$ , we can now write any  $\mathbf{G}$ -symmetric spin-chain Hamiltonian in the schematic form

$$H[\{t_{\mathbf{d}}\}] = \sum_{\mathbf{d}} \sum_{\ell} t_{\mathbf{d}}(\ell) \mathcal{K}_{\mathbf{d}}(\ell) + \text{h.c.}, \quad (3.31)$$

where  $\mathcal{K}_{\mathbf{d}}(\ell)$  is some product of string operators  $S_{d_1} \cdots S_{d_n}$  on an interval of length  $\ell$  on the lattice,  $\mathbf{d} \equiv (d_1, \dots, d_n)$  denotes a collection of dyons, and  $t_{\mathbf{d}}(\ell) \in \mathbb{C}$  are coupling constants of the theory. This can also be written in terms of operators  $A$  and  $B$  defined in (3.27). This Hamiltonian is block-diagonal with respect to the decomposition (3.26),

$$H = \bigoplus_{\mathbf{g}' \in \mathbf{G}} H_{\mathbf{g}'} = \begin{pmatrix} H_{\mathbf{g}'_1} & & \\ & H_{\mathbf{g}'_2} & \\ & & \ddots \end{pmatrix}, \quad (3.32)$$

where  $H_{\mathbf{g}'}$  corresponds to a spin chain with the symmetry-twisted boundary condition  $\mathbf{g}' \in \mathbf{G}$ . For example in the case of  $\mathbf{G} = \mathbb{Z}_2 = \{0, 1\}$ ,  $H_{\mathbf{g}'=0}$  and  $H_{\mathbf{g}'=1}$  corresponds to periodic and anti-periodic boundary conditions (3.30), respectively. The full decomposition

<sup>11</sup>Note that we are using additive notation for  $\alpha \in \text{Rep}(\mathbf{G})$  since for the case of groups we are considering, finite Abelian groups, we have  $\text{Rep}(\mathbf{G}) \simeq \mathbf{G}$ . Therefore, the operator  $\mathcal{O}_{-\alpha,i+1}$  is labeled by an element  $-\alpha \in \text{Rep}(\mathbf{G})$ . For example, consider the group  $\mathbb{Z}_4 = \{0, 1, 2, 3\}$ . Then,  $-1 \sim 3$  since everything is defined modulo 4.



(3.16) is obtained by further decomposing into eigenspaces of the symmetry operator (3.24)

$$H_{\mathbf{g}'} = \bigoplus_{\alpha' \in \text{Rep}(\mathbf{G})} H_{(\mathbf{g}', \alpha')} = \begin{pmatrix} H_{(\mathbf{g}', \alpha'_1)} & & \\ & H_{(\mathbf{g}', \alpha'_2)} & \\ & & \ddots \end{pmatrix}. \quad (3.33)$$

Now for each anyonic charge  $d' \in \mathcal{A}$ , there is a sector  $H_{d'=(\mathbf{g}', \alpha')} = P_{\alpha'} H_{\mathbf{g}'} P_{\alpha'} = H_{\mathbf{g}'} P_{\alpha'}$  corresponding to a symmetry sector labeled by  $\alpha' \in \text{Rep}(\mathbf{G})$  and a symmetry-twisted boundary condition labeled by  $\mathbf{g}' \in \mathbf{G}$ . We have defined the projection operator into a symmetry sector  $\alpha$  by

$$P_{\alpha} \equiv \frac{1}{|\mathbf{G}|} \sum_{\mathbf{h} \in \mathbf{G}} R_{\alpha}^{-1}(\mathbf{h}) \mathcal{U}_{\mathbf{h}}. \quad (3.34)$$

Note that we have identified  $\Gamma_{(\mathbf{g}, 0)}$  as boundary symmetries while  $\Gamma_{(0, \alpha)}$  corresponded to operators related to symmetry-twisted boundary conditions. We could have done it the other way around, this is related to the existence of so-called electric-magnetic dualities that we will discuss shortly. The reader might also wonder why we do not think of both of these as boundary symmetries, this is related to 't Hooft anomaly between these lines. These anomalies also play a related role when considering gapped boundary conditions, as they serve as obstruction to condensing certain anyons simultaneously. We will discuss this point in the following section.

### 3.4 Gapped boundaries as gapped phases

So far, we have argued that the space of boundary conditions of a bulk topological gauge theory with gauge group  $\mathbf{G}$  in 2+1 dimensions is equivalent to the space of  $\mathbf{G}$ -symmetric quantum systems in 1+1 dimensions. We can further ask what this correspondence can tell us about  $\mathbf{G}$ -symmetric theories. To answer this question, we remind the reader that the possible gapped boundary conditions of a topological gauge theory with the gauge group  $\mathbf{G}$  has been classified and correspond to so-called Lagrangian subgroups of  $\mathcal{A}$ . These are maximal subsets<sup>12</sup>  $\mathcal{L} \subset \mathcal{A}$  of bulk line operators (anyons) that can simultaneously be condensed on the boundary [141–143]. Physically, the subgroup  $\mathcal{L}$  corresponds to the largest possible subsets of anyons that satisfy: 1) they are all bosons and 2) they all have trivial mutual braiding with each other. Another interesting point of view is that  $\mathcal{L}$  are maximal 1-form subgroups of  $\mathcal{A}$  with vanishing 't Hooft anomalies (3.5) and (3.6). This means that there is no obstruction to condensing those anyons simultaneously [104, 144]. This in turn gives a classification of possible gapped phases of  $\mathbf{G}$ -symmetric quantum theories at the boundary. The classification of gapped boundaries is therefore equivalent to the classification of Lagrangian subgroups. This classification for a topological gauge theory with the gauge group  $\mathbf{G}$  is given by the tuple  $(\mathbf{H}, \psi)$  where [145, 146]

$$\mathbf{H} \subset \mathbf{G}, \quad [\psi] \in H^2(\mathbf{H}, \mathbf{U}(1)). \quad (3.35)$$

Physically, a pair  $(\mathbf{H}, \psi)$  labelling a gapped boundary condition corresponds to a gapped phase where the  $\mathbf{G}$  symmetry has been spontaneously broken to a subgroup  $\mathbf{H}$  but with a

---

<sup>12</sup>We have used the same symbol for Lagrangian subgroups and the space of local operators in Section 2.2. These should not be confused with each other.

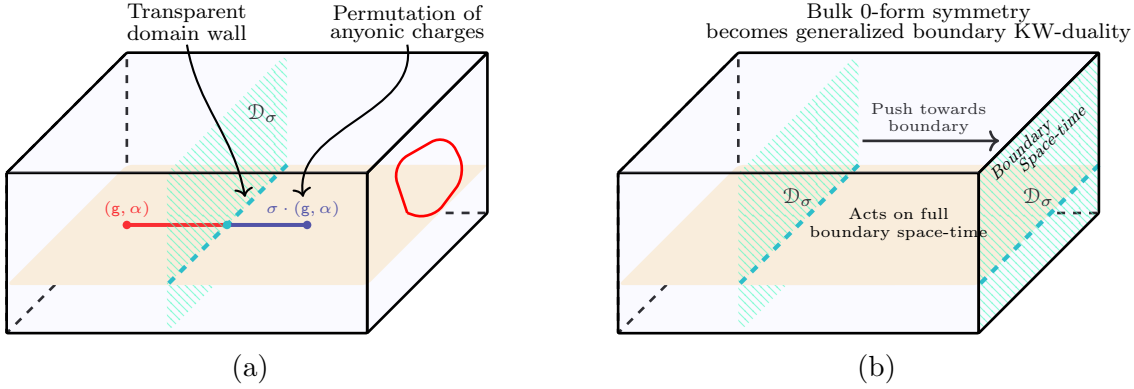


Figure 6: Illustration of the  $2 + 1d$  spacetime with a boundary  $1 + 1d$  spacetime. The green hatched surface corresponds to a 0-form bulk symmetry  $\mathcal{D}_\sigma[\Sigma]$ ,  $\sigma \in \mathcal{G}[\mathbf{G}]$ , known as anyonic symmetry. **(a)** When a 1-form symmetry is brought to the boundary, it becomes a topological line operator of a  $1 + 1d$  theory and thus a 0-form symmetry. Furthermore when the bulk symmetry surface  $\Sigma$  is oriented along time, it splits space-time into two regions and functions as a transparent domain wall. The domain wall is transparent to a line operator  $\mathcal{W}_{(\mathbf{g}, \alpha)}[\gamma]$  as it can penetrate through, although with the cost of transforming its charge to  $(\mathbf{g}', \alpha') = \sigma \cdot (\mathbf{g}, \alpha)$ . **(b)** When the 0-form symmetry surface is brought to a boundary, it acts on the full boundary spacetime as a duality transformation.

possible SPT twist encoded in the 2-cocycle  $\psi$ . This is consistent with previously known classifications of  $1 + 1$  dimensional  $\mathbf{G}$ -symmetric phases using tensor-network methods [65, 147–149]. Given a Lagrangian subgroup  $\mathcal{L}$ , one can construct a boundary Hamiltonian which only includes the operators  $S_d$  where  $d \in \mathcal{L}$

$$H_{\mathcal{L}} = - \sum_{d \in \mathcal{L}} \sum_i S_d(i, i+1). \quad (3.36)$$

Due to the trivial mutual braiding between any pair of operators in  $\mathcal{L}$ , all terms in this Hamiltonian commute, therefore such a Hamiltonian is a *fixed-point Hamiltonian*. The ground states are in the simultaneous  $+1$  eigenspace of the all operators  $S_d$  labeled by anyons  $d \in \mathcal{L}$ . Additionally  $S_d$  for any  $d \notin \mathcal{L}$ , does not commute with at least some subset of operators in the Hamiltonian (3.36). As a consequence, the expectation values of string operators  $S_d$  are given by

$$\langle S_d \rangle_{\text{GS}} = \begin{cases} 1, & \text{if } d \in \mathcal{L}, \\ 0, & \text{if } d \notin \mathcal{L}. \end{cases} \quad (3.37)$$

Equivalently, anyons in  $\mathcal{L}$  are condensed (i.e. they become part of the ground-state of the system at the boundary) while those outside this set are confined and form the excitations at the boundary. Furthermore, this construction gives us the order parameters corresponding to each gapped  $\mathbf{G}$ -symmetric phase [65, 149, 150]. These order parameters naturally play an essential role in identifying the tuple  $(\mathbf{H}, \psi)$  corresponding to each Lagrangian subgroup  $\mathcal{L}$  as described later in Sec. 4.1.

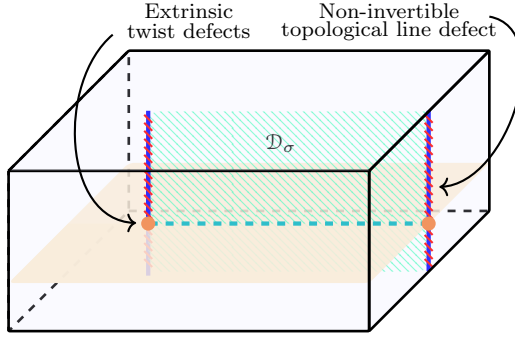


Figure 7: When the edge of the surface is brought the boundary, its shadow will be a topological line operator on the boundary. However, these line operators will be non-invertible, as boundary operators alone cannot annihilate them.

To avoid confusion, let us clarify what we mean by the notion of  $G$ -symmetric gapped phase. We define a gapped phase as follows: any two gapped  $G$ -symmetric Hamiltonians connected by a continuous  $G$ -symmetric gapped path is said to belong to the same phase<sup>13</sup>. In other words, each topologically-connected component of the space of all gapped  $G$ -symmetric Hamiltonians is a distinct gapped phase. The Lagrangian subgroups discussed above correspond to these phases. Specific  $G$ -symmetric Hamiltonians might have more symmetries and structures beyond  $G$ , for example, it might have global  $U(1)$  symmetry. From a physical point of view, there might exist phases related to the spontaneous-breaking of  $U(1)$  symmetry without affecting the  $G$ -symmetry. Such phases might correspond to the same Lagrangian subgroups as they might be connected through a  $G$ -symmetric gapped path that explicitly breaks  $U(1)$  symmetry (see Figure 8). In order to distinguish those phases, one has to look at the space of  $G \times U(1)$ -symmetric theories and appropriately modify the definition of “gapped phase” [144].

<sup>13</sup>By a  $G$ -symmetric path, we mean a deformation of the Hamiltonian in a given gapped phase by a family of Hamiltonians depending on a set of parameters. As we change the parameters, the corresponding Hamiltonian changes producing a path in the space of  $G$ -symmetric Hamiltonians.

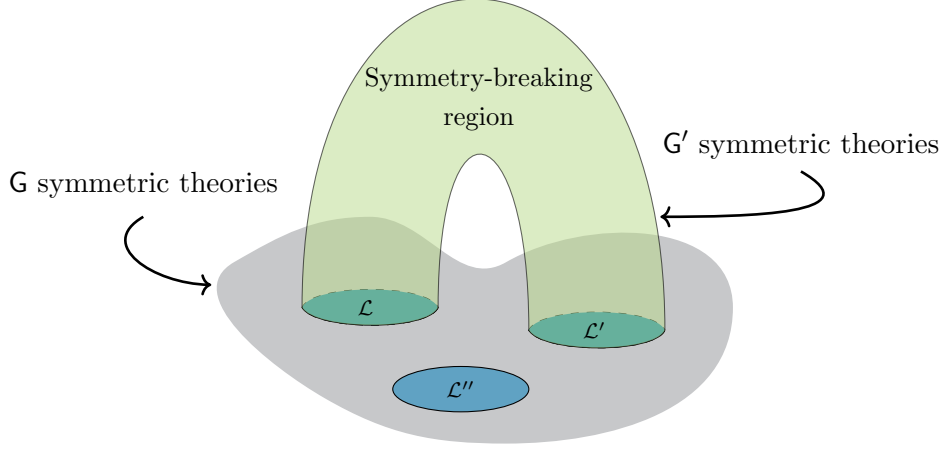


Figure 8: The grey surface corresponds to the space of  $G$  symmetric theories, while the regions  $\mathcal{L}$ ,  $\mathcal{L}'$  and  $\mathcal{L}''$  are three different gapped phases. These phases are considered different, only if  $G$ -symmetry is preserved. However, if we allow perturbations that break the symmetry down to a subgroup  $G' \subset G$ , the space of theories will get enlarged. Now it might be possible to connect two previously different phases  $\mathcal{L}$  and  $\mathcal{L}'$  through a symmetry-breaking region (which one might call a symmetry-breaking “wormhole”). In such a scenario,  $\mathcal{L}$  and  $\mathcal{L}'$  are the same phase in the space of  $G'$ -symmetric theories. The notion of gapped phase therefore depends on the space of theories under consideration.

### 3.5 From bulk symmetries to boundary dualities

We have seen how line operators (or 1-form symmetries) in the bulk of a  $2+1d$  topologically ordered system, corresponds to (0-form) global symmetries of  $1+1d$  quantum systems. One could wonder about the 0-form (anyonic) symmetries  $\mathcal{G}[G]$  present in the bulk of a  $2+1d$  topological phase, and naturally ask what do they represent in the space of  $G$ -symmetric  $1+1d$  theories? This symmetry group is a subgroup  $\mathcal{G}[G] \subset S_{|\mathcal{A}|}$  of the group of permutations  $S_{|\mathcal{A}|}$  of charges in  $\mathcal{A}$  satisfying

$$\mathcal{G}[G] = \{ \sigma \in S_{|\mathcal{A}|} \mid S_{\sigma(d), \sigma(d')} = S_{dd'} \text{ and } T_{\sigma(d), \sigma(d')} = T_{dd'} \}, \quad (3.38)$$

where  $S$  and  $T$  are defined as in (3.7). In other words, these are all possible ways of permuting charges while preserving all topological properties like fusion rules and braiding statistics. We denote elements in  $\mathcal{G}[G]$  by  $\mathcal{D}_\sigma$ . In particular, for the case of Abelian topological gauge theories, the group of 0-form symmetries  $\mathcal{G}[G]$  for any generic finite Abelian group  $G = \prod_{i=1}^n \mathbb{Z}_{N_i}$  are generated by three kinds of symmetry operations [151–153]

1. *Universal kinematical symmetries:* These are induced from the automorphisms of the group  $G$ . For every automorphism  $\varphi : G \rightarrow G$ , one obtains a 0-form symmetry  $\sigma_\varphi : \mathcal{A} \rightarrow \mathcal{A}$  in  $\mathcal{G}[G]$ , which acts on a dyon  $d = (g, \alpha) \in \mathcal{A}$  as

$$\sigma_\varphi : (g, \alpha) \rightarrow (\varphi(g), (\varphi^{-1})^*(\alpha)), \quad (3.39)$$

where  $\varphi^* : \text{Rep}(\mathbf{G}) \rightarrow \text{Rep}(\mathbf{G})$  defined as  $[\varphi^* \mathbf{R}_\alpha](\mathbf{g}) \equiv \mathbf{R}_\alpha(\varphi(\mathbf{g}))$ . This thus maps  $\alpha \in \text{Rep}(\mathbf{G})$  to some other  $\alpha' \in \text{Rep}(\mathbf{G})$ .

2. *Universal dynamical symmetries*: These correspond to elements in  $H^2(\mathbf{G}, \mathbf{U}(1))$ , where for  $\mathbf{G}$  is of the form (2.8). The corresponding cohomology group is

$$H^2(\mathbf{G}, \mathbf{U}(1)) = \prod_{i < j} \mathbb{Z}_{\text{gcd}(N_i, N_j)}. \quad (3.40)$$

For each cohomology class, there is an associated alternating bicharacter<sup>14</sup>

$$\mathbf{c}_\ell(\mathbf{g}, \mathbf{h}) = \exp \left\{ 2\pi i \sum_{i,j} \frac{\ell_{ij} \mathbf{g}_i \mathbf{h}_j}{\text{gcd}(N_i, N_j)} \right\}, \quad (3.41)$$

with  $\ell_{ij} = -\ell_{ji}$  and  $\mathbf{g} = (\mathbf{g}_1, \dots, \mathbf{g}_n)$ , and  $\mathbf{h} = (\mathbf{h}_1, \dots, \mathbf{h}_n)$ . Given such a bicharacter, one obtains a 0-form symmetry  $\sigma_\mathbf{c}$  which maps the dyon  $d = (\mathbf{g}, \alpha)$  as

$$\sigma_\mathbf{c} : (\mathbf{g}, \alpha) \mapsto (\mathbf{g}, \alpha_\mathbf{g}^\mathbf{c}), \quad (3.42)$$

where the transformed representation  $\alpha_\mathbf{g}^\mathbf{c}$  has the form  $\mathbf{R}_{\alpha_\mathbf{g}^\mathbf{c}}(\cdot) = \mathbf{R}_\alpha(\cdot) \mathbf{c}_\ell(\mathbf{g}, \cdot)$ .

3. *Partial electric-magnetic dualities*: These correspond to performing an electric-magnetic duality on a given factor  $\mathbb{Z}_{N_j}$  in  $\mathbf{G}$ . Concretely, an electric-magnetic duality acting on the  $j^{\text{th}}$  factor transforms the dyons  $d \in \mathcal{A}$  as

$$\sigma_j : \begin{aligned} (\mathbf{g}_1, \dots, \mathbf{g}_{j-1}, \mathbf{g}_j, \mathbf{g}_{j+1}, \dots, \mathbf{g}_n) &\mapsto (\mathbf{g}_1, \dots, \mathbf{g}_{j-1}, \alpha_j, \mathbf{g}_{j+1}, \dots, \mathbf{g}_n), \\ (\alpha_1, \dots, \alpha_{j-1}, \alpha_j, \alpha_{j+1}, \dots, \alpha_n) &\mapsto (\alpha_1, \dots, \alpha_{j-1}, \mathbf{g}_j, \alpha_{j+1}, \dots, \alpha_n). \end{aligned} \quad (3.43)$$

Since the 0-form symmetry group  $\mathcal{G}[\mathbf{G}]$  acts on the 1-form symmetries  $\mathcal{A}$ , the combined symmetry structure forms a 2-group structure. Note that even though  $\mathbf{G}$  and  $\mathcal{A}$  are Abelian, the group  $\mathcal{G}[\mathbf{G}]$  can be non-Abelian.

Since elements in  $\mathcal{G}[\mathbf{G}]$  are standard symmetries in  $2 + 1d$ , they are defined on  $2d$  surfaces. When  $\mathcal{D}_\sigma[\Sigma]$  is put on a time slice as in Figure 4b, they act on the Hilbert space by permuting anyons as shown. However, we can orient the surface in different ways. For example, when it is oriented as in Figure 6a, it splits the space into two regions and corresponds to a domain wall. Whenever a string operator crosses such a domain wall, it is transformed according to the corresponding anyonic symmetry. For this reason, these domain walls are called transparent domain walls [154]. These are also called invertible domain walls. The set of all possible gapped domain walls between a topological order and itself can be found using Lagrangian subgroups, with the help of the folding trick [143]. Only a subset of these are transparent.

Now, if we push the surface towards the boundary as in Figure 6b, we end up with a new kind of object from the boundary point of view. The surface now acts on the entire space-time, thus acts on the full boundary theory and can in principle change it to a completely

<sup>14</sup>An alternating bicharacter is a group homomorphism  $\mathbf{c} : \mathbf{G} \times \mathbf{G} \rightarrow \mathbb{C}^*$  in both arguments which satisfies the property  $\mathbf{c}(\mathbf{g}, \mathbf{g}) = 1$  for all  $\mathbf{g} \in \mathbf{G}$  [153].

different theory. In other words, 0-form symmetries in  $2 + 1d$  corresponds to dualities between different  $1 + 1d$  theories. It is natural to call these  $(-1)$ -form symmetry operators (see also [155]).

It is instructive to reinterpret this spacetime logic from a spatial Hamiltonian/Hilbert space level. On a fixed-time slice, domain wall in Figure 6a corresponds to a line-like domain wall with the property

$$\begin{array}{c} \mathcal{W}_{(\mathbf{g}, \alpha)} \quad \mathcal{D}_\sigma \quad \mathcal{W}_{\sigma \cdot (\mathbf{g}, \alpha)} \\ \text{---} \text{---} \text{---} \end{array} \quad (3.44)$$

This is the standard view of transparent domain walls in the topological order literature [136–139, 154]. However, if we bring this domain wall to the boundary as in Figure 6b, then we see that

$$\begin{array}{c} \text{---} \end{array} \rightarrow \begin{array}{c} \text{---} \end{array} \rightarrow \begin{array}{c} \text{---} \end{array}, \quad (3.45)$$

i.e. boundary operators maps to other boundary operators

$$S_d(a, b) \mapsto \hat{\mathcal{D}}_\sigma \cdot S_d(a, b) \equiv S_{\sigma \cdot d}(a, b). \quad (3.46)$$

This action has the following properties

$$\begin{aligned} \hat{\mathcal{D}}_\sigma \cdot \mathbb{I} &= \mathbb{I}, \\ \left( \hat{\mathcal{D}}_\sigma \cdot S_d(a, b) \right)^\dagger &= \hat{\mathcal{D}}_\sigma \cdot S_d(a, b)^\dagger, \\ \hat{\mathcal{D}}_\sigma \cdot \sum_{i=1}^n c_i S_{d_i}(a_i, b_i) &= \sum_{i=1}^n c_i \hat{\mathcal{D}}_\sigma \cdot S_{d_i}(a_i, b_i), \\ \hat{\mathcal{D}}_\sigma \cdot \prod_{i=1}^n S_{d_i}(a_i, b_i) &= \prod_{i=1}^n \hat{\mathcal{D}}_\sigma \cdot S_{d_i}(a_i, b_i), \end{aligned} \quad (3.47)$$

where  $c_i$ s are constants. These imply that the map  $\hat{\mathcal{D}}_\sigma : \text{SOA}[\mathbf{G}] \mapsto \text{SOA}[\mathbf{G}]$  is an algebra homomorphism. Furthermore, since it just permutes the generators of  $\text{SOA}[\mathbf{G}]$  (3.46) while preserving (3.5) and (3.6), it is a non-trivial automorphism of the algebra of boundary operators  $\text{SOA}[\mathbf{G}]$ . It is useful to also consider how such dualities act on states by assuming the existence of a unitary operator on the Hilbert space with the property

$$U_\sigma S_d(a, b) U_\sigma^\dagger = \hat{\mathcal{D}}_\sigma \cdot S_d(a, b) = S_{\sigma \cdot d}(a, b). \quad (3.48)$$

The existence of such unitary operator is guaranteed according to Theorem 3.3 of [156]. Here  $\text{SOA}[\mathbf{G}]$  corresponds to our *bond algebra*. Note that all dualities we are discussing here are called self-dualities in the terminology of [156], since we are using a bond algebra large enough to contain any  $\mathbf{G}$ -symmetric spin-chain Hamiltonian. We will briefly discuss action of dualities on non-symmetric theories in Section 3.7.

The unitary map preserves the trivial sector in (3.23) (see Appendix A). From (3.44) and (3.18), it then follows that the non-contractible operators transform according to

$$U_\sigma \Gamma_d U_\sigma^\dagger = \Gamma_{\sigma \cdot d}, \quad U_\sigma \mathcal{Y}_{d'} U_\sigma^\dagger = \mathcal{Y}_{\sigma \cdot d'}. \quad (3.49)$$

In particular, when combined with (3.23), we see that the duality permutes the superselection sectors non-trivially

$$U_\sigma : \mathcal{H}_{d'} \mapsto \mathcal{H}_{\sigma \cdot d'}, \quad (3.50)$$

the same way as anyons are permuted. On the level of the sectors of the String Operator Algebra we thus have

$$\widehat{\mathcal{D}}_\sigma \cdot \text{SOA}[\mathbf{G}] = \bigoplus_{d' \in \mathcal{A}} U_\sigma \text{SOA}_{d'}[\mathbf{G}] U_\sigma^\dagger = \bigoplus_{d' \in \mathcal{A}} \text{SOA}_{\sigma \cdot d'}[\mathbf{G}]. \quad (3.51)$$

Taking the transformation (3.49) together with the identifications (3.24) and (3.25), we see that symmetry sectors and boundary conditions get non-trivially mixed under these dualities. For example we have that the symmetry operator  $\mathcal{U}_{\mathbf{g}}$  (3.24) maps to  $\mathcal{U}_{\mathbf{g}^\vee} \mathcal{T}_{\alpha^\vee}$  where  $(\mathbf{g}^\vee, \alpha^\vee) = \sigma \cdot (\mathbf{g}, 0)$ . This is an alternate way of stating (3.50).

As a simple example consider the electric-magnetic duality  $\sigma \cdot (\mathbf{g}, \alpha) = (\alpha, \mathbf{g})$  which exists for any finite Abelian group  $\mathbf{G}$ . Under this duality  $\mathcal{U}_{\mathbf{g}}$  and  $\mathcal{T}_\alpha$  are swapped (see equation (3.49)). Transforming both states and operators, we find the following relation between matrix elements

$$\langle \mathbf{g}', \alpha' | \mathcal{U}_{\mathbf{g}} | \mathbf{g}'', \alpha'' \rangle = \langle \alpha', \mathbf{g}' | \mathcal{T}_{\alpha=\mathbf{g}} | \alpha'', \mathbf{g}'' \rangle. \quad (3.52)$$

In the simplest case of  $\mathbf{G} = \mathbb{Z}_2$ , this relation can be checked explicitly using

$$\begin{aligned} \mathcal{U} &= \begin{matrix} & |0,0\rangle & |0,1\rangle & |1,0\rangle & |1,1\rangle \\ \begin{matrix} \langle 0,0| \\ \langle 0,1| \\ \langle 1,0| \\ \langle 1,1| \end{matrix} & \begin{pmatrix} +\mathbb{I} & 0 & 0 & 0 \\ 0 & -\mathbb{I} & 0 & 0 \\ 0 & 0 & +\mathbb{I} & 0 \\ 0 & 0 & 0 & -\mathbb{I} \end{pmatrix} \end{matrix}, \\ \mathcal{T} &= \begin{matrix} & |0,0\rangle & |0,1\rangle & |1,0\rangle & |1,1\rangle \\ \begin{matrix} \langle 0,0| \\ \langle 0,1| \\ \langle 1,0| \\ \langle 1,1| \end{matrix} & \begin{pmatrix} +\mathbb{I} & 0 & 0 & 0 \\ 0 & +\mathbb{I} & 0 & 0 \\ 0 & 0 & -\mathbb{I} & 0 \\ 0 & 0 & 0 & -\mathbb{I} \end{pmatrix} \end{matrix}. \end{aligned} \quad (3.53)$$

The upper two blocks correspond to a periodic  $\mathbb{Z}_2$ -symmetric spin chain in the even and odd symmetry sectors. Similarly, the lower two blocks correspond to an anti-periodic spin chain.

### 3.6 Action of dualities on Hamiltonians

We have seen that how 0-form symmetries in the bulk act on the boundary Hilbert space, we can now turn to their actions on Hamiltonians. We will see that bulk 0-form symmetries become dualities in the space of  $\mathbf{G}$ -symmetries theories. As discussed above, any



G-symmetric Hamiltonian  $H$  in  $1 + 1d$  is constructed out of boundary operators  $S_d(a, b)$ , defined in (3.31), and hence is an element of  $\mathbb{SOA}[\mathbb{G}]$ . Bringing the domain wall  $\mathcal{D}_\sigma[\Sigma]$  to the boundary will therefore map  $H$  to a dual Hamiltonian

$$H \longrightarrow H^\vee \equiv \widehat{\mathcal{D}}_\sigma \cdot H = U_\sigma H U_\sigma^\dagger, \quad (3.54)$$

where in the second equality, we have used the fact that duality symmetry could be represented by a unitary operator  $U_\sigma$  acting on the Hilbert space (see Section 3.5). More precisely, the action on a generic Hamiltonian of the form (3.31) becomes

$$\begin{aligned} H^\vee[\{t_{\mathbf{d}}\}] &= \sum_{\mathbf{d}} \sum_{\ell} t_{\mathbf{d}}(\ell) \left[ \widehat{\mathcal{D}}_\sigma \cdot \mathcal{K}_{\mathbf{d}}(\ell) \right] + \text{h.c.}, \\ &= \sum_{\mathbf{d}} \sum_{\ell} t_{\mathbf{d}}(\ell) \mathcal{K}_{\sigma \cdot \mathbf{d}}(\ell) + \text{h.c.}, \\ &= \sum_{\mathbf{d}} \sum_{\ell} t_{\sigma^{-1} \cdot \mathbf{d}}(\ell) \mathcal{K}_{\mathbf{d}}(\ell) + \text{h.c.} \\ &= H[\{t_{\sigma^{-1} \cdot \mathbf{d}}\}], \end{aligned} \quad (3.55)$$

where of course  $U_\sigma \mathcal{K}_{\mathbf{d}} U_\sigma^\dagger = U_\sigma S_{d_1} \dots S_{d_n} U_\sigma^\dagger = S_{\sigma \cdot d_1} \dots S_{\sigma \cdot d_n} = \mathcal{K}_{\sigma \cdot \mathbf{d}}$ , which is the consequence of a nontrivial action of dualities on global sectors, as given in (3.50). In other words, the duality acts on coupling constants and permutes twisted sectors as

$$H_{(\mathbf{g}, \alpha)}^\vee[\{t_{\mathbf{d}}\}] = H_{\sigma \cdot (\mathbf{g}, \alpha)}[\{t_{\sigma^{-1} \cdot \mathbf{d}}\}]. \quad (3.56)$$

Since the Hamiltonians are related by a unitary map (3.54), their energy spectra are preserved up to a permutation of sectors

$$E_n^{(\mathbf{g}, \alpha)}[\{t_{\mathbf{d}}\}] = E_n^{\sigma \cdot (\mathbf{g}, \alpha)}[\{t_{\sigma^{-1} \cdot \mathbf{d}}\}], \quad (3.57)$$

where  $n$  labels the eigenvalues.

Furthermore, correlation functions of symmetric operators also transform naturally under the action of duality. Consider a correlation function of the following kind

$$\langle S_{d_1}(\ell_1) S_{d_2}(\ell_2) \dots \rangle_{\beta, H_d} := \text{tr}_{\mathcal{H}} \left[ S_{d_1}(\ell_1) S_{d_2}(\ell_2) \dots e^{-\beta H_{\mathbb{E}}} P_\alpha \right], \quad (3.58)$$

where  $S_d(\ell)$  is the boundary operator obtained from a topological line operator labelled by  $d$  of length  $\ell$ . Since the dyonic labels  $d \in \mathcal{A}$  transform under duality, one obtains a dual correlation function with an equivalent expectation value

$$\langle S_{d_1} S_{d_2} \dots \rangle_{\beta, H_d} = \langle S_{\sigma(d_1)} S_{\sigma(d_2)} \dots \rangle_{\beta, H_d^\vee} \quad (3.59)$$

In this paper, we will show how these dualities are powerful tools to constrain and determine portions of the phase diagrams and compute exact conformal spectra of many non-trivial phase transitions.

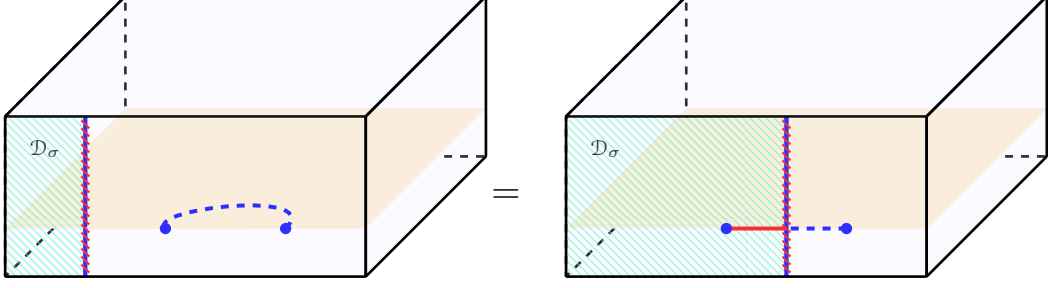


Figure 9: Duality  $\mathcal{D}_\sigma$  acting on part of boundary. When dragged over local non-symmetric operators,  $\mathcal{O}_{\alpha,i}$ , the duality becomes non-local. The edge of the duality region can become a (possibly non-invertible) symmetry of the boundary, for boundaries that are self-dual under  $\sigma$ .

### 3.7 Action of dualities on non-symmetric theories

We have so far considered the action of dualities on the space of  $G$ -symmetric Hamiltonians which are constructed out of string operator algebra  $\text{SOA}[G]$ . This is a subalgebra of the algebra of all linear operators  $\mathcal{L}(\mathcal{H})$  on a Hilbert space  $\mathcal{H}$ , as discussed in Section 2.2. On the Hilbert space of the spin chain, string operators with charge  $d = (0, \alpha)$  are given by

$$S_{(0,\alpha)}(\ell) = \mathcal{O}_{\alpha,i} \mathcal{O}_{-\alpha,j}, \quad (3.60)$$

where  $i$  and  $j$  are the endpoints of the interval  $\ell$ . These operators are symmetric and belong to  $\text{SOA}[G]$ . However,  $\mathcal{O}_{\alpha,i}$  itself is not symmetric and hence does not belong to  $\text{SOA}[G]$ , but it belongs to  $\mathcal{L}(\mathcal{H})$ . When a duality acts on  $\text{SOA}[G]$ , it is local. By this, we mean that the support of symmetric operators (for example the interval  $\ell$  in (3.60)) are preserved under duality. Due to this property,  $G$ -symmetric local Hamiltonians are mapped to dual local Hamiltonians, which are also  $G$ -symmetric.

However, nothing prevents us to act with duality on the space of all operators  $\mathcal{L}(\mathcal{H})$ . However, it turns out that the mapping of non-symmetric operators becomes non-local. In order to see this, first notice that under a duality  $\sigma$ ,  $S_{(0,\alpha)}(\ell) = \mathcal{O}_{\alpha,i} \mathcal{O}_{-\alpha,j}$  is mapped to  $S_{\sigma \cdot (0,\alpha)}(\ell)$ . Now consider acting duality on part of spacetime boundary. We see that when the boundary  $\partial\Sigma$  of a duality domain wall  $\mathcal{D}_\sigma[\Sigma]$  is moved across a non-symmetric operator, we find the following relation (see also Figure 9)

$$\begin{array}{c} \mathcal{O}_{-\alpha,j} \quad \mathcal{O}_{\alpha,i} \\ \bullet \quad \bullet \\ \text{---} \text{---} \text{---} S_{(0,\alpha)} \text{---} \text{---} \text{---} \\ \text{---} \text{---} \text{---} \sigma \text{---} \text{---} \text{---} \end{array} = \begin{array}{c} \mathcal{O}_{-\alpha,j} \quad S_{\sigma \cdot (0,\alpha)} \\ \bullet \quad \bullet \\ \text{---} \text{---} \text{---} S_{(0,\alpha)} \text{---} \text{---} \text{---} \\ \text{---} \text{---} \text{---} \sigma \text{---} \text{---} \text{---} \end{array} . \quad (3.61)$$

In other words, as a duality wall is dragged over a local operator, a non-local operator emerges. If the  $1d$  quantum spin chain was infinitely long, we could drag  $\mathcal{O}_{j,-\alpha}$  to  $j \rightarrow -\infty$  and the non-symmetric local operator would be mapped to an operator with infinite





theories. These insights will be used in section 5 to apply Topological Holography to the study of concrete spin chains with various symmetry groups.

The elements of the duality group  $\mathcal{G}[\mathbf{G}]$  are by definition automorphisms of  $\text{SOA}[\mathbf{G}]$  and thus preserve the properties of the local operator algebra. The action of these dualities on Hamiltonians, as described in (3.46) and (3.54), will therefore give rise to dual Hamiltonians with similar properties. In particular, the behavior of correlation functions such as exponential and algebraic decay in gapped and critical systems, respectively, are preserved under the duality mapping. Therefore, if  $H$  is gapped or gapless then  $H^\vee$  will be also be gapped or gapless, respectively. However, the duality can act non-trivially on global symmetry properties such as symmetry sectors of the Hilbert space and twisted boundary conditions. Therefore, certain aspects of the boundary theory described by  $H$  are not preserved. For example the partition function and hence the spectrum of the theory can change. We exploit this to compute the full spectra of conformal field theories describing the critical phenomena of several non-trivial phase transitions.

## 4.1 Gapped phases and web of dualities

The first question is how are gapped phases mapped to each other? Recall that gapped phases are classified by Lagrangian subgroups  $\mathcal{L} \subset \mathcal{A}$ , which are collections of charges  $d = (\mathbf{g}, \alpha) \in \mathcal{A}$  that simultaneously condense in that phase. The action of anyonic symmetries  $\sigma \in \mathcal{G}[\mathbf{G}]$  on anyonic charges can be lifted to sets of charges by acting elements-wise on each anyonic charge individually. Thus if  $\mathcal{L} = \{d_1, d_2, \dots\}$  then  $\sigma \cdot \mathcal{L} \equiv \{\sigma \cdot d_1, \sigma \cdot d_2, \dots\}$ . Note that acting on a Lagrangian subgroup

$$\mathcal{L} \longmapsto \mathcal{L}^\vee = \sigma \cdot \mathcal{L}, \quad (4.1)$$

gives rise to another set of anyonic charges  $\mathcal{L}^\vee$  which also satisfy the Lagrangian subgroup conditions as the action of  $\sigma$  (by definition (3.38)) preserves the braiding and fusion properties of anyons ((3.1), (3.5), and (3.6)). In other words, maximal non-anomalous subgroups of the 1-form symmetry  $\mathcal{A}$  (of the bulk topological order) are permuted amongst each other under the action of dualities. As discussed earlier, for each gapped phase we can write an exactly solvable fixed-point Hamiltonian (3.36). It then follows from (3.54) and (3.55) that the dualities in  $\mathcal{G}[\mathbf{G}]$  map fixed-point Hamiltonians in the gapped phase  $\mathcal{L}$  to a dual Hamiltonian which is the fixed-point Hamiltonian of the gapped phase  $\mathcal{L}^\vee = \sigma \cdot \mathcal{L}$

$$H_{\mathcal{L}} \longmapsto H_{\mathcal{L}}^\vee = \widehat{\mathcal{D}}_\sigma \cdot H_{\mathcal{L}} = H_{\mathcal{L}^\vee}. \quad (4.2)$$

However, how about a more generic non-fixed-point Hamiltonian  $H[\{t_{\mathbf{d}}\}]$  (3.31) that is  $\mathbf{G}$ -symmetric? By definition, each gapped phase is path-connected. This means that we can find a continuous one-parameter family  $H_{\mathcal{L}}(s)$ ,  $s \in [0, 1]$ , of Hamiltonians in the gapped phase  $\mathcal{L}$  where  $H_{\mathcal{L}}(0)$  is the fixed-point Hamiltonian and  $H_{\mathcal{L}}(1)$  is any arbitrary Hamiltonian in the same phase. After the duality transformation, the path  $H_{\mathcal{L}}^\vee(s) \equiv \widehat{\mathcal{D}}_\sigma \cdot H_{\mathcal{L}}(s)$  is still a continuous function of  $s$ . This can be seen as follows:  $H_{\mathcal{L}}(s)$  is a linear superposition of products of boundary operators  $S_{\mathbf{d}}(a, b)$  (3.31) where the coefficients  $\{t_{\mathbf{d}}(s)\}$  are continuous functions of  $s \in [0, 1]$ . The duality acts term-wise as in (3.55) and hence coefficients are merely permuted, i.e.  $t_{\mathbf{d}}(s)$  are replaced by  $t_{\sigma^{-1} \cdot \mathbf{d}}(s)$ , and thus are still continuous functions of  $s$ . Therefore, the path remains connected after the duality. Furthermore  $H_{\mathcal{L}}^\vee(s)$

is a one-parameter family of gapped Hamiltonians since duality maps gapped phases onto gapped phases. This means that there are no second-order phase transition along the path after duality. This however does not rule out the possibility of first-order transitions. Note that the duality is unitarily implementable (3.54) and preserves the spectrum (3.57) along the path. Therefore, there cannot be any level-crossing along the path after the duality since there were none before the duality by assumption. This consequently excludes first-order transitions along the path. Finally, it follows from (4.2) that  $H_{\mathcal{L}}^{\vee}(0)$  is a fixed-point Hamiltonian in  $\mathcal{L}^{\vee}$  because  $H_{\mathcal{L}}(0)$  is the fixed-point Hamiltonian in  $\mathcal{L}$ . From this argument, we can conclude that the whole path  $H_{\mathcal{L}}^{\vee}(s)$  is in  $\mathcal{L}^{\vee}$  as there is no phase transition along the path.

Note that if a generic Hamiltonian  $H[\{t_a\}]$  (3.31) is gapped, it must either be in a phase labelled by a Lagrangian subgroup  $\mathcal{L}$  or sits at a first-order transition and has ground-state degeneracies. We will see examples of this later. By gapped phase, we always exclude such first-order transitions.

We will call the group structure of a Lagrangian subgroup  $\mathcal{L}$  the *fusion structure* of the corresponding gapped phase. Following the discussion around (3.37), we can interpret this fusion structure as the algebra of order parameters for the gapped phase. From the same line of argument as above, we can see that the two Lagrangian subgroups  $\mathcal{L}$  and  $\mathcal{L}^{\vee} = \sigma \cdot \mathcal{L}$  must be isomorphic as groups. In other words, we can conclude that only gapped phases with the same fusion structure can be dual to each other. Both of these phases have  $G$ -symmetric Hamiltonians but the symmetry could be spontaneously broken to subgroups with different SPT twists  $(H_{\mathcal{L}}, \psi_{\mathcal{L}})$  and  $(H_{\mathcal{L}^{\vee}}, \psi_{\mathcal{L}^{\vee}})$ . This information can be derived out of  $\mathcal{L}$  and  $\mathcal{L}^{\vee}$  and thus depends on more than their group structure; it depends on their specific embedding inside  $\mathcal{A}$ .

Let us explain how to extract  $(H_{\mathcal{L}}, \psi_{\mathcal{L}})$  from the Lagrangian subgroup  $\mathcal{L}$ . Consider the lowest-energy eigen-state  $|\Psi_d^{(0)}\rangle$  of the fixed-point Hamiltonian  $H_{\mathcal{L}}$  in the super-selection sector  $d = (g, \alpha) \in \mathcal{A}$ . Now let us consider the action of a string operator  $S_{\bar{d}}(\ell)$  on the state  $|\Psi_d^{(0)}\rangle$  where  $\bar{d} = (\bar{g}, \bar{\alpha}) \in \mathcal{L}$ . Since  $\bar{d}$  is in the set of condensed dyons in the gapped phase labelled by  $\mathcal{L}$ , the true ground-state must satisfy

$$S_{\bar{d}}(\ell)|\Psi_d^{(0)}\rangle = R_{\bar{\alpha}}(g)R_{\alpha}(\bar{g})|\Psi_d^{(0)}\rangle \stackrel{!}{=} |\Psi_d^{(0)}\rangle, \quad \forall \bar{d} \in \mathcal{L}, \quad (4.3)$$

or in other words  $R_{\bar{\alpha}}(g)R_{\alpha}(\bar{g}) = 1$  (see (2.17) for the definition of  $R_{\alpha}(g)$ ). This implies that the true ground-states belong to the twisted sectors  $d \in \mathcal{L} \subset \mathcal{A}$ . Define the magnetic projector  $\Pi : \mathcal{A} \simeq G \times \text{Rep}(G) \rightarrow G$  given by  $\Pi(g, \alpha) = g$ . In the gapped phase  $\mathcal{L}$ , the symmetry has been spontaneously broken down to  $\Pi(\mathcal{L}) = H_{\mathcal{L}} \subset G$ . The ground-states are thus given by  $|\text{GS}_{h,\alpha}\rangle \equiv |\Psi_{h,\alpha}^{(0)}\rangle$  where  $(h, \alpha) \in \mathcal{L}$ . These correspond to the ground-state with symmetry-twisted boundary condition  $h \in H_{\mathcal{L}}$ . In order to compute the SPT twist  $\Psi_{\mathcal{L}}$ , consider the expectation value of the remaining-symmetry operators  $\mathcal{U}_{\bar{h}}$  for  $\bar{h} \in H$  in the ground-state

$$\langle \text{GS}_{h,\alpha} | \mathcal{U}_{\bar{h}} | \text{GS}_{h,\alpha} \rangle = R_{\alpha}(\bar{h}) = R_{\alpha}^{-1}(h). \quad (4.4)$$

The last equality follows from  $R_{\bar{\alpha}}(g)R_{\alpha}(\bar{g}) = 1$ . Let us define the  $U(1)$  phase

$$\psi_{\mathcal{L}}(h, \bar{h}) \equiv \langle \text{GS}_{h,\alpha} | \mathcal{U}_{\bar{h}} | \text{GS}_{h,\alpha} \rangle = R_{\alpha}(\bar{h}). \quad (4.5)$$

One can readily check that this satisfies the group 2-cocycle condition [42]. In fact, the cohomology class  $[\psi_{\mathcal{L}}]$  belongs to the second group-cohomology group  $H^2(\mathbf{H}, \mathbf{U}(1))$ , which characterizes the SPT phase  $\mathcal{L}$  [42, 48] and the phase (4.5) is the topological response when the model is coupled to a background  $\mathbf{H}$ -gauge field whose holonomy in the space and time directions are  $\bar{\mathbf{h}}$  and  $\mathbf{h}$  respectively. Since  $\mathbf{H}$  is finite and Abelian, it takes the general form  $\mathbf{H} = \prod_i \mathbb{Z}_{N_i}$  with the corresponding second cohomology group

$$H^2(\mathbf{H}, \mathbf{U}(1)) = \prod_{i < j} \mathbb{Z}_{\gcd(N_i, N_j)}. \quad (4.6)$$

Concretely, any such SPT is labeled by a list of integers  $p_{ij} \in \mathbb{Z}_{\gcd(N_i, N_j)}$ . These numbers can be extracted by comparing (4.5) with the following representative 2-cocycle

$$\psi(\mathbf{h}, \bar{\mathbf{h}}) = \exp \left( \sum_{i < j} \frac{2\pi i p_{ij}}{\gcd(N_i, N_j)} \mathbf{h}_i \bar{\mathbf{h}}_j \right). \quad (4.7)$$

From this, we see that non-trivial SPT phases appear when the condensed generators of  $\mathcal{L}$  are dyonic. The integers  $p_{ij}$  correspond to which magnetic and electric charges are combined to form the dyons condensed in  $\mathcal{L}$ .

Another important observation from our construction is that certain Hamiltonians can have non-trivial emergent symmetries. First let us define the stabilizer subgroup of a gapped phase

$$\text{Stab}(\mathcal{L}) \equiv \{ \sigma \in \mathcal{G}[\mathbf{G}] \mid \sigma \cdot \mathcal{L} = \mathcal{L} \}. \quad (4.8)$$

By construction, any gapped Hamiltonian  $H_{\mathcal{L}}[\{t_{\mathbf{d}}\}]$  maps to another Hamiltonian  $\widehat{\mathcal{D}}_{\sigma} \cdot H_{\mathcal{L}}[\{t_{\mathbf{d}}\}]$  in the same phase under dualities  $\sigma \in \text{Stab}(\mathcal{L})$ . However, there can exist points in a gapped phase  $\mathcal{L}$  that are self-dual

$$H[\{t_{\mathbf{d}}^*\}] = \widehat{\mathcal{D}}_{\sigma} \cdot H[\{t_{\mathbf{d}}\}], \quad (4.9)$$

for some  $\sigma \in \text{Stab}(\mathcal{L})$ . Such self-dual Hamiltonians will have emergent symmetries beyond the global  $\mathbf{G}$ -symmetry. These emergent symmetries can however be non-invertible and form a fusion category. They are edges of the duality walls coming from the bulk, related to twist defects, from the point of view of topological holography (see Figure 7). The largest such emergent symmetries happen at points that are self-dual under the full  $\text{Stab}(\mathcal{L})$ .

As a simple example, consider  $\mathbf{G} = \mathbb{Z}_2 \times \mathbb{Z}_4$  where we have

$$\mathcal{A} = \left\{ (\mathbf{g}_1, \mathbf{g}_2, \alpha_1, \alpha_2) \mid \mathbf{g}_1, \alpha_1 = 0, 1 \text{ and } \mathbf{g}_2, \alpha_2 = 0, 1, 2, 3 \right\}. \quad (4.10)$$

There are ten Lagrangian subgroups labeled as  $\mathcal{L}_1, \dots, \mathcal{L}_{10}$  (see Section 5 for details) with the following fusion structures

$$\mathcal{L}_1, \dots, \mathcal{L}_8 \simeq \mathbb{Z}_2 \times \mathbb{Z}_4, \quad \mathcal{L}_9, \mathcal{L}_{10} \simeq \mathbb{Z}_2 \times \mathbb{Z}_2 \times \mathbb{Z}_2. \quad (4.11)$$

Therefore, there are two different types of fusion structures. So there only exist dualities between the gapped phases in the set  $\{\mathcal{L}_1, \dots, \mathcal{L}_8\}$  and similarly between the ones in  $\{\mathcal{L}_9, \mathcal{L}_{10}\}$  but not between these sets. Beyond electric-magnetic dualities, there are other dualities mixing the  $\mathbb{Z}_2$  and  $\mathbb{Z}_4$  electric and magnetic charges. The duality group turns out



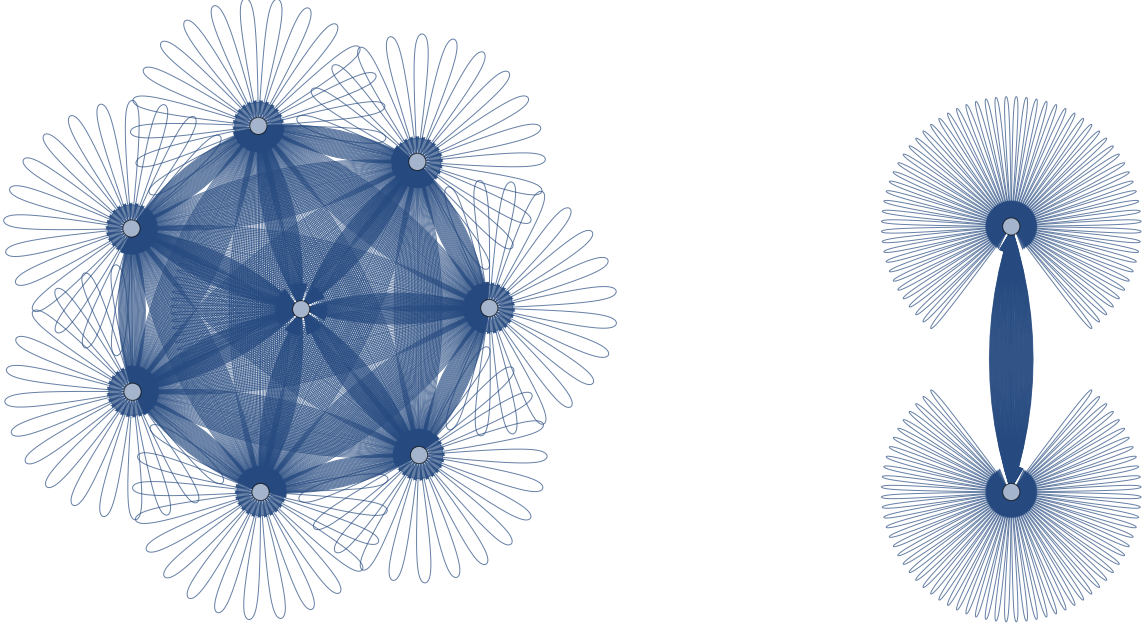


Figure 10: Web of dualities of  $G = \mathbb{Z}_2 \times \mathbb{Z}_4$ : each node corresponds to a gapped phase and each line depicts a duality transformation between these phases. The web of dualities has two connected components, corresponding to the two possible fusion structures for theories with  $G = \mathbb{Z}_2 \times \mathbb{Z}_4$  global symmetry.

to be  $\mathcal{G}[G] = (D_4 \times D_4) \rtimes \mathbb{Z}_2$ , which is a non-Abelian group of order 128. We can draw a *web of dualities* that shows how gapped phases are related by dualities. A web of dualities can be drawn as follows: represent each gapped phase by a node and for each  $\sigma \in \mathcal{G}[G]$  draw a line connecting gapped phases mapped under this duality. We have illustrated the web of dualities for  $G = \mathbb{Z}_2 \times \mathbb{Z}_4$  in Figure 10. As can be seen, the web of dualities is disconnected and each connected component corresponds to a fusion structure. More generally the set of possible fusion structures is given as follows: any subgroup (up to isomorphism)  $F$  of  $\mathcal{A} \simeq G \times G$  satisfying  $|F| = |G|$  is a possible fusion structure. Each of these would then correspond to a connected component in a web-of-dualities graph.<sup>16</sup> In Figure (10), lines that connect a node  $\mathcal{L}$  to itself correspond to elements of  $\text{Stab}(\mathcal{L})$ . These are the source of emergent non-invertible symmetries as discussed above.

Another example is  $G = \mathbb{Z}_N$ . For any  $p$  and  $q$  such that  $pq = N$ , we have a fusion structure  $F = \mathbb{Z}_p \times \mathbb{Z}_q$ . Furthermore, there is a Lagrangian subgroup for any  $H \subset G$  which means that we have a Lagrangian subgroup given by  $\mathcal{L}_p \simeq \mathbb{Z}_p \times \mathbb{Z}_{N/p}$ . This phase spontaneously breaks  $\mathbb{Z}_N \rightarrow \mathbb{Z}_p$ . Clearly, any gapped phase  $\mathcal{L}_p$  comes with a pair  $\mathcal{L}_{N/p}$  with isomorphic fusion structure:  $\mathcal{L}_p \simeq \mathcal{L}_{N/p}$ . Under electric-magnetic duality, these are mapped into each other  $\mathcal{L}_p \xrightarrow{\text{EM}} \mathcal{L}_{N/p}$ . There cannot exist dualities that connect phases in other ways, as they have different fusion structures.

We believe that there always exist at least one duality between two gapped phases with

<sup>16</sup>Our statement here are about dualities obtained from this construction. There might exist dualities beyond the topological holography framework where this might not be true.

the same fusion structure (which implies that number of connected component of a web-of-duality graph is equal to the number of fusion structures). We have implicitly assumed this in the discussion above and will assume this to be true in what follows.

Let us summarize the main points

1. Properties of  $\mathbf{G}$ -symmetric Hamiltonians  $H[\{t_{\mathbf{d}}\}]$  such as being gapped, gapless, critical, or at a first-order transition is preserved under duality transformations.
2. Each gapped phase  $\mathcal{L}$  is characterized by a pair  $(\mathbf{H}_{\mathcal{L}}, \psi_{\mathcal{L}})$ , corresponding to a spontaneous symmetry-breaking down to a subgroup  $\mathbf{H}_{\mathcal{L}} \subset \mathbf{G}$  together with an SPT twist  $\psi_{\mathcal{L}} \in H^2(\mathbf{H}_{\mathcal{L}}, \mathbf{U}(1))$ . The data  $(\mathbf{H}_{\mathcal{L}}, \psi_{\mathcal{L}})$  can be conveniently obtained from the dyons in  $\mathcal{L}$ .
3. Each gapped phase has a fusion structure corresponding to the algebra of condensed order parameters  $\mathcal{L} \subset \mathcal{A}$ . Only gapped phases with isomorphic fusion structures  $\mathcal{L} \simeq \mathcal{L}'$  can be dual to each other. The web of dualities splits into connected components, one for each type of fusion structure.
4. For any gapped phase  $\mathcal{L}$ , one can associate a stabilizer subgroup  $\text{Stab}(\mathcal{L}) \subset \mathcal{G}[\mathbf{G}]$ . Any Hamiltonian in the gapped phase  $\mathcal{L}$  will be dual to another Hamiltonian in the same phase under dualities  $\sigma \in \text{Stab}(\mathcal{L})$ . Any such Hamiltonian at a self-dual point  $H[\{t_{\mathbf{d}}^*\}] = \widehat{\mathcal{D}}_{\sigma} \cdot H[\{t_{\mathbf{d}}^*\}]$  has extra emergent symmetries. These symmetries can be non-invertible which form a fusion category rather than a group.

## 4.2 Gapless phases, phase transitions, and critical points

Having discussed some of the properties of dualities with regards to gapped phases, we will now turn to critical points between gapped phases. All these properties can help constrain and map out phase-diagrams as we will see in examples (see Section 5).

It is convenient to define  $\text{Crit}[\mathcal{L}_1, \dots, \mathcal{L}_k]$  as the set of (multi-)critical points between gapped phases  $\mathcal{L}_1, \dots, \mathcal{L}_k$ . Here is a summary of various properties of dualities when acting on critical points:

1. *Self-duality*: If  $H[\{t_{\mathbf{d}}^*\}]$  is self-dual under a duality  $\sigma$  (or subgroup  $\mathcal{S} \subset \mathcal{G}[\mathbf{G}]$ ) then it cannot be in any gapped phase  $\mathcal{L}$  that is not self-dual under the same dualities  $\sigma \cdot \mathcal{L} \neq \mathcal{L}$ . In particular, if no gapped phase is self-dual under  $\sigma$  (or  $\mathcal{S}$ ) then  $H[\{t_{\mathbf{d}}^*\}]$  must either be gapless (critical or otherwise) or degenerate/at a first-order transition.
  - (a) If a critical point is self-dual under a subgroup  $\mathcal{S} \subset \mathcal{G}[\mathbf{G}]$  and  $\mathcal{L}$  is a gapped phase connected to this critical point, then it is a critical point between at least  $|\text{Orb}_{\mathcal{S}}(\mathcal{L})|$  number of gapped phases.
  - (b) If a Hamiltonian  $H[\{t_{\mathbf{d}}^*\}]$  (gapped or gapless) is self-dual under a subgroup  $\mathcal{S}$  of dualities, then this implies that there are topological defect lines commuting with it and therefore has new emergent symmetries. These emergent symmetries can be non-invertible.
2. *Critically*: Consider a critical point  $\mathcal{C} \in \text{Crit}[\mathcal{L}_1, \dots, \mathcal{L}_k]$  and a duality  $\sigma$  such that  $\sigma \cdot \mathcal{L}_i = \mathcal{L}_i^{\vee}$ . Then, the critical point will be mapped to  $\mathcal{C}^{\vee} \equiv \sigma \cdot \mathcal{C} \in \text{Crit}[\mathcal{L}_1^{\vee}, \dots, \mathcal{L}_k^{\vee}]$ . There are a few consequences:

- (a) In fact, there will be a bijection between the set of all critical points  $\text{Crit}[\mathcal{L}_1, \dots, \mathcal{L}_k]$  and  $\text{Crit}[\mathcal{L}_1^\vee, \dots, \mathcal{L}_k^\vee]$  induced by any such duality  $\sigma$ .
- (b) The set of critical points  $\text{Crit}[\mathcal{L}_1, \dots, \mathcal{L}_k]$  depends only on the fusion structures. More precisely, there is a bijection

$$\text{Crit}[\mathcal{L}_1, \dots, \mathcal{L}_k] \simeq \text{Crit}[\mathcal{L}'_1, \dots, \mathcal{L}'_k], \quad (4.12)$$

if  $\mathcal{L}_i \simeq \mathcal{L}'_i$  for all  $i$  (same fusion structure). By this, we mean that for any critical point between  $\mathcal{L}_1, \dots, \mathcal{L}_k$ , there is one (and only one) critical point between  $\mathcal{L}'_1, \dots, \mathcal{L}'_k$ . If  $\text{Crit}[\mathcal{L}_1, \dots, \mathcal{L}_k]$  has lines or surfaces of critical points, then so will  $\text{Crit}[\mathcal{L}'_1, \dots, \mathcal{L}'_k]$ . Note that the conformal field theories mapped to each other under this bijection need not be equivalent and can have different scaling operators. But if one has a marginal operator, then so will the other.

- (c) While a gapped phase is characterized by a fusion structure, a (multi-)critical point is characterized by a collection of fusion structures. The space of  $G$ -symmetric CFTs can be decomposed based on fusion structures.

Let us elaborate on some of these points. The first point follows from the discussion of the previous section. Imagine there exist a Hamiltonian  $H[\{t_d^*\}]$  which is self-dual under a subgroup  $\mathcal{S}$ , then which phase does it describe? Since dualities map gapped phases into each other according to (4.2), then any gapped phase that is not self-dual under  $\mathcal{S}$  is forbidden. However, if no gapped phase is self-dual, then  $H[\{t_d^*\}]$  cannot be any gapped phase. It must therefore be gapless or at a first-order transition with ground-state degeneracy.

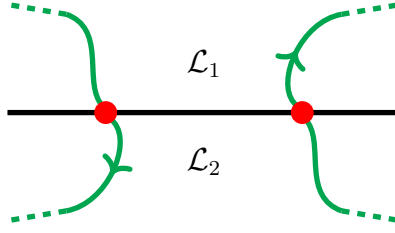
Point (1a) can be seen as follows: consider a path  $H_{\mathcal{L}}(s)$  connecting a gapped point ( $H_{\mathcal{L}}(0)$ ) in phase  $\mathcal{L}$  to a critical point  $\mathcal{C}$  ( $H_{\mathcal{L}}(1)$ ). Under dualities in  $\mathcal{S}$ ,  $H_{\mathcal{L}}^\vee(1) = H_{\mathcal{L}}(1)$ , under the assumption of self-duality of  $\mathcal{C}$ . However, the gapped portion of the path can be mapped to other gapped phases. Let us define the orbit of the action of  $\mathcal{S}$  on  $\mathcal{L}$  as

$$\text{Orb}_{\mathcal{S}}(\mathcal{L}) \equiv \{\sigma \cdot \mathcal{L}, \forall \sigma \in \mathcal{S}\}. \quad (4.13)$$

We can therefore connect any pair of gapped phases in  $\text{Orb}_{\mathcal{S}}(\mathcal{L})$  with a continuous path of Hamiltonians going through  $\mathcal{C}$ . Thus we conclude that  $\mathcal{C}$  is a multi-critical point between all gapped phases in  $\text{Orb}_{\mathcal{S}}(\mathcal{L})$ . However, there could be other gapped phases attached to  $\mathcal{C}$  with different fusion structures.

Point (1b) follows from the discussion in previous section, which naturally holds for any self-dual Hamiltonian and not just gapped ones.

The second point can be argued as follow. By assumption, we have tuned a Hamiltonian  $H_{\mathcal{C}}[\{t_d\}]$  to a critical point  $\mathcal{C} \in \text{Crit}[\mathcal{L}_1, \dots, \mathcal{L}_k]$ . Under a duality transformation  $H_{\mathcal{C}}^\vee[\{t_d\}] = \widehat{\mathcal{D}}_\sigma \cdot H_{\mathcal{C}}[\{t_d\}]$ , the critical point  $\mathcal{C}$  is mapped to another critical point  $\mathcal{C}^\vee \equiv \sigma \cdot \mathcal{C}$ . The question is, which transition does  $\mathcal{C}^\vee$  describe? Consider a path  $H(s)$  going from  $\mathcal{L}_1$ , through  $\mathcal{C}$ , to  $\mathcal{L}_2$ . After duality, this path maps into a path going from  $\mathcal{L}_1^\vee$ , through  $\mathcal{C}^\vee$ , to  $\mathcal{L}_2^\vee$ , where  $\mathcal{L}_i^\vee = \sigma \cdot \mathcal{L}_i$ . Repeating this for all pairs in the set  $\{\mathcal{L}_1, \dots, \mathcal{L}_k\}$  proves that  $\mathcal{C}^\vee \in \text{Crit}[\mathcal{L}_1^\vee, \dots, \mathcal{L}_k^\vee]$ . The above discussion implies that a duality induces a map between spaces  $\text{Crit}[\mathcal{L}_1, \dots, \mathcal{L}_k] \rightarrow \text{Crit}[\mathcal{L}_1^\vee, \dots, \mathcal{L}_k^\vee]$ . This map was not one-to-one then  $\sigma \cdot \mathcal{C}_1 = \sigma \cdot \mathcal{C}_2$ . However, this is not possible since the duality just permutes the coefficients (3.31) and therefore is trivially invertible. The surjectivity of the map can be argued as follows. Assume that there is phase  $\mathcal{C}' \in \text{Crit}[\mathcal{L}_1^\vee, \dots, \mathcal{L}_k^\vee]$  that is not the image of a point in



$\text{Crit}[\mathcal{L}_1, \dots, \mathcal{L}_k]$  under a duality  $\sigma$ . However, applying  $\sigma^{-1}$  to  $\mathcal{C}'$  would necessarily give us a point in the set  $\text{Crit}[\mathcal{L}_1, \dots, \mathcal{L}_k]$ . This can be seen by taking a continuous path from  $\mathcal{L}_1^\vee$  and  $\mathcal{L}_2^\vee$  that passes through  $\mathcal{C}'$ . The image of this path under  $\sigma^{-1}$  would be a path from  $\mathcal{L}_1$  to  $\mathcal{L}_2$  and passes through a critical phase between them. Hence  $\sigma^{-1} \cdot \mathcal{C}' \in \text{Crit}[\mathcal{L}_1, \dots, \mathcal{L}_k]$ . This shows point (2a).

To elaborate point (2b) and (2c), let  $\text{Fus}[\mathbf{G}] = \{\mathbf{F}_1, \dots, \mathbf{F}_r\}$  be the set of possible fusion structures of gapped phases of  $\mathbf{G}$ -symmetric systems and define  $\text{Crit}[\mathbf{F}_{i_1}, \dots, \mathbf{F}_{i_k}]$  with  $i_1 \leq \dots \leq i_k$  to be the set of critical phases between gapped phases with fusion structures  $\mathbf{F}_{i_1}, \dots, \mathbf{F}_{i_k}$ . This space is bigger than  $\text{Crit}[\mathcal{L}_1, \dots, \mathcal{L}_k]$  since it also contains all critical points  $\text{Crit}[\mathcal{L}'_1, \dots, \mathcal{L}'_k]$  satisfying  $\mathcal{L}_j \simeq \mathcal{L}'_j \simeq \mathbf{F}_{i_j}$ . We can decompose the subset of critical points within the space of  $\mathbf{G}$ -symmetric systems as

$$\text{Crit}[\mathbf{G}] = \bigcup_{k \geq 2} \bigcup_{\substack{i_1, \dots, i_k=1 \\ i_1 \leq \dots \leq i_k}}^r \text{Crit}[\mathbf{F}_{i_1}, \dots, \mathbf{F}_{i_k}]. \quad (4.14)$$

Dualities can only map critical points within each block  $\text{Crit}[\mathbf{F}_{i_1}, \dots, \mathbf{F}_{i_k}]$  but not between different blocks.

### 4.3 Conformal spectroscopy from dualities

In previous section, we discussed which kinds of global constraints dualities in  $\mathcal{G}[\mathbf{G}]$  impose on the space of  $\mathbf{G}$ -symmetric Hamiltonians. It is instructive to see how these dualities act in a spacetime formulation, or in other words on the level of partition functions. Since partition functions contain the full spectrum of a theory, it can be a powerful tool when combined with dualities. For example, we will see that it can be used to compute the conformal spectrum of many non-trivial phase transitions relatively easily. The conformal spectrum contains information about scaling dimensions of the universality class of the phase transitions.

In order to see the action of dualities on partition functions, it is useful to define a generalized twisted partition function as [88]

$$\mathcal{Z}_{\mathbf{g}, \mathbf{h}} = \text{tr}_{\mathcal{H}} \left( \mathcal{U}_{\mathbf{h}} e^{-\beta H_{\mathbf{g}}} \right), \quad (4.15)$$

where  $\mathcal{U}_{\mathbf{h}}$  is the  $\mathbf{G}$  symmetry operator and  $H_{\mathbf{g}}$  is a  $\mathbf{G}$ -symmetric Hamiltonian with symmetry-twisted boundary condition labeled by  $\mathbf{g}$ . One can think of this as being a normal partition function with the insertion of a symmetry operator  $\mathcal{U}_{\mathbf{h}}$  in the space direction and a  $\mathcal{U}_{\mathbf{g}}$  in the time direction (see Figure 11). To see how the presence of a defect in the time

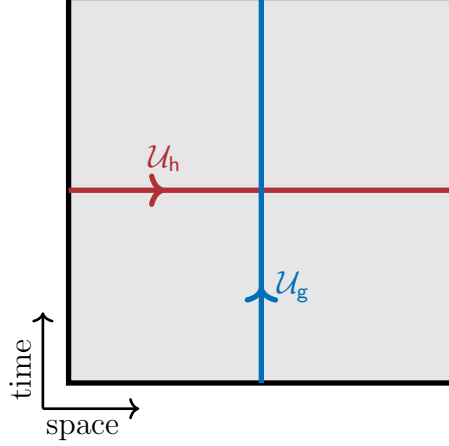


Figure 11: The insertion of symmetry line defects along space and time directions.

direction leads to a twisted boundary condition (see Appendix D). We are considering the generalized partition functions because dualities mix all sectors non-trivially, as we will see.

The projection operator to symmetry sector  $\alpha \in \text{Rep}(\mathbf{G})$  is given by

$$P_\alpha = \frac{1}{|\mathbf{G}|} \sum_{\mathbf{h} \in \mathbf{G}} \mathbf{R}_\alpha^{-1}(\mathbf{h}) \mathcal{U}_h. \quad (4.16)$$

One can readily confirm that  $P_\alpha^2 = P_\alpha$  and  $P_\alpha^\dagger = P_\alpha$ . Conversely, the symmetry operator can be written in terms of projectors  $P_\alpha$

$$\mathcal{U}_h = \sum_{\alpha \in \text{Rep}(\mathbf{G})} \mathbf{R}_\alpha(\mathbf{h}) P_\alpha. \quad (4.17)$$

Using the projectors,  $\mathbf{G}$ -twisted *characters* are defined as

$$\chi_d = \text{tr}_{\mathcal{H}} \left( P_\alpha e^{-\beta H_{\mathbf{g}}} \right) = \text{tr}_{\mathcal{H}_\alpha} \left( q^{H_{(\mathbf{g}, \alpha)}} \right), \quad (4.18)$$

where  $d = (\mathbf{g}, \alpha)$ ,  $q \equiv e^{-\beta}$ , and  $\mathcal{H}_\alpha = P_\alpha \mathcal{H}$ . Due to the projection operator, this object contains the spectrum of our Hamiltonian with twisted boundary condition  $\mathbf{g}$  in the symmetry sector  $\alpha$ . Using (4.16) and (4.17), we can express the partition functions and characters in terms of one another via

$$\mathcal{Z}_{\mathbf{g}, \mathbf{h}} = \sum_{\alpha \in \text{Rep}(\mathbf{G})} \mathbf{R}_\alpha(\mathbf{h}) \chi_{d=(\mathbf{g}, \alpha)}, \quad (4.19)$$

and

$$\chi_d = \frac{1}{|\mathbf{G}|} \sum_{\mathbf{h} \in \mathbf{G}} \mathbf{R}_\alpha^{-1}(\mathbf{h}) \mathcal{Z}_{\mathbf{g}, \mathbf{h}}. \quad (4.20)$$

Under a duality  $\sigma$ , Hamiltonian  $H_{\mathbf{g}}$  transforms to  $H_{(\mathbf{g}, \alpha)}^\vee[\{t\mathbf{d}\}] = H_{\sigma \cdot (\mathbf{g}, \alpha)}[\{t_{\sigma^{-1}} \cdot \mathbf{d}\}]$  (see equation (3.56)). By inserting this in (4.18), the characters transform as

$$\chi_d \longmapsto \chi_d^\vee = \text{tr}_{\mathcal{H}} \left( q^{H_{(\mathbf{g}, \alpha)}^\vee} \right) = \text{tr}_{\mathcal{H}} \left( q^{H_{\sigma \cdot (\mathbf{g}, \alpha)}} \right) = \chi_{\sigma \cdot (\mathbf{g}, \alpha)}. \quad (4.21)$$

Therefore, the dual twisted partition functions are given by

$$\begin{aligned}\mathcal{Z}_{\mathbf{g}^\vee, \mathbf{h}^\vee}^\vee &= \sum_{\alpha^\vee \in \text{Rep}(\mathbf{G})} R_{\alpha^\vee}(\mathbf{h}^\vee) \chi_{d^\vee}^\vee \\ &= \sum_{\alpha^\vee \in \text{Rep}(\mathbf{G})} R_{\alpha^\vee}(\mathbf{h}^\vee) \chi_{(\widehat{\mathbf{g}}, \widehat{\alpha})},\end{aligned}\tag{4.22}$$

where we have defined

$$(\widehat{\mathbf{g}}, \widehat{\alpha}) = \sigma \cdot (\mathbf{g}^\vee, \alpha^\vee).\tag{4.23}$$

Using (4.20), this can be written as

$$\begin{aligned}\mathcal{Z}_{\mathbf{g}^\vee, \mathbf{h}^\vee}^\vee &= \frac{1}{|\mathbf{G}|} \sum_{\alpha^\vee} R_{\alpha^\vee}(\mathbf{h}^\vee) \sum_{\mathbf{h}} R_{\widehat{\alpha}}^{-1}(\mathbf{h}) \mathcal{Z}_{\widehat{\mathbf{g}}, \mathbf{h}} \\ &= \frac{1}{|\mathbf{G}|} \sum_{\mathbf{g}, \mathbf{h}, \alpha^\vee} R_{\alpha^\vee}(\mathbf{h}^\vee) R_{\widehat{\alpha}}^{-1}(\mathbf{h}) \delta_{\widehat{\mathbf{g}}, \widehat{\alpha}} \mathcal{Z}_{\mathbf{g}, \mathbf{h}}.\end{aligned}\tag{4.24}$$

In other words, under a duality generalized twisted partition functions transform linearly

$$\mathcal{Z}_{\mathbf{g}^\vee, \mathbf{h}^\vee}^\vee = \frac{1}{|\mathbf{G}|} \sum_{\mathbf{g}, \mathbf{h} \in \mathbf{G}} \eta(\mathbf{g}, \mathbf{h}, \mathbf{g}^\vee, \mathbf{h}^\vee) \mathcal{Z}_{\mathbf{g}, \mathbf{h}},\tag{4.25}$$

where the coefficients are

$$\eta(\mathbf{g}, \mathbf{h}, \mathbf{g}^\vee, \mathbf{h}^\vee) \equiv \sum_{\alpha^\vee \in \text{Rep}(\mathbf{G})} R_{\alpha^\vee}(\mathbf{h}^\vee) R_{\widehat{\alpha}}^{-1}(\mathbf{h}) \delta_{\widehat{\mathbf{g}}, \widehat{\alpha}}.\tag{4.26}$$

Starting from a model with periodic boundary condition, the partition function is given by  $\mathcal{Z}_{0,0}$  and the partition function of the dual theory is given by  $\mathcal{Z}_{0,0}^\vee$ . However, it is clear from (4.25) that the dual partition function  $\mathcal{Z}_{0,0}^\vee$  depends on all generalized twisted partition functions  $\mathcal{Z}_{\mathbf{g}, \mathbf{h}}$  of the original theory. This is another manifestation of how dualities act on twisted sectors.

Physically, the factor  $\eta_\sigma$  corresponds to the partition function of a theory living on the duality wall  $\mathcal{D}_\sigma[\Sigma]$  living in the  $2 + 1d$  bulk TQFT (see Figure 6b). In terms of  $\eta$  factors, the fusion of domain walls (3.2) in the bulk is given

$$\eta_{\sigma_1 \sigma_2}(\mathbf{g}, \mathbf{h}, \mathbf{g}'', \mathbf{h}'') = \frac{1}{|\mathbf{G}|} \sum_{\mathbf{g}', \mathbf{h}'} \eta_{\sigma_1}(\mathbf{g}, \mathbf{h}, \mathbf{g}', \mathbf{h}') \eta_{\sigma_2}(\mathbf{g}', \mathbf{h}', \mathbf{g}'', \mathbf{h}'').\tag{4.27}$$

While (4.25) holds for any  $\mathbf{G}$ -symmetric theory, it is particularly powerful at critical points with conformal symmetry. In such cases, the partition functions are expressed in terms of Virasoro characters of the primary fields in the theory. From (4.25), we can therefore directly compute the spectrum of a dual conformal field theory from any other with known partition functions. We will exploit this formula to explicitly predict the conformal spectrum of non-trivial phase transitions and confirm these predictions numerically.

## 4.4 Duality: a gauging perspective

The relation between twisted partition functions  $\mathcal{Z}_{\mathbf{g},\mathbf{h}}$  and dual twisted partition functions  $\mathcal{Z}_{\mathbf{g}^\vee,\mathbf{h}^\vee}^\vee$  (4.25) can often be conveniently expressed as a generalized gauging of the global  $\mathbf{G}$  symmetry. We first note that,  $\mathcal{Z}_{\mathbf{g},\mathbf{h}}$  can be equivalently understood as the partition functions of the model described by the Hamiltonian  $H$  coupled to a background  $\mathbf{G}$  gauge field whose holonomies in the space and time directions of the spacetime torus are  $\mathbf{g}$  and  $\mathbf{h}$  respectively. Since gauge fields for finite groups have a vanishing field strength, the gauge equivalence classes of such gauge fields can be labelled the holonomies around non-contractible cycles of the manifold. Therefore we may write

$$\mathcal{Z}_{\mathbf{g},\mathbf{h}} \equiv \mathcal{Z}[A], \quad \mathcal{Z}_{\mathbf{g}^\vee,\mathbf{h}^\vee}^\vee \equiv \mathcal{Z}[A^\vee]. \quad (4.28)$$

Then the duality expression, (4.24), can be expressed as

$$\mathcal{Z}[A^\vee] = \frac{1}{|\mathbf{G}|} \sum_A \mathcal{Z}[A] \eta(A, A^\vee). \quad (4.29)$$

We will find that in several duality transformations, the object  $\eta(A, A^\vee)$  reduces to a topological term in terms of the backgrounds  $A$  and  $A^\vee$ . Such topological terms are expressed most conveniently in terms of gauge fields defined on oriented triangulations of the spacetime manifold as illustrated in Fig. 3. A gauge field is defined via a coloring of the 1-simplices by group labels such that the composition of the group labels on the boundary of any 2-simplex or plaquette evaluates to the identity element in  $\mathbf{G}$ . This is nothing but the cocycle or flatness condition for the gauge field  $A$ . The gauge field  $A$  can be dualized to obtain a network of  $\mathbf{G}$  symmetry domain wall. Concretely, the gauge field  $A_{ij} \in \mathbf{G}$  assigned to the 1-simplex  $\langle ij \rangle$  dualizes to a symmetry domain wall corresponding to the same group element living on the 1-simplex of the dual triangulation. Furthermore, the cocycle condition simply translates to the fact that the symmetry domain walls fuse according the group product in  $\mathbf{G}$  (see Fig. 12). Note that, if in  $d+1$  dimensions, a  $d$ -simplex would be dual to a 1-simplex and therefore the symmetry domain walls would be defined on  $d$ -simplices, which as described earlier, is the correct dimension for 0-form symmetry defects (see Appendix E for details).

In two dimensions, the types of topological terms that appear are typically of the form

$$S_{\text{top}} \propto \int_{\Sigma} A_1 \cup A_2, \quad (4.30)$$

where  $A_1$  and  $A_2$  are some discrete gauge fields. A generic topological term would contain a sum of terms of the form (4.30). When  $\Sigma$  is a two torus, the topological term  $S_{\text{top}}$  can be expressed in terms of the holonomies of  $A_{1,2}$  as

$$\int_{\Sigma} A_1 \cup A_2 = (\text{hol}_x(A_1)\text{hol}_t(A_2) - \text{hol}_x(A_2)\text{hol}_t(A_1)), \quad (4.31)$$

where  $\text{hol}_{x,t}(A_i)$  is the holonomy of the gauge field  $A_i$  along the  $x, t$  cycle respectively.

In Sec. 3.5, we described how the 0-form symmetry group of  $2+1d$  topological gauge theories is generated by three kinds of symmetry transformations, namely (i) universal kinematical symmetries, (ii) universal dynamical symmetries and (iii) partial electric-magnetic



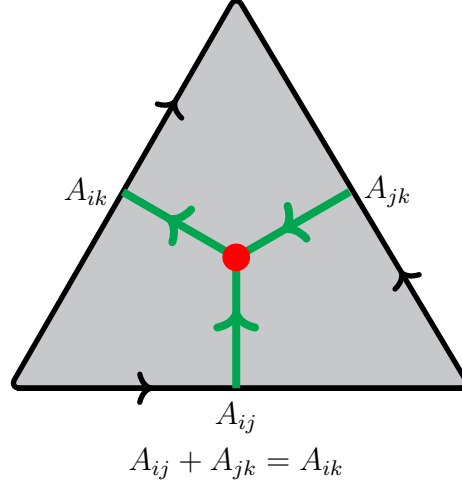


Figure 12: A gauge field corresponding to a finite Abelian group  $G$  is given by a  $G$  coloring of 1-simplices (in black) or equivalently a network of symmetry domain walls (in green). The cocycle condition for the gauge field  $A$  translates to a consistent group composition of the symmetry domain walls.

dualities. In turn, there are correspondingly three kinds of generators of the duality group acting on the space of  $G$ -symmetric quantum systems. These three families of generators have a natural action on the twisted partition functions  $\mathcal{Z}[A]$ .

1. Universal kinematical symmetries: These dualities are labelled by elements of the automorphism group of  $G$ . An automorphism  $\varphi$ , maps a generator  $\mathbf{g}_j$  of the group  $G$  into a new group element  $\varphi(\mathbf{g}_j)$  of the same order. Correspondingly, the automorphism group acts on the background gauge field by mapping  $A_j$  to  $A_j^\vee = \varphi(A_j)$ . More precisely, the dual partition function has the form

$$\sigma_\varphi : \mathcal{Z}[A] \mapsto \mathcal{Z}^\vee[A^\vee] = \sum_{A \in H^1(\Sigma, G)} \mathcal{Z}[A] \delta_{A, \varphi(A^\vee)}, \quad (4.32)$$

where  $\varphi(A) = (\varphi(A_1), \varphi(A_2), \dots)$ .

2. Universal dynamical symmetries: These dualities are labelled by elements  $\mathbf{c}_\ell \in H^2(G, \mathbf{U}(1))$ , which also labels  $1+1d$   $G$  SPTs. In particular, the partition function of a  $G$ -SPT, coupled to a background  $G$  gauge field  $A$  is (in the topological limit) a pure  $\mathbf{U}(1)$  phase. Concretely, for a finite group  $G = \prod_i \mathbb{Z}_{N_i}$ , the group cocycles are given in (3.41). The corresponding topological response theory of the SPT labelled by  $\mathbf{c}_\ell$  coupled to a  $G$  background  $A$  is

$$\mathcal{Z}_{\text{SPT}-\mathbf{c}_\ell}[A] = \exp \left\{ 2\pi i \sum_{i < j} \int_\Sigma \frac{\ell_{ij}}{\text{gcd}(N_i, N_j)} A_i \cup A_j \right\}. \quad (4.33)$$

Then the duality  $\sigma_{\mathbf{c}_\ell}$  acts on the twisted partition functions as

$$\sigma_{\mathbf{c}_\ell} : \mathcal{Z}[A] \mapsto \mathcal{Z}[A] \mathcal{Z}_{\text{SPT}-\mathbf{c}_\ell}[A]. \quad (4.34)$$

Therefore the universal dynamical symmetries correspond to pasting  $G$ -SPTs.



3. Partial electric-magnetic dualities: These are generalized Kramers-Wannier dualities [91, 158, 162] that are obtained by gauging a certain  $\mathbb{Z}_{N_j}$  factor in the group  $\mathbf{G}$ . The resulting theory has a dual (or quantum)  $\mathbf{G}$  global symmetry. The twisted partition functions transform as follows under such duality operations

$$\mathcal{Z}^\vee[\cdots, A_j^\vee, \cdots] = \frac{1}{N_j} \sum_{A_j \in H^1(\Sigma, \mathbb{Z}_{N_j})} \exp\left(\frac{2\pi i}{N_j} \int_\Sigma A_j \cup A_j^\vee\right) \mathcal{Z}[\cdots, A_j, \cdots], \quad (4.35)$$

More general duality operation can be obtained by taking various combinations of these kinds of duality generators. These often take the form of generalized gauging in the presence of topological terms. Such interpretations would be discussed in more detail in subsequent sections. It should be noted that gauging in the presence of an SPT or topological twist has been known in the string theory and conformal field theory literature for more than thirty years as orbifolding in the presence of discrete torsion [163, 164].

## 5 Examples

In this section, we study the space of quantum spin chains for specific examples of global symmetry  $\mathbf{G}$  using the formalism of topological holography introduced in prior sections. In particular, we will describe all gapped phases, their order parameters, and fundamental excitations. We will write down certain minimal Hamiltonians that capture all the essential (symmetry related) features of such systems. Using dualities, we predict phase diagrams of these models, and numerically verify the theoretical predictions. Finally, we analytically compute and numerically verify the conformal spectrum of various non-trivial topological phase transitions.

The dualities discussed in this paper are particularly powerful for global symmetries  $\mathbf{G}$  that have large duality groups but very few fusion structures. As explained in Sections 4.1 and 4.2, gapped phases and critical points with different fusion structures cannot be mapped onto each other under duality. Having a single fusion structure and many dualities can vastly constrain the possible phase diagram. Groups like  $\mathbb{Z}_N$  belong to the opposite limit where there are few dualities and many fusion structures. Therefore, dualities put modest constraints on possible phase diagrams. Nonetheless, we will start by the examples of  $\mathbb{Z}_2$  and  $\mathbb{Z}_N$  as they are the building blocks of more interesting examples.

On the other limit, global symmetries such as  $\mathbb{Z}_2 \times \mathbb{Z}_2$  or  $\mathbb{Z}_3 \times \mathbb{Z}_3$  have only a single fusion structure but a large duality group. Hence, these examples are particularly well-suited to be studied using topological holography.

For a basic derivation of topological holography using an exactly-solvable model in the bulk, see Appendix C.

### 5.1 $\mathbb{Z}_2$ symmetric quantum spin chains

Let us consider the simplest finite Abelian group  $\mathbf{G} = \mathbb{Z}_2$ . We are interested in analyzing the phase diagram of  $\mathbb{Z}_2$  symmetric quantum systems using the holographic approach outlined

in previous sections. To this end, we consider an auxiliary bulk  $2 + 1d$  theory which hosts the  $\mathbb{Z}_2$  topological order whose topological line operators are labelled by

$$\mathcal{A}[\mathbb{Z}_2] = \{1, e, m, f\} = \mathbb{Z}_2 \times \text{Rep}(\mathbb{Z}_2) \simeq \mathbb{Z}_2 \times \mathbb{Z}_2, \quad (5.1)$$

where we have associated the group elements  $\{(0, 0), (0, 1), (1, 0), (1, 1)\} \in \mathcal{A}[\mathbb{Z}_2]$  with the label set  $\{1, e, m, f\}$ . In other words, the lines corresponding to the group elements  $(1, 0)$  and  $(0, 1)$  in  $\mathcal{A}[\mathbb{Z}_2]$  are the magnetic and electric line operators while the  $(1, 1)$  element corresponds to the dyonic line obtained via a fusion of the electric and magnetic lines labelled as  $f$ . The  $\mathbb{Z}_2$  topological order has a 0-form global symmetry group

$$\mathcal{G}[\mathbb{Z}_2] = \mathbb{Z}_2 = \{id, \sigma\}, \quad (5.2)$$

whose generator acts as an outer automorphism on the 1-form symmetry group  $\mathbb{Z}_2 \times \mathbb{Z}_2$ , that exchanges  $e \leftrightarrow m$  and leaves the product  $f = em$  invariant. The  $\mathbb{Z}_2$  gauge theory admits two gapped boundaries corresponding to the  $\mathbb{Z}_2$  subgroups of  $\mathcal{A}[\mathbb{Z}_2]$  generated by  $e$  and  $m$ . These two gapped boundaries condense the magnetic and electric excitations respectively and will be denoted as  $\mathcal{L}_e = \{1, e\}$  and  $\mathcal{L}_m = \{1, m\}$ .

The phase diagram of  $1+1d$   $\mathbb{Z}_2$  symmetric quantum systems can be captured by an effective spin chain that arises at the lattice on the regularized boundary of the  $\mathbb{Z}_2$  topological order defined on a semi-infinite cylinder [120]. As discussed in Sec. 3.2, the action of the open  $e$  and  $m$  operators restricted to the boundary can be captured by a quantum spin chain defined on a 1D lattice with a local Hilbert space  $\mathcal{H}_i = \mathbb{C}^2$ . From (3.28), it can be seen that the minimal operators subtended from the bulk topological magnetic and electric operators are

$$S_m = A_i = \sigma_i^x, \quad S_e = B_{i,i+1} = \sigma_i^z \sigma_{i+1}^z, \quad (5.3)$$

where  $\sigma_i^\mu$  are Pauli operators acting on the local Hilbert space  $\mathcal{H}_i$ . Applying electric-magnetic duality (5.2) swaps electric and magnetic lines  $S_m \leftrightarrow S_e$ , which in turn becomes the well-known Kramers-Wannier duality on the spin chain, which acts on symmetry operators as (3.46)

$$\widehat{\mathcal{D}}_\sigma \cdot (\sigma_i^z \sigma_{i+1}^z) = \sigma_{i+1}^x \quad \widehat{\mathcal{D}}_\sigma \cdot (\sigma_i^x) = \sigma_i^z \sigma_{i+1}^z. \quad (5.4)$$

One immediately recognizes these operators as those appearing in the transverse field Ising (TFI) model, which is the paradigmatic quantum spin chain with a global  $\mathbb{Z}_2$  symmetry. The fixed point Hamiltonians that describe the two gapped phases, i.e., the ferromagnetic and the paramagnetic phase of the TFI model are obtained as the Hamiltonians corresponding to the electric and magnetic gapped boundaries of the  $\mathbb{Z}_2$  gauge theory

$$H_e = - \sum_{i=1}^L \sigma_i^z \sigma_{i+1}^z, \quad H_m = - \sum_{i=1}^L \sum_i \sigma_i^x. \quad (5.5)$$

The simplest Hamiltonian capable of capturing the phase diagram of  $\mathbb{Z}_2$  symmetric quantum systems is simply a linear combination of these two fixed point Hamiltonians

$$H(\lambda) = \lambda H_m + (1 - \lambda) H_e. \quad (5.6)$$

Next, we organize the Hilbert space of the TFI model using the bulk topological considerations. Firstly, since all the non-contractible line operators  $\Gamma_d$  with  $d \in \mathcal{A}[\mathbb{Z}_2]$  commute

with all the boundary operators  $\mathcal{O}_{g,i}$  and  $\mathcal{O}_{\alpha,i}\mathcal{O}_{-\alpha,i+1}$ , we may simultaneously diagonalize all the  $\Gamma_d$  operators, which leads to a decomposition of the boundary Hilbert space into super-selection sectors

$$\mathcal{H} = \bigoplus_{d' \in \mathcal{A}[\mathbb{Z}_2]} \mathcal{H}_{d'}, \quad \text{where} \quad \Gamma_d \Big|_{\mathcal{H}_{d'}} = e^{i\theta_{dd'}} = (-1)^{\mathbf{g}\alpha' + \mathbf{g}'\alpha}, \quad (5.7)$$

where  $\exp\{i\theta_{dd'}\}$  is the Hopf-linking phase between the  $d = (\mathbf{g}, \alpha)$  and  $d' = (\mathbf{g}', \alpha')$  topological line operators (bulk anyons). Furthermore, we can diagonalize a maximal commuting subalgebra of boundary operators to define a basis for  $\mathcal{H}_{d'}$ . We choose to diagonalize the operators  $\mathcal{O}_{\alpha,i}\mathcal{O}_{-\alpha,i+1} = \sigma_i^z \sigma_{i+1}^z$ . Doing so, we may construct the basis  $\{|\mathbf{a}, d'\rangle\}$ , with  $\mathbf{a} \in C^1(\Lambda, \mathbb{Z}_2)$ , the space of  $\mathbb{Z}_2$  valued 1-cochains defined on the regularized boundary lattice  $\Lambda$ . The various finite local operators in eq. (5.3) act on the basis states as

$$\sigma_i^z \sigma_{i+1}^z |\mathbf{a}, d'\rangle = (-1)^{a_{i,i+1}} |\mathbf{a}, d'\rangle, \quad \prod_i (\sigma_i^x)^{\lambda_i} |\mathbf{a}, d'\rangle = |\mathbf{a} + \delta\boldsymbol{\lambda}, d'\rangle, \quad (5.8)$$

where  $\boldsymbol{\lambda} \in C^0(\Lambda, \mathbb{Z}_2)$ . Here,  $a_{i,i+1} = 0, 1$  corresponds to a domain-wall configuration in the spin chain. For example,  $a_{i,i+1} = \sigma_{i+1} - \sigma_i$ , where  $\sigma_i = 0, 1$  are labels of up and down spins. The action of  $\sigma_i^x$  flips a spin  $\sigma_i \rightarrow \sigma_i + 1$  at site  $i$ , which in turn flips two domain walls attached to it. This is encoded in the notation  $\mathbf{a} \rightarrow \mathbf{a} + \delta\boldsymbol{\lambda}$ , which explicitly means  $a_{i,i+1} \rightarrow a_{i,i+1} + \lambda_{i+1} - \lambda_i$ . In other word,  $\mathbf{a}$  can be thought of as a  $\mathbb{Z}_2$  gauge field and  $\mathbf{a} \rightarrow \mathbf{a} + \delta\boldsymbol{\lambda}$  as a gauge transformation. Similarly, the non-contractible line operators in the bulk become the symmetry operator  $\Gamma_{(\mathbf{g},0)} \equiv \mathcal{U}_{\mathbf{g}}$  and the boundary condition twist operator  $\Gamma_{(0,\alpha)} \equiv \mathcal{T}_{\alpha}$  as defined in (3.29). More explicitly, these operators are given by

$$\mathcal{U}_{\mathbf{g}} = \left( \prod_{i=1}^L \sigma_i^x \right)^{\mathbf{g}}, \quad \mathcal{T}_{\alpha} = \left( \prod_{i=1}^L \sigma_i^z \sigma_{i+1}^z \right)^{\alpha}. \quad (5.9)$$

Note that the Kramers-Wannier duality  $\sigma$  (5.4) swaps these operators. These act on the basis states as

$$\begin{aligned} \mathcal{U}_{\mathbf{g}} |\mathbf{a}, d'\rangle &= (-1)^{\mathbf{g}\alpha'} |\mathbf{a}, d'\rangle, \\ \mathcal{T}_{\alpha} |\mathbf{a}, d'\rangle &= (-1)^{\mathbf{g}'\alpha} |\mathbf{a}, d'\rangle = (-1)^{\text{hol}(\mathbf{a})\alpha} |\mathbf{a}, d'\rangle, \end{aligned} \quad (5.10)$$

where in the second line, we have used  $\text{hol}(\mathbf{a}) := \sum_i a_{i,i+1} = \mathbf{g}'$ . Here, the holonomy  $\text{hol}(\mathbf{a})$  can be thought of as the flux  $\oint_{\gamma} \mathbf{a}$  of  $\mathbb{Z}_2$  gauge field  $\mathbf{a}$ , where  $\gamma$  is a loop around the spatial direction. The flux  $\text{hol}(\mathbf{a}) = \mathbf{g}'$  is created by the insertion of symmetry operator  $\mathcal{U}_{\mathbf{g}'}$  in the time direction, which gives rise to the boundary condition above.

Finally, the endpoint of the semi-infinite operators  $\mathcal{W}_d$  serve to toggle between super-selection sectors. This can be readily seen from the commutation relations between the semi-infinite lines  $\mathcal{Y}_d$  and the non-contractible bulk line operators  $\Gamma_d$  (3.19) and (3.20). The operator  $\mathcal{Y}_e$ , ending on the site  $i$  on the effective spin chain, anticommutes with  $\sigma_i^x$ , and therefore effectively acts as the  $\sigma_i^z$  operator (see (3.64)). As a consequence, it modifies the charge, i.e.,  $\mathcal{U}_{\mathbf{g}}$  eigenvalue of the superselection sector. Similarly, the semi-infinite line  $\mathcal{Y}_m$  ending on the link  $(L, 1)$  on the effective spin chain, anticommutes with a single link operator  $\sigma_L^z \sigma_1^z$ . As a consequence, this modifies the eigenvalue of the  $\mathcal{T}_{\alpha}$ . More explicitly,

from (5.9) we have  $\mathcal{T}_\alpha = (\sigma_L^z \sigma_{L+1}^z)^\alpha$ . The presence of an infinite  $\mathcal{Y}_{(\mathbf{g}', 0)} = (\mathcal{Y}_m)^{\mathbf{g}'}$  ending on the link  $(L, 1)$  imposes the twisted boundary condition

$$\sigma_{L+1}^z = (-1)^{\mathbf{g}'} \sigma_1^z. \quad (5.11)$$

To summarize, the semi-infinite line operators act on the Hilbert space sectors as

$$\mathcal{Y}_d : \mathcal{H}_{d'} \mapsto \mathcal{H}_{d+d'}. \quad (5.12)$$

In addition to the boundary Hilbert space, the space of local operators on the spin chain admits a decomposition into superselection sectors labelled by  $d \in \mathcal{A}$ , since the local operators in (5.3) commute with  $\Gamma_d$  for all  $d$ . In particular, the Hamiltonian admits a decomposition  $H(\lambda) = \oplus_d H_d(\lambda)$ .

The spectrum of Hamiltonian  $H_d(\lambda)$  can be obtained by coupling the model to a background  $\mathbb{Z}_2$  gauge field and computing the partition function. Different gauge inequivalent configurations of a  $\mathbb{Z}_2$  gauge field  $A$  are labelled by the holonomies  $(\mathbf{g}, \mathbf{h}) \in H^1(T^2, \mathbb{Z}_2)$  of  $A$  in the space and time direction, respectively. The partition function in a symmetry twisted sector or equivalently coupled to a background  $\mathbb{Z}_2$  gauge field  $A = (\mathbf{g}, \mathbf{h})$  is

$$\mathcal{Z}[A, \lambda] \equiv \mathcal{Z}_{\mathbf{g}, \mathbf{h}}(\lambda) = \text{Tr}_{\mathcal{H}} \left[ \mathcal{U}_{\mathbf{h}} e^{-\beta H_{\mathbf{g}}(\lambda)} \right]. \quad (5.13)$$

Then, the twisted characters, which contain a trace of states in a sector labelled by  $d = (\mathbf{g}, \alpha) \in \mathcal{A}[\mathbb{Z}_2]$  is

$$\chi_d(\lambda) = \text{Tr}_{\mathcal{H}} \left[ P_\alpha e^{-\beta H_g(\lambda)} \right] = \frac{1}{2} \sum_{\mathbf{h} \in \mathbb{Z}_2} (-1)^{\alpha \mathbf{h}} \mathcal{Z}_{\mathbf{g}, \mathbf{h}}, \quad (5.14)$$

where  $P_\alpha$  is a projector, defined in (4.16), onto  $\alpha \in \text{Rep}(\mathbb{Z}_2)$ . These characters transform under the action of the generator  $\sigma$  of the 0-form symmetry group  $\mathcal{G}[\mathbb{G}]$  (5.2) of the bulk as  $\chi_d(\lambda) \mapsto \chi_d^\vee(\lambda)$ , where

$$\chi_d^\vee(\lambda) = \text{Tr}_{\mathcal{H}} \left[ P_{\alpha^\vee} e^{-\beta H_{g^\vee}^\vee(\lambda)} \right], \quad (5.15)$$

with  $\sigma \cdot (\mathbf{g}, \alpha) = (\mathbf{g}^\vee, \alpha^\vee)$ . The Hamiltonian  $H^\vee$  is obtained from the action (5.4) on (5.6). From this we obtain  $H^\vee(\lambda) = U_P H(1 - \lambda) U_P^\dagger$ , where  $U_P$  is a permutation of super-selection sectors. When decomposed into the sectors (5.7), this explicitly becomes

$$\begin{pmatrix} H_{P+}^\vee & & & \\ & H_{P-}^\vee & & \\ & & H_{A+}^\vee & \\ & & & H_{A-}^\vee \end{pmatrix}(\lambda) = \begin{pmatrix} H_{P+} & & & \\ & H_{A+} & & \\ & & H_{P-} & \\ & & & H_{A-} \end{pmatrix}(1 - \lambda). \quad (5.16)$$

Here  $P$  and  $A$  label periodic and anti-periodic boundary conditions, respectively, while  $+$  and  $-$  label the even and odd  $\mathbb{Z}_2$  symmetry sectors. A physical consequence of the duality is that the spectrum of the Hamiltonians,  $H(\lambda)$  and  $H^\vee(\lambda)$ , on either side of the duality are the same but are permuted (see also (3.56) and (3.57)). From this, we can see that characters transform as

$$\chi_d(\lambda) \mapsto \chi_d^\vee(\lambda) = \chi_{\sigma \cdot d}(\sigma \cdot \lambda), \quad \sigma \cdot \lambda = 1 - \lambda, \quad (5.17)$$

where  $\sigma \cdot (\mathbf{g}, \alpha) = (\alpha, \mathbf{g})$ .

It is also useful to see how the twisted partition functions transform under duality. To do so, we first write the twisted characters  $\chi_d$ , in terms of the twisted partition functions  $\mathcal{Z}_{\mathbf{g}, \mathbf{h}}$  explicitly

$$\begin{aligned}\chi_1(\lambda) &= \frac{1}{2} (\mathcal{Z}_{0,0}(\lambda) + \mathcal{Z}_{0,1}(\lambda)), & \chi_e(\lambda) &= \frac{1}{2} (\mathcal{Z}_{0,0}(\lambda) - \mathcal{Z}_{0,1}(\lambda)), \\ \chi_m(\lambda) &= \frac{1}{2} (\mathcal{Z}_{1,0}(\lambda) + \mathcal{Z}_{1,1}(\lambda)), & \chi_f(\lambda) &= \frac{1}{2} (\mathcal{Z}_{1,0}(\lambda) - \mathcal{Z}_{1,1}(\lambda)),\end{aligned}\tag{5.18}$$

which implies the equality of the following combinations of twisted partition functions

$$\begin{aligned}\chi_1^\vee(\lambda) &= \frac{1}{2} (\mathcal{Z}_{0,0}^\vee(\lambda) + \mathcal{Z}_{0,1}^\vee(\lambda)) = \frac{1}{2} (\mathcal{Z}_{0,0}(1-\lambda) + \mathcal{Z}_{0,1}(1-\lambda)) = \chi_1(\sigma \cdot \lambda) \\ \chi_e^\vee(\lambda) &= \frac{1}{2} (\mathcal{Z}_{0,0}^\vee(\lambda) - \mathcal{Z}_{0,1}^\vee(\lambda)) = \frac{1}{2} (\mathcal{Z}_{1,0}(1-\lambda) + \mathcal{Z}_{1,1}(1-\lambda)) = \chi_m(\sigma \cdot \lambda) \\ \chi_m^\vee(\lambda) &= \frac{1}{2} (\mathcal{Z}_{1,0}^\vee(\lambda) + \mathcal{Z}_{1,1}^\vee(\lambda)) = \frac{1}{2} (\mathcal{Z}_{0,0}(1-\lambda) - \mathcal{Z}_{0,1}(1-\lambda)) = \chi_e(\sigma \cdot \lambda) \\ \chi_f^\vee(\lambda) &= \frac{1}{2} (\mathcal{Z}_{1,0}^\vee(\lambda) - \mathcal{Z}_{1,1}^\vee(\lambda)) = \frac{1}{2} (\mathcal{Z}_{1,0}(1-\lambda) - \mathcal{Z}_{1,1}(1-\lambda)) = \chi_f(\sigma \cdot \lambda).\end{aligned}\tag{5.19}$$

Finally, the transformation of twisted sectors can be expressed as

$$\mathcal{Z}_{\mathbf{g}^\vee, \alpha^\vee} = \frac{1}{2} \sum_{\mathbf{g}, \mathbf{g}=0}^1 (-1)^{\mathbf{g}^\vee \mathbf{h} - \mathbf{h}^\vee \mathbf{g}} \mathcal{Z}_{\mathbf{g}, \mathbf{h}},\tag{5.20}$$

which is a special case of (4.25). This is nothing but a discrete Fourier transform of twisted partition functions. Written in the language of gauging and cup products, this can be succinctly written as

$$\mathcal{Z}^\vee[A^\vee, \lambda] = \frac{1}{\sqrt{|H^1(T^2, \mathbb{Z}_2)|}} \sum_A (-1)^{\int_{T^2} A \cup A^\vee} \mathcal{Z}[A, 1-\lambda].\tag{5.21}$$

This is a well-known modern perspective on Kramers-Wannier duality [91, 162].

The two Lagrangian subgroups  $\mathcal{L}_e$  and  $\mathcal{L}_m$  correspond to ferromagnetic and paramagnetic phases of  $\mathbb{Z}_2$ -symmetric quantum system. The Kramers-Wannier duality maps  $\mathcal{L}_e \leftrightarrow \mathcal{L}_m$  and thus ferromagnetic to paramagnetic phase and vice versa. The order parameter  $S_e = \sigma_i^z \sigma_j^z$  for condensing  $e$  satisfies

$$\begin{aligned}\lim_{|i-j| \rightarrow \infty} \langle \text{GS}_{\text{FM}} | \sigma_i^z \sigma_j^z | \text{GS}_{\text{FM}} \rangle &\neq 0, \\ \lim_{|i-j| \rightarrow \infty} \langle \text{GS}_{\text{PM}} | \sigma_i^z \sigma_j^z | \text{GS}_{\text{PM}} \rangle &= 0,\end{aligned}\tag{5.22}$$

and thus becomes the order parameter for the ferromagnetic phase, detecting the long-range spin order after spontaneous breaking of  $\mathbb{Z}_2$  symmetry. The order parameter  $S_m = \prod_{k=i}^j \sigma_k^x$  for condensing  $m$  satisfies

$$\begin{aligned}\lim_{|i-j| \rightarrow \infty} \langle \text{GS}_{\text{FM}} | \prod_{k=i}^j \sigma_k^x | \text{GS}_{\text{FM}} \rangle &= 0, \\ \lim_{|i-j| \rightarrow \infty} \langle \text{GS}_{\text{PM}} | \prod_{k=i}^j \sigma_k^x | \text{GS}_{\text{PM}} \rangle &\neq 0,\end{aligned}\tag{5.23}$$

and becomes the disorder parameter for the ferromagnetic phase. As expected, the order and disorder parameters are swapped under Kramer's Wannier duality.

Let us now consider the Kramers-Wannier self-dual region between ferromagnetic and paramagnetic phases. The self-dual point/region of the phase diagram of  $\mathbb{Z}_2$ -symmetric quantum systems cannot be in a phase corresponding to either of the two Lagrangian subgroups, i.e, in either of the two gapped phases. As a consequence, it must be either gapless, critical or a first-order transition (gapped but with degeneracy). The minimal self-dual point  $\lambda = 1/2$  in the Hamiltonian (5.6) is well-known to be in universality class of the Ising CFT with central charge  $c = \frac{1}{2}$ . This is the simplest non-trivial minimal model  $\mathcal{M}(4, 3)$ . There are three primary operators in the critical Ising CFT: the identity operator  $\mathbb{I}$ , the spin field  $\sigma$ , and the energy operator  $\epsilon$  with conformal dimensions  $(h, \bar{h})$  being  $(0, 0)$ ,  $(\frac{1}{16}, \frac{1}{16})$ , and  $(\frac{1}{2}, \frac{1}{2})$ , respectively [165]. Therefore, the partition function in the untwisted sector  $(g, h) = (0, 0)$  is given by

$$\mathcal{Z}_{0,0} = |\chi_0|^2 + |\chi_{\frac{1}{2}}|^2 + |\chi_{\frac{1}{16}}|^2. \quad (5.24)$$

The Ising CFT has a  $\mathbb{Z}_2$  global symmetry or equivalently a  $\mathbb{Z}_2$  topological defect line under which the eigenvalues of the three primaries are  $+1, -1$  and  $+1$ , respectively. Therefore, the partition functions with the insertion of  $\mathbb{Z}_2$  symmetry line in the spatial direction is given by [88]

$$\mathcal{Z}_{0,1} = |\chi_0|^2 + |\chi_{\frac{1}{2}}|^2 - |\chi_{\frac{1}{16}}|^2. \quad (5.25)$$

Here  $|\chi_i|^2 = \chi_i \bar{\chi}_i$  is the (product of) Virasoro characters of the Ising CFT obtained by tracing over the conformal tower obtained from a primary operator of conformal dimension  $(i, i)$ , not to be confused with the twisted  $\mathbb{Z}_2$  characters defined in (5.14). In terms of the  $\mathbb{Z}_2$  twisted characters, these take the form

$$\chi_1 = |\chi_0|^2 + |\chi_{\frac{1}{2}}|^2, \quad \chi_e = |\chi_{\frac{1}{16}}|^2. \quad (5.26)$$

Additionally, the theory has a  $\mathbb{Z}_2$  twisted Hilbert space, known as the defect Hilbert space in the CFT literature. In the lattice model, this is realized within the Hamiltonian with anti-periodic boundary conditions. The defect Hilbert space too has three primary operators denoted as  $\psi, \bar{\psi}$  and  $\mu$  with conformal dimensions  $(\frac{1}{2}, 0), (0, \frac{1}{2})$  and  $(\frac{1}{16}, \frac{1}{16})$ . The  $\mathbb{Z}_2$  eigenvalues of these three primary operators are  $-1, -1$  and  $+1$  respectively. Therefore the  $\mathbb{Z}_2$  twisted sectors with antiperiodic boundary conditions take the form

$$\begin{aligned} \mathcal{Z}_{1,0} &= |\chi_{\frac{1}{16}}|^2 + \chi_0 \bar{\chi}_{\frac{1}{2}} + \chi_{\frac{1}{2}} \bar{\chi}_0, \\ \mathcal{Z}_{1,1} &= |\chi_{\frac{1}{16}}|^2 - \chi_0 \bar{\chi}_{\frac{1}{2}} - \chi_{\frac{1}{2}} \bar{\chi}_0. \end{aligned} \quad (5.27)$$

The  $\mathbb{Z}_2$  twisted characters, in the anti-periodic sector are

$$\chi_m = |\chi_{\frac{1}{16}}|^2, \quad \chi_f = \chi_0 \bar{\chi}_{\frac{1}{2}} + \chi_{\frac{1}{2}} \bar{\chi}_0. \quad (5.28)$$

The fact that  $\chi_e = \chi_m$  is a direct consequence of the Kramers-Wannier self-duality of the Ising critical point.

Finally, we note, that the holographic approach can be used to analyze more general Hamiltonians, i.e., those which are subtended from non-minimal bulk strings. For instance,

consider the Hamiltonian built from, bulk  $e$  and  $m$  string operators of length 2. On the boundary Hilbert space, these act as

$$\mathcal{O}_{\mathbf{g},j}\mathcal{O}_{\mathbf{g},j+1} = \sigma_j^x \sigma_{j+1}^x, \quad \mathcal{O}_{\alpha,j}\mathcal{O}_{-\alpha,j+2} = \sigma_j^z \sigma_{j+2}^z. \quad (5.29)$$

The Hamiltonian obtained upon including these deformations to the transverse field Ising model is known as the anisotropic next-nearest-neighbor Ising (ANNNI) model [166–168]

$$H_{\text{ANNNI}}(\lambda, \tau) = \lambda H_m + (1 - \lambda) H_e - \tau \sum_j [\sigma_j^x \sigma_{j+1}^x + \sigma_j^z \sigma_{j+2}^z]. \quad (5.30)$$

Note that the model is self-dual for any  $\tau$ , when  $\lambda = \frac{1}{2}$ . Along the self-dual line, this model has a rich phase diagram which contains an extended  $c = 1/2$  Ising critical phase as well as the tri-critical Ising fixed point, Lifshitz transition and degenerate gapped regions (first-order transitions). This is consistent with the possible phases along the self-dual line as constrained by considerations mentioned in Sec. 4.2. Namely that the gapped phases  $\mathcal{L}_e$  and  $\mathcal{L}_m$  cannot exist along this line. Instead, this line contains different types of transitions between these two phases. In particular, by varying  $\lambda$  we can exit the self-dual line and enter one of the gapped phases  $\mathcal{L}_e$  or  $\mathcal{L}_m$ .

Another class of non-minimal Kramers-Wannier self-dual deformations of the Ising model are generated by the operators

$$\mathcal{O}_{\mathbf{g},j}\mathcal{O}_{\alpha,j+1}\mathcal{O}_{-\alpha,j+2} + \mathcal{O}_{\alpha,j}\mathcal{O}_{-\alpha,j+1}\mathcal{O}_{\mathbf{g},j+2} = \sigma_j^x \sigma_{j+1}^z \sigma_{j+2}^z + \sigma_j^z \sigma_{j+1}^z \sigma_{j+2}^x. \quad (5.31)$$

The corresponding model, known as Fendeleý-O’Brien model [168, 169], also hosts the tri-critical Ising critical point. The tri-critical Ising (TCI) model corresponds to the minimal model  $\mathcal{M}(4, 5)$ , with central charge  $c = 7/10$ . These models clearly also have a  $\mathbb{Z}_2$  global symmetry and can therefore be organized a twisted  $\mathbb{Z}_2$  characters labelled by  $d \in \mathcal{A}[\mathbb{Z}_2]$ . These twisted characters take the form [170, 171]

$$\begin{aligned} \chi_1^{\text{TCI}} &= |\chi_0|^2 + |\chi_{1/10}|^2 + |\chi_{\frac{3}{5}}|^2 + |\chi_{\frac{3}{2}}|^2, \\ \chi_e^{\text{TCI}} &= |\chi_{\frac{3}{80}}|^2 + |\chi_{\frac{7}{16}}|^2, \\ \chi_m^{\text{TCI}} &= |\chi_{\frac{3}{80}}|^2 + |\chi_{\frac{7}{16}}|^2, \\ \chi_f^{\text{TCI}} &= \chi_{\frac{6}{10}} \bar{\chi}_{\frac{1}{10}} + \chi_{\frac{1}{10}} \bar{\chi}_{\frac{6}{10}} + \chi_{\frac{3}{2}} \bar{\chi}_0 + \chi_0 \bar{\chi}_{\frac{3}{2}}. \end{aligned} \quad (5.32)$$

The Kramers-Wannier self-duality is manifest from the fact that  $\chi_e = \chi_m$ . We note that the TCI model realizes an emergent  $\mathcal{N} = 1$  superconformal algebra. The algebra is generated by two primaries, i.e., supercharges with scaling dimensions  $(3/2, 0)$  and  $(0, 3/2)$ . As can be seen from (5.32), these appear in the  $\mathbb{Z}_2$  twisted Hilbert space sector, i.e., in the lattice model with anti-periodic boundary conditions with respect to the  $\mathbb{Z}_2$  symmetry and furthermore transform under a non-trivial  $\mathbb{Z}_2$  representation.

## 5.2 $\mathbb{Z}_N$ symmetric quantum spin chains

As discussed in Sec. 4.1, the symmetry group  $G = \mathbb{Z}_N$  has in general several different fusion structures and few dualities. Therefore, it belongs to the limit of examples where

topological holography is not very powerful and constraining. Nonetheless, it is instructive to go through some details as these become useful for more general examples. For a more powerful application of topological holography, the reader can skip to the next example with  $G = \mathbb{Z}_2 \times \mathbb{Z}_2$ .

Any such finite Abelian group  $G$  can be decomposed into a product of finite Abelian groups of prime power order, i.e.,

$$\mathbb{Z}_N = \mathbb{Z}_{p_1^{\ell_1}} \times \mathbb{Z}_{p_2^{\ell_2}} \times \dots, \quad (5.33)$$

where  $p_i$  are all distinct prime numbers and  $\ell_i \in \mathbb{Z}_{\geq 0}$ . In order to organize our understanding of  $G$  symmetric quantum systems, we follow the outlined strategy of first studying a  $G$ -topological order in  $2 + 1d$ . The topological line operators of the  $G$  topological order are labelled by elements in the group

$$\mathcal{A}[\mathbb{Z}_N] = \mathbb{Z}_N \times \text{Rep}(\mathbb{Z}_N) \simeq \mathbb{Z}_N \times \mathbb{Z}_N = \langle m, e | m^N = e^N = 1 \rangle. \quad (5.34)$$

The 0-form symmetry group of the  $\mathbb{Z}_N$  gauge theory is given by [153]

$$\mathcal{G}[\mathbb{Z}_N] = \text{Aut}(\mathbb{Z}_N) \rtimes \mathbb{Z}_2 = \mathbb{Z}_N^\times \rtimes \mathbb{Z}_2, \quad (5.35)$$

where the  $\mathbb{Z}_2$  subgroup is generated by the electromagnetic duality which acts as

$$\sigma : e \longleftrightarrow m, \quad (5.36)$$

while  $\mathbb{Z}_N^\times$  is the group under multiplication modulo  $N$  formed by the set of integers which are coprime with respect to  $N$ . Some examples are  $\mathbb{Z}_4^\times = \mathbb{Z}_2$ ,  $\mathbb{Z}_8^\times = \mathbb{Z}_2 \times \mathbb{Z}_2$ ,  $\mathbb{Z}_9^\times = \mathbb{Z}_6$  and  $\mathbb{Z}_{27}^\times = \mathbb{Z}_{18}$ . For any prime number  $p$ ,  $\mathbb{Z}_p^\times = \mathbb{Z}_{p-1}$ . A useful relation for later purposes is

$$\text{Aut}(\mathbb{Z}_N) = \left( \text{Aut}(\mathbb{Z}_{p_1^{\ell_1}}^\times) \times \text{Aut}(\mathbb{Z}_{p_2^{\ell_2}}^\times) \times \dots \right). \quad (5.37)$$

The group  $\mathbb{Z}_N^\times$  acts on  $\mathbb{Z}_N$  by mapping its generator to some other element of order  $N$ . Concretely, for  $\mathbb{Z}_N = \{0, 1, \dots, N\}$ , let a generator  $s$  of  $\mathbb{Z}_N^\times$  act as  $s(1) = j$ , where  $\text{gcd}(j, N) = 1$ . Then the action of  $s$  on the line operators of the  $\mathbb{Z}_N$  gauge theory is given by

$$s : e^a m^b \longmapsto e^{ja} m^{f(j)b}, \quad (5.38)$$

where  $j \times f(j) = 1 \pmod N$ . For the case, where  $N$  itself is prime, the generator of  $\mathbb{Z}_N^\times$  takes the form

$$s : e^a m^b \longmapsto e^{2a} m^{(\frac{N-1}{2})b}, \quad (5.39)$$

Note that  $(N-1)/2 \in \mathbb{Z}$  for all primes except  $N=2$ , for which  $\mathbb{Z}_2^\times$  is trivial.

Next, we move onto the gapped boundaries for  $\mathbb{Z}_N$  gauge theory. As discussed in section 3.4, the possible  $\mathbb{Z}_N$  symmetric gapped phases are in bijective correspondence to the subgroups of  $\mathbb{Z}_N$ . To see this, we write the group in terms of a product of indecomposable groups

$$\mathbb{Z}_N = \mathbb{Z}_{p_1^{\ell_1} p_2^{\ell_2} \dots p_M^{\ell_M}}. \quad (5.40)$$



Subgroups then take the form

$$H_{\mathbf{r}} = Z_{p_1^{r_1} p_2^{r_2} \dots p_M^{r_M}} \subseteq Z_{p_1^{\ell_1} p_2^{\ell_2} \dots p_M^{\ell_M}} = \mathbb{Z}_N, \quad (5.41)$$

where  $0 \leq r_i \leq \ell_i$ . Consequently, the number of subgroups are  $\prod_{i=1}^M (\ell_i + 1)$  and are labelled by an  $M$  component vector  $\mathbf{r}$ . We similarly, can label Lagrangian subgroups by an  $\mathbf{r}$ , which take the form

$$\mathcal{L}_{\mathbf{r}} = \langle e^{\alpha(\mathbf{r})}, m^{\mathbf{g}(\mathbf{r})} \rangle := \langle e^{\prod_i p_i^{r_i}}, m^{\prod_i p_i^{\ell_i - r_i}} \rangle. \quad (5.42)$$

Having described the line operators (1-form symmetries) labelled by  $\mathcal{A}[\mathbb{Z}_N]$ , the 0-form symmetries  $\mathcal{G}[\mathbf{G}]$  and the set of gapped boundaries of the  $\mathbf{G} = \mathbb{Z}_N$  gauge theory, we are now in a position to discuss the phase space of  $\mathbb{Z}_N$  symmetric quantum systems.

Using the approach defined previously, we can obtain an effective spin chain on the 1D boundary of the topological gauge theory defined on a spatial semi-infinite cylinder. The effective spin chain, is defined on a lattice whose sites are endowed with a local Hilbert space  $\mathcal{H}_i \simeq \mathbb{C}^N$ . The space of local operators  $\mathcal{L}(\mathcal{H}_i)$  are spanned by  $X_i$  and  $Z_i$ , which satisfy the  $\mathbb{Z}_N$  clock algebra (see section 2.2

$$X_i^a Z_j^b = \omega_N^{ab\delta_{ij}} Z_j^b X_i^a, \quad (5.43)$$

where  $a, b = 0, \dots, N-1$  and  $\omega_N \equiv \exp(2\pi i/N)$ . The local operator  $\mathcal{O}_{\alpha,i} = Z_i^\alpha$  transforms in the representation  $\alpha \in \text{Rep}(\mathbb{Z}_N)$ , while the global  $\mathbb{Z}_N$  symmetry is generated by the operator  $\mathcal{U}_{\mathbf{g}} = \prod_i X_i^{\mathbf{g}}$ . The minimal operators subtended from the bulk topological magnetic and electric operators,  $m^{\mathbf{g}}$  and  $e^\alpha$  respectively are (3.28)

$$\mathcal{O}_{g,i} = X_i^{\mathbf{g}}, \quad \mathcal{O}_{\alpha,i} \mathcal{O}_{-\alpha,i+1} = Z_i^\alpha Z_{i+1}^{-\alpha}, \quad (5.44)$$

More, generally an open dyonic line operator labelled by  $d = (\mathbf{g}, \alpha) \in \mathcal{A}[\mathbb{Z}_N]$  and with its two ends on the 1D boundary subtends the following string operator on the effective spin-chain

$$\mathcal{S}_{(\mathbf{g},\alpha)}(\ell) = Z_{i_1}^\alpha \left( \bigotimes_{k=1}^{n-1} X_{i_k}^{\mathbf{g}} \right) Z_{i_n}^{-\alpha}. \quad (5.45)$$

These operators satisfy certain important properties that encode the topological data of the bulk  $\mathbb{Z}_N$  gauge theory. By using the graphical notation for string operators

$$S_d(\ell) = \bullet \xrightarrow{d} \bullet, \quad (5.46)$$

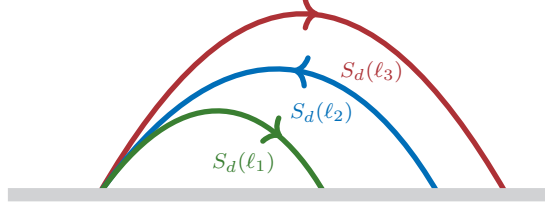


Figure 13: Configuration of string operators corresponding to the algebra (5.49) computing self-statistics of bulk anyonic excitations from boundary spin chain.

one can readily check that these string operators satisfy the following algebraic relations

$$\begin{aligned}
& \text{Diagram 1: } \text{---} \xrightarrow{d} \text{---} = \text{---} \xrightarrow{d} \text{---} \\
& \text{Diagram 2: } \begin{array}{c} \xrightarrow{d_2} \\ \xrightarrow{d_1} \end{array} = R_{\alpha_2^{-1}}(g_1) R_{\alpha_1}(g_2) \begin{array}{c} \xrightarrow{d_1} \\ \xrightarrow{d_2} \end{array} \\
& \text{Diagram 3: } \begin{array}{c} \xrightarrow{d_2} \\ \xrightarrow{d_1} \end{array} = e^{i\theta_{d_1 d_2}} \begin{array}{c} \xrightarrow{d_1} \\ \xrightarrow{d_2} \end{array} \\
& \text{Diagram 4: } \begin{array}{c} \xrightarrow{d_2} \\ \xrightarrow{d_1} \end{array} = R_{\alpha_2}(g_1) \begin{array}{c} \xrightarrow{d_2} \\ \xrightarrow{d_1} \end{array} \\
& \text{Diagram 5: } \begin{array}{c} \xrightarrow{d_2} \\ \xrightarrow{d_1} \end{array} = R_{\alpha_2^{-1}}(g_1) \begin{array}{c} \xrightarrow{d_1} \\ \xrightarrow{d_2} \end{array}
\end{aligned} \tag{5.47}$$

where  $\exp \{i\theta_{dd'}\} = R_{\alpha}(g') R_{\alpha'}(g)$ . In the above equations we have use the shorthand

$$\begin{array}{c} \xrightarrow{d_2} \\ \xrightarrow{d_1} \end{array} \equiv \mathcal{S}_{d_2}(\ell) \mathcal{S}_{d_1}(\ell). \tag{5.48}$$

Additionally, if we consider three oriented segments  $\ell_{1,2,3}$  as in Figure 13, which share a common initial point, the corresponding string operators satisfy the algebraic relation [172]

$$\mathcal{S}_d(\ell_1) \mathcal{S}_d(\ell_2) \mathcal{S}_d(\ell_3) = e^{i\theta_d} \mathcal{S}_d(\ell_3) \mathcal{S}_d(\ell_2) \mathcal{S}_d(\ell_1), \tag{5.49}$$

where  $\exp \{i\theta_d\} = R_{\alpha}(g)$ . The algebra generated by these string operators is the String Operator Algebra (SOA)

$$\text{SOA}[\mathbb{Z}_N] = \text{Spac}_{\mathbb{C}} \{ \mathcal{S}_d(\ell) \mid \forall d \text{ and } \forall \ell \}, \tag{5.50}$$

which is the algebra of local  $\mathbb{Z}_N$ -symmetric operators that are the building blocks of  $\mathbb{Z}_N$ -symmetric Hamiltonians. To see this, note that the most general  $\mathbb{Z}_N$ -symmetric operator on a segment  $\ell$  is spanned by operators of the form

$$\mathcal{K}(\ell) = \mathcal{O}_{\alpha_1, i_1} \mathcal{O}_{g_1, i_1} \cdots \mathcal{O}_{\alpha_n, i_n} \mathcal{O}_{g_n, i_n}, \tag{5.51}$$

with the constraint that  $\sum_{k=1}^n \alpha_{i_k} = 0 \bmod N$ . Such operators are elements of the SOA since we can always decompose these (up to a  $U(1)$  phase) into a product of string operators as (See also figure 14).

$$\mathcal{K}(\ell) = \left( \prod_{k=1}^{n-1} \mathcal{S}_{d_k}(\ell_{i_k}) \right) \mathcal{S}_{(\mathbf{g}'_n, 1)}(i_n), \quad (5.52)$$

where  $d_k = (\mathbf{g}_k, \sum_{j=1}^k \alpha_j)$  and  $\ell_i$  correspond to a single link  $\ell_i = \{i, i+1\}$ . The decomposition of symmetric operators  $\mathcal{K}(\ell)$  into links (5.52) may not be the most economical as it assigns a ‘ $d$ ’ label to each link. Often  $\mathcal{K}(\ell)$  can be decomposed using longer string operators and thus fewer labels. For any symmetric operator  $\mathcal{K}(\ell)$ , there is always a minimal decomposition, which contains the minimum number of string operators. Thus any symmetric operator can be labeled by its corresponding set of minimal labels  $\mathbf{d} \equiv (d_1, \dots, d_n)$  as

$$\mathcal{K}_{\mathbf{d}}(\ell) = \mathcal{S}_{d_1}(\ell_1) \dots \mathcal{S}_{d_n}(\ell_n), \quad (5.53)$$

where  $\ell_i$  are non-overlapping sub-segments of  $\ell$  of various lengths such that  $\ell = \cup_i \ell_i$ .

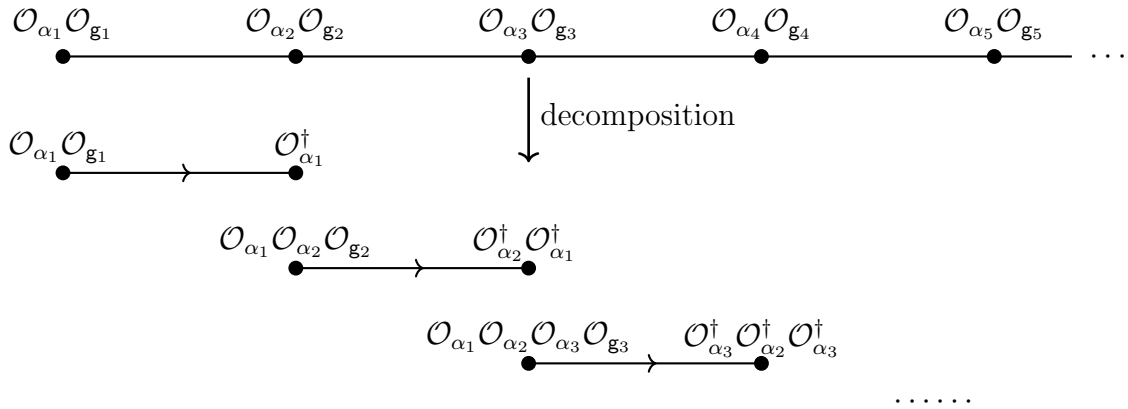


Figure 14: Any  $\mathbb{Z}_N$ -symmetric operator acting on a finite region can be decomposed into a product of string operators.

As described in the previous section, the gapped phases/ground states realized in  $\mathbf{G}$  symmetric quantum systems are in correspondence with gapped boundaries of a  $\mathbf{G}$  topological gauge theory, classified by Lagrangian subgroups. Furthermore, we can construct the fixed-point Hamiltonian within each phase directly from the operators corresponding to the line operators allowed to end on a given gapped boundary  $\mathcal{L}_{\mathbf{r}}$  in eq. (5.42). Such a fixed point Hamiltonian takes the form

$$H_{\mathbf{r}} = - \sum_j \left[ Z_j^{\alpha(\mathbf{r})} Z_{j+1}^{-\alpha(\mathbf{r})} + X_j^{\mathbf{g}(\mathbf{r})} + \text{H.c.} \right]. \quad (5.54)$$

The ground state realized for a Hamiltonian labelled by  $\mathbf{r}$ , breaks the global symmetry down to the subgroup  $\mathbf{H}_{\mathbf{r}}$  in eq. (5.41). This can be seen from the fact that the expectation value

$$\lim_{|i-j| \rightarrow \infty} \langle Z_i^{\alpha(\mathbf{r})} Z_j^{-\alpha(\mathbf{r})} \rangle \neq 0, \quad (5.55)$$

Furthermore, from the property of cluster decomposition, this implies that

$$\langle Z_i^{\alpha(r)} \rangle \neq 0, \quad (5.56)$$

which transforms non-trivially under  $\mathbb{Z}_N/\mathbf{H}_r$ . Meanwhile, it can be readily checked that the ground state is invariant under the subgroup  $\mathbf{H}_r \subseteq \mathbb{Z}_N$  generated by  $\mathcal{U}_{\mathbf{g}(r)}$ . A general Hamiltonian capable of realizing all the gapped phases is simply obtained by adding terms corresponding to each Lagrangian subgroup

$$H(\boldsymbol{\lambda}) = \sum_r \lambda_r H_r. \quad (5.57)$$

Finally, let us point out that the critical transitions  $\mathcal{C}_{p,q}$  between two gapped phases  $\mathcal{L}_p$  and  $\mathcal{L}_q$  labeled by two integers  $p$  and  $q$  such that  $pq = N$  is electric-magnetic self-dual. Using (4.24) and the electric-magnetic duality  $\sigma : (\mathbf{g}, \alpha) = (\alpha, \mathbf{g})$ , we see that  $(\omega = \exp(\frac{2\pi i}{N}))$

$$\mathcal{Z}_{\mathbf{g}^\vee, \mathbf{h}^\vee}(\mathcal{C}_{p,q}) = \frac{1}{N} \sum_{\mathbf{g}, \mathbf{h}=0}^{N-1} \omega^{\mathbf{g}^\vee \mathbf{h} - \mathbf{h}^\vee \mathbf{g}} \mathcal{Z}_{\mathbf{g}, \mathbf{h}}(\mathcal{C}_{p,q}). \quad (5.58)$$

It is known that the critical transition between ferromagnetic and paramagnetic phases of  $N$ -state Potts model is described by  $\mathbb{Z}_N$  parafermion CFT [173] and hence  $\mathcal{Z}_{\mathbf{g}, \mathbf{h}}(\mathcal{C}_{p,q})$  is the generalized twisted partition function of this CFT. The relation (5.58) is exactly the sum rule for twisted partition functions of the parafermion CFTs, which reflects the self-duality [174, 175] (for a brief review, see appendix A of [175]. The relevant sum rule is given in equation (A.8)).

### 5.3 $\mathbb{Z}_2 \times \mathbb{Z}_2$ symmetric quantum spin chains

The dualities discussed in this paper are most useful when the duality group is large as compared with the number of possible fusion structures. In the case of  $\mathbb{Z}_N$ , we have the opposite limit, there are few dualities but many fusion structures. Hence, dualities are not very powerful in constraining the phase diagram.

In this section, we consider quantum systems with  $\mathbf{G} = \mathbb{Z}_2 \times \mathbb{Z}_2$  global symmetry, which belong to the opposite limit; there is a non-Abelian duality group of order 72 and six gapped phases with the same fusion structure. We will see that this can help us to determine the rich phase diagram of models with  $\mathbb{Z}_2 \times \mathbb{Z}_2$  global symmetry. In particular, there will be interesting critical points and lines, as well as regions with large emergent symmetries. Besides constraining and predicting a phase diagram using topological holography, our construction provides order parameters that we will use to numerically verify the theoretically obtained phase diagram.

Parts of this phase-diagram was analysed long ago using topological holography and non-abelian dualities in [121, 122]. The ideas in this paper were inspired by and developed shortly after the work in [121, 122], though it remained unpublished until now.

## Dualities

In the holographic bulk, we consider a  $2+1d$   $G$  topological gauge theory whose line operators are labelled by elements (anyons) in  $\mathcal{A}$  where

$$\mathcal{A}[\mathbb{Z}_2 \times \mathbb{Z}_2] = \mathbb{Z}_2^2 \times \text{Rep}(\mathbb{Z}_2) \simeq \mathbb{Z}_2^2 \times \mathbb{Z}_2^2 = \langle m_L, m_R, e_L, e_R \rangle. \quad (5.59)$$

Here the  $(\mathbf{g}_1, \mathbf{g}_2, \alpha_1, \alpha_2)$  charge of each anyon is  $m_L = (1, 0, 0, 0)$ ,  $m_R = (0, 1, 0, 0)$ ,  $e_L = (0, 0, 1, 0)$  and  $e_R = (0, 0, 0, 1)$ . Let us now explore the 0-form symmetry group  $\mathcal{G}[G]$ . Three symmetry operations are immediately obtained as the electromagnetic duality  $\sigma_L$  and  $\sigma_R$  on the two  $\mathbb{Z}_2$  “layers” denoted as  $L$  and  $R$  respectively, along with the layer-swapping  $L \leftrightarrow R$  denoted as  $f$  such that

$$\begin{aligned} \sigma_L &: \{m_L \mapsto e_L, e_L \mapsto m_L\}, \\ \sigma_R &: \{m_R \mapsto e_R, e_R \mapsto m_R\}, \\ f &: \{m_L \mapsto m_R, m_R \mapsto m_L, e_L \mapsto e_R, e_R \mapsto e_L\}, \end{aligned} \quad (5.60)$$

where all the other generators of  $\mathcal{A}[\mathbb{Z}_2 \times \mathbb{Z}_2]$  that have not been shown are invariant. Together,  $\sigma_L, \sigma_R$  and  $f$  form the group  $D_4 = \mathbb{Z}_4 \rtimes \mathbb{Z}_2$ . However the duality group turns out to be significantly larger. Here, we present the generators that will turn out to be useful in understanding the phase-diagram of the model.

$$\begin{aligned} h_1 &: \{m_R \mapsto m_L m_R, e_L \mapsto e_L e_R\}, \\ h_2 &: \{m_L \mapsto m_L m_R, e_R \mapsto e_L e_R\}, \\ h_3 &: \{m_L \mapsto m_R, m_R \mapsto m_L, e_L \mapsto e_R, e_R \mapsto e_L\}, \end{aligned} \quad (5.61)$$

and

$$\begin{aligned} k_1 &: \{m_L \mapsto m_L e_R, m_R \mapsto m_R e_L\}, \\ k_2 &: \{e_L \mapsto e_L m_R, e_R \mapsto e_R m_L\}, \\ k_3 &: \{m_L \mapsto e_R, m_R \mapsto e_L, e_L \mapsto m_R, e_R \mapsto m_L\}. \end{aligned} \quad (5.62)$$

The transformations  $h_1, h_2, h_3, k_1$  and  $k_2, k_3$  generate the group  $S_3 \times S_3$  as

$$\begin{aligned} S_3 &= \left\langle k_1, k_2, k_3 \mid k_1^2 = 1, (k_2 k_3)^3 = 1, k_1 (k_2 k_3) k_1^{-1} = (k_2 k_3)^{-1} \right\rangle, \\ S_3 &= \left\langle h_1, h_2, h_3 \mid h_1^2 = 1, (h_2 h_3)^3 = 1, h_1 (h_2 h_3) h_1^{-1} = (h_2 h_3)^{-1} \right\rangle, \end{aligned} \quad (5.63)$$

and  $h_i k_j = k_j h_i$  for  $i, j = 1, 2, 3$ . The previous generators  $\sigma_{L,R}$  and  $f$  are related to these generators via the relations

$$h_3 = f, \quad k_3 = \sigma_L \sigma_R f, \quad (5.64)$$

implying that  $\sigma_R$  and  $f$  can be expressed in terms of these generators, and we only need to add  $\sigma_L$  to the set of generators. The  $\mathbb{Z}_2$  group generated by  $\sigma_L$  act on  $S_3 \times S_3$ , by swapping the two  $S_3$  copies

$$\sigma_L k_i \sigma_L^{-1} = h_i, \quad i = 1, 2, 3. \quad (5.65)$$

Therefore the full 0-form symmetry group  $\mathcal{G}[G]$  is

$$\mathcal{G}[\mathbb{Z}_2 \times \mathbb{Z}_2] = \langle \sigma_L, h_1, k_1, h_2 h_3, k_2 k_3 \rangle = (S_3 \times S_3) \rtimes \mathbb{Z}_2. \quad (5.66)$$

Lagrangian subgroups	Generating set	Image of $\Pi$	$H$	$\psi(h_1, h_2)$	Gapped phase
$\mathcal{L}_1$	$e_L, e_R$	$1_L, 1_R$	$\mathbb{I}$	1	SSB
$\mathcal{L}_2$	$m_L, e_R$	$m_L$	$\mathbb{Z}_2^L$	1	$\text{PSB}_L$
$\mathcal{L}_3$	$e_L, m_R$	$m_R$	$\mathbb{Z}_2^R$	1	$\text{PSB}_R$
$\mathcal{L}_4$	$e_L e_R, m_L m_R$	$m_L m_R$	$\mathbb{Z}_2^D$	1	$\text{PSB}_D$
$\mathcal{L}_5$	$e_L m_R, m_L e_R$	$m_R, m_L$	$\mathbb{Z}_2^L \times \mathbb{Z}_2^R$	$(-1)^{h_{1,L} h_{2,R}}$	$\text{SPT}_1$
$\mathcal{L}_6$	$m_L, m_R$	$m_R, m_L$	$\mathbb{Z}_2^L \times \mathbb{Z}_2^R$	1	$\text{SPT}_0$

Table 1: Table of Lagrangian subgroups (gapped phases) for  $G = \mathbb{Z}_2 \times \mathbb{Z}_2$ . Here,  $\mathbb{Z}_2^L, \mathbb{Z}_2^R$  and  $\mathbb{Z}_2^D$  denote the left, the right and the diagonal  $\mathbb{Z}_2$  subgroups of  $\mathbb{Z}_2 \times \mathbb{Z}_2$ , respectively. All gapped phases have the same fusion structure  $\mathcal{L}_i \simeq \mathbb{Z}_2 \times \mathbb{Z}_2$  for all  $i$ .  $H$  and  $\psi$  are the unbroken subgroup of  $G$  and the SPT twist of the given phase respectively. These can be extracted from the corresponding Lagrangian subgroup (see Section 4.1). For the

This is a group of order

$$|\mathcal{G}[\mathbb{Z}_2 \times \mathbb{Z}_2]| = (3!)^2 \times 2 = 72. \quad (5.67)$$

These bulk 0-form symmetries in  $2 + 1$  dimensions become dualities in  $1 + 1$  dimensions. This group can be generated by fewer generators, however we have chosen these as they reveal the structure of the phase-diagram more transparently.

## Gapped Phases, Order Parameters, and Excitations

The bulk topological gauge theory admits a set of six gapped boundaries as enumerated in Table 1. Each gapped boundary can be labelled equivalently by a tuple  $(H, \psi)$ , where  $H \subseteq \mathbb{Z}_2 \times \mathbb{Z}_2$  and  $\psi \in H^2(H, \text{U}(1))$ . The subgroups corresponding to each of the six Lagrangian subgroups are given in Table 1. The cohomology group  $H^2(\mathbb{Z}_2, \text{U}(1)) = \mathbb{Z}_1$ , while  $H^2(\mathbb{Z}_2 \times \mathbb{Z}_2, \text{U}(1)) = \mathbb{Z}_2$ . Therefore, there are two Lagrangian subgroups  $\mathcal{L}_5$  and  $\mathcal{L}_6$  corresponding to  $H = \mathbb{Z}_2 \times \mathbb{Z}_2$ . In particular,  $\mathcal{L}_5$  and  $\mathcal{L}_6$  are labelled by the non-trivial and trivial cohomology class in  $H^2(\mathbb{Z}_2 \times \mathbb{Z}_2, \text{U}(1))$ , respectively.

Having described the properties of the bulk  $\mathbb{Z}_2 \times \mathbb{Z}_2$  gauge theory that are of interest, we now analyze the phase diagram of 1D quantum systems with  $\mathbb{Z}_2 \times \mathbb{Z}_2$  global symmetry. As before, it is useful to have a quantum spin system in mind, both for concreteness as well as to be able to numerically verify various theoretical predictions. The effective spin chain is obtained at the boundary of a 2D  $G$  gauge theory defined on a semi-infinite cylinder. The Hilbert space of the 1D quantum system decomposes into a tensor product of local Hilbert spaces  $\mathcal{H}_i \simeq \mathbb{C}_L^2 \otimes \mathbb{C}_R^2$  assigned to the site  $i$ . The local operators acting on the spin chain are obtained by bringing minimal-length bulk line operators to the open boundary. The generators of  $\mathcal{A}[\mathbb{Z}_2 \times \mathbb{Z}_2]$  become the following operators when brought to the 1D boundary (see (3.27) and (3.28))

$$\begin{aligned} e_L &\longrightarrow \sigma_{i,L}^z \sigma_{i+1,L}^z, & m_L &\longrightarrow \sigma_{i,L}^x \\ e_R &\longrightarrow \sigma_{i,R}^z \sigma_{i+1,R}^z, & m_R &\longrightarrow \sigma_{i,R}^x. \end{aligned} \quad (5.68)$$

The symmetry generator is given by

$$\mathcal{U}_{\mathbf{g}_L, \mathbf{g}_R} = \bigotimes_i^L (\sigma_{i,L}^x)^{\mathbf{g}_L} \otimes (\sigma_{i,R}^x)^{\mathbf{g}_R}. \quad (5.69)$$

The fixed-point Hamiltonians corresponding to the different gapped phases can be read off from the generators of the corresponding Lagrangian subgroups. Note that some of the Lagrangian subgroups, in  $\mathcal{L}_4$  and  $\mathcal{L}_5$  are generated by dyons which are not in the generator set of  $\mathcal{A}[\mathbb{Z}_2 \times \mathbb{Z}_2]$ . We need to additionally specify the operators that are subtended on the boundary by corresponding minimal length bulk dyonic operators. The generators of  $\mathcal{L}_4$  can be immediately obtained by taking a product of generators of  $\mathcal{A}[\mathbb{Z}_2 \times \mathbb{Z}_2]$ , i.e.

$$e_L e_R \longrightarrow \sigma_{i,L}^z \sigma_{i,R}^z \sigma_{i+1,L}^z \sigma_{i+1,R}^z, \quad m_L m_R \longrightarrow \sigma_{i,L}^x \sigma_{i,R}^x. \quad (5.70)$$

The generators of  $\mathcal{L}_5$  require slight care such that the operators corresponding to  $e_L m_R$  commute with the operators corresponding to  $e_R m_L$  regardless of their location. For a more systematic construction of the spin chain and string operators see Appendix A. The minimal operators take the form

$$e_L m_R \longrightarrow \sigma_{i,L}^z \sigma_{i+1,L}^z \sigma_{i+1,R}^x, \quad m_L e_R \longrightarrow \sigma_{i,L}^x \sigma_{i,R}^z \sigma_{i+1,R}^z. \quad (5.71)$$

Having defined the set of operators, which correspond to the generators of each of the Lagrangian subgroups, we can straightforwardly write down the fixed-point Hamiltonian (3.36) for each of the gapped phases

$$\begin{aligned} H_1 &= - \sum_i [\sigma_{i,L}^z \sigma_{i+1,L}^z + \sigma_{i,R}^z \sigma_{i+1,R}^z], \\ H_2 &= - \sum_i [\sigma_{i,L}^x + \sigma_{i,R}^z \sigma_{i+1,R}^z], \\ H_3 &= - \sum_i [\sigma_{i,L}^z \sigma_{i+1,L}^z + \sigma_{i,R}^x], \\ H_4 &= - \sum_i [\sigma_{i,L}^z \sigma_{i,R}^z \sigma_{i+1,L}^z \sigma_{i+1,R}^z + \sigma_{i,L}^x \sigma_{i,R}^x], \\ H_5 &= - \sum_i [\sigma_{i,L}^z \sigma_{i+1,L}^z \sigma_{i+1,R}^x + \sigma_{i,L}^x \sigma_{i,R}^z \sigma_{i+1,R}^z], \\ H_6 &= - \sum_i [\sigma_{i,L}^x + \sigma_{i,R}^x]. \end{aligned} \quad (5.72)$$

From the point of view of the bulk topological order, the different gapped boundaries are characterized by condensation of anyons in their corresponding Lagrangian subgroups (3.37). To detect condensation of  $e_L$ ,  $e_R$ , and  $e_L e_R$ , we have the order parameters

$$\begin{aligned} S_{e_L}(i, j) &= \sigma_{i,L}^z \sigma_{j,L}^z, & S_{e_R}(i, j) &= \sigma_{i,R}^z \sigma_{j,R}^z, \\ S_{e_L e_R}(i, j) &= \sigma_{i,L}^z \sigma_{i,R}^z \sigma_{j,L}^z \sigma_{j,R}^z. \end{aligned} \quad (5.73)$$

A non-zero vacuum expectation-value for these operators for  $|i - j| \rightarrow \infty$  implies long-range spin-spin correlations and thus long-range order. Since these operators are bi-local,

the property of cluster decomposition of correlation functions induces genuinely local order parameters. Thus the local order parameters  $\sigma_{i,L}^z$ ,  $\sigma_{i,R}^z$  and  $\sigma_{i,L}^z \sigma_{i,R}^z$  can be used to detect the spontaneous symmetry-breaking. Holographically, the condensation of electric excitations, imply that the corresponding symmetry is broken. Similarly, the condensation of  $m_L$ ,  $m_R$ , and  $m_L m_R$  are detected by the condensation of the following string operators

$$\begin{aligned} S_{m_L}(i, j) &= \prod_{k=i}^j \sigma_{k,L}^x, & S_{m_R}(i, j) &= \prod_{k=i}^j \sigma_{k,R}^x, \\ S_{m_L m_R}(i, j) &= \prod_{k=i}^j \sigma_{k,L}^x \sigma_{k,R}^x. \end{aligned} \quad (5.74)$$

These are the disorder parameters, relative to the spin order parameters in (5.73). Thus the condensation of magnetic excitations imply that the corresponding symmetry is unbroken. Finally, the condensation of the dyons  $e_L m_R$  and  $m_L e_R$  for the gapped phase  $\mathcal{L}_5$  can be detected by

$$\begin{aligned} S_{e_L m_R}(i, j) &= \sigma_{i,L}^z \left( \bigotimes_{k=i+1}^j \sigma_{k,R}^x \right) \sigma_{j,L}^z, \\ S_{m_L e_R}(i, j) &= \sigma_{i,R}^z \left( \bigotimes_{k=i}^{j-1} \sigma_{k,L}^x \right) \sigma_{j,R}^z. \end{aligned} \quad (5.75)$$

These are the non-local string order-parameters for SPT phases [65, 176, 177]. Thus the condensation of dyonic excitations (for Lagrangian subgroups that are generated by dyonic generators) implies that the corresponding phase is an SPT phase. We emphasize that all order parameters for all possible gapped phases naturally emerge out of the holographic construction.

The next question is: what are the fundamental excitations of a given gapped phase? For example, consider the gapped phase  $\mathcal{L}_1$ . In this phase, the anyons in  $\mathcal{L}_1 = \{1, e_L, e_R, e_L e_R\}$  are condensed and become the order parameters (5.73), as explained above. On the other hand, it costs finite energy to create anyons that are confined on the boundary and thus such confined anyons correspond to excitations. However, any two anyon that differ by a condensed anyon correspond to identical boundary excitations. The equivalence classes of boundary excitations are thus given by

$$\begin{aligned} \phi_1^{\text{SSB}} &= \{1, e_L, e_R, e_L e_R\}, \\ \phi_{m_L}^{\text{SSB}} &= \{m_L, m_L e_L, m_L e_R, m_L e_L e_R\}, \\ \phi_{m_R}^{\text{SSB}} &= \{m_R, m_R e_L, m_R e_R, m_R e_L e_R\}, \\ \phi_{m_L m_R}^{\text{SSB}} &= \{m_L m_R, m_L m_R e_L, m_L m_R e_R, m_L m_R e_L e_R\}, \end{aligned} \quad (5.76)$$

Together  $\phi_1^{\text{SSB}}$ ,  $\phi_{m_L}^{\text{SSB}}$ ,  $\phi_{m_R}^{\text{SSB}}$  and  $\phi_{m_L m_R}^{\text{SSB}}$  are the objects of the category of excitations  $\text{Vec}_{\mathbb{Z}_2 \times \mathbb{Z}_2}$  within the gapped phase corresponding  $\mathcal{L}_1$ . Physically, these excitations are nothing but string operators (5.74) corresponding to  $m_L$ ,  $m_R$  and  $m_L m_R$ , i.e., the  $\mathbb{Z}_2 \times \mathbb{Z}_2$  symmetry operators restricted to a finite segment. Since the ground-state spontaneously breaks the  $\mathbb{Z}_2 \times \mathbb{Z}_2$  symmetry, these symmetry operators create domain-walls which are the familiar excitations within this phase. Similarly, the fundamental excitations within other gapped phases  $\mathcal{L}_i$  can be obtained straightforwardly.



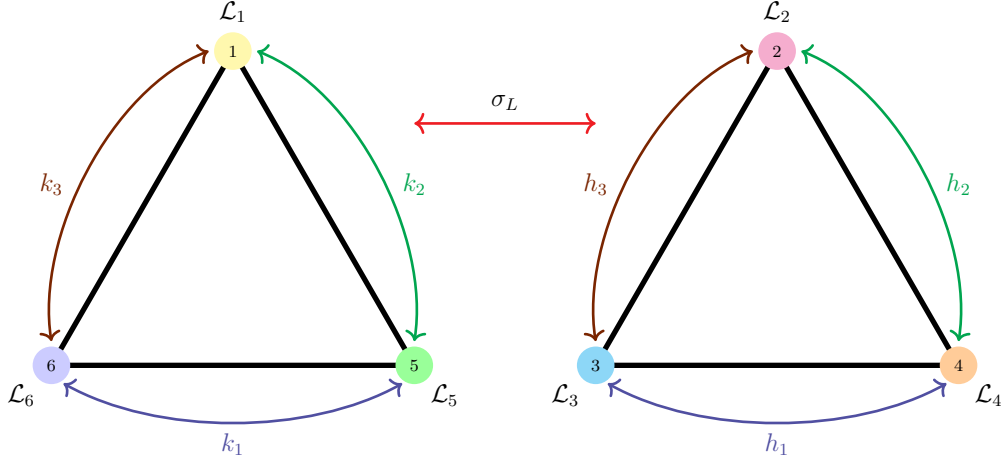


Figure 15: Duality mapping between different gapped phases. The gapped phases labelled by Lagrangian subgroups in the set  $T_2 = \{\mathcal{L}_1, \mathcal{L}_5, \mathcal{L}_6\}$  and  $T_1 = \{\mathcal{L}_2, \mathcal{L}_3, \mathcal{L}_4\}$  transform under duality subgroup  $S^3 = \langle k_1, k_2, k_3 \rangle$  (depicted in solid lines) and  $S^3 = \langle h_1, h_2, h_3 \rangle$  (depicted in dashed lines) respectively. The order two duality generator  $\sigma_L$  maps between the two sets.

### The minimal Hamiltonian and its phase diagram

A minimal Hamiltonian capable of accessing all the gapped phases arising within  $\mathbb{Z}_2^2$  symmetric quantum systems is obtained as a sum of the six fixed point Hamiltonians given in (5.72)

$$H(\lambda) = \sum_{a=1}^6 \lambda_a H_a. \quad (5.77)$$

The phase diagram of this model is parameterized by six real parameters  $\lambda_1, \dots, \lambda_6$ . We can develop an understanding of the topology of the phase diagram as well as the nature of transitions realized by using dualities inherited from the 0-form symmetry group  $\mathcal{G}[\mathbb{Z}_2 \times \mathbb{Z}_2]$  of the corresponding topological order.

The action of the duality group  $\mathcal{G}[\mathbb{Z}_2 \times \mathbb{Z}_2] = (S_3 \times S_3) \rtimes \mathbb{Z}_2$ , can be conveniently understood by partitioning the set of gapped phases into 2 disjoint subsets with Lagrangian subgroups  $T_1 = \{\mathcal{L}_2, \mathcal{L}_3, \mathcal{L}_4\}$  and  $T_2 = \{\mathcal{L}_1, \mathcal{L}_5, \mathcal{L}_6\}$ . The first  $S_3$  subgroup, generated by  $h_i$ ,  $i = 1, 2, 3$  (5.63), acts as the permutation of the three Lagrangian subgroups in  $T_1$  while leaving the Lagrangian subgroups in  $T_2$  invariant. The second  $S_3$  subgroup, generated by  $k_i$ ,  $i = 1, 2, 3$  (5.63), acts as the permutation of the three Lagrangian subgroups in  $T_2$  while leaving the Lagrangian subgroups in  $T_1$  invariant.

Finally, the transformation  $\sigma_L$ , which generates a  $\mathbb{Z}_2$  subgroup of  $\mathcal{G}[\mathbb{Z}_2 \times \mathbb{Z}_2]$ , acts via an outer automorphism on  $S_3 \times S_3$ , which exchanges the two copies of  $S_3$ . Naturally it also acts by exchanging the two sets of gapped phases,

$$\mathcal{L}_1 \xleftrightarrow{\sigma_L} \mathcal{L}_2, \quad \mathcal{L}_5 \xleftrightarrow{\sigma_L} \mathcal{L}_4, \quad \mathcal{L}_6 \xleftrightarrow{\sigma_L} \mathcal{L}_3. \quad (5.78)$$

From this, we see that the action of the duality group on the set of Lagrangian subgroups is geometrically the symmetries of two triangles (See Figure 15). One might wonder whether this abstract symmetry reflects a geometrical structure within the phase diagram. As discussed previously, these symmetries act on the set of anyons which induces an action on operators in the spin chain (3.46). In particular, the fixed-point Hamiltonians transform as their corresponding Lagrangian subgroups which in turn induces a permutation of coupling constants  $\lambda_a$  in (5.77).

In summary, the dualities of the Hamiltonian (5.77) for a fixed set of parameters  $\lambda_a$  are as follows: there is a dual Hamiltonian for (1) any permutation of  $\{\lambda_2, \lambda_3, \lambda_4\}$ , (2) any permutation of  $\{\lambda_1, \lambda_5, \lambda_6\}$ , and (3) any mapping of parameters between these sets. Since a six-dimensional phase diagram is hard to visualize, we will break it down to interesting subspaces. Let us focus on the three phases in  $T_1$  by setting  $\lambda_1 = \lambda_5 = \lambda_6 = 0$ ,

$$H_{T_1}(\lambda_2, \lambda_3, \lambda_4) = \lambda_2 H_2 + \lambda_3 H_3 + \lambda_4 H_4. \quad (5.79)$$

Here  $H_2, H_3$ , and  $H_4$  are the fixed-point Hamiltonian for the partially spontaneously-broken phases corresponding to  $\mathbf{H} = \mathbb{Z}_2^L$ ,  $\mathbf{H} = \mathbb{Z}_2^R$ , and  $\mathbf{H} = \mathbb{Z}_2^D$  (see Table 1 and equation (5.72)).

This Hamiltonian is dual to any other Hamiltonian related by a permutation of its coefficients. Since the overall scaling of the Hamiltonian has no physical consequences, we can express  $\lambda_2, \lambda_3$ , and  $\lambda_4$  in spherical coordinates [121]

$$\lambda_2 = \sin \theta \cos \phi, \quad \lambda_3 = \sin \theta \sin \phi, \quad \lambda_4 = \cos \theta. \quad (5.80)$$

For  $(\theta, \phi) = (\pi/2, 0)$ ,  $(\theta, \phi) = (\pi/2, \pi/2)$ , and  $(\theta, \phi) = (0, 0)$ , we get the fixed-point (exactly-solvable) Hamiltonians for the gapped phases  $\mathcal{L}_2$ ,  $\mathcal{L}_3$ , and  $\mathcal{L}_4$ , respectively. The quadrant of the sphere spanned by these three points has a particularly nice structure and is easiest visualized through projection of  $(\theta, \phi)$  onto the plane  $\lambda_2 + \lambda_3 + \lambda_4 = 1$ . Any point on this triangle corresponds to a particular set of parameters in the Hamiltonian (5.79), its corners are the fixed-point Hamiltonians and symmetry of the triangle maps parameters  $\lambda_a$  to dual parameters  $\lambda_a^\vee$ . We can use the properties of dualities described in Section 4 to sketch out a phase diagram. We assume that only the three gapped phases  $\mathcal{L}_2$ ,  $\mathcal{L}_3$ , and  $\mathcal{L}_4$  can appear in this  $2d$ -slice of the phase diagram.

Dualities are a powerful tool to make non-perturbative statement which constrain the possible phase diagram. A possible way of reasoning using dualities is as follows <sup>17</sup>

1. The center of the triangle is self-dual under  $S_3 \times S_3$ , thus it cannot be in any of the six gapped phases and must be a phase transition.
2. Note that

$$H_{T_1}(1, 1, 0) = - \sum_i [\sigma_{i,L}^x + \sigma_{i,L}^z \sigma_{i+1,L}^z + \sigma_{i,R}^x + \sigma_{i,R}^z \sigma_{i+1,R}^z], \quad (5.81)$$

is the Hamiltonian of the two decoupled copies of the critical Ising chain. Therefore, it is a second-order phase transition described by a conformal field theory with central

---

<sup>17</sup>For notational simplicity, we will parameterize Hamiltonians with points lying outside of the  $\lambda_2 + \lambda_3 + \lambda_4 = 1$  plane. However, through scaling, this parameterization is equivalent to the one for which  $\lambda_a$ s are lying on the plane.

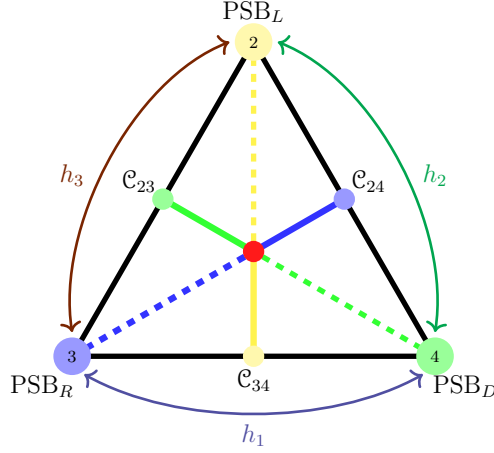


Figure 16: Illustration of a triangle on the plane  $\lambda_2 + \lambda_3 + \lambda_4 = 1$  and  $\lambda_1 = \lambda_5 = \lambda_6 = 0$ . The  $S_3$  subgroup of dualities generated  $h_1, h_2$ , and  $h_3$  acts on the Hamiltonians in this region as the symmetries of the triangle. The colored lines correspond to self-dual points under the various reflections while the red point is self-dual under the full  $S_3$  subgroup.

charge  $c = 1$  and nine primary fields corresponding to pair-wise combinations of Ising primaries  $\mathbb{I}$ ,  $\epsilon$ , and  $\sigma$  with conformal weights  $(0, 0)$ ,  $(\frac{1}{2}, \frac{1}{2})$ , and  $(\frac{1}{16}, \frac{1}{16})$ , respectively. This corresponds to the point  $\mathcal{C}_{23}$  in Figure 16. By duality, this point is mapped to the points  $\mathcal{C}_{24}$  and  $\mathcal{C}_{34}$ . From the properties discussed in Section 4, these two other points must therefore also be critical with central charge  $c = 1$ .

3. The corners of the triangle are fixed-point Hamiltonians and thus are guaranteed to be gapped. The line that goes from the  $\mathcal{L}_2$  corner to  $\mathcal{C}_{34}$  is self-dual under the reflection of the triangle that swaps  $\mathcal{L}_3$  and  $\mathcal{L}_4$ . Due to this self-duality, only the gapped phase  $\mathcal{L}_2$  or a phase-transition is allowed on this line. Repeating this argument for the other reflection-self-dual lines in Figure 16, it is reasonable to expect that the dashed parts of the lines are gapped while the solid parts are phase-transitions, either first-order or second-order.
4. At the Ising<sup>2</sup> transition  $\mathcal{C}_{23}$ , there exist a spinless marginal operator  $\epsilon_L \epsilon_R$  with conformal weight  $(1, 1)$ . Deforming the theory with this marginal operator

$$S(\lambda) = S_{\text{Ising}^2} + \lambda \int d^2z \epsilon_L(z) \epsilon_R(z), \quad (5.82)$$

it remains conformal and all scaling dimensions change continuously as long as the  $\epsilon_L \epsilon_R$  perturbation remains marginal. On the spin-chain level, this corresponds to deforming the theory (5.81) from  $\mathcal{C}_{23}$  towards the center of the triangle  $\mathcal{C}_{234}$

$$H_{T_1}(1, 1, \lambda) = H_{T_1}(1, 1, 0) - \lambda \sum_i [\sigma_{i,L}^z \sigma_{i,R}^z \sigma_{i+1,L}^z \sigma_{i+1,R}^z + \sigma_{i,L}^x \sigma_{i,R}^x]. \quad (5.83)$$

Assuming that this line remains marginal until the center, the solid parts of the lines in Figure 16 must be critical with  $c = 1$ .

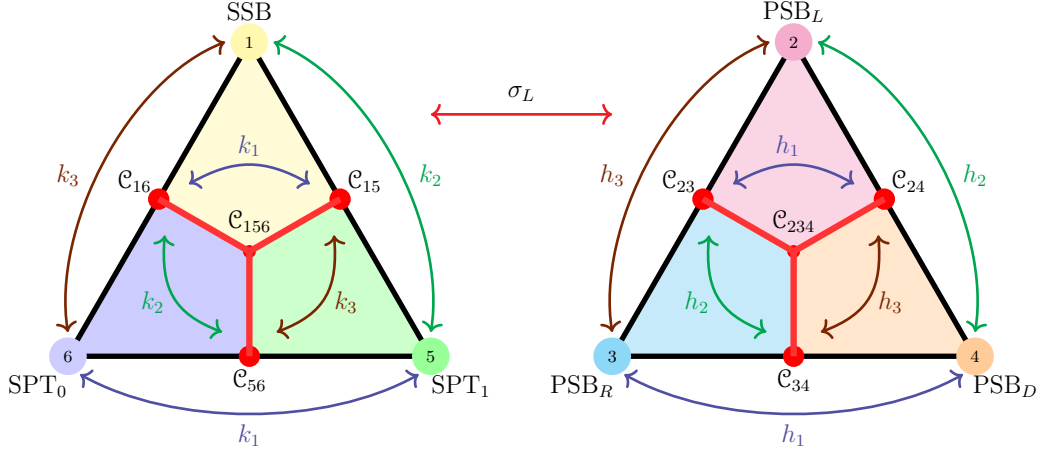


Figure 17: Phase diagram on two different planes in the six-dimensional parameter space ( $T_1$  on the right and  $T_2$  on the left). The edges of the triangles are gapped fixed points, the colored regions are gapped phases, while the red points and lines are  $c = 1$  critical transitions.

Note that the same arguments can be made for the triangle  $T_2$ , though the triangle now lives on the plane  $\lambda_2 = \lambda_3 = \lambda_4 = 0$  within the six-dimensional phase-diagram

$$H_{T_2}(\lambda_1, \lambda_5, \lambda_6) = \lambda_1 H_1 + \lambda_5 H_5 + \lambda_6 H_6. \quad (5.84)$$

A possible phase diagram based on these arguments is shown in Figure 17, where the red lines correspond to a critical line described by  $c = 1$  conformal field theories and the colored regions are the various gapped phases. The  $\mathcal{C}_{56}$  transition corresponds to a critical point that goes beyond the Landau paradigm, since such a transition ought to be “Landau-forbidden” [178, 179]. However, here the “Landau-allowed” and “Landau-forbidden” transitions appear on an equal footing. In particular, there is a duality-mapping between Ising<sup>2</sup> transitions  $\mathcal{C}_{16}$  or  $\mathcal{C}_{23}$  to the topological criticality  $\mathcal{C}_{56}$ , which we will exploit to compute the exact conformal spectrum of this transition shortly.

So far, we have constructed a potential phase diagram on two different planes in six-dimensional parameter space. We can in principle go beyond this and explore other regions in the phase diagram. Dualities prove useful in this regard as well. Let us look at the known critical point  $\mathcal{C}_{23}$ . The only  $\mathbb{Z}_2 \times \mathbb{Z}_2$  symmetric relevant operators at this critical point are  $\epsilon_L$  and  $\epsilon_R$  both with conformal weight  $(\frac{1}{2}, \frac{1}{2})$ , which can be thought of as energy-density operators of the form

$$\begin{aligned} \epsilon_L &\sim \sigma_{i,L}^z \sigma_{i+1,L}^z - \sigma_{i,L}^x, \\ \epsilon_R &\sim \sigma_{i,R}^z \sigma_{i+1,R}^z - \sigma_{i,R}^x. \end{aligned} \quad (5.85)$$

The relative sign comes from the fact that  $\epsilon \rightarrow -\epsilon$  under Kramers-Wannier duality. Perturbing the  $\mathcal{C}_{23}$  critical point (5.81) with these two relevant operators

$$H = H_{T_1}(1, 1, 0) + \delta_L \sum_i [\sigma_{i,L}^z \sigma_{i+1,L}^z - \sigma_{i,L}^x] + \delta_R \sum_i [\sigma_{i,R}^z \sigma_{i+1,R}^z - \sigma_{i,R}^x], \quad (5.86)$$

we see that this flows to four different gapped phases; (1)  $\text{PSB}_L$  ( $\delta_L < 0$ ,  $\delta_R > 0$ ), (2)  $\text{PSB}_R$  ( $\delta_L > 0$ ,  $\delta_R < 0$ ), (3)  $\text{SSB}$  ( $\delta_L > 0$ ,  $\delta_R > 0$ ), (4)  $\text{SPT}_0$  ( $\delta_L < 0$ ,  $\delta_R < 0$ ). Thus,

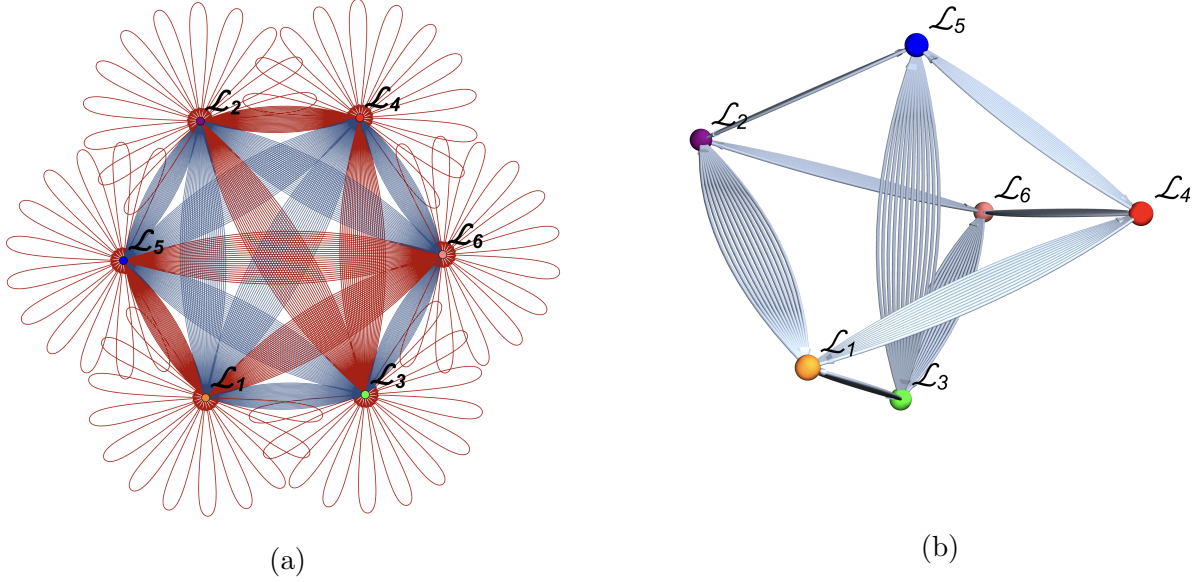


Figure 18: (a) The web of dualities of  $G = \mathbb{Z}_2 \times \mathbb{Z}_2$ . Nodes correspond to gapped phases while lines denote the action of dualities on gapped phases. The highlighted red lines correspond to order-3 dualities, revealing the asymmetry amongst the six phases. (b) The visualization of order-4 dualities.

$\mathcal{C}_{23}$  is a multi-critical point between four phases and only the first two transitions lie on the plane. This analysis is done purely using decoupled Ising chains, but all other critical points related to  $\mathcal{C}_{23}$  by duality, will also be multicritical points with two relevant operators. Therefore, the gapped phases of the two triangles meet in the region between the triangles. The structure of the region interpolating between triangles can be further constrained using dualities. For example, consider the following plane in (5.77)

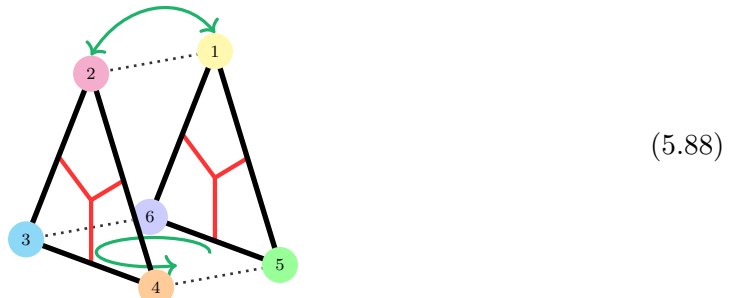
$$H(\lambda, \tilde{\lambda}, \tilde{\lambda}, \tilde{\lambda}, \lambda, \lambda) = \lambda(H_1 + H_5 + H_6) + \tilde{\lambda}(H_2 + H_3 + H_4). \quad (5.87)$$

Since the overall scaling does not matter, without loss of generality, we will restrict ourselves to the line  $\lambda + \tilde{\lambda} = 1$ . This line is self-dual under  $S_3 \times S_3$  and the center point  $\lambda = \tilde{\lambda} = \frac{1}{2}$  is self-dual under the full duality group  $(S_3 \times S_3) \rtimes \mathbb{Z}_2$ . Since no gapped phase is self-dual under these subgroups, the whole line must correspond to phase transitions. In particular, note that this line interpolates between the critical points  $\mathcal{C}_{156}$  ( $\lambda = 1, \tilde{\lambda} = 0$ ) and  $\mathcal{C}_{234}$  ( $\lambda = 0, \tilde{\lambda} = 1$ ). Therefore, the centers of the two triangles (see Figure 17) are connected by a critical line and the center of the line  $\mathcal{C}_{123456}$  is a multi-critical point connecting all gapped phases (see Figure 19).

One might wonder whether there exist other  $S_3$  subgroups of dualities permuting three different gapped phases and thus creating a similar structure in the phase diagram as in Figure 17. This possibility can be excluded by examining the web of dualities shown in Figure 18a where the action of dualities on the six gapped phases are illustrated by lines. The red lines correspond to order-3 group elements, from which, it is clear that any other  $S_3$  subgroup connect the same sets of gapped phases.

In Figure 18b, we have illustrated the action of order-4 elements. These order-4 elements

map between corners of one triangle and the corners of the other triangle, and thus establish connections between the triangles. They are part of  $D_4$  subgroups of dualities which are symmetries of squares. One example is as follows



where  $\mathcal{L}_3, \mathcal{L}_4, \mathcal{L}_5$ , and  $\mathcal{L}_6$  form a square. There exists a  $D_4$  subgroup corresponding to the symmetries of this square ( $D_4$  contains two order 4 elements, pure rotation and reflection-rotation). The two other gapped boundaries just map onto each other under these  $D_4$  dualities, thus no gapped phase is self-dual under these dualities. There are 18 order 4 dualities, corresponding to the 9 different possible squares we can form between the corners of the triangles.

We can use self-duality to find critical points between the two triangles. For example, consider these Hamiltonians that are self-dual under a  $\mathbb{Z}_2 \subset D_4$  that swap  $i \leftrightarrow j$  corners between the two triangles

$$H_{ij} = H_i + H_j, \quad i = 2, 3, 4, \quad j = 1, 5, 6. \quad (5.89)$$

In particular, consider  $H_{21}$  which is nothing but a critical Ising chain with  $c = \frac{1}{2}$  coupled to a trivially-gapped chain. Between any pair of gapped phases of the two triangles, there is a  $c = \frac{1}{2}$  transition, self-dual under various  $\mathbb{Z}_2$  dualities. One can think of the interpolation of the two triangles in Figure 17 in different ways. Consider  $H_{36}$  and  $H_{45}$ : there exists a plane with a triangle with the  $c = \frac{1}{2}$  transitions  $H_{36}$  and  $H_{45}$  as two of the corners and  $\mathcal{C}_{123456}$  its center. The last corner is gapped (the transition exists, but on a rotated plane). This plane can for example be parametrized using Hamiltonian (5.77) as

$$\begin{pmatrix} \lambda_1 \\ \lambda_2 \\ \lambda_3 \\ \lambda_4 \\ \lambda_5 \\ \lambda_6 \end{pmatrix} = \begin{pmatrix} a + b - 1 \\ a + b - 1 \\ a \\ a \\ b \\ b \end{pmatrix}, \quad (5.90)$$

where  $(a, b) = (1, 0)$  and  $(a, b) = (0, 1)$  are the two  $c = \frac{1}{2}$  points and  $(a, b) = (1, 1)$  is  $\mathcal{C}_{123456}$ . The  $c = 1$  point  $\mathcal{C}_{123456}$  is therefore surrounded by  $c = \frac{1}{2}$  points, corresponding to various different interpolations between the two triangles in the six-dimensional space. See figure 19. Furthermore, there are also points that are self-dual under the full  $D_4$  subgroup corresponding to the square formed by  $i_1, i_2, j_1, j_2$

$$H_{i_1 i_2, j_1 j_2} = H_{i_1} + H_{i_2} + H_{j_1} + H_{j_2}, \quad \begin{aligned} i_1, i_2 &= 2, 3, 4, \\ j_1, j_2 &= 1, 5, 6. \end{aligned} \quad (5.91)$$

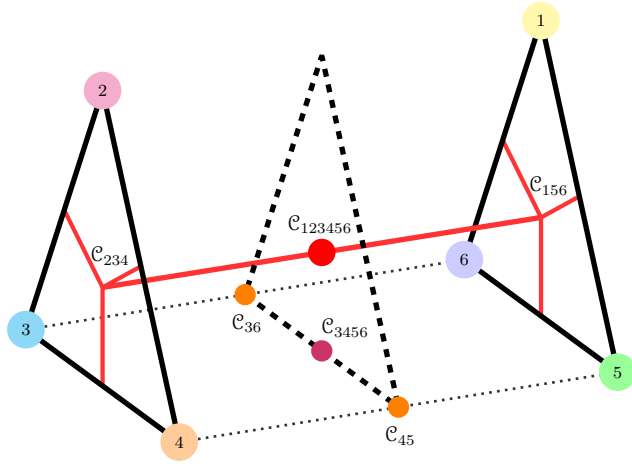


Figure 19: Sketch of critical lines in the six-dimensional parameter space for (5.77). All red lines correspond to  $c = 1$  conformal field theories. The lines on the left triangle are self-dual under the subgroup of dualities  $\mathbb{Z}_2 \times S_3$ , generated by  $h_1, h_2, h_3$  and one single  $k_i$  (depending on line). The red lines on the right triangle are self-dual under  $S_3 \times \mathbb{Z}_2$ , with  $k$  and  $h$  swapped. The line between the triangles correspond to (5.87) and is self-dual under  $S_3 \times S_3$  while the point  $\mathcal{C}_{123456}$  is self-dual under the full duality group  $\mathcal{G}[\mathbb{Z}_2 \times \mathbb{Z}_2] = (S_3 \times S_3) \rtimes \mathbb{Z}_2$ . This fully self-dual point is a multicritical point connecting all six gapped phases. The orange points are self-dual under  $\mathbb{Z}_2$  subgroups that map between the triangles and correspond to  $c = \frac{1}{2}$  transitions. There is such a transition in the six-dimensional parameter space between any two gapped phases belonging to different triangles. These  $c = \frac{1}{2}$  transitions lie pairwise on triangles (dashed lines) around the fully self-dual point. Finally, the point  $\mathcal{C}_{3456}$  is self-dual under the  $D_4$  symmetry of the bottom square. This is a multi-critical point between four gapped phases. There are nine such critical points around  $\mathcal{C}_{123456}$ , corresponding to the different squares. Although it is not illustrated in the figure, the line connecting the bottom critical points of the two triangles through  $\mathcal{C}_{3456}$  is also critical. Crossing the center triangles along different regions also lead to transitions.

This critical point  $\mathcal{C}_{3456}$  also lies on the plane (5.90) with  $(a, b) = (\frac{1}{2}, \frac{1}{2})$  (see Figure 19) and its central charge is  $c = 1$ .

As discussed in section 3.8, self-dual Hamiltonians will have new emergent symmetries. For example, this implies that the gapped and gapless Hamiltonians along the self-dual lines in Figure 16 should have emergent symmetries. In particular, let us consider the line from  $\mathcal{C}_{23}$  to  $\mathcal{C}_{234}$  (the Hamiltonian in (5.83)), which is self-dual under  $h_3$ . This Hamiltonian is clearly symmetric under  $\mathcal{U}_L = \prod_i \sigma_{i,L}^x$ ,  $\mathcal{U}_R = \prod_i \sigma_{i,R}^x$ , and  $h_3$ , which swaps the two chains. Together, these form the enhanced symmetry group  $D_4$ . Furthermore, the Hamiltonian is self-dual under  $\sigma_L \sigma_R$ , which is nothing but a simultaneous Kramers-Wannier duality on both chains. These further enhance the symmetries with non-invertible symmetries, as discussed in section 3.8. In fact, the specific Hamiltonian (5.83) is nothing but the Ashkin-Teller model where it is known to have  $D_4$  global symmetry. For  $\lambda \in [0, 1]$ , the model is in



the universality class of the  $c = 1$   $\mathbb{Z}_2$ -orbifold compact boson CFT with orbifold radius

$$R_O^2 = \frac{\pi}{2} [\arccos(-\lambda)]^{-1}. \quad (5.92)$$

For  $\lambda = 0$ ,  $R_O = 1$ , which corresponds to the Ising<sup>2</sup> point [180], while  $\lambda = 1$  corresponds to  $R_O = 1/\sqrt{2}$ , known as the KT point.

Topological holography implies that there are many more emergent symmetries in these models. We will explore these emergent non-invertible symmetries further in [160].

## Numerical verification of phase diagram

So far, we have used dualities to construct a potential phase diagram for the minimal  $\mathbb{Z}_2 \times \mathbb{Z}_2$  symmetric lattice Hamiltonian. Since topological holography provides us with various tools such as order parameters for each gapped phase, we can numerically verify the proposed phase diagram. We have performed DMRG calculations on the Hamiltonian (5.77) and computed various order parameters on the planes of the triangles 17. We numerically computed the three order parameters that can distinguish the three gapped phases of the triangle  $T_1$  in Figure 17 and the results are shown in Figure 20. Each gapped phase has two order parameters but we only shown the simplest ones as they are enough to distinguish phases. The points on the triangles denote parameters of the Hamiltonian (5.79) on the plane  $\lambda_2 + \lambda_3 + \lambda_4 = 1$ , and the color denotes the value of correlation function. We clearly see that the order parameters associated to each gapped phase is equal to 1 (or non-zero) in the predicted gapped regions of Figure 17. From the point of view of topological order, the non-zero expectation values of the order parameters correspond to the condensation of various anyons in the Lagrangian subgroups for the given gapped phase.

Along the predicted gapless lines, there is faint silhouette in the numerical calculation of Figure 20. These are again consistent with the predictions as the DMRG algorithm converges slower near critical points. We further verify these critical lines by computing their entanglement entropy and extracting their central charge using the Cardy Formula [182]

$$S_L(x) = \frac{c}{3} \left[ \frac{L}{\pi} \sin \left( \frac{\pi x}{L} \right) \right] + C'. \quad (5.93)$$

Here,  $L$  is the length of the chain,  $x$  is the entanglement cut,  $c$  is the central charge, and  $C'$  is a non-universal constant. This formula holds for periodic boundary conditions. DMRG converges slower for periodic boundary conditions but for the computation of central charge, it is known to converge faster. We have computed the entanglement entropy along two lines: (1) from  $\mathcal{C}_{23}$  to the center of the triangle  $\mathcal{C}_{234}$  and then a bit further out, and (2) the line between the centers of the two triangles  $\mathcal{C}_{234}$  and  $\mathcal{C}_{156}$ , as described below (5.87) (see figure 19). In Figure 21, the numerically-computed value of the central charge is shown along these two lines. We see that  $c$  is equal to 1 to high level of accuracy, exactly in the regions predicted. As an example of how these values are extracted from entanglement entropy, the entropy of the fully  $(S_3 \times S_3) \rtimes \mathbb{Z}_2$  self-dual point  $\mathcal{C}_{123456}$  ( $\lambda = \tilde{\lambda} = \frac{1}{2}$  in (5.87)) is shown in figure 22.



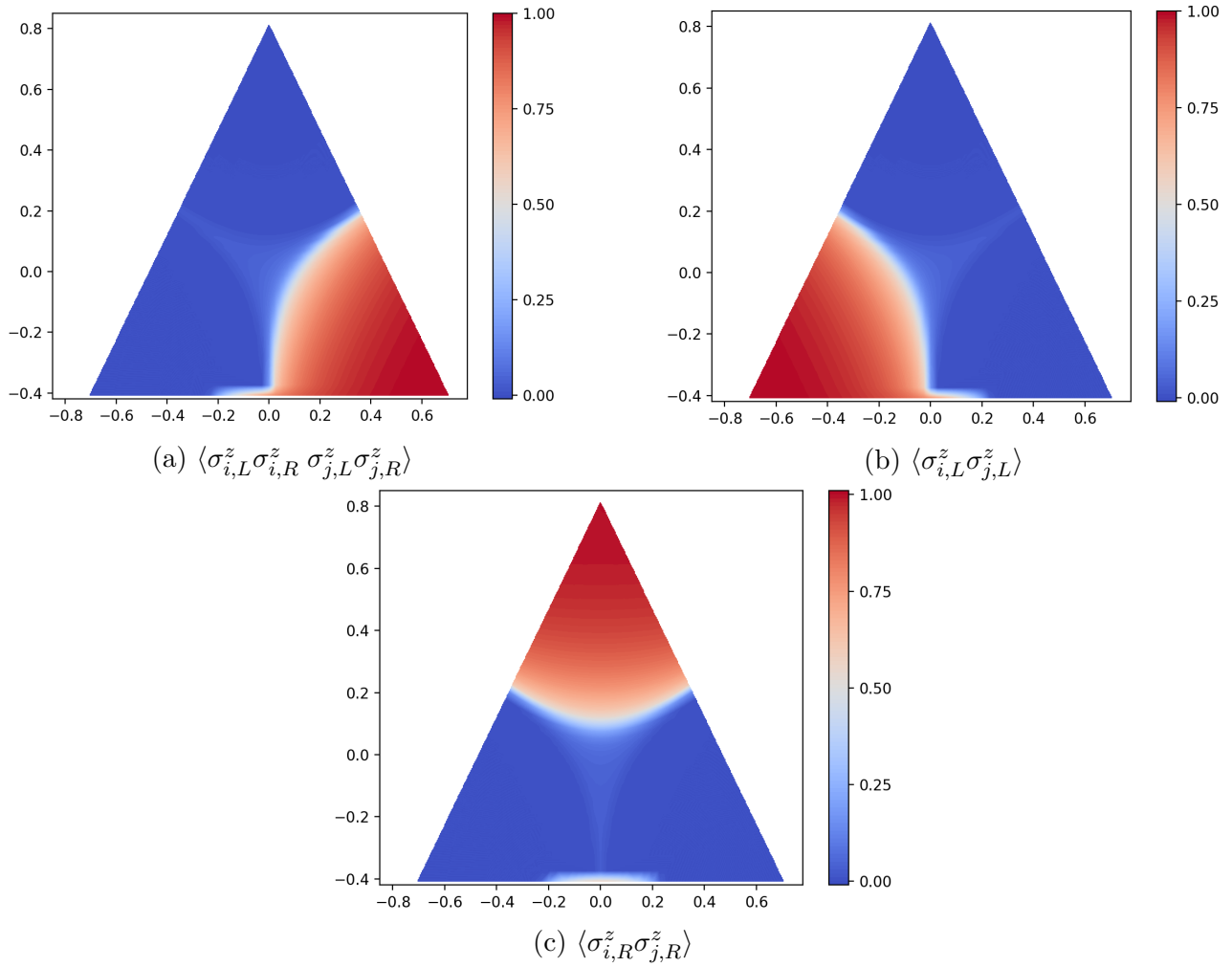


Figure 20: Numerical calculation of correlation functions of (5.79) on the plane  $\lambda_2 + \lambda_3 + \lambda_4 = 1$  ( $0 \leq \lambda_i \leq 1$ ) using DMRG algorithm. The code was implemented in **Julia** using **iTensor** library [181]. The simulation was done on a spin chain with  $N = 2 \times 100$  spin- $\frac{1}{2}$  sites with open boundary conditions. In order to avoid cat states in spontaneously-broken phase due to finite-size effects, the symmetry was weakly-broken at the boundary using a small pinning field with strength  $\eta < 0.05$ . In order to capture long-range correlations while avoiding boundary effects, we chose  $|i - j| = \frac{1}{2}L$ .

### Conformal spectrum of critical points

In the previous sections, using topological holography, we constructed a potential phase diagram and verified its gapped and critical regions numerically. In this section, we will further use the vast web of dualities to compute the full conformal spectra of various transitions.

Let us remind the reader of the logic of Section 4.3 in a simpler setting. The generalized

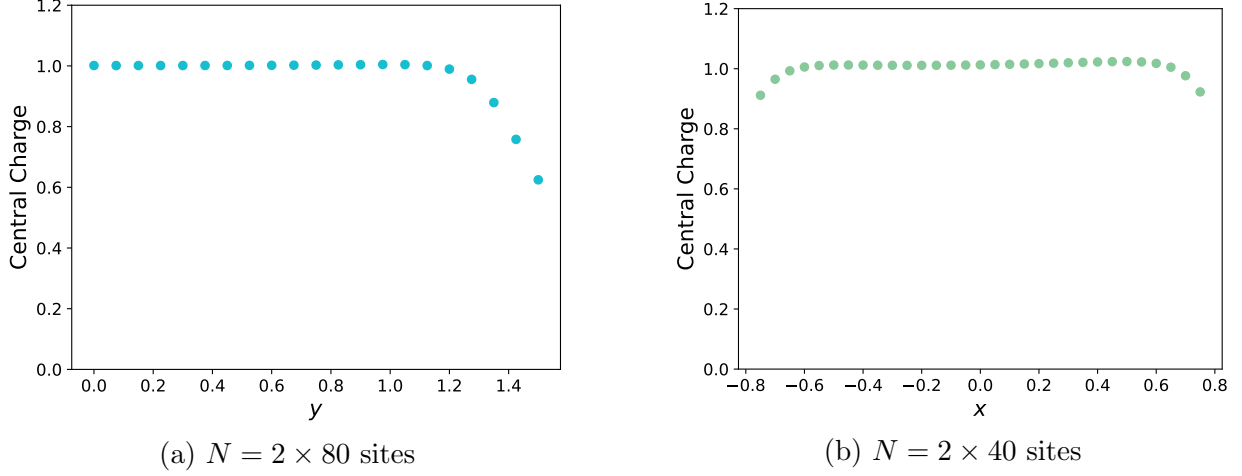


Figure 21: Numerical computation of the central charge along two different lines: (a) the line inside a triangle, from  $\mathcal{C}_{23}$  ( $y = 0$ ) to the center of the triangle  $\mathcal{C}_{234}$  ( $y = 1$ ) and then a bit further out, and (2) the line between the centers of the two triangles  $\mathcal{C}_{234}$  ( $x = -0.5$ ) and  $\mathcal{C}_{156}$  ( $x = 0.5$ ). The point  $x = 0$  is the fully self-dual point  $\mathcal{C}_{123456}$ . In the gapped regions near criticality we have  $c = 0$ , but see a decay on these plots due to finite-size effects and slow convergence of the DMRG algorithm.

twisted partition functions of the Hamiltonian (5.77) are given by

$$\begin{aligned} \mathcal{Z}_{\mathbf{g},\mathbf{h}}(\lambda) &= \text{Tr}_{\mathcal{H}} \left( \mathcal{U}_{\mathbf{h}} e^{-\beta H_{\mathbf{g}}(\lambda)} \right) \\ &= \sum_{\alpha_L, \alpha_R=0}^1 e^{i\pi[\alpha_L \mathbf{h}_L + \alpha_R \mathbf{h}_R]} \chi_{d=(\mathbf{g},\alpha)}(\lambda), \end{aligned} \quad (5.94)$$

where  $\mathbf{g} = (\mathbf{g}_L, \mathbf{g}_R)$  and  $\mathbf{h} = (\mathbf{h}_L, \mathbf{h}_R)$  are  $\mathbb{Z}_2 \times \mathbb{Z}_2$  elements corresponding to inserting a symmetry line-operator along time and space directions, respectively.  $H_{\mathbf{g}}(\lambda)$  is the Hamiltonian with twisted boundary condition  $\mathbf{g}$  and  $\mathcal{U}_{\mathbf{h}}$  is the symmetry operator. There is a sector for each bulk anyon  $d = (\mathbf{g}, \alpha) \in \mathcal{A}$  corresponding to twisted boundary condition  $\mathbf{g}$  and symmetry sector  $\alpha$  and the spectrum in this sector is given by the character  $\chi_d(\lambda)$ . Under a duality  $\sigma \in \mathcal{G}[\mathbb{Z}_2 \times \mathbb{Z}_2] = (S_3 \times S_3) \rtimes \mathbb{Z}_2$ , the characters transform as

$$\chi_d(\lambda) = \text{Tr}_{\mathcal{H}} \left[ P_{\alpha} e^{-\beta H_{\mathbf{g}}(\lambda)} \right] = \text{Tr}_{\mathcal{H}} \left[ P_{\alpha^{\vee}} e^{-\beta H_{\mathbf{g}^{\vee}}(\sigma \cdot \lambda)} \right] = \chi_{\sigma \cdot d}^{\vee}(\sigma \cdot \lambda), \quad (5.95)$$

where  $\sigma \cdot \lambda$  corresponds to the permuted parameters under duality. Therefore, knowing the spectrum in all twisted sectors at the point  $\lambda$ , we can compute the spectrum at the point  $\sigma \cdot \lambda$  using dualities. Using this, we can also compute the partition function for the dual theory using (4.22) and (4.24).

Let us start with the critical point  $\mathcal{C}_{16}$  between the ferromagnetic (fully-broken) and paramagnetic (unbroken) gapped phases which is described by two decoupled critical Ising chains. The generalized twisted partition functions of a single Ising CFT is given by [88, 165]

$$\begin{aligned} \mathcal{Z}_{0,0}^{\text{Ising}} &= |\chi_0|^2 + |\chi_{\frac{1}{2}}|^2 + |\chi_{\frac{1}{16}}|^2, & \mathcal{Z}_{1,0}^{\text{Ising}} &= \chi_0 \bar{\chi}_{\frac{1}{2}} + \chi_{\frac{1}{2}} \bar{\chi}_0 + |\chi_{\frac{1}{16}}|^2, \\ \mathcal{Z}_{0,1}^{\text{Ising}} &= |\chi_0|^2 + |\chi_{\frac{1}{2}}|^2 - |\chi_{\frac{1}{16}}|^2, & \mathcal{Z}_{1,1}^{\text{Ising}} &= |\chi_{\frac{1}{16}}|^2 - \chi_0 \bar{\chi}_{\frac{1}{2}} - \chi_{\frac{1}{2}} \bar{\chi}_0, \end{aligned} \quad (5.96)$$

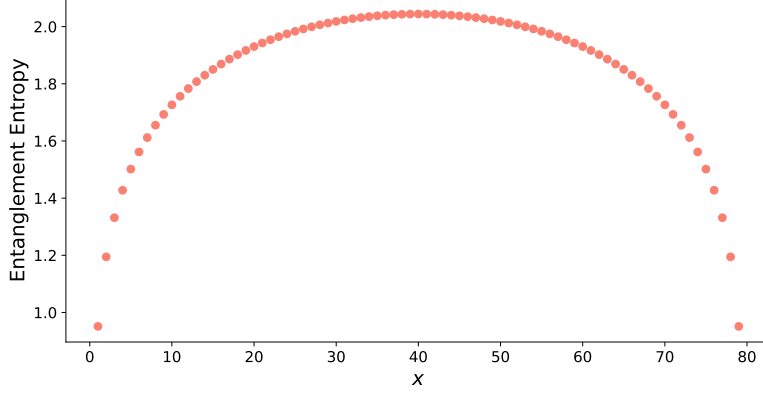


Figure 22: Numerical computation of entanglement entropy for the fully  $\mathcal{G}[\mathbb{Z}_2 \times \mathbb{Z}_2] = (S_3 \times S_3) \rtimes \mathbb{Z}_2$  self-dual point (equation (5.87) for  $\lambda = \tilde{\lambda}$ ), using DMRG. The spin-chain has  $N = 2 \times 80$  sites with periodic boundary conditions. When fitted to the function (5.93), we find the central charge  $c \approx 1.0040$ .

and the  $\mathbb{Z}_2$  characters in terms of the Virasoro characters are given by

$$\begin{aligned} \chi_1^{\text{Ising}} &= |\chi_0|^2 + |\chi_{\frac{1}{2}}|^2, & \chi_e^{\text{Ising}} &= |\chi_{\frac{1}{16}}|^2, \\ \chi_m^{\text{Ising}} &= |\chi_{\frac{1}{16}}|^2, & \chi_{em}^{\text{Ising}} &= \chi_0 \bar{\chi}_{\frac{1}{2}} + \chi_{\frac{1}{2}} \bar{\chi}_0. \end{aligned} \quad (5.97)$$

The generalized twisted partition functions at  $\mathcal{C}_{16}$  are thus given by

$$\mathcal{Z}_{\mathbf{g}, \mathbf{h}}(\mathcal{C}_{16}) = \mathcal{Z}_{\mathbf{g}_L, \mathbf{h}_L}^{\text{Ising}} \times \mathcal{Z}_{\mathbf{g}_R, \mathbf{h}_R}^{\text{Ising}}. \quad (5.98)$$

Similarly, the  $\mathbb{Z}_2 \times \mathbb{Z}_2$  characters can be written in terms of Virasoro characters as

$$\chi_{d=(\mathbf{g}, \alpha)}(\mathcal{C}_{16}) = \chi_{\mathbf{g}_L, \alpha_L}^{\text{Ising}} \times \chi_{\mathbf{g}_R, \alpha_R}^{\text{Ising}}. \quad (5.99)$$

The partition function and spectrum of any critical point related to  $\mathcal{C}_{16}$  by duality can be readily computed using the above data.

To illustrate our approach, we use this transition and the duality maps  $k_2$  and  $k_1$  to obtain the universality classes of the  $\mathcal{C}_{56}$  and  $\mathcal{C}_{15}$  transitions, respectively (see Figure 17). Since the duality operation  $k_2$  leaves  $\mathcal{L}_6$  invariant and maps  $\mathcal{L}_1$  and  $\mathcal{L}_5$  into each other, it maps between  $\mathcal{C}_{16}$  and  $\mathcal{C}_{56}$ . Similarly,  $k_1$  leaves  $\mathcal{L}_1$  invariant and maps  $\mathcal{L}_6$  and  $\mathcal{L}_5$  into each other, therefore it maps  $\mathcal{C}_{16}$  and  $\mathcal{C}_{15}$  into each other. Denoting the  $\mathbb{Z}_2 \times \mathbb{Z}_2$  characters at the transition  $\mathcal{C}_{ij}$  as  $\chi_d(\mathcal{C}_{ij})$  with  $d \in \mathcal{A}[\mathbb{Z}_2 \times \mathbb{Z}_2]$  we have the relations

$$\chi_d(\mathcal{C}_{56}) = \chi_{k_2(d)}(\mathcal{C}_{16}), \quad \chi_d(\mathcal{C}_{15}) = \chi_{k_1(d)}(\mathcal{C}_{16}) \quad (5.100)$$

From (5.97), the characters of these two transitions can be immediately read off. They take the following explicit form for the  $\mathcal{C}_{56}$  transition

$$\begin{aligned}
\chi_1(\mathcal{C}_{56}) &= \chi_1(\mathcal{C}_{16}) = (|\chi_0|^2 + |\chi_{\frac{1}{2}}|^2)^2, \\
\chi_{e_L}(\mathcal{C}_{56}) &= \chi_{e_L m_R}(\mathcal{C}_{16}) = (|\chi_{\frac{1}{16}}|^2)^2, \\
\chi_{e_R}(\mathcal{C}_{56}) &= \chi_{e_R m_L}(\mathcal{C}_{16}) = (|\chi_{\frac{1}{16}}|^2)^2, \\
\chi_{m_L}(\mathcal{C}_{56}) &= \chi_{m_L}(\mathcal{C}_{16}) = |\chi_{\frac{1}{16}}|^2 (|\chi_0|^2 + |\chi_{\frac{1}{2}}|^2), \\
\chi_{m_R}(\mathcal{C}_{56}) &= \chi_{m_R}(\mathcal{C}_{16}) = |\chi_{\frac{1}{16}}|^2 (|\chi_0|^2 + |\chi_{\frac{1}{2}}|^2),
\end{aligned} \tag{5.101}$$

etc., and similarly for the  $\mathcal{C}_{15}$  transition

$$\begin{aligned}
\chi_1(\mathcal{C}_{15}) &= \chi_1(\mathcal{C}_{16}) = (|\chi_0|^2 + |\chi_{\frac{1}{2}}|^2)^2, \\
\chi_{e_L}(\mathcal{C}_{15}) &= \chi_{e_L}(\mathcal{C}_{16}) = |\chi_{\frac{1}{16}}|^2 (|\chi_0|^2 + |\chi_{\frac{1}{2}}|^2), \\
\chi_{e_R}(\mathcal{C}_{15}) &= \chi_{e_R}(\mathcal{C}_{16}) = |\chi_{\frac{1}{16}}|^2 (|\chi_0|^2 + |\chi_{\frac{1}{2}}|^2), \\
\chi_{m_L}(\mathcal{C}_{15}) &= \chi_{m_L e_R}(\mathcal{C}_{16}) = (|\chi_{\frac{1}{16}}|^2)^2, \\
\chi_{m_R}(\mathcal{C}_{15}) &= \chi_{m_R e_L}(\mathcal{C}_{16}) = (|\chi_{\frac{1}{16}}|^2)^2.
\end{aligned} \tag{5.102}$$

Note that the identity sector  $\chi_1$  is invariant under all dualities since dualities descend from global symmetries of the  $\mathbf{G}$  topological gauge theory under which the identity (transparent) line operator always remains invariant. We can also explicitly compute the exact partition functions of these critical points using (4.22). For example, the partition function of the critical point  $\mathcal{C}_{56}$  for, say, periodic boundary condition, is given by

$$\mathcal{Z}_{(0,0),(0,0)}(\mathcal{C}_{56}) = \frac{1}{4} \sum_{\substack{\mathbf{h}_L, \mathbf{h}_R \\ \alpha'_L, \alpha'_R}} (-1)^{-\alpha'_L \mathbf{h}_L - \alpha'_R \mathbf{h}_R} \mathcal{Z}_{\alpha'_R, \alpha'_L}^{\text{Ising}} \mathcal{Z}_{\mathbf{h}_L, \mathbf{h}_R}^{\text{Ising}}. \tag{5.103}$$

Substituting Ising partition functions in terms of Virasoro characters, this expression gives

$$\begin{aligned}
\mathcal{Z}_{(0,0),(0,0)}(\mathcal{C}_{56}) &= |\chi_0|^4 + |\chi_{\frac{1}{2}}|^4 + 2|\chi_0|^2 |\chi_{\frac{1}{2}}|^2 \\
&\quad + 2|\chi_{\frac{1}{16}}|^4 + \chi_0^2 \bar{\chi}_{\frac{1}{2}}^2 + 2|\chi_0|^2 |\chi_{\frac{1}{2}}|^2 + \bar{\chi}_0^2 \chi_{\frac{1}{2}}^2.
\end{aligned} \tag{5.104}$$

Interestingly,  $\mathcal{C}_{56}$  is a “Landau-forbidden” transition, corresponding to a topological criticality between trivial and non-trivial SPT phases. The full conformal spectrum, including information about which operator drives this transition was gained from the simple Ising CFT together with a duality.

The conformal spectrum of the topological transition  $\mathcal{C}_{56}$  was recently computed in [179] using a lattice map specific to a spin-chain model. They found the following expression

$$\mathcal{Z}'_{(0,0),(0,0)}(\mathcal{C}_{56}) = \frac{1}{2} \sum_{\mathbf{g}_L, \mathbf{g}_R} \mathcal{Z}_{\mathbf{g}_L, \mathbf{g}_R}^{\text{Ising}} \mathcal{Z}_{\mathbf{g}_L, \mathbf{g}_R}^{\text{Ising}}. \tag{5.105}$$

Despite looking very different from (5.103), they are both exactly equal to (5.104). The reason two very different expression give rise to the same partition function is due to the fact that there are several dualities mapping  $\mathcal{C}_{16}$  to  $\mathcal{C}_{56}$ . Note that the method used in [179] is specific to the model while our derivation is not model specific and is therefore applicable

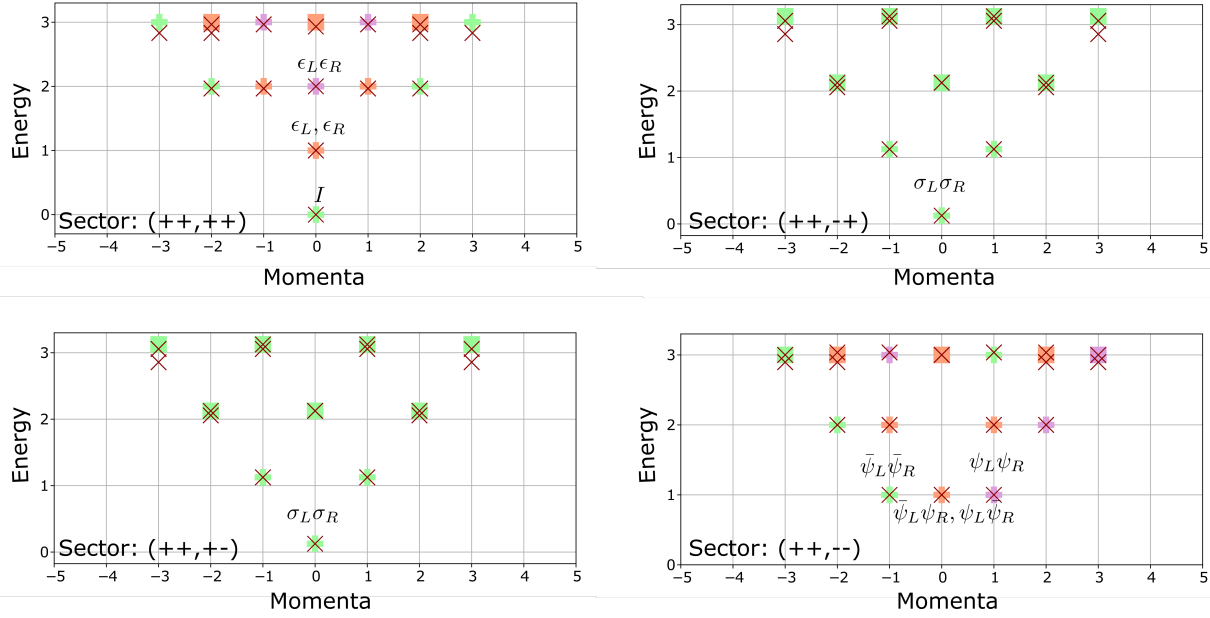


Figure 23: The figure shows a comparison between the analytically-computed conformal spectrum of the transition between the  $\mathbb{Z}_2 \times \mathbb{Z}_2$  symmetric SPT and PM and the numerically-obtained spectrum for the Hamiltonian  $H_{56}$  in (5.89) using exact diagonalization. All the numerics have been performed for spin chains of length  $L = 12$ , i.e., spin-chains containing 24  $\mathbb{Z}_2$ -spins using the Python package QuSpin [183]. The subplots (a)-(d) correspond to  $\mathbb{Z}_2 \times \mathbb{Z}_2$  eigensectors  $(++)$ ,  $(+-)$ ,  $(-+)$  and  $(--)$  and with periodic boundary conditions. Single and double degenerate states in the conformal towers are depicted using plus signs and squares respectively. For all other boundary conditions, the numerical and analytical results match as well.

in a much wider context. Similarly, the conformal spectrum of the other transitions  $\mathcal{C}_{ij}$  can be computed using our method.

In order to numerically verify the analytical results above, we use exact diagonalization of the Hamiltonian (5.77) at various critical points  $\lambda = \lambda_c$  and assign a momentum to each eigenstate. As an example, the spectrum of the topological criticality  $\mathcal{C}_{56}$ , decomposed into different symmetry eigensectors, is shown in Figure 23. The crosses are the numerically-computed spectrum while the other points are the analytical results given in (5.101). As one can see, the two are in good agreement, even for relatively small system sizes. See Appendix G for a comparison between the numerically obtained and theoretically predicted conformal spectrum at the  $\mathcal{C}_{15}$ ,  $\mathcal{C}_{34}$  and  $\mathcal{C}_{24}$  transitions.

As discussed above, the spectrum along the Ashkin-Teller line is known to belong to the  $c = 1$   $\mathbb{Z}_2$ -orbifold compact boson universality class at various compactification radii. The conformal spectrum of this CFT is given a  $U(1)$  current operator and vertex operators [180]. From this, we can again use dualities to find the conformal spectrum along any point of the critical lines in Figure 17.

## Beyond minimal $\mathbb{Z}_2 \times \mathbb{Z}_2$ spin chain models

So far we have studied the minimal model, i.e., those containing operators subtended from the shortest possible strings, in quite some detail. Our construction, however, works for any  $\mathbb{Z}_2 \times \mathbb{Z}_2$  symmetric spin chain, since any such Hamiltonian is an element of the string operator algebra  $\text{SOA}[\mathbb{Z}_2 \times \mathbb{Z}_2]$ . To illustrate this, it is instructive to briefly study the simplest non-minimal  $\mathbb{Z}_2 \times \mathbb{Z}_2$  symmetric Hamiltonians.

For simplicity, let us start with the following minimal Hamiltonian

$$H_{16} = - \sum_{\mu=L,R} \sum_i [S_{e_\mu}(i, i+1) + S_{m_\mu}(i)], \quad (5.106)$$

which from (5.72) and (5.89) we see are two decoupled critical Ising chains. There are two simple extensions we could consider: (1) by using longer string operators or (2) the products of two minimal operators. Using these operators, let us consider two possible deformations of (5.106)

$$\begin{aligned} \Delta H_{\text{ANNNI}, \mu} &= - \sum_i [S_{e_\mu}(i, i+2) + S_{m_\mu}(i, i+1)] \\ &= - \sum_i [\sigma_{i,\mu}^z \sigma_{i+2,\mu}^z + \sigma_{i,\mu}^x \sigma_{i+1,\mu}^x], \\ \Delta H_{\text{F-O'B}, \mu} &= - \sum_i [S_{e_\mu}(i, i+1) S_{m_\mu}(i+2) + S_{m_\mu}(i) S_{e_\mu}(i, i+1)] \\ &= - \sum_i [\sigma_{i,\mu}^z \sigma_{i+1,\mu}^z \sigma_{i+2,\mu}^x + \sigma_{i,\mu}^x \sigma_{i+1,\mu}^z \sigma_{i+2,\mu}^z], \end{aligned} \quad (5.107)$$

where  $\mu = L, R$ . With these deformations, the model is still self-dual under electric-magnetic dualities and the two chains remain decoupled. These are the ANNNI and the Fendley-O'Brien models, respectively [166–169]. On a single chain, these models realize various interesting points such as the  $c = 7/10$  tri-critical Ising (TCI) universality class, a  $c = 3/2$  critical phase that realizes decoupled Ising and Luttinger Liquid phases as well as two and four-fold degenerate ground states [167]. Using these terms,  $\mathcal{C}_{16}$  has a four-dimensional parameter space of deformations parametrized as

$$H_{16}^{\text{def}}(\{t_\mu, s_\mu\}) = H_{16} + \sum_{\mu=L,R} (t_\mu \Delta H_{\text{ANNNI}, \mu} + s_\mu \Delta H_{\text{F-O'B}, \mu}). \quad (5.108)$$

This parameter space therefore contains interesting critical points, Lifshitz transitions, etc between the paramagnetic ( $\text{SPT}_0$ ) and ferromagnetic (SSB) phases, realized as decoupled chains. Using dualities, we can find novel transitions between any other gapped phases. As an example, we can use the duality  $k_2$  (see Figure 17), to obtain a four-dimensional space of deformations of the topological critical transition between  $\text{SPT}_0$  and  $\text{SPT}_1$   $\mathcal{C}_{56}$ . The dual Hamiltonian has the form

$$H_{56}^{\text{def}}(\{t_\mu, s_\mu\}) = H_{56} + \sum_{\mu=L,R} [t_\mu \Delta H_{\text{ANNNI}, \mu}^\vee + s_\mu \Delta H_{\text{F-O'B}, \mu}^\vee], \quad (5.109)$$

where

$$\begin{aligned}
\Delta H_{\text{ANNI},L}^{\vee} &= - \sum_i [S_{e_L m_R}(i, i+2) + S_{m_L}(i, i+1)] \\
&= - \sum_i [\sigma_{i,L}^z \sigma_{i+1,R}^x \sigma_{i+2,L}^z \sigma_{i+2,R}^x + \sigma_{i,L}^x \sigma_{i+1,L}^x] \\
\Delta H_{\text{ANNI},R}^{\vee} &= - \sum_i [S_{m_L e_R}(i, i+2) + S_{m_R}(i, i+1)] \\
&= - \sum_i [\sigma_{i,R}^x \sigma_{i+1,R}^x + \sigma_{i,L}^x \sigma_{i,R}^z \sigma_{i+1,L}^z \sigma_{i+2,R}^z] \\
\Delta H_{\text{F-O'B},L}^{\vee} &= - \sum_i [S_{e_L m_R}(i, i+1) S_{m_L}(i+2) + S_{m_L}(i) S_{e_L m_R}(i+1, i+2)] \\
&= - \sum_i [\sigma_{i,L}^z \sigma_{i+1,L}^z \sigma_{i+1,R}^x \sigma_{i+2,L}^x + \sigma_{i,L}^x \sigma_{i+1,L}^z \sigma_{i+2,L}^z \sigma_{i+2,R}^x] \\
\Delta H_{\text{F-O'B},R}^{\vee} &= - \sum_i [S_{m_L e_R}(i, i+1) S_{m_R}(i+2) + S_{m_R}(i) S_{m_L e_R}(i+1, i+2)] \\
&= - \sum_i [\sigma_{i,L}^x \sigma_{i,R}^z \sigma_{i+1,R}^z \sigma_{i+2,R}^x + \sigma_{i,R}^x \sigma_{i+1,L}^z \sigma_{i+1,R}^z \sigma_{i+2,R}^z] .
\end{aligned} \tag{5.110}$$

For any point  $(t_L, t_R, s_L, s_R)$  corresponding to an interesting transition in (5.108), we can find a topological transition in (5.109). Among the interesting points, consider the doubled tri-critical Ising CFT at four different points

$$(t_L, t_R, s_L, s_R) \in \{(t^*, t^*, 0, 0), (t^*, 0, 0, s^*), (0, t^*, s^*, 0), (0, 0, s^*, s^*)\}, \tag{5.111}$$

where  $t^* \approx 246$  and  $s^* = 0.428$  [167, 168]. For the above parameters, the model (5.109) realizes (non-minimal) topological transitions between the trivial and non-trivial SPT phases with central charge  $c = 7/5$ . The conformal spectrum (or partition function) in all the different  $\mathbb{Z}_2 \times \mathbb{Z}_2$  twisted sectors can readily be obtained using this duality. The conformal spectrum of this topological transition in a few example sectors are given by

$$\begin{aligned}
\chi_1^{\vee} &= (\chi_1^{\text{TCI}})^2 = (|\chi_0|^2 + |\chi_{1/10}|^2 + |\chi_{\frac{3}{5}}|^2 + |\chi_{\frac{3}{2}}|^2)^2, \\
\chi_{e_L}^{\vee} &= \chi_e^{\text{TCI}} \chi_m^{\text{TCI}} = (|\chi_{\frac{3}{80}}|^2 + |\chi_{\frac{7}{16}}|^2)^2, \\
\chi_{e_R}^{\vee} &= \chi_e^{\text{TCI}} \chi_m^{\text{TCI}} = (|\chi_{\frac{3}{80}}|^2 + |\chi_{\frac{7}{16}}|^2)^2, \\
\chi_{m_L}^{\vee} &= \chi_1^{\text{TCI}} \chi_m^{\text{TCI}} = (|\chi_{\frac{3}{80}}|^2 + |\chi_{\frac{7}{16}}|^2) (|\chi_0|^2 + |\chi_{1/10}|^2 + |\chi_{\frac{3}{5}}|^2 + |\chi_{\frac{3}{2}}|^2), \\
\chi_{m_R}^{\vee} &= \chi_1^{\text{TCI}} \chi_m^{\text{TCI}} = (|\chi_{\frac{3}{80}}|^2 + |\chi_{\frac{7}{16}}|^2) (|\chi_0|^2 + |\chi_{1/10}|^2 + |\chi_{\frac{3}{5}}|^2 + |\chi_{\frac{3}{2}}|^2), \\
\chi_{e_L e_R}^{\vee} &= (\chi_f^{\text{TCI}})^2 = \left( \chi_{\frac{6}{10}} \bar{\chi}_{\frac{1}{10}} + \chi_{\frac{1}{10}} \bar{\chi}_{\frac{6}{10}} + \chi_{\frac{3}{2}} \bar{\chi}_0 + \chi_0 \bar{\chi}_{\frac{3}{2}} \right)^2.
\end{aligned} \tag{5.112}$$

Similarly, we can also compute the exact partition functions of (5.109) at the non-minimal topological critical point. For example, for periodic boundary conditions we have

$$\begin{aligned}
\mathcal{Z}_{(0,0),(0,0)}^{\vee} &= \chi_1^{\vee} + \chi_{e_L}^{\vee} + \chi_{e_R}^{\vee} + \chi_{e_L e_R}^{\vee}, \\
&= (|\chi_0|^2 + |\chi_{1/10}|^2 + |\chi_{\frac{3}{5}}|^2 + |\chi_{\frac{3}{2}}|^2)^2 + 2 (|\chi_{\frac{3}{80}}|^2 + |\chi_{\frac{7}{16}}|^2)^2 \\
&\quad + \left( \chi_{\frac{6}{10}} \bar{\chi}_{\frac{1}{10}} + \chi_{\frac{1}{10}} \bar{\chi}_{\frac{6}{10}} + \chi_{\frac{3}{2}} \bar{\chi}_0 + \chi_0 \bar{\chi}_{\frac{3}{2}} \right)^2.
\end{aligned} \tag{5.113}$$

The conformal spectrum can be readily read. The theory has several relevant perturbations, some of these are responsible for driving the topological transition. Using topological holography, we can also find many other interesting transitions. More detailed study will be presented elsewhere.

## Gauging perspective

Having explored various aspects of the phase diagram of  $\mathbb{Z}_2 \times \mathbb{Z}_2$  symmetric quantum systems in some detail, we now shift directions towards interpreting the action of dualities in the partition functions in terms of (topological) gauging. First, we focus on the duality transformations  $h_i$  which generate an  $S_3$  subgroup (5.63) of the full duality group  $\mathcal{G}[\mathbb{Z}_2 \times \mathbb{Z}_2]$ . Notably, the dualities  $h_i$  map non-trivially between phases that are labelled by distinct  $\mathbb{Z}_2$  subgroup (i.e.  $\mathbb{Z}_2^L, \mathbb{Z}_2^R$ , and  $\mathbb{Z}_2^D$ ) of  $\mathbb{Z}_2 \times \mathbb{Z}_2$  (see Table 1). These dualities originate from automorphisms of  $\mathbb{Z}_2 \times \mathbb{Z}_2$ , which form the group  $S_3$ . Twisted partition functions transform as follows under  $h_i$  (see (4.22))

$$\begin{aligned} h_1 : \mathcal{Z}[A_L, A_R] &\mapsto \mathcal{Z}[A_L, A_L + A_R], \\ h_2 : \mathcal{Z}[A_L, A_R] &\mapsto \mathcal{Z}[A_L + A_R, A_R], \\ h_3 : \mathcal{Z}[A_L, A_R] &\mapsto \mathcal{Z}[A_R, A_L]. \end{aligned} \quad (5.114)$$

where  $A_L$  and  $A_R$  are background  $\mathbb{Z}_2$  gauge fields. It can be verified that these transforms form the group  $S_3$  by choosing the two generators as  $h_3 h_1$  and  $h_2$ .  $h_3 h_1$  is an order-3 element, which acts as

$$\begin{aligned} (h_3 h_1) : \mathcal{Z}[A_L, A_R] &\mapsto \mathcal{Z}[A_L + A_R, A_L], \\ (h_3 h_1)^2 : \mathcal{Z}[A_L, A_R] &\mapsto \mathcal{Z}[A_R, A_L + A_R], \\ (h_3 h_1)^3 : \mathcal{Z}[A_L, A_R] &\mapsto \mathcal{Z}[A_L, A_R]. \end{aligned} \quad (5.115)$$

Similarly,  $h_2$  is an order-2 element and the group relation  $h_2(h_3 h_1)h_2^{-1} = (h_3 h_1)^2$  can also be explicitly verified. In order to construct the transformation of the twisted partition functions under the full group  $\mathcal{G}[\mathbb{Z}_2 \times \mathbb{Z}_2]$ , we need the action of an additional element  $\sigma_L$ , which acts simply as electromagnetic or Kramers-Wannier duality on the layer labelled  $L$

$$\sigma_L : \mathcal{Z}[A_L, A_R] \mapsto \mathcal{Z}^\vee[A_L^\vee, A_R] = \frac{1}{\sqrt{|H^1(\Sigma, \mathbb{Z}_2)|}} \sum_{A_L} \mathcal{Z}[A_L, A_R] e^{i\pi \int_\Sigma A_L \cup A_L^\vee}. \quad (5.116)$$

The remaining operations corresponding to  $k_i \in \mathcal{G}[\mathbb{Z}_2 \times \mathbb{Z}_2]$  can be obtained by using the group relation  $k_i = \sigma_L h_i \sigma_L^{-1}$ . They take the explicit form

$$\begin{aligned} k_1 : \mathcal{Z}[A_L, A_R] &\mapsto \mathcal{Z}^\vee[A_L^\vee, A_R^\vee] = \mathcal{Z}[A_L, A_R] e^{i\pi \int_\Sigma A_L \cup A_R}, \\ k_2 : \mathcal{Z}[A_L, A_R] &\mapsto \mathcal{Z}^\vee[A_L^\vee, A_R^\vee] = \frac{1}{\sqrt{|H^1(\Sigma, \mathbb{Z}_2^2)|}} \sum_{A_L, A_R} \mathcal{Z}[A_L, A_R] e^{i\pi \int_\Sigma (A_L^\vee - A_L) \cup (A_R^\vee - A_R)}, \\ k_3 : \mathcal{Z}[A_L, A_R] &\mapsto \mathcal{Z}^\vee[A_L^\vee, A_R^\vee] = \frac{1}{\sqrt{|H^1(\Sigma, \mathbb{Z}_2^2)|}} \sum_{A_L, A_R} \mathcal{Z}[A_L, A_R] e^{i\pi \int_\Sigma A_L \cup A_R^\vee + A_R \cup A_L^\vee}. \end{aligned} \quad (5.117)$$



Lagrangian subgroups	Generating set	Image of $\Pi$	$H$	$\psi(h_1, h_2)$	Gapped phase
$\mathcal{L}_1$	$e_L, e_R$	$1_L, 1_R$	$\mathbb{I}$	1	SSB
$\mathcal{L}_2$	$m_L, e_R$	$m_L$	$\mathbb{Z}_3^L$	1	$\text{PSB}_L$
$\mathcal{L}_3$	$e_L, m_R$	$m_R$	$\mathbb{Z}_3^R$	1	$\text{PSB}_R$
$\mathcal{L}_4$	$e_L e_R^2, m_L m_R$	$m_L m_R$	$\mathbb{Z}_3^D$	1	$\text{PSB}_D$
$\mathcal{L}_5$	$e_L e_R, m_L^2 m_R$	$m_L^2 m_R$	$\mathbb{Z}_3^A$	1	$\text{PSB}_A$
$\mathcal{L}_6$	$m_L, m_R$	$m_L, m_R$	$\mathbb{Z}_3^L \times \mathbb{Z}_3^R$	1	$\text{SPT}_0$
$\mathcal{L}_7$	$m_L e_R, e_L^2 m_R$	$m_L, m_R$	$\mathbb{Z}_3^L \times \mathbb{Z}_3^R$	$\omega_3^{h_{1,L} h_{2,R}}$	$\text{SPT}_1$
$\mathcal{L}_8$	$m_L e_R^2, e_L m_R$	$m_L, m_R$	$\mathbb{Z}_3^L \times \mathbb{Z}_3^R$	$\omega_3^{2h_{1,L} h_{2,R}}$	$\text{SPT}_2$

Table 2: The Lagrangian subgroups for  $G = \mathbb{Z}_3 \times \mathbb{Z}_3$ .  $\mathbb{Z}_3^L, \mathbb{Z}_3^R, \mathbb{Z}_3^D$ , and  $\mathbb{Z}_3^A$  are the left, right, diagonal, and anti-diagonal  $\mathbb{Z}_3$  subgroups of  $\mathbb{Z}_3 \times \mathbb{Z}_3$ , respectively.  $\mathcal{L}_i$  for  $i = 6, 7, 8$  are the three gapped SPT states. The 2-cocycle is evaluated on the group elements  $h_i = (h_{i,L}, h_{i,R}) \in H$  for  $i = 1, 2$  and  $\omega_3 = e^{2\pi i/3}$ .

The duality  $k_1$  corresponds to modifying the partition function of the theory by a topological phase. This topological phase is precisely the response theory corresponding to a  $\mathbb{Z}_2 \times \mathbb{Z}_2$  SPT. Therefore,  $k_1$  can be physically interpreted as pasting a non-trivial SPT on the theory. The remaining dualities are gauging or orbifold like dualities. It can be shown that the transformations in (5.117) satisfy the group relations of  $\mathcal{G}[\mathbb{Z}_2 \times \mathbb{Z}_2] = (S_3 \times S_3) \rtimes \mathbb{Z}_2$  (See Appendix F).

## 5.4 $\mathbb{Z}_3 \times \mathbb{Z}_3$ symmetric quantum spin chains

To examine a more complicated situation, we could consider  $\mathbb{Z}_2 \times \mathbb{Z}_3$ . However, this group is isomorphic to  $\mathbb{Z}_6$ , which has been explored in Section 5.2. Therefore, next we consider the example of  $G = \mathbb{Z}_3 \times \mathbb{Z}_3$ . As in the previous example, this symmetry group has a single fusion structure and many dualities. In fact, the order of the duality group is 1152, therefore this case belongs to the limit where topological holography is particularly powerful. In this section, we restrict ourselves to study very few details and a deeper analysis will appear elsewhere.

As usual, we consider a  $2 + 1d$   $\mathbb{Z}_3 \times \mathbb{Z}_3$  topological gauge theory whose line operators are labelled by elements in the group

$$\mathcal{A}[\mathbb{Z}_3 \times \mathbb{Z}_3] = \mathbb{Z}_3^L \times \mathbb{Z}_3^R \times \text{Rep}(\mathbb{Z}_3^L \times \mathbb{Z}_3^R) \simeq \mathbb{Z}_3^4 \simeq \langle m_L, m_R, e_L, e_R \rangle, \quad (5.118)$$

where the generators satisfy the following relations  $e_L^3 = m_L^3 = e_R^3 = m_R^3 = 1$ .

Following the recipe detailed in Sec. 3.2, we obtain a  $1 + 1d$  quantum spin chain that provides a concrete realization of a  $\mathbb{Z}_3 \times \mathbb{Z}_3$  symmetric system. The Hilbert space of the spin chain decomposes into on-site Hilbert spaces

$$\mathcal{H}_i = \mathcal{H}_{i,L} \otimes \mathcal{H}_{i,R}, \quad \mathcal{H}_{i,L} \simeq \mathcal{H}_{i,R} \simeq \mathbb{C}^3. \quad (5.119)$$

There is a natural action of generalized Pauli operators  $(X_{i,L}, Z_{i,L})$  on the on-site Hilbert space  $\mathcal{H}_{i,L}$  which satisfy the  $\mathbb{Z}_3$  clock and shift algebra in (5.43) with  $N = 3$ . Similarly there is a set of operators  $(X_{i,R}, Z_{i,R})$  that act on  $\mathcal{H}_{i,R}$  and satisfy an isomorphic algebra. The generators of  $\mathcal{A}[\mathbb{Z}_3 \times \mathbb{Z}_3]$  become the following operators when brought to the 1D boundary (see (3.27) and (3.28))

$$\begin{aligned} e_L &\longrightarrow Z_{i,L} Z_{i+1,L}^\dagger, & m_L &\longrightarrow X_{i,L}, \\ e_R &\longrightarrow Z_{i,R} Z_{i+1,R}^\dagger, & m_R &\longrightarrow X_{i,R}. \end{aligned} \quad (5.120)$$

The global symmetry operator for  $\mathbf{g} = (\mathbf{g}_L, \mathbf{g}_R) \in \mathbb{Z}_3 \times \mathbb{Z}_3$  has the form

$$\mathcal{U}_{\mathbf{g}} = \bigotimes_i (X_{i,L})^{\mathbf{g}_L} \otimes (X_{i,R})^{\mathbf{g}_R}. \quad (5.121)$$

### Gapped phases, order parameters, and excitations

There are 8 Lagrangian subgroups of  $\mathcal{A}[\mathbb{Z}_3 \times \mathbb{Z}_3]$ , which correspond to 8 distinct gapped phases (see Table 2). Using the holographic correspondence in (5.120), we can construct the fixed-point Hamiltonians associated to each of the gapped phases in Table 2. The Hamiltonian associated to the SSB phase is given by<sup>18</sup>

$$H_1 = - \sum_i \left[ Z_{i,L} Z_{i+1,L}^\dagger + Z_{i,R} Z_{i+1,R}^\dagger \right] + \text{h.c.} \quad (5.122)$$

The fixed-point Hamiltonians associated to the four possible partial symmetry-breaking phases are

$$\begin{aligned} H_2 &= - \sum_i \left[ X_{i,L} + Z_{i,R} Z_{i+1,R}^\dagger \right] + \text{h.c.}, \\ H_3 &= - \sum_i \left[ Z_{i,L} Z_{i+1,L}^\dagger + X_{i,R} \right] + \text{h.c.}, \\ H_4 &= - \sum_i \left[ Z_{i,L} Z_{i,R}^\dagger Z_{i+1,L}^\dagger Z_{i+1,R} + X_{i,R} X_{i,R} \right] + \text{h.c.}, \\ H_5 &= - \sum_i \left[ Z_{i,L} Z_{i,R} Z_{i+1,L}^\dagger Z_{i+1,R}^\dagger + X_{i,L}^\dagger X_{i,R} \right] + \text{h.c.} \end{aligned} \quad (5.123)$$

Finally, the fixed-point Hamiltonians of SPT phases are given by

$$\begin{aligned} H_6 &= - \sum_i \left[ X_{i,L} + X_{i,R} \right] + \text{h.c.}, \\ H_7 &= - \sum_i \left[ X_{i,L} Z_{i,R} Z_{i+1,R}^\dagger + Z_{i,L}^\dagger Z_{i+1,L} X_{i+1,R} \right] + \text{h.c.}, \\ H_8 &= - \sum_i \left[ X_{i,L} Z_{i,R}^\dagger Z_{i+1,R} + Z_{i,L} Z_{i+1,L}^\dagger X_{i+1,R} \right] + \text{h.c.}, \end{aligned} \quad (5.124)$$

These are all commuting fixed-point models, a fact that can be easily checked using the clock algebra (5.43). =

---

<sup>18</sup>We label the Hamiltonians with the corresponding gapped phase, described by a Lagrangian subgroup. Therefore, the Hamiltonian associated to the Lagrangian subgroup  $\mathcal{L}_i$  in Table 2 is denoted as  $H_i$ .

As discussed in 3.4, the order parameter corresponding to the condensation of an anyon  $d$  of a Lagrangian subgroup is given by the string operator  $S_d(i, j)$  labeled by  $d$ , where  $i$  and  $j$  are the endpoints of the operator on the lattice. A non-zero expectation value for  $S_d(i, j)$  in the limit  $|i - j| \rightarrow \infty$  corresponds to a long-range ordered ground-state. The holographic perspective suggests that the condensation of charges  $e_L$ ,  $e_R$ ,  $e_L e_R$ , and  $e_L e_R^2$  will be detected by the following string operators

$$\begin{aligned} S_{e_L}(i, j) &= Z_{i,L} Z_{j,L}^\dagger, & S_{e_R}(i, j) &= Z_{i,R} Z_{j,R}^\dagger, \\ S_{e_L e_R}(i, j) &= Z_{i,L} Z_{i,R} Z_{j,L}^\dagger Z_{j,R}^\dagger, & S_{e_L e_R^2}(i, j) &= Z_{i,L} Z_{i,R}^\dagger Z_{j,L}^\dagger Z_{j,R}, \end{aligned} \quad (5.125)$$

Alternatively, by cluster decomposition, the local order parameters  $Z_{i,L}$ ,  $Z_{i,R}$ ,  $Z_{i,L} Z_{i,R}$  and  $Z_{i,L} Z_{i,R}^\dagger$  can be used to detect the spontaneous symmetry-breaking to  $\mathbb{Z}_3^L$ ,  $\mathbb{Z}_3^R$ ,  $\mathbb{Z}_3^D$ , and  $\mathbb{Z}_3^A$  symmetries in the ground state, respectively (see Table 2). Similarly, the condensation of fluxes  $m_L$ ,  $m_R$ ,  $m_L m_R$ , and  $m_L m_R^2$  will be detected by the following string operators

$$\begin{aligned} S_{m_L}(i, j) &= \prod_{k=i}^j X_{k,L}, & S_{m_R}(i, j) &= \prod_{k=i}^j X_{k,R}, \\ S_{m_L m_R}(i, j) &= \prod_{k=i}^j X_{k,L} X_{k,R}, & S_{m_L m_R^2}(i, j) &= \prod_{k=i}^j X_{k,L} X_{k,R}^\dagger, \end{aligned} \quad (5.126)$$

These are the disorder parameters and their condensation does not break any symmetry. Finally, we construct the string order-parameters corresponding to the condensation of dyonic generators of the Lagrangian subgroups. They are given by

$$\begin{aligned} S_{e_L m_R^2}(i, j) &= Z_{i,L} \left( \bigotimes_{k=i+1}^j X_{k,R}^\dagger \right) Z_{j,L}^\dagger, & S_{m_L e_R}(i, j) &= Z_{i,R} \left( \bigotimes_{k=i}^{j-1} X_{k,L} \right) Z_{j,R}^\dagger, \\ S_{e_L m_R}(i, j) &= Z_{i,L} \left( \bigotimes_{k=i+1}^j X_{k,R}^\dagger \right) Z_{j,L}^\dagger, & S_{m_L^2 e_R}(i, j) &= Z_{i,R} \left( \bigotimes_{k=i}^{j-1} X_{k,L}^\dagger \right) Z_{j,R}^\dagger, \end{aligned} \quad (5.127)$$

which detect SPT phases. Denoting the ground-state of the gapped phase  $\mathcal{L}_i$  by  $|\text{GS}_{\mathcal{L}_i}\rangle$ , we have

$$\lim_{|j_1 - j_2| \rightarrow \infty} \langle \text{GS}_{\mathcal{L}_i} | S_d(j_1, j_2) | \text{GS}_{\mathcal{L}_i} \rangle = \begin{cases} \text{constant}, & \forall d \in \mathcal{L}_i, \\ 0, & \forall d \notin \mathcal{L}_i. \end{cases} \quad (5.128)$$

The fundamental excitations within each gapped phase that correspond to the set of confined anyons. Any two anyons that only differ by a condensed anyon create the same excitation and are thus identified. For example, consider the Lagrangian subgroup  $\mathcal{L}_6$ . It is be readily checked that possible equivalence classes of excitations are given by<sup>19</sup>

$$\begin{aligned} \phi_{e_L}^{\text{SPT}_0} &= \langle e_L m_L, e_L m_R \rangle, & \phi_{e_L^2}^{\text{SPT}_0} &= \langle e_L^2 m_L, e_L^2 m_R \rangle, \\ \phi_{e_R}^{\text{SPT}_0} &= \langle e_R m_L, e_R m_R \rangle, & \phi_{e_R^2}^{\text{SPT}_0} &= \langle e_R^2 m_L, e_R^2 m_R \rangle, \\ \phi_{e_L e_R}^{\text{SPT}_0} &= \langle e_L e_R m_L, e_L e_R m_R \rangle, & \phi_{e_L^2 e_R}^{\text{SPT}_0} &= \langle e_L^2 e_R m_L, e_L^2 e_R m_R \rangle, \\ \phi_{e_L e_R^2}^{\text{SPT}_0} &= \langle e_L e_R^2 m_L, e_L e_R^2 m_R \rangle, & \phi_{e_R^2 e_R^2}^{\text{SPT}_0} &= \langle e_R^2 e_R^2 m_L, e_R^2 e_R^2 m_R \rangle, \end{aligned} \quad (5.129)$$

<sup>19</sup>Here by  $\langle \cdots \rangle$  denotes the set generated by the dyons inside.

which together with the trivial  $\phi_1^{\text{SPT}_0} = \langle m_L, m_R \rangle$  form the object of the category  $\text{Rep}(\mathbb{Z}_3 \times \mathbb{Z}_3)$ . The anyon in the subscript of each  $\phi$  corresponds to the representative of the confined anyons and the corresponding string operators create fundamental excitations (domain wall) (see (5.125), (5.126), and (5.127)). Similar considerations determine the category of excitations associated to other gapped phases.

We thus see that the holographic perspective could easily determine various gapped phases, their order parameters, and excitations.

## Dualities, and their action on anyons and gapped phases

We now study the action of the duality group on the gapped phases. The duality group  $\mathcal{G}[\mathbf{G}]$  for  $\mathbf{G} = \mathbb{Z}_3^L \times \mathbb{Z}_3^R$  has order 1152 and is isomorphic to the Weyl group of the exceptional Lie algebra  $F_4$  (see App. B for details)

$$\mathcal{G}[\mathbb{Z}_3^L \times \mathbb{Z}_3^R] = W(F_4). \quad (5.130)$$

The group is generated by  $\{\sigma_L, h_1, h_2, k\}$ . The generators act on the anyons and gapped phases as follows

- (a) **Universal dynamical dualities:** These are classified by  $H^2(\mathbf{G}, \text{U}(1)) = \mathbb{Z}_3$  and its actions on anyons is

$$k : \{m_L \mapsto m_L e_R^2, m_R \mapsto e_L m_R\}, \quad (5.131)$$

and its non-trivial action on gapped phases is

$$\mathcal{L}_6 \xrightarrow{k} \mathcal{L}_8 \xrightarrow{k} \mathcal{L}_7 \xrightarrow{k} \mathcal{L}_6. \quad (5.132)$$

This satisfies  $k^3 = 1$ . Physically,  $k$  corresponds to a domain wall in the bulk with the  $\text{SPT}_2$  ( $\mathcal{L}_8$ ) phase. The duality above is just stacking of  $\mathbb{Z}_3 \times \mathbb{Z}_3$  SPT phases.

- (b) **Universal kinematical dualities:** These are related to  $\text{Aut}(\mathbb{Z}_3 \times \mathbb{Z}_3) = \text{GL}_2(\mathbb{F}_3) = Q_8 \rtimes S_3$ . Their actions on anyons are

$$\begin{aligned} h_1 : \{m_L \mapsto m_R, m_R \mapsto m_L, e_L \mapsto e_R, e_R \mapsto e_L\}, \\ h_2 : \{m_R \mapsto m_L m_R, e_L \mapsto e_L e_R^2\}. \end{aligned} \quad (5.133)$$

and hence their nontrivial action on gapped phases are

$$\begin{aligned} \mathcal{L}_2 \xleftrightarrow{h_1} \mathcal{L}_3, \quad \mathcal{L}_7 \xleftrightarrow{h_1} \mathcal{L}_8, \\ \mathcal{L}_3 \xrightarrow{h_2} \mathcal{L}_4 \xrightarrow{h_2} \mathcal{L}_5 \xrightarrow{h_2} \mathcal{L}_3. \end{aligned} \quad (5.134)$$

They act on  $k$  as  $h_1 k h_1^{-1} = k^{-1}$  and  $h_2 k h_2^{-1} = k$ . Together, they generate

$$\langle k, h_1, h_2 \rangle = \mathbb{Z}_3 \rtimes \text{GL}_2(\mathbb{F}_3). \quad (5.135)$$

- (c) **Partial electric-magnetic duality:** The action on anyons is

$$\sigma_L : \{m_L \mapsto e_L, e_L \mapsto m_L\}, \quad (5.136)$$

and the mapping of gapped phases are

$$\mathcal{L}_1 \xleftrightarrow{\sigma_L} \mathcal{L}_2, \quad \mathcal{L}_3 \xleftrightarrow{\sigma_L} \mathcal{L}_6, \quad \mathcal{L}_4 \xleftrightarrow{\sigma_L} \mathcal{L}_8, \quad \mathcal{L}_5 \xleftrightarrow{\sigma_L} \mathcal{L}_7. \quad (5.137)$$

This satisfies  $\sigma_L^2 = 1$  and generates a  $\mathbb{Z}_2$  subgroup. Together,  $\sigma_L, k, h_1$ , and  $h_2$  generate the full group  $\mathcal{G}[\mathbb{Z}_3 \times \mathbb{Z}_3]$ . It is convenient to also define  $\sigma_R = h_1 \sigma_L h_1$ .

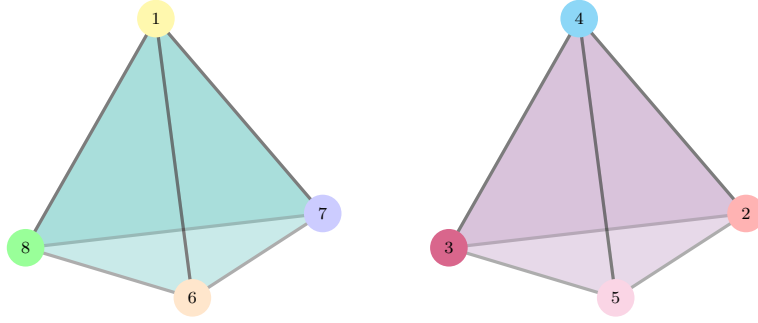


Figure 24: The action of the  $S_4$  subgroup of dualities (5.139) and (5.140) on gapped boundaries can geometrically be thought of as the isometries of two regular tetrahedra as illustrated above. There is a duality/isometry for any permutation of the vertices within each tetrahedron.

### The minimal Hamiltonian and its phase diagram

Similar to the  $\mathbb{Z}_2 \times \mathbb{Z}_2$  case, we consider the minimal Hamiltonian containing all gapped phases and many interesting transitions of  $\mathbb{Z}_3 \times \mathbb{Z}_3$  symmetric theories. This is given by

$$H = \sum_{a=1}^8 t_a H_a, \quad t_a \in \mathbb{R}, \quad (5.138)$$

where each term is given in (5.122), (5.123), and (5.124). There are many other interesting models one could write using the minimal string operators, but for this example we will restrict ourselves to this simple model. Furthermore, we only make a few observations about the phase-diagram, and a more detailed analysis will appear elsewhere.

The duality group contains many interesting subgroups, one particularly interesting subgroup is generated by the dualities

$$\begin{aligned} a : \{m_L \mapsto m_R^2, m_R \mapsto m_L^2, e_L \mapsto e_R^2, e_R \mapsto e_L^2\}, \\ \sigma_L \sigma_R : \{m_L \mapsto e_L, m_R \mapsto e_R, e_L \mapsto m_L, e_R \mapsto m_R\}, \\ b : \{m_L \mapsto m_R, m_R \mapsto m_L^2 m_R^2, e_L \mapsto m_L^2 e_L^2 m_R^2 e_R, e_R \mapsto e_L^2 m_R^2\}. \end{aligned} \quad (5.139)$$

These generate the group of permutations of four objects

$$\langle a, \sigma_L \sigma_R, b \rangle = S_4 \subset \mathcal{G}[\mathbb{Z}_2 \times \mathbb{Z}_2]. \quad (5.140)$$

The action of this group on Lagrangian subgroups give rise to two orbits

$$\text{Orb}_1 = \{\mathcal{L}_1, \mathcal{L}_6, \mathcal{L}_7, \mathcal{L}_8\}, \quad \text{Orb}_2 = \{\mathcal{L}_2, \mathcal{L}_3, \mathcal{L}_4, \mathcal{L}_5\}, \quad (5.141)$$

and the action of each group element is to permute the gapped phases within these two sets. Note that the second orbit consists of all gapped phases in which  $\mathbb{Z}_3 \times \mathbb{Z}_3$  symmetry partially breaks down to  $\mathbb{Z}_3$  while the first orbit consists of the SSB phase and all the unbroken (SPT) phases (see Table 2). Geometrically,  $S_4$  is the isometry group of the regular tetrahedron and each gapped phases can be thought of as a vertex of a tetrahedron

(see Figure 24). In order to realize these abstract tetrahedra in the 8-dimensional phase diagram, consider the restrictions of (5.138) to the two different 4-dimensional subspaces

$$\begin{aligned} H_{\text{Orb}_1} &= t_1 H_1 + t_6 H_6 + t_7 H_7 + t_8 H_8, \\ H_{\text{Orb}_2} &= t_2 H_2 + t_3 H_3 + t_4 H_4 + t_5 H_5. \end{aligned} \quad (5.142)$$

In (5.140), there is a duality for any possible permutation of the four parameters in these two Hamiltonians. Since the discussion is the same, we will restrict ourselves to the first Hamiltonian  $H_{\text{Orb}_1}$ . The overall scale does not matter, and without loss of generality, we can restrict ourselves to the 3-dimensional subspace

$$t_1 + t_6 + t_7 + t_8 = 1. \quad (5.143)$$

This is exactly a tetrahedron with the the four fixed-point Hamiltonians at its vertices  $(t_1, t_2, t_3, t_4) = (1, 0, 0, 0)$ ,  $(t_1, t_2, t_3, t_4) = (0, 1, 0, 0)$ , etc. Using similar arguments and assumptions that led to Figure 17, we can construct the simplest possible phase-diagram for  $H_{\text{Orb}_1}$ , as can be seen in Figure 25.

One way to argue for such a phase diagram is as follows. Since  $S_4$  dualities act on the tetrahedron parameterizing  $H_{\text{Orb}_1}$  as its isometries, they naturally induce maps on any point in the tetrahedron. The blue vertices are fixed-point Hamiltonians  $H_1, H_6, H_7$ , and  $H_8$ . The center of the tetrahedron is self-dual under  $S_4$  and therefore has to be a transition since no Lagrangian subgroup is self-dual under  $S_4$ . Now consider the subgroup  $S_3 \subset S_4$  corresponding to all permutations of  $t_6, t_7$ , and  $t_8$  that leave  $t_1$  invariant. The Hamiltonians on the self-dual line must either be transitions<sup>20</sup> or in the gapped phase  $\mathcal{L}_1$  (assuming that  $\mathcal{L}_1, \mathcal{L}_6, \mathcal{L}_7$ , and  $\mathcal{L}_8$  are the only gapped phases in this tetrahedron). Starting from the fixed-point Hamiltonian  $H_1$ , we can move along the self-dual line. Assuming that the Hamiltonians remain in the same phase  $\mathcal{L}_1$ , a transition must occur when we reach the  $S_4$  self-dual point in the center. Also, consider the  $\mathbb{Z}_2$  subgroup swapping  $\mathcal{L}_7$  and  $\mathcal{L}_8$ , the plane of reflection is  $\mathbb{Z}_2$  self-dual and similar arguments can be used. Repeating this logic for all the subgroups of  $S_4$ , the minimal phase diagram is given by Figure 25. The blue points are the four gapped fixed-point Hamiltonians, the yellow regions are gapped phases, red dots, the green lines and red surfaces are transitions.

For some of the red points, we can make a slightly stronger statement. The red point at  $(t_1, t_6, t_7, t_8) = (1, 1, 0, 0)$  corresponds to two decoupled copies of critical 3-state Potts model. This critical point is thus described by two copies of the  $\mathbb{Z}_3$  parafermion CFT with  $c = \frac{8}{5}$ . Unlike the case of Ising<sup>2</sup> CFT, this critical point does not have a marginal operator, therefore, we expect that the green lines and the red surface attached to it to be first-order transitions. All the critical points in the center of the edges (1-simplices) are dual to this point thus also critical with  $c = \frac{8}{5}$ . Remaining are the four red points at the center of the triangles (2-simplices) that are self-dual under  $S_3$  subgroups of  $S_4$ . Duality does not completely fix the type of transition but it seems reasonable to expect them to be critical.

It is important to note that dualities do not completely fix the phase diagram and we have to make a few assumptions to construct the phase diagram in Figure 25. More complicated scenarios are possible. However, by knowing the phase diagram only in a small corner of the tetrahedron is enough to completely determine the rest of the tetrahedron by dualities.

---

<sup>20</sup>Recall that we consider anything beyond gapped phases (with non-degenerate ground states) labeled by Lagrangian subgroups as transitions. This in principle could be gapless phases.

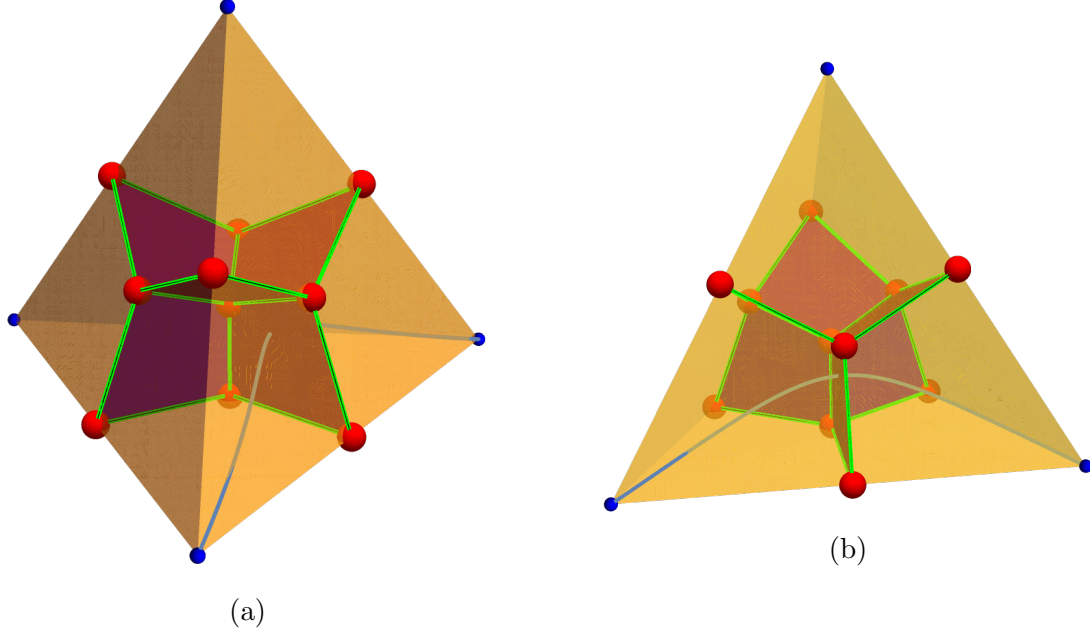


Figure 25: A proposed phase diagram for the minimal  $\mathbb{Z}_3 \times \mathbb{Z}_3$  Hamiltonian at  $t_2 = t_3 = t_4 = t_5 = 0$ . The two figures correspond to (different angles of) the subspace  $t_1 + t_6 + t_7 + t_8 = 1$  (or equivalently a quadrant of  $S^3 \subset \mathbb{R}^4$ ). The blue points are fixed-point Hamiltonians, the yellow regions are gapped phases, the green lines and red surfaces are expected to be first-order transitions while the red points are expected to be second-order transitions. The curve between the fixed-point Hamiltonians  $H_1$  and  $H_6$  is parameterized as (5.145).

As a preliminary numerical analysis, we have performed DMRG calculations of some order parameters along a simple curve. Since overall scaling of Hamiltonians does not matter, we can parameterize a three-sphere in four dimensions as

$$\begin{pmatrix} t_1 \\ t_6 \\ t_7 \\ t_8 \end{pmatrix} = \begin{pmatrix} \cos \phi_1 \\ \cos \phi_2 \sin \phi_1 \\ \cos \phi_3 \sin \phi_1 \sin \phi_2 \\ \sin \phi_1 \sin \phi_2 \sin \phi_3 \end{pmatrix}. \quad (5.144)$$

Consider the curve

$$\begin{pmatrix} \phi_1(s) \\ \phi_2(s) \\ \phi_3(s) \end{pmatrix} = \frac{\pi}{2} \begin{pmatrix} s \\ 1-s \\ s \end{pmatrix}. \quad (5.145)$$

from  $\mathcal{L}_1$  to  $\mathcal{L}_6$  crossing our predicted transition surface at  $s = \frac{2}{3}$  or  $\phi_1 = \frac{\pi}{3} \approx 1.0472$  (see Figure 25). The order parameter for the condensation of  $e_L$  and  $e_R$  on this curve is shown in Figure 26. Exactly at  $\phi_1 = \frac{\pi}{3}$ , we see a sharp transition consistent with a first-order transition, as predicted. However, further numerical analysis is needed to confirm this more convincingly. We leave a more complete analysis of  $\mathbb{Z}_3 \times \mathbb{Z}_3$  symmetric models using topological holography for future work.

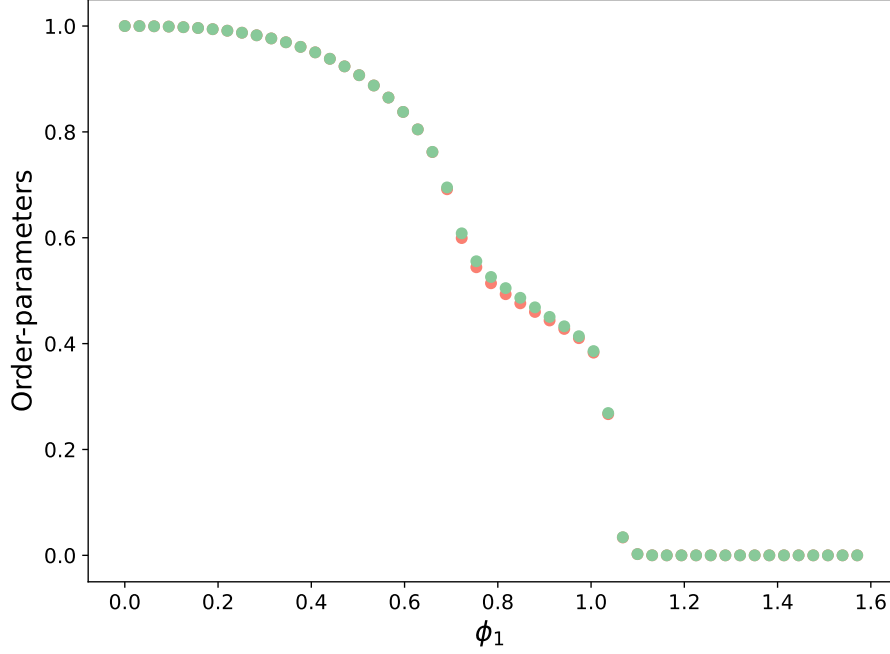


Figure 26: DMRG calculations of order parameters  $\langle Z_i^L \rangle$  and  $\langle Z_i^R \rangle$  detecting condensation of  $e_L$  and  $e_R$  along the curve (5.145). The calculation was performed for  $N = 2 \times 80$   $\mathbb{Z}_3$  spins for open boundary conditions. The transition happened at the expected point  $\phi_1 = \frac{\pi}{3} \approx 1.0472$ .

### Predictions of conformal spectra of nontrivial critical points

We will now briefly turn to the second application of topological holography of computing conformal spectrum of non-trivial transitions. Consider the topological phase transition  $\mathcal{C}_{67}$  between  $\text{SPT}_0$  ( $\mathcal{L}_6$ ) and  $\text{SPT}_1$  ( $\mathcal{L}_7$ ). The duality  $\sigma_L h_2^2 \sigma_R k^2$

$$\begin{aligned} \mathcal{L}_1 &\xrightarrow{k^2} \mathcal{L}_1 \xrightarrow{\sigma_R} \mathcal{L}_3 \xrightarrow{h_2^2} \mathcal{L}_5 \xrightarrow{\sigma_L} \mathcal{L}_7, \\ \mathcal{L}_6 &\xrightarrow{k^2} \mathcal{L}_7 \xrightarrow{\sigma_R} \mathcal{L}_4 \xrightarrow{h_2^2} \mathcal{L}_3 \xrightarrow{\sigma_L} \mathcal{L}_6, \end{aligned} \quad (5.146)$$

maps  $\mathcal{C}_{16}$ , described by decoupled  $\mathbb{Z}_3$  parafermion CFTs to the topological transitions  $\mathcal{C}_{67}$

$$\mathcal{C}_{16} \xrightarrow{\sigma_L h_2^2 \sigma_R k^2} \mathcal{C}_{67}. \quad (5.147)$$

Under this duality, we have

$$(\mathbf{g}_L, \alpha_L, \mathbf{g}_R, \alpha_R) \xrightarrow{\sigma_L h_2^2 \sigma_R k^2} (2\mathbf{g}_R + \alpha_L, 2\alpha_R, -2\mathbf{g}_L + \alpha_R, \alpha_L). \quad (5.148)$$

We can now use (4.26) to relate the dual twisted partition functions and the original ones ( $\omega = \exp(2\pi i/3)$ )

$$\mathcal{Z}_{\mathbf{g}^\vee, \mathbf{h}^\vee}^\vee = \frac{1}{9} \sum_{\substack{\mathbf{g}_L, \mathbf{g}_R \\ \mathbf{h}_L, \mathbf{h}_R}} \omega^{[(\mathbf{g}_L - 2\mathbf{g}_R^\vee)(\mathbf{h}_L^\vee - 2\mathbf{h}_R) + (\mathbf{g}_R + 2\mathbf{g}_L^\vee)(\mathbf{h}_R^\vee - \mathbf{h}_L)]} \mathcal{Z}_{\mathbf{g}_L, \mathbf{h}_L}^{3\text{-Para}} \mathcal{Z}_{\mathbf{g}_R, \mathbf{h}_R}^{3\text{-Para}}. \quad (5.149)$$



Topological criticality with no defect										
$h + \bar{h}$	0	$\frac{4}{15}$	$\frac{4}{5}$	$\frac{14}{15}$	$\frac{8}{5}$	$\frac{4}{3}$	$\frac{8}{3}$	$\frac{22}{15}$	$\frac{17}{15}$	$\frac{17}{15}$
$h - \bar{h}$	0	0	0	0	0	0	0	0	+1	-1
multiplicity	1	4	2	4	1	4	4	8	4	4
$(\alpha_L, \alpha_R)$	(0,0)	(1,0)(0,1) (2,0)(0,2)	(0,0)	(1,1)(1,2) (2,1)(2,2)	(0,0)	(1,1)(1,2) (2,1)(2,2)	(1,0)(0,1) (2,0)(0,2)	(1,0)(0,1) (2,0)(0,2)	(1,1)(1,2) (2,1)(2,2)	(1,1)(1,2) (2,1)(2,2)

Table 3: The spectrum of primary fields for topological transitions ( $\mathcal{C}_{67}$ ,  $\mathcal{C}_{68}$ , and  $\mathcal{C}_{78}$ ) between  $\mathbb{Z}_3 \times \mathbb{Z}_3$  SPT phases for periodic boundary condition. With this boundary conditions, the spectrum and  $\mathbb{Z}_3 \times \mathbb{Z}_3$  transformation properties are the same for these three transitions.

where  $\mathcal{Z}_{\mathbf{g}, \mathbf{h}}^{3\text{-Para}}$  are the twisted partition functions of  $\mathbb{Z}_3$  parafermion CFT,  $\mathcal{Z}^\vee = \mathcal{Z}(\mathcal{C}_{67})$  and  $\mathbf{g}^\vee = (\mathbf{g}_L^\vee, \mathbf{g}_R^\vee)$  and  $\mathbf{h}^\vee = (\mathbf{h}_L^\vee, \mathbf{h}_R^\vee)$ . As a concrete check, we can see that the partition function in the untwisted sector (periodic boundary conditions) is given by

$$\begin{aligned} \mathcal{Z}_{(0,0)(0,0)}(\mathcal{C}_{67}) = & 4|\chi_{\frac{2}{3}}|^4 + 8|\chi_{\frac{1}{15}}|^2|\chi_{\frac{2}{3}}|^2 + 4\chi_0\chi_{\frac{1}{15}}\chi_{\frac{2}{5}}\bar{\chi}_{\frac{2}{3}} + 4\chi_{\frac{2}{5}}\chi_{\frac{2}{3}}\bar{\chi}_0\chi_{\frac{1}{15}} \\ & + |\chi_0|^4 + 2|\chi_{\frac{2}{5}}|^2|\chi_0|^2 + 4|\chi_{\frac{2}{3}}|^2|\chi_0|^2 + \left(2|\chi_{\frac{1}{15}}|^2 + |\chi_{\frac{2}{5}}|^2\right)^2. \end{aligned} \quad (5.150)$$

In [179], the spectrum of the topological transition  $\mathcal{C}_{67}$  was obtained using a specific lattice mapping giving rise to a diagonal orbifold similar to (5.105). Our result (5.150) for periodic boundary condition reproduces the result of [179] (equation E.7). The spectrum of primary fields for this transition with periodic boundary condition is tabulated in Table 3. As can be seen in the table, there are three  $\mathbb{Z}_3 \times \mathbb{Z}_3$  symmetric relevant operators, two with scaling dimension  $\frac{4}{5}$  and one with scaling dimension  $\frac{8}{5}$ . Hence, this is a multicritical point between up to six different gapped phases. In [179], it was shown that one of the operators with scaling dimension  $\frac{4}{5}$  is responsible for topological transition  $\mathcal{C}_{67}$ . Similar to the  $\mathbb{Z}_2 \times \mathbb{Z}_2$ , we expect that the other relevant operators flow to gapped phases in other tetrahedron (see Figure 24).

Similarly, we can obtain the other topological transitions. For example using the duality  $\sigma_R h_2^2 \sigma_R : \mathcal{C}_{16} \mapsto \mathcal{C}_{68}$ , we find

$$\mathcal{Z}_{\mathbf{g}^\vee, \mathbf{h}^\vee}(\mathcal{C}_{68}) = \frac{1}{9} \sum_{\substack{\mathbf{g}_L, \mathbf{g}_R \\ \mathbf{h}_L, \mathbf{h}_R}} \omega^{[(\mathbf{g}_R - \mathbf{g}_R^\vee)(\mathbf{h}_L^\vee - \mathbf{h}_L) + (\mathbf{g}_L + \mathbf{g}_L^\vee)(\mathbf{h}_R^\vee - 2\mathbf{h}_R)]} \mathcal{Z}_{\mathbf{g}_L, \mathbf{h}_L}^{3\text{-Para}} \mathcal{Z}_{\mathbf{g}_R, \mathbf{h}_R}^{3\text{-Para}}. \quad (5.151)$$

More transparently, using  $k : \mathcal{C}_{67} \mapsto \mathcal{C}_{68}$  and  $k^2 : \mathcal{C}_{67} \mapsto \mathcal{C}_{78}$ , we have

$$\begin{aligned} \mathcal{Z}_{\mathbf{g}^\vee, \mathbf{h}^\vee}(\mathcal{C}_{68}) &= \omega^{\mathbf{g}_L^\vee \mathbf{h}_R^\vee - \mathbf{g}_R^\vee \mathbf{h}_L^\vee} \mathcal{Z}_{\mathbf{g}^\vee, \mathbf{h}^\vee}^{3\text{-Para}}(\mathcal{C}_{67}), \\ \mathcal{Z}_{\mathbf{g}^\vee, \mathbf{h}^\vee}(\mathcal{C}_{78}) &= \omega^{2(\mathbf{g}_L^\vee \mathbf{h}_R^\vee - \mathbf{g}_R^\vee \mathbf{h}_L^\vee)} \mathcal{Z}_{\mathbf{g}^\vee, \mathbf{h}^\vee}^{3\text{-Para}}(\mathcal{C}_{67}). \end{aligned} \quad (5.152)$$

The phase factors are the topological partition functions for the SPT phase on the duality domain-wall labeled by  $k$  and  $k^2$ . Both of these partition functions are equal to  $\mathcal{C}_{67}$  in the untwisted sector (i.e.  $(\mathbf{g}_L^\vee, \mathbf{g}_R^\vee) = (0, 0)$ ) and one might consider these transition to belong

to the same universality class, as has been pointed out in [179]. However, they differ in the twisted sectors due to the effect of the topological SPT phase. In other words, these CFTs have the same conformal spectra but in the twisted sectors the Virasoro primaries (and their descendants) transform differently under global  $\mathbb{Z}_3 \times \mathbb{Z}_3$  symmetry. Therefore, these CFTs belong to the same universality class if we only consider conformal symmetry but they belong to topologically-distinct universality classes if we also consider the global  $\mathbb{Z}_3 \times \mathbb{Z}_3$  symmetry. In Table 4, we have tabulated the conformal spectra of these three transitions with twisted boundary condition  $(\mathbf{g}_L^\vee, \mathbf{g}_R^\vee) = (1, 1)$ . As can be seen, conformal spectra are identical but the transformation properties of fields under  $\mathbb{Z}_3 \times \mathbb{Z}_3$  symmetry are different, illustrating the topological-distinctness of these criticalities.

As another application, consider the duality  $k : \mathcal{C}_{16} \mapsto \mathcal{C}_{18}$  and  $k^2 : \mathcal{C}_{16} \mapsto \mathcal{C}_{17}$ . The corresponding Hamiltonian for transitions are

$$\begin{aligned} H(\mathcal{C}_{18}) &= - \sum_i \left[ Z_i^L (Z_{i+1}^L)^2 + Z_i^R (Z_{i+1}^R)^2 + Z_i^L (Z_{i+1}^L)^2 X_{i+1}^R + (X_i^L)^2 Z_i^R (Z_{i+1}^R)^2 \right] + \text{h.c.}, \\ H(\mathcal{C}_{17}) &= - \sum_i \left[ Z_i^L (Z_{i+1}^L)^2 + Z_i^R (Z_{i+1}^R)^2 + Z_i^L (Z_{i+1}^L)^2 (X_{i+1}^R)^2 + X_i^L Z_i^R (Z_{i+1}^R)^2 \right] + \text{h.c.} \end{aligned} \quad (5.153)$$

These critical spin-chain models couple between the two chains and are in general complicated to analyze. However, using dualities at the level of partition functions, we can find their exact spectra

$$\begin{aligned} \mathcal{Z}_{\mathbf{g}^\vee, \mathbf{h}^\vee}(\mathcal{C}_{18}) &= \omega^{\mathbf{g}_L^\vee \mathbf{h}_R^\vee - \mathbf{g}_R^\vee \mathbf{h}_L^\vee} \mathcal{Z}_{\mathbf{g}^\vee, \mathbf{h}^\vee}(\mathcal{C}_{16}), \\ \mathcal{Z}_{\mathbf{g}^\vee, \mathbf{h}^\vee}(\mathcal{C}_{17}) &= \omega^{2(\mathbf{g}_L^\vee \mathbf{h}_R^\vee - \mathbf{g}_R^\vee \mathbf{h}_L^\vee)} \mathcal{Z}_{\mathbf{g}^\vee, \mathbf{h}^\vee}(\mathcal{C}_{16}). \end{aligned} \quad (5.154)$$

We again see that  $\mathcal{C}_{16}$ ,  $\mathcal{C}_{17}$ , and  $\mathcal{C}_{18}$  have identical partition functions for periodic boundary conditions (i.e.  $(\mathbf{g}_L^\vee, \mathbf{g}_R^\vee) = (0, 0)$ ). Naively, one would think that all these transitions are described by two decoupled  $\mathbb{Z}_3$  parafermion universality class. However, we find that the partition functions do not match in all twisted sectors. In particular, the SPT twist can still be detected in the twisted sectors and therefore, these transitions can be distinguished. We call these criticalities *topological spontaneous symmetry-breaking transitions*. Using the language of [119], the  $\mathcal{C}_{68}$ ,  $\mathcal{C}_{78}$ ,  $\mathcal{C}_{17}$  and  $\mathcal{C}_{18}$  are nontrivial  $\mathbb{Z}_3 \times \mathbb{Z}_3$  symmetry-enriched CFTs. Similar to gapped SPT phases, they can be distinguished by their edge modes.

## Prediction of new nonconformal phase transitions

There has been convincing recent evidence based on numerical studies that the  $\mathbb{Z}_3$  symmetric quantum spin systems (see (5.57) for  $N = 3$ ) in general with complex parameters ( $\lambda \in \mathbb{C}$ ) host generic, i.e., non-fine-tuned phase transitions with a dynamical critical exponent  $z > 1$  [184]. The low-energy description of such a transition is not given by a conventional conformal field theory. In fact, the example of the non-conformal transition realized in the  $\mathbb{Z}_3$  spin chain is claimed to be the first such strongly-coupled, generic transition between gapped phases. Naturally, the  $\mathbb{Z}_3 \times \mathbb{Z}_3$  model also hosts decoupled doubled non-conformal transitions in the model

$$H = t_1 H_1^{\text{non-c}} + t_2 H_2^{\text{non-c}}, \quad (5.155)$$

where  $H_i^{\text{non-c}}$  is a  $\mathbb{Z}_3$ -symmetric Hamiltonian at a non-conformal transition on the  $i^{\text{th}}$  chain. Using the vast web of dualities and the decoupled Hamiltonian (5.155), we can in principle

Topological criticalities ( $\mathcal{C}_{67}, \mathcal{C}_{68}, \mathcal{C}_{78}$ ) with defect $\mathcal{U}_{1,1}$																	
$h + \bar{h}$	$\frac{4}{15}$	$\frac{14}{15}$	$\frac{4}{3}$	$\frac{22}{15}$	$\frac{8}{3}$	$\frac{2}{3}$	$\frac{4}{5}$	$\frac{22}{15}$	$\frac{7}{15}$	$\frac{3}{5}$	$\frac{9}{5}$	$\frac{19}{15}$	$\frac{17}{15}$	2			
$h - \bar{h}$	0	0	0	0	0	$\pm\frac{2}{3}$	$\pm\frac{2}{3}$	$\pm\frac{2}{3}$	$\pm\frac{1}{3}$	$\pm\frac{1}{3}$	$\pm\frac{1}{3}$	$\pm\frac{1}{3}$	$\pm 1$	$\pm\frac{2}{3}$			
multiplicity	2	1	1	4	2	2	4	2	2	4	4	2	2	4			
$(\alpha_L, \alpha_R)_{\mathcal{C}_{67}}$	$\begin{pmatrix} (0,0) \\ (2,1) \end{pmatrix}$	$(1,2)$	$(1,2)$	$\begin{pmatrix} (0,0) \\ (2,1) \end{pmatrix}$	$\begin{pmatrix} (0,0) \\ (2,1) \end{pmatrix}$	$\begin{pmatrix} (0,1) \\ (2,0) \end{pmatrix}$	$\begin{pmatrix} (1,1) \\ (1,0) \end{pmatrix}$	$\begin{pmatrix} (0,2) \\ (2,2) \end{pmatrix}$	$\begin{pmatrix} (0,1) \\ (2,0) \end{pmatrix}$	$\begin{pmatrix} (0,1) \\ (2,0) \end{pmatrix}$	$\begin{pmatrix} (1,1) \\ (1,0) \end{pmatrix}$	$\begin{pmatrix} (0,2) \\ (2,2) \end{pmatrix}$	$\begin{pmatrix} (1,1) \\ (1,0) \end{pmatrix}$	$\begin{pmatrix} (0,2) \\ (2,0) \end{pmatrix}$	$(1,2)$	$\begin{pmatrix} (1,1) \\ (1,0) \end{pmatrix}$	$\begin{pmatrix} (0,2) \\ (2,2) \end{pmatrix}$
$(\alpha_L, \alpha_R)_{\mathcal{C}_{68}}$	$\begin{pmatrix} (0,0) \\ (1,2) \end{pmatrix}$	$(2,1)$	$(2,1)$	$\begin{pmatrix} (0,0) \\ (1,2) \end{pmatrix}$	$\begin{pmatrix} (0,0) \\ (1,2) \end{pmatrix}$	$\begin{pmatrix} (1,0) \\ (0,2) \end{pmatrix}$	$\begin{pmatrix} (0,1) \\ (2,0) \end{pmatrix}$	$\begin{pmatrix} (1,1) \\ (2,2) \end{pmatrix}$	$\begin{pmatrix} (1,0) \\ (0,2) \end{pmatrix}$	$\begin{pmatrix} (1,0) \\ (0,2) \end{pmatrix}$	$\begin{pmatrix} (0,1) \\ (2,0) \end{pmatrix}$	$\begin{pmatrix} (1,1) \\ (2,2) \end{pmatrix}$	$\begin{pmatrix} (0,1) \\ (2,0) \end{pmatrix}$	$\begin{pmatrix} (1,1) \\ (0,2) \end{pmatrix}$	$(2,1)$	$\begin{pmatrix} (0,1) \\ (2,0) \end{pmatrix}$	$\begin{pmatrix} (1,1) \\ (2,2) \end{pmatrix}$
$(\alpha_L, \alpha_R)_{\mathcal{C}_{78}}$	$\begin{pmatrix} (2,1) \\ (1,2) \end{pmatrix}$	$(0,0)$	$(0,0)$	$\begin{pmatrix} (2,1) \\ (1,2) \end{pmatrix}$	$\begin{pmatrix} (2,1) \\ (1,2) \end{pmatrix}$	$\begin{pmatrix} (1,1) \\ (2,2) \end{pmatrix}$	$\begin{pmatrix} (1,0) \\ (2,0) \end{pmatrix}$	$\begin{pmatrix} (0,1) \\ (0,2) \end{pmatrix}$	$\begin{pmatrix} (1,1) \\ (2,2) \end{pmatrix}$	$\begin{pmatrix} (1,1) \\ (2,2) \end{pmatrix}$	$\begin{pmatrix} (1,0) \\ (2,0) \end{pmatrix}$	$\begin{pmatrix} (0,1) \\ (0,2) \end{pmatrix}$	$\begin{pmatrix} (1,0) \\ (2,0) \end{pmatrix}$	$\begin{pmatrix} (0,1) \\ (0,2) \end{pmatrix}$	$(0,0)$	$\begin{pmatrix} (1,0) \\ (2,0) \end{pmatrix}$	$\begin{pmatrix} (0,1) \\ (0,2) \end{pmatrix}$

Table 4: The spectrum of primary fields for the topological criticalities  $\mathcal{C}_{67}, \mathcal{C}_{68}$ , and  $\mathcal{C}_{78}$ ) with the twisted boundary condition  $(\mathbf{g}_L^\vee, \mathbf{g}_R^\vee) = (1, 1)$ . These three critical points have the same conformal spectrum but the action of the global  $\mathbb{Z}_3 \times \mathbb{Z}_3$  symmetries differs. As  $\mathbb{Z}_3 \times \mathbb{Z}_3$  symmetry-enriched CFTs, these criticalities are topologically distinct and belong to different universality classes.

find many new non-trivial non-conformal transitions. These new transitions will generically couple the two chains and correspond to phase transitions between non-trivial, potentially topological, phases.

## 5.5 $\mathbb{Z}_2 \times \mathbb{Z}_4$ symmetric quantum spin chains

We now turn to the  $\mathbb{Z}_2^L \times \mathbb{Z}_4^R$  global symmetry. Even though this example mixes  $\mathbb{Z}_2$  and  $\mathbb{Z}_4$  symmetry, surprisingly there is a large duality group of order 128. This symmetry group has two different fusion structures. Although there is more than one fusion structure, this example still belongs to the limit where topological holography is powerful. A thorough analysis of the phase diagram of such models will appear elsewhere. In this example, we restrict ourselves to computing the conformal spectra of a few interesting phase transitions.

The group of excitations of the bulk theory is

$$\mathcal{A} = \mathbb{Z}_2^L \times \mathbb{Z}_4^R \times \text{Rep}(\mathbb{Z}_2^L \times \mathbb{Z}_4^R) \simeq \mathbb{Z}_2^L \times \mathbb{Z}_4^R \times \mathbb{Z}_2^L \times \mathbb{Z}_4^R \simeq \langle e_L, m_L, e_R, m_R \rangle, \quad (5.156)$$

where the generators satisfy the following relations

$$e_L^2 = m_L^2 = 1, \quad e_R^4 = m_R^4 = 1. \quad (5.157)$$

There are 10 Lagrangian subgroups/gapped phases as tabulated in Table 5. The Hilbert space of the corresponding spin chain is

$$\mathcal{H} = \bigotimes_{i \in \text{sites}} \mathbb{C}^2 \otimes \mathbb{C}^4. \quad (5.158)$$

Lagrangian subgroups	Generating set	Fusion Structure	Image of $\Pi$	H	$\psi(\mathbf{h}_1, \mathbf{h}_2)$	Gapped phase
$\mathcal{L}_1$	$e_L, e_R$	$\mathbb{Z}_2 \times \mathbb{Z}_4$	$1_L, 1_R$	$\mathbb{I}$	1	SSB
$\mathcal{L}_2$	$m_L, e_R$	$\mathbb{Z}_2 \times \mathbb{Z}_4$	$m_L$	$\mathbb{Z}_2^L$	1	$\text{PSB}_L$
$\mathcal{L}_3$	$e_L, m_R$	$\mathbb{Z}_2 \times \mathbb{Z}_4$	$m_R$	$\mathbb{Z}_4^R$	1	$\text{PSB}_R$
$\mathcal{L}_4$	$e_L e_R, m_L m_R^2$	$\mathbb{Z}_2 \times \mathbb{Z}_4$	$m_L m_R^2$	$\mathbb{Z}_2^D$	1	$\text{PSB}[\mathbb{Z}_2^D]$
$\mathcal{L}_5$	$e_L, e_R^2, m_R^2$	$\mathbb{Z}_2 \times \mathbb{Z}_2 \times \mathbb{Z}_2$	$m_R^2$	$\mathbb{Z}_2^{(4)}$	1	$\text{PSB}[\mathbb{Z}_2^{(4)}]$
$\mathcal{L}_6$	$e_L e_R^2, m_L m_R$	$\mathbb{Z}_2 \times \mathbb{Z}_4$	$m_L m_R$	$\mathbb{Z}_4^D$	1	$\text{PSB}[\mathbb{Z}_4^D]$
$\mathcal{L}_7$	$m_L, e_R^2, m_R^2$	$\mathbb{Z}_2 \times \mathbb{Z}_2 \times \mathbb{Z}_2$	$m_L, m_R^2$	$\mathbb{Z}_2 \times \mathbb{Z}_2^{(4)}$	1	$\text{SPT}_0^{(1)}$
$\mathcal{L}_8$	$e_L m_R^2, m_L e_R$	$\mathbb{Z}_2 \times \mathbb{Z}_4$	$m_L, m_R^2$	$\mathbb{Z}_2 \times \mathbb{Z}_2^{(4)}$	$(-1)^{h_{1,L} h_{2,R}}$	$\text{SPT}_1^{(1)}$
$\mathcal{L}_9$	$m_L, m_R$	$\mathbb{Z}_2 \times \mathbb{Z}_4$	$m_L, m_R$	$\mathbb{Z}_2^L \times \mathbb{Z}_4^R$	1	$\text{SPT}_0^{(2)}$
$\mathcal{L}_{10}$	$e_L m_R, m_L e_R^2$	$\mathbb{Z}_2 \times \mathbb{Z}_4$	$m_R, m_L$	$\mathbb{Z}_2^L \times \mathbb{Z}_4^R$	$(-1)^{h_{1,L} h_{2,R}}$	$\text{SPT}_1^{(2)}$

Table 5: The Lagrangian subgroups for  $\mathbf{G} = \mathbb{Z}_2^L \times \mathbb{Z}_4^R$  and their various properties.  $\mathbb{Z}_2^D$  and  $\mathbb{Z}_4^D$  denote the “diagonal” subgroups, and  $\mathbb{Z}_2^{(4)}$  denotes the  $\mathbb{Z}_2$  subgroup of  $\mathbb{Z}_4$ . There are two classes of SPT states denoted as  $\text{SPT}^{(1)}$ , protected by  $\mathbb{Z}_2 \times \mathbb{Z}_2^{(4)}$  symmetry, and  $\text{SPT}^{(2)}$ , protected by  $\mathbb{Z}_2^L \times \mathbb{Z}_4^R$  symmetry. Since  $H^2(\mathbb{Z}_2 \times \mathbb{Z}_4, \text{U}(1)) \simeq H^2(\mathbb{Z}_2 \times \mathbb{Z}_2, \text{U}(1)) \simeq \mathbb{Z}_2$ , each classes of SPT states contains two inequivalent phases denoted as  $\text{SPT}_0^{(1)}$  and  $\text{SPT}_1^{(1)}$  for the first class and  $\text{SPT}_0^{(2)}$  and  $\text{SPT}_1^{(2)}$  for the second class. The 2-cocycle is evaluated on the group elements  $\mathbf{h}_i = (h_{i,L}, h_{i,R}) \in \mathbf{H}$  for  $i = 1, 2$ .

The symmetry operator

$$\mathcal{U}_{\mathbf{g}_L, \mathbf{g}_R} = \bigotimes_i (\sigma_i^x)^{\mathbf{g}_L} \otimes X_i^{\mathbf{g}_R}, \quad \mathbf{g}_L = 0, 1, \quad \mathbf{g}_R = 0, 1, 2, 3. \quad (5.159)$$

$X_i$  and  $Z_i$  denote the  $\mathbb{Z}_4$  generalizations of Pauli matrices. The spin-chain operators corresponding to the electric and magnetic bulk excitations are given by (see equation (3.28))

$$\begin{aligned} e_L &\longrightarrow \sigma_i^z \sigma_{i+1}^z, & m_L &\longrightarrow \sigma_i^x \\ e_R &\longrightarrow Z_i Z_{i+1}^3, & m_R &\longrightarrow X_i. \end{aligned} \quad (5.160)$$

Spin-chain operators for other dyons can be obtained similarly. The fixed-point Hamiltonians associated to each of the gapped phases can be obtained using (3.36). The Hamiltonian associated to the SSB phase is given by<sup>21</sup>

$$H_1 = - \sum_i [\sigma_i^z \sigma_{i+1}^z + Z_i Z_{i+1}^3] + \text{h.c.} \quad (5.161)$$

The fixed-point Hamiltonians associated to the five possible partial symmetry-breaking

<sup>21</sup>We label the Hamiltonians with the corresponding gapped phase, described by a Lagrangian subgroup. Therefore, the Hamiltonian associated to the Lagrangian subgroup  $\mathcal{L}_i$  in Table 5 is denoted as  $H_i$ .

phases are

$$\begin{aligned}
H_2 &= - \sum_i [\sigma_i^x + Z_i Z_{i+1}^3] + \text{h.c.}, \\
H_3 &= - \sum_i [\sigma_i^z \sigma_{i+1}^z + X_i] + \text{h.c.}, \\
H_4 &= - \sum_i [\sigma_i^z \sigma_{i+1}^z Z_i Z_{i+1}^3 + \sigma_i^x X_i^2] + \text{h.c.}, \\
H_5 &= - \sum_i [\sigma_i^z \sigma_{i+1}^z + Z_i^2 Z_{i+1}^2 + X_i^2 X_{i+1}^2] + \text{h.c.}, \\
H_6 &= - \sum_i [\sigma_i^z \sigma_{i+1}^z Z_i^2 Z_{i+1}^2 + \sigma_i^x X_i] + \text{h.c.}.
\end{aligned} \tag{5.162}$$

The fixed-point Hamiltonians corresponding to  $\mathbb{Z}_2 \times \mathbb{Z}_2^{(4)}$  SPT phases are

$$\begin{aligned}
H_7 &= - \sum_i [\sigma_i^x + Z_i^2 Z_{i+1}^2 + X_i^2] + \text{h.c.}, \\
H_8 &= - \sum_i [\sigma_i^z \sigma_{i+1}^z X_{i+1}^2 + \sigma_i^x Z_i Z_{i+1}^3] + \text{h.c.},
\end{aligned} \tag{5.163}$$

while  $\mathbb{Z}_2 \times \mathbb{Z}_4$  SPT phases are

$$\begin{aligned}
H_9 &= - \sum_i [\sigma_i^x + X_i] + \text{h.c.}, \\
H_{10} &= - \sum_i [\sigma_i^z \sigma_{i+1}^z X_{i+1} + \sigma_i^x Z_i^2 Z_{i+1}^2] + \text{h.c.}.
\end{aligned} \tag{5.164}$$

Similar to the previous examples, one can study the phase diagram of the simplest minimal model  $H = \sum_{a=1}^{10} t_a H_a$  using dualities. However, here we will confine ourselves to the study of few transitions.

The duality group is generated by partial electric-magnetic dualities, universal kinematical dualities (elements of  $\text{Aut}(\mathbb{Z}_2 \times \mathbb{Z}_4) \simeq D_4$ ), and universal dynamical dualities (elements of  $H^2(\mathbb{Z}_2 \times \mathbb{Z}_4, \text{U}(1)) \simeq \mathbb{Z}_2$ ). However, it turns out that the following three dualities generate the full duality group  $\mathcal{G}[\mathbb{Z}_2 \times \mathbb{Z}_4]$

$$\begin{aligned}
\sigma_L &: \{m_L \mapsto e_L, e_L \mapsto m_L\}, \\
\sigma_R &: \{m_R \mapsto e_R, e_R \mapsto m_R\}, \\
k &: \{m_L \mapsto m_L e_R^2, m_R \mapsto e_L m_R\}.
\end{aligned} \tag{5.165}$$

Physically  $k \in H^2(\mathbb{Z}_2 \times \mathbb{Z}_4, \text{U}(1))$  corresponds to a domain wall in the bulk with a  $\mathbb{Z}_2 \times \mathbb{Z}_4$  SPT phase. The duality group is

$$\mathcal{G}[\mathbb{Z}_2 \times \mathbb{Z}_4] = (D_4 \times D_4) \rtimes \mathbb{Z}_2. \tag{5.166}$$

The minimal transition  $\mathcal{C}_{19}$  between  $\mathcal{L}_1$  and  $\mathcal{L}_9$  is given by decoupled copies of Ising and  $\mathbb{Z}_4$  parafermion CFTs (see Appendix G for their twisted partition functions). Under the duality  $k$ ,  $\mathcal{L}_1$  is invariant while  $\mathcal{L}_9 \mapsto \mathcal{L}_{10}$  which maps  $\mathcal{C}_{19}$  to the topological SSB transition  $\mathcal{C}_{1,10}$ . The twisted partition functions of  $\mathcal{C}_{1,10}$  is given by the following orbifold

$$\mathcal{Z}_{(\mathfrak{g}_L^\vee, \mathfrak{g}_R^\vee), (\mathfrak{h}_L^\vee, \mathfrak{g}_R^\vee)}(\mathcal{C}_{1,10}) = (-1)^{\mathfrak{h}_L^\vee \mathfrak{g}_R^\vee - \mathfrak{h}_R^\vee \mathfrak{g}_L^\vee} \mathcal{Z}_{\mathfrak{g}_L^\vee, \mathfrak{h}_L^\vee}^{\text{Ising}} \mathcal{Z}_{\mathfrak{g}_R^\vee, \mathfrak{h}_R^\vee}^{4-\text{Para}}, \tag{5.167}$$

where  $\mathcal{Z}_{\mathbf{g}_R^\vee, \mathbf{h}_R^\vee}^{4\text{-Para}}$  denotes the twisted partition function of  $\mathbb{Z}_4$  parafermion CFT. The phase factor in (5.167) is the partition function of the SPT phase on the duality domain-wall labeled by  $k$ . Similar to the previous  $\mathbb{Z}_3 \times \mathbb{Z}_3$  example, the partition function with periodic boundary condition is identical to that of the decoupled Ising and  $\mathbb{Z}_4$  parafermion CFTs ( $\mathcal{C}_{19}$  transition). However, the twisted sectors of  $\mathcal{C}_{1,10}$  criticality is twisted by the SPT cocycle and hence differs from  $\mathcal{C}_{19}$ . This is another example of topological SSB or, in the language of [119], a nontrivial  $\mathbb{Z}_2 \times \mathbb{Z}_4$  symmetry-enriched CFT.

Consider the duality

$$\sigma : \{m_L \mapsto e_L m_R^2, e_L \mapsto m_L e_R^2, m_R \mapsto m_L e_R^3, e_R \mapsto e_L m_R\}, \quad (5.168)$$

which maps  $\mathcal{L}_1 \mapsto \mathcal{L}_{10}$  and  $\mathcal{L}_9 \mapsto \mathcal{L}_8$ . Therefore, this maps  $\mathcal{C}_{19}$  to  $\mathcal{C}_{8,10}$  which is the criticality between the two nontrivial SPT phases protected by  $\mathbb{Z}_2 \times \mathbb{Z}_2^{(4)}$  and  $\mathbb{Z}_2 \times \mathbb{Z}_4$  symmetries, respectively. The generalized twisted partition functions are

$$\mathcal{Z}_{(\mathbf{g}^\vee, \mathbf{h}^\vee)}(\mathcal{C}_{8,10}) = \frac{1}{8} \sum_{\substack{\mathbf{g}_L, \mathbf{g}_R \\ \mathbf{h}_L, \mathbf{h}_R}} (-1)^{[(\mathbf{g}_L - \mathbf{g}_R^\vee)(\mathbf{h}_L^\vee - 2\mathbf{h}_R) - \mathbf{h}_L \mathbf{g}_L^\vee]_\omega [(\mathbf{g}_R - 2\mathbf{g}_L^\vee)(\mathbf{h}_R^\vee - 2\mathbf{h}_L) - 3\mathbf{g}_R^\vee \mathbf{h}_R]} \mathcal{Z}_{\mathbf{g}_L, \mathbf{h}_L}^{\text{Ising}} \mathcal{Z}_{\mathbf{g}_R, \mathbf{h}_R}^{4\text{-Para}}. \quad (5.169)$$

## 5.6 $\mathbb{Z}_2 \times \mathbb{Z}_2 \times \mathbb{Z}_2$ symmetric quantum spin chains

Topological holography is extremely powerful for symmetry groups of the form  $\mathbb{Z}_2 \times \cdots \times \mathbb{Z}_2$ . These groups have a single fusion structure and many dualities. For  $\mathbf{G} = \mathbb{Z}_2 \times \mathbb{Z}_2 \times \mathbb{Z}_2$ , the duality group is  $\mathcal{G}[\mathbf{G}] \simeq S_8$  with over forty thousand dualities. For  $\mathbf{G} = \mathbb{Z}_2^{\times 4}$ , the duality group is  $O_8^+(2) \rtimes \mathbb{Z}_2$  with over 350 million dualities. In this example, we will not delve into great details, as the space of  $\mathbb{Z}_2^{\times 3}$  theories is very rich. Further investigation will appear elsewhere. Here, we will make few simple remarks to highlight the rich geometric structure of the minimal-model phase diagram.

The bulk theory has 64 anyons

$$\mathcal{A} = \mathbf{G} \times \text{Rep}(\mathbf{G}) \simeq \mathbf{G}^2 = \langle m_1, m_2, m_3, e_1, e_2, e_3 \rangle. \quad (5.170)$$

The duality group is generated by

1. **Partial electric-magnetic dualities:** There are three independent partial em dualities which we denote as  $\sigma_i$  with  $i = 1, 2, 3$ , which act on the generators of  $\mathcal{A}$  as

$$\sigma_i : \begin{bmatrix} m_j \\ e_j \end{bmatrix} \mapsto \begin{bmatrix} (1 - \delta_{ij})m_j + \delta_{ij}e_j \\ (1 - \delta_{ij})e_j + \delta_{ij}m_j \end{bmatrix}. \quad (5.171)$$

2. **Universal kinematical symmetries:** These dualities are related to automorphism group of  $\mathbb{Z}_2^{\times 3}$ . They are given by

$$\begin{aligned} h_1 &: \{m_1 \mapsto m_2, m_2 \mapsto m_1, e_1 \mapsto e_2, e_2 \mapsto e_1\}, \\ h_2 &: \{m_1 \mapsto m_2, m_2 \mapsto m_3, m_3 \mapsto m_1, e_1 \mapsto e_2, e_2 \mapsto e_3, e_3 \mapsto e_1\}, \\ h_3 &: \{m_1 \mapsto m_1 m_2, e_2 \mapsto e_1 e_2\}. \end{aligned} \quad (5.172)$$

Together,  $h_1$  and  $h_2$  generate the permutation group of three elements  $S_3$ , while the full group generated by  $h_1$ ,  $h_2$  and  $h_3$  is the group  $\text{PSL}(3, 2)$  of order 168.

3. **Universal dynamical symmetries:** These dualities are classified by  $H^2(\mathbf{G}, \mathbf{U}(1)) = \mathbb{Z}_2^3$  and correspond to bulk duality-walls with SPT phases. They act on anyons as

$$\begin{aligned} k_1 &: \{e_1 \mapsto e_1 m_2, e_2 \mapsto m_1 e_2\}, \\ k_2 &: \{e_2 \mapsto e_2 m_3, e_3 \mapsto m_2 e_3\}, \\ k_3 &: \{e_1 \mapsto e_1 m_3, e_3 \mapsto m_1 e_3\}. \end{aligned} \tag{5.173}$$

It turns out that the full group  $\mathcal{G}[\mathbf{G}] = S_8$  can be generated by  $\sigma_1, k_1$  and  $k_2$ .

Lagrangian subgroups	Generating set	H	$\psi(\mathbf{h}, \bar{\mathbf{h}})$
$\mathcal{L}_1$	$e_1, e_2, e_3$	$\mathbb{I}$	1
$\mathcal{L}_2$	$m_1, e_2, e_3$	$\mathbb{Z}_2^{(1)}$	1
$\mathcal{L}_3$	$e_1, m_2, e_3$	$\mathbb{Z}_2^{(2)}$	1
$\mathcal{L}_4$	$e_1, e_2, m_3$	$\mathbb{Z}_2^{(3)}$	1
$\mathcal{L}_5$	$m_1 m_2, e_3, e_1 e_2$	$\mathbb{Z}_2^{(1-2)}$	1
$\mathcal{L}_6$	$m_2 m_3, e_1, e_2 e_3$	$\mathbb{Z}_2^{(2-3)}$	1
$\mathcal{L}_7$	$m_1 m_3, e_2, e_1 e_3$	$\mathbb{Z}_2^{(1-3)}$	1
$\mathcal{L}_8$	$m_1 m_2 m_3, e_1 e_2, e_2 e_3$	$\mathbb{Z}_2^{(1-2-3)}$	1
$\mathcal{L}_9$	$m_1, m_2, e_3$	$\mathbb{Z}_2^{(1)} \times \mathbb{Z}_2^{(2)}$	1
$\mathcal{L}_{10}$	$m_1 e_2, m_2 e_1, e_3$	$\mathbb{Z}_2^{(1)} \times \mathbb{Z}_2^{(2)}$	$(-1)^{h_1 \bar{h}_2}$
$\mathcal{L}_{11}$	$e_1, m_2, m_3$	$\mathbb{Z}_2^{(2)} \times \mathbb{Z}_2^{(3)}$	1
$\mathcal{L}_{12}$	$e_1, m_2 e_3, m_3 e_2$	$\mathbb{Z}_2^{(2)} \times \mathbb{Z}_2^{(3)}$	$(-1)^{h_2 \bar{h}_3}$
$\mathcal{L}_{13}$	$m_1, e_2, m_3$	$\mathbb{Z}_2^{(1)} \times \mathbb{Z}_2^{(3)}$	1
$\mathcal{L}_{14}$	$m_1 e_3, e_2, m_3 e_1$	$\mathbb{Z}_2^{(1)} \times \mathbb{Z}_2^{(3)}$	$(-1)^{h_1 \bar{h}_3}$
$\mathcal{L}_{15}$	$m_1 m_2, e_1 e_2, m_3$	$\mathbb{Z}_2^{(1-2)} \times \mathbb{Z}_2^{(3)}$	1
$\mathcal{L}_{16}$	$m_1 m_2 e_3, e_1 e_2, m_3 e_1$	$\mathbb{Z}_2^{(1-2)} \times \mathbb{Z}_2^{(3)}$	$(-1)^{h_1 \bar{h}_3 + h_2 \bar{h}_3}$
$\mathcal{L}_{17}$	$m_1, m_2 m_3, e_2 e_3$	$\mathbb{Z}_2^{(1)} \times \mathbb{Z}_2^{(2-3)}$	1
$\mathcal{L}_{18}$	$m_1 e_2, m_2 m_3 e_1, e_2 e_3$	$\mathbb{Z}_2^{(1)} \times \mathbb{Z}_2^{(2-3)}$	$(-1)^{h_1 \bar{h}_2 + h_1 \bar{h}_3}$
$\mathcal{L}_{19}$	$m_1 m_3, m_2, e_1 e_3$	$\mathbb{Z}_2^{(1-3)} \times \mathbb{Z}_2^{(2)}$	1
$\mathcal{L}_{20}$	$m_1 m_3 e_2, m_2 e_1, e_1 e_3$	$\mathbb{Z}_2^{(1-3)} \times \mathbb{Z}_2^{(2)}$	$(-1)^{h_1 \bar{h}_2 + h_2 \bar{h}_3}$
$\mathcal{L}_{21}$	$m_1 m_2, m_2 m_3, e_1 e_2 e_3$	$\mathbb{Z}_2^{(1-2)} \times \mathbb{Z}_2^{(2-3)}$	1
$\mathcal{L}_{22}$	$m_1 m_2 e_3, m_2 m_3 e_1, e_1 e_2 e_3$	$\mathbb{Z}_2^{(1-2)} \times \mathbb{Z}_2^{(2-3)}$	$(-1)^{h_1 \bar{h}_2 + h_2 \bar{h}_3 + h_3 \bar{h}_1}$
$\mathcal{L}_{23}$	$m_1, m_2, m_3$	$\mathbb{Z}_2^{(1)} \times \mathbb{Z}_2^{(2)} \times \mathbb{Z}_2^{(3)}$	1
$\mathcal{L}_{24}$	$m_1 e_2, m_2 e_1, m_3$	$\mathbb{Z}_2^{(1)} \times \mathbb{Z}_2^{(2)} \times \mathbb{Z}_2^{(3)}$	$(-1)^{h_1 \bar{h}_2}$
$\mathcal{L}_{25}$	$m_1, m_2 e_3, m_3 e_2$	$\mathbb{Z}_2^{(1)} \times \mathbb{Z}_2^{(2)} \times \mathbb{Z}_2^{(3)}$	$(-1)^{h_2 \bar{h}_3}$
$\mathcal{L}_{26}$	$m_1 e_3, m_2, m_3 e_1$	$\mathbb{Z}_2^{(1)} \times \mathbb{Z}_2^{(2)} \times \mathbb{Z}_2^{(3)}$	$(-1)^{h_3 \bar{h}_1}$
$\mathcal{L}_{27}$	$m_1 e_2 e_3, m_2 e_1, m_3 e_1$	$\mathbb{Z}_2^{(1)} \times \mathbb{Z}_2^{(2)} \times \mathbb{Z}_2^{(3)}$	$(-1)^{h_1 \bar{h}_2 + h_1 \bar{h}_3}$
$\mathcal{L}_{28}$	$m_1 e_2, m_2 e_1 e_3, m_3 e_2$	$\mathbb{Z}_2^{(1)} \times \mathbb{Z}_2^{(2)} \times \mathbb{Z}_2^{(3)}$	$(-1)^{h_1 \bar{h}_2 + h_2 \bar{h}_3}$
$\mathcal{L}_{29}$	$m_1 e_3, m_2 e_3, m_3 e_1 e_2$	$\mathbb{Z}_2^{(1)} \times \mathbb{Z}_2^{(2)} \times \mathbb{Z}_2^{(3)}$	$(-1)^{h_1 \bar{h}_3 + h_2 \bar{h}_3}$
$\mathcal{L}_{30}$	$m_1 e_2 e_3, m_2 e_1 e_3, m_3 e_1 e_2$	$\mathbb{Z}_2^{(1)} \times \mathbb{Z}_2^{(2)} \times \mathbb{Z}_2^{(3)}$	$(-1)^{h_1 \bar{h}_2 + h_2 \bar{h}_3 + h_3 \bar{h}_1}$

Table 6: Lagrangian subgroups for  $G = \mathbb{Z}_2 \times \mathbb{Z}_2 \times \mathbb{Z}_2$ .  $\mathbb{Z}_2^{(i-j)}$  means the diagonal subgroup of  $\mathbb{Z}_2^i \times \mathbb{Z}_2^j$ , while  $\mathbb{Z}_2^{(1-2-3)}$  denotes the diagonal subgroup of  $\mathbb{Z}_2 \times \mathbb{Z}_2 \times \mathbb{Z}_2$ . The 2-cocycles labelling the SPTs are evaluated on group elements  $\mathbf{h} = (h_1, h_2, h_3)$ ,  $\bar{\mathbf{h}} = (\bar{h}_1, \bar{h}_2, \bar{h}_3)$ , where  $\mathbf{h}, \bar{\mathbf{h}} \in H$ . When  $H \subset \mathbb{Z}_2^3$ , for example,  $H = \mathbb{Z}_2^{(1)} \times \mathbb{Z}_2^{(2)}$  for  $\mathcal{L}_{10}$ , we use the same notation but simply set  $h_3 = \bar{h}_3 = 0$ .



All Lagrangian subgroups/gapped phases are tabulated in Table 6.

Similar to the previous examples, we can write a fixed-point Hamiltonian for each of the thirty gapped phases in Table 6. With this, we can consider the minimal Hamiltonian

$$H = \sum_{a=1}^{30} t_a H_a, \quad t_a \in \mathbb{R}. \quad (5.174)$$

The action of the duality group on this Hamiltonian corresponds to certain permutations of the coupling constants  $t_a$ . The phase is 30-dimensional and complicated to describe. Here, we will make a few remarks about the phase diagram by attempting to decompose it into smaller known pieces. For example, we find several subgroups of  $\mathcal{G}[\mathbf{G}] \simeq S_8$  isomorphic to  $(S_3 \times S_3) \rtimes \mathbb{Z}_2$ . One such subgroups  $(S_3 \times S_3) \rtimes \mathbb{Z}_2 = \langle a, b \rangle$  is generated by

$$a : \begin{pmatrix} m_1 \\ m_2 \\ m_3 \\ e_1 \\ e_2 \\ e_3 \end{pmatrix} \mapsto \begin{pmatrix} e_1 m_2 e_3 \\ m_2 \\ m_1 m_2 m_3 e_1 e_3 \\ m_1 m_2 e_3 \\ m_1 m_2 e_1 e_2 e_3 \\ e_3 \end{pmatrix} \quad b : \begin{pmatrix} m_1 \\ m_2 \\ m_3 \\ e_1 \\ e_2 \\ e_3 \end{pmatrix} \mapsto \begin{pmatrix} m_1 m_3 \\ m_1 m_3 e_1 e_3 \\ m_1 m_3 e_1 e_2 e_3 \\ m_1 e_2 e_3 \\ m_1 m_2 e_1 e_2 e_3 \\ e_1 m_2 e_3 \end{pmatrix} \quad (5.175)$$

Upon further study, one finds that the first  $S_3$  subgroup permutes the Lagrangian subgroups  $T_1 = \{\mathcal{L}_4, \mathcal{L}_{26}, \mathcal{L}_{27}\}$  while the other  $S_3$  subgroup permutes phases in  $T_2 = \{\mathcal{L}_{11}, \mathcal{L}_{14}, \mathcal{L}_{16}\}$ . Finally, the remaining  $\mathbb{Z}_2$  subgroup permutes  $T_1$  and  $T_2$ . In other words, these six gapped phases generate a phase diagram identical to Figure 17. Similarly, there are other  $(S_3 \times S_3) \rtimes \mathbb{Z}_2$  subgroups generating similar triangles often with shared corners generating an interesting geometrical shape. However, there is slight difference to the case of  $\mathbf{G} = \mathbb{Z}_2 \times \mathbb{Z}_2$ : consider the Hamiltonian  $H_1 + H_{23}$  corresponding to three decoupled critical Ising chains with  $c = \frac{3}{2}$ . While two decoupled Ising chains had a single marginal operator, this CFT has three marginal operators generating three different  $c = \frac{3}{2}$  lines (potentially planes or volumes) of CFTs.

This suggests a simple geometric picture of the phase diagram. For  $\mathbf{G} = \mathbb{Z}_2$ , the minimal model was essentially corresponded to a 1-simplex with ferromagnetic and paramagnetic fixed-point Hamiltonians as vertices and a  $c = \frac{1}{2}$  in the center. For  $\mathbf{G} = \mathbb{Z}_2 \times \mathbb{Z}_2$ , these 1-simplices become boundaries of 2-simplices (triangles in Figure 17) with interesting new features in the interior of the 2-simplices and a transitions with  $c = 1$ . For  $\mathbf{G} = \mathbb{Z}_2 \times \mathbb{Z}_2 \times \mathbb{Z}_2$ , it appears that that several 2-simplices are glued together to form higher-dimensional geometric shapes (potentially 3-simplices similar to Figure 25) with new features in the interior and  $c = \frac{3}{2}$  criticalities. It is easy to see such a pattern persists as the symmetry group is extended by more copies of  $\mathbb{Z}_2$ .

This example contains many interesting transitions including Landau-type, topological, topological SSB, and deconfined quantum critical transitions. However, there is a new kind of transition which is both deconfined and topological (for example between  $\mathcal{L}_{10}$  and  $\mathcal{L}_{14}$  or between  $\mathcal{L}_{20}$  and  $\mathcal{L}_{22}$ ). We call such transitions *Topological Deconfined Criticality*. As far as we aware, such transitions have not been studied in the literature. Using topological holography, we can compute the exact conformal spectra of many of these transitions and study their properties in detail. The in-depth analysis will appear elsewhere.

## 6 Summary and future directions

In this work, we have outlined a framework to systematically study the global symmetry aspects of symmetric quantum systems in a given dimension using a topologically-ordered system in one higher dimension. The main idea of this work can be stated as a fruitful interplay between (1) (*the topological nature of*) *symmetry*, (2) *holography*, and (3) *dualities*. This led to a framework which is general in the sense that it can be applied to any dimension and to a broad class of symmetry structures, in particular those with finitely many symmetry operators. As illustrated in Section 5, using  $2+1d$  topologically ordered systems and  $1+1d$  quantum spin chains, topological holography is not merely an abstract framework but can be used to extract physically-interesting information for concrete condensed matter systems.

Let us briefly summarize the main results of this work pertaining to the study of  $1+1d$  quantum systems which are symmetric under a finite Abelian group  $G$ , using the framework of topological holography. In Section 3, we built up the basic foundation by combining the two main ingredients in our story, i.e. symmetry and holography. Using a  $2+1d$  topological  $G$ -gauge theory, we showed that its 1-form symmetries (generated by topological line operators) can be used to construct the space of  $G$ -symmetric operators or equivalently the space of  $G$ -symmetric  $1+1d$  theories. More precisely, the space of  $G$ -symmetric operators was encapsulated in an algebra dubbed the String Operator Algebra  $\text{SOA}[G]$ , which was used to parameterize the space of  $G$ -symmetric theories. To demonstrate the utility of this somewhat abstract holographic framework, we showed how concrete generalized spin models can be efficiently studied using these structures. Among our results, we could classify all gapped phases and explicitly construct the fixed-point (i.e. exactly-solvable) Hamiltonians and order parameters for each of them.

We then included the third main ingredient of our story, i.e., dualities. Within the holographic approach, dualities descend from 0-form symmetries of the  $2+1d$  topological gauge theory, i.e., permutations of anyons or topological line operators of the topological gauge theory which preserve all the correlation functions such as braiding (self and mutual) statistics. These dualities form a group denoted as  $\mathcal{G}[G]$  and each duality operation is associated with a codimension-1 (i.e., a two dimensional surface) topological operator/defect in the holographic bulk. Bringing the topological surfaces to the boundary leads to the action of dualities on the space of  $G$ -symmetric theories. We explicitly worked out the action of dualities on  $\text{SOA}[G]$ . Since any Hamiltonian can be constructed from elements of  $\text{SOA}[G]$ , we thus deduced the action of dualities on generic symmetric Hamiltonians. We argued that the action of dualities restricted to the space of symmetric theories is local while the same action on the space of all operators, including the non-symmetric ones, is in general non-local. Another important observation was the emergence of new symmetries in self-dual theories. Such symmetries are associated to certain topological line defects and are generically non-Abelian and sometimes non-invertible.

Remarkably all these non-trivial lessons about  $G$  symmetric theories were extracted by simple algebraic manipulations on the set of anyons.

In Section 4, we studied some of the implications of the framework we laid out in the previous section. It is known that gapped boundaries in  $2+1d$  can be labeled by a subgroup  $H$  of  $G$  and an SPT twist, i.e., an element of  $H^2(H, U(1))$ . We explained how

this data can be extracted easily from the condensed set of anyons that label a particular gapped boundary. An important question is—for which symmetry groups is topological holography most powerful? We could answer this question by introducing the notion of fusion structure of a gapped phase. We explained that this concept quantifies the power of applicability of topological holography—less number of fusion structures and larger duality group is the regime in which topological holography is more powerful. Additionally, the fusion structures were shown to impose constraints on possible dualities between gapped phases and critical points/regions. Using these constraints, we uncovered that the space of  $G$ -symmetric conformal field theories can be decomposed into blocks that are labeled by a subset of possible fusion structures for a given global symmetry  $G$ .

Possibly, the most powerful aspect of the topological holography is that it provides tools to obtain the spectrum of the dual critical transitions, using the spectra of a known transition as input. We derived a general formula for the generalized symmetry-twisted partition functions of dual transitions, which could be computed using the transformation of anyons under the duality in question. We thus demonstrated that topological holography can be used to extract stringent constraints on the structure of the phase diagram and compute physical quantities.

Finally, we illustrated this claim in Section 5, by applying the above framework to various examples of the symmetry group  $G$ . We numerically verified our predictions of phase-diagrams and conformal spectra of non-trivial critical transitions based on topological holography. We studied various new types of phase-transitions using dualities.

There are many open research directions that follow from our work and would enrich the formalism of topological holography. Let us briefly list some of them:

- **Non-Abelian and non-invertible symmetries:** In this work, we have focused on elucidating the details of the formalism for the case of finite Abelian group symmetries. An obvious generalization would be to consider symmetries corresponding to a non-Abelian discrete group  $G$  or more generally, a non-invertible fusion category  $\mathcal{C}$ . In these cases, the bulk topological order would be the Turaev-Viro-Barrett-Westbury statesum model [185, 186] or equivalently the Levin-Wen Hamiltonian models [14] constructed with the fusion category  $\text{Vec}_G$  and  $\mathcal{C}$  as input respectively (see [94]).
- **Anomalous quantum systems:** Another natural extension of the present work is to holographically study quantum systems with 't Hooft anomalies (or Lieb-Schultz-Mattis constraints) for finite Abelian groups. Holographically these symmetry structures correspond to Abelian Dijkgraaf-Witten theory with non-trivial cohomology twists  $[\omega] \in H^3(G, U(1))$ .
- **Fermionic systems:** We have only considered bulk theories which are described by Abelian bosonic TQFTs with gapped boundaries, which are known to be described by Dijkgraaf-Witten theories [144]. Another generalization of the present paper would be to consider  $2+1d$  topologically-ordered systems with elementary fermionic excitations whose low-energy description are given by (Abelian or non-Abelian) spin-TQFT [16, 61, 62, 187] which have a richer structure. One difference is that the boundary of such theories can host topologically non-trivial phases, even in the absence of any global symmetries. Therefore, the classification of beyond-Landau phases is richer in the context of fermionic systems. The study of gapped phases and phase transitions from a holographic perspective would be an interesting extension of the present work.

- **Higher dimensions:** Generalizations to higher dimensions, in particular, to explore the application of topological holography to  $2+1$  quantum magnets, which are known to possess rich phase diagrams would be an extremely interesting direction. Much less is known about  $3+1d$  topological order as compared with  $2+1d$  topological order. Moreover  $3+1d$  topological orders generically contain topological line and surface operators, i.e., 2-form and 1-form symmetries respectively, which holographically map to 1-form and 0-form symmetries respectively. The boundary theories can therefore have much richer symmetry structures which form some kind of a fusion 2-category.
- **Gauging anyonic symmetries:** It is known that gauging anyonic symmetries of  $2+1d$  topological orders lead to new topological phases called twist liquids [139, 140] with generically non-invertible topological operators. On the other hand, gauging anyonic symmetries is related to orbifolding the edge CFT. It would be very interesting to be able to understand the gapped boundaries of these exotic phases in terms of the gapped boundaries of the parent topological order, such as the relation between their phase diagrams, through the lens of topological holography (see [188, 189] for related studies pertaining to gapless edges of topological orders in  $2+1d$  and  $3+1d$  respectively).

We believe that topological holography is a valuable tool in the study of symmetric quantum systems and uncovering its full scope and details would enrich our understanding of the phase diagrams, their possible geometrical interpretation, and in general the nature and the possible unification of the theory of phase transitions between various types of quantum phases of matter. The above-mentioned research directions would pave the way for such an understanding.

## Acknowledgements

We would like to thank Benjamin Beri, Gunnar Müller, Clement Delcamp and Jens H. Bardarson for fruitful discussions. We thank Kevin Costello for critical comments on a draft of this work. The work of SFM is funded by the Natural Sciences and Engineering Research Council of Canada (NSERC) and also in part by the Alfred P. Sloan Foundation, grant FG-2020-13768. AT is supported by the Swedish Research Council (VR) through grants number 2019-04736 and 2020-00214.

## A From $G$ -topological orders to $G$ -symmetric quantum spin chains

In this appendix we provide some computational details pertaining to how  $2+1$ -dimensional  $G$  topological gauge theories can be employed as a theoretical tool to study the space of  $1+1$ -dimensional  $G$ -symmetric quantum spin chains. Our approach takes as an input a discrete Abelian group  $G$  and the corresponding  $G$  topological gauge theory  $\mathcal{T}_G$  with a trivial action, also referred to as  $G$  quantum double. We study the theory  $\mathcal{T}_G$  on a spatial semi-infinite cylinder and show that the algebra of bulk line operators restricted to the

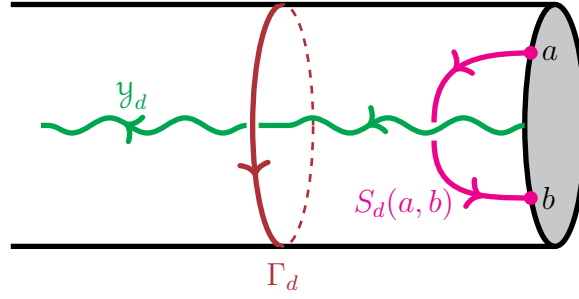


Figure 27: An illustration of the different kinds of topological line operators for a topological order defined on a semi-infinite cylinder.

spatial circle, i.e., the boundary of the cylinder is isomorphic to the algebra of  $G$  symmetric operators acting on the Hilbert space of the circle. We use this insight to flesh out the space of  $G$  symmetric quantum spin models.

The theory  $\mathcal{T}_G$  contains a set of anyons or line operators which fall into two classes, namely Wilson lines and 't-Hooft lines. The Wilson lines are labelled by a charge  $\alpha \in \text{Rep}(G)$  while the 't-Hooft lines are labelled by a flux  $g \in G$ . Therefore the most general line operator corresponds to a charge-flux composite also known as a dyon and carries the label  $d \equiv (g, \alpha) \in \mathcal{A}$ . We divide the non-trivial line operators into three families (i) line operators  $\Gamma_d$  which wrap the non-contractible cycle  $[\ell_x]$  of the cylinder<sup>22</sup>, (ii) line operators  $\mathcal{Y}_d$  defined on the line  $\ell_{y,a}$  that have one end on the boundary at  $a$ , the other end at infinity and are oriented away from the boundary and (iii) line operators with both ends on the boundary, denoted as  $S_d(a, b)$  which have support on some oriented open line  $\gamma_{ab}$  from the point  $a$  to the point  $b$  on the boundary. In addition, there are bulk line operators defined on contractible loops which act trivially on the boundary theory as they commute with all other operators in the theory. Note that the line operators of the type  $\mathcal{Y}_d$  and  $S_d$  are labelled only by the location of the end points of the lines they have support on because the precise (bulk) location of these lines can be deformed by the action of the trivial contractible loop operators. To summarize, the total set of operators that act non-trivially on the boundary Hilbert space is

$$\left\{ \Gamma_d, \mathcal{Y}_d(a), S_d(a, b) \right\}_{d \in \mathcal{A}; a, b \in S^1}. \quad (\text{A.1})$$

The algebra of these operators takes the form

$$X_d(\ell) X_{d'}(\ell') = e^{i\theta_{dd'} \text{Intersect}[\ell, \ell']} X_{d'}(\ell') X_d(\ell), \quad (\text{A.2})$$

where  $X_d(\ell)$ ,  $X_{d'}(\ell')$  denotes a line operator of the type in eq. (A.1) with  $d, d' \in \mathcal{A}$  and  $\ell, \ell'$  one of the three kinds of lines described above.  $\text{Intersect}[\ell, \ell']$  is the oriented intersection number of the lines  $\ell$  and  $\ell'$  and  $\exp \{i\theta_{dd'}\} = R_\alpha(g') R_{\alpha'}(g)$  which corresponds to the phase accrued when dyons  $d$  and  $d'$  braid. Graphically, the commutation relations of the line operators can be extracted from local moves of the form (3.5). More explicitly, the line

<sup>22</sup>Here  $[\cdot]$  refers to a homology class.

operators satisfy the following algebraic relations

$$\begin{aligned}
\Gamma_d \Gamma_{d'} &= \Gamma_{d'} \Gamma_d, \\
\Gamma_d \mathcal{Y}_{d'}(a) &= e^{i\theta_{dd'}} \mathcal{Y}_{d'}(a) \Gamma_d, \\
\mathcal{Y}_d(a) \mathcal{Y}_{d'}(b) &= \mathcal{Y}_{d'}(b) \mathcal{Y}_d(a), \\
S_d(a, b) \mathcal{Y}_{d'}(c) &= e^{i\theta_{dd'} \text{Intersect}[\gamma_{ab}, \ell_{y,c}]} \mathcal{Y}_{d'}(c) S_d(a, b), \\
S_d(a, b) S_{d'}(a', b') &= e^{i\theta_{dd'} \text{Intersect}[\gamma_{ab}, \gamma_{a'b'}]} S_{d'}(a', b') S_d(a, b), \\
S_d(a, b) \Gamma_{d'} &= \Gamma_{d'} S_d(a, b).
\end{aligned} \tag{A.3}$$

Notably in the above expressions, the intersection number remains unaltered if we deform the lines  $\gamma_{ab}$  and  $\ell_{y,a}$  as long as we keep the end-points fixed. Therefore, one is free to choose any representative line in order to evaluate the algebra.

Having described the operator algebra, we now move on to analyzing how one may organize the boundary Hilbert space  $\mathcal{H}$ . Since all the  $\Gamma_d$  operators mutually commute, we may block-diagonalize  $\mathcal{H}$  into superselection sectors which are eigenspaces of  $\Gamma_d$

$$\begin{aligned}
\mathcal{H} &= \bigoplus_{d \in \mathcal{A}} \mathcal{H}_d \\
\mathcal{H}_d &= \left\{ |\psi\rangle \mid \Gamma_{d'} |\psi\rangle = e^{i\theta_{dd'}} |\psi\rangle \right\}.
\end{aligned} \tag{A.4}$$

Using the algebraic relations in eq. (A.3), it can be seen that the remaining operators  $\{\mathcal{Y}_d(a)\}$  and  $\{S_d(a, b)\}$  act on the sectors  $\mathcal{H}_{d'}$  as

$$\begin{aligned}
\mathcal{Y}_d(a) : \mathcal{H}_{d'} &\mapsto \mathcal{H}_{d' \otimes d} \\
S_d(a, b) : \mathcal{H}_{d'} &\mapsto \mathcal{H}_{d'},
\end{aligned} \tag{A.5}$$

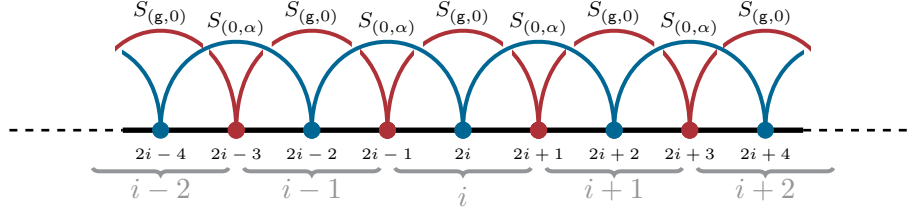
where  $d \otimes d' = (\mathbf{g} + \mathbf{g}', \alpha + \alpha')$ . Since the subspace  $\mathcal{H}_d$  is left invariant under the action of each  $S_d(a, b)$ , we can span  $\mathcal{H}_d$  using a basis that diagonalizes a maximally commuting subalgebra of the algebra generated by  $\{S_d(a, b)\}$ . For our purposes, it will prove useful to resolve the boundary into  $2L$  points where  $L$  is some integer. We allow pure charges/fluxes to terminate at odd/even points on the boundary, while more general dyonic operators need to be defined with a choice of framing. We label the points on the boundary as  $x_i$  with  $i = 1, \dots, 2L$ . Any pure charge or flux operator can be decomposed as a product of minimal length operators

$$A_j^{\mathbf{g}} \equiv S_{(\mathbf{g}, 0)}(x_{2j-1}, x_{2j+1}), \quad B_{j,j+1}^{\alpha} \equiv S_{(0, \alpha)}(x_{2j}, x_{2j+2}). \tag{A.6}$$

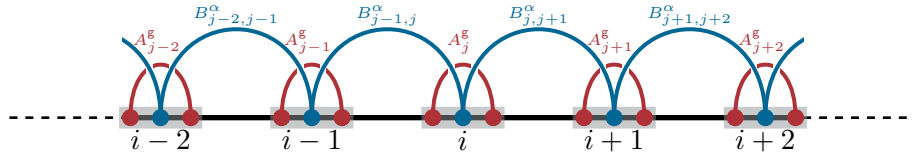
Note that the operators  $A^{\mathbf{g}}$  act on-site on an effective  $L$ -site pseudo-spin chain while the operator  $B^{\alpha}$  acts on two neighboring sites. The algebra satisfied by these operators can be read-off from eq. (A.3) and takes the form

$$A_k^{\mathbf{g}} B_{j,j+1}^{\alpha} = R_{\alpha}(\mathbf{g})^{\delta_{k,j} - \delta_{k,j+1}} B_{j,j+1}^{\alpha} A_k^{\mathbf{g}} \tag{A.7}$$

with the additional constraint that  $\prod_j A_j^{\mathbf{g}} = \Gamma_{(\mathbf{g}, 0)}$  and  $\prod_j B_{j,j+1}^{\alpha} = \Gamma_{(0, \alpha)}$ . We identify  $A_j^{\mathbf{g}}$  as the local representative of the global symmetry operator corresponding to the element  $\mathbf{g} \in \mathbf{G}$ . Therefore,  $\Gamma_{(\mathbf{g}, 0)}$  is nothing but the global symmetry operator. In order to construct the entire Hilbert space, one first starts with a reference state in  $\mathcal{H}_{(0,0)}$  and uses the operator



(a) The construction of an effective pseudo-spin chain on the boundary of a  $2 + 1d$  topological gauge theory involves regularizing the  $1 + 1d$  boundary such that the electric and magnetic topological lines can end on the even and odd points of the points of the regularized lattice.



(b) The corresponding pseudo-spin chain is obtained by representing the algebra of bulk topological line operators on a tensor product Hilbert space. Every even site of the regularized  $1 + 1d$  boundary of the topological gauge theory realizes a local Hilbert space for the pseudo spin chain, on which the minimal magnetic operators act on site, while the minimal electric operators act on two neighboring sites.

Figure 28: Effective an effective pseudo spin chain on the boundary of a  $2 + 1d$  topological gauge theory.

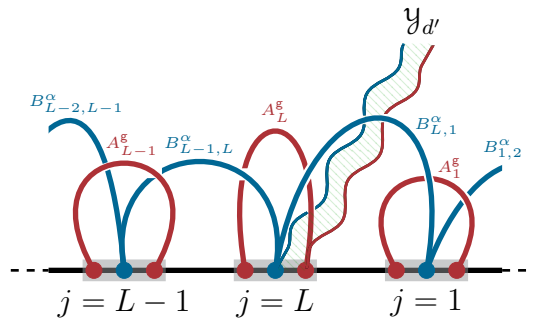


Figure 29: Within the holographic construction, one can obtain a sector  $\mathcal{H}_{d'} := \mathcal{H}_{(\mathbf{g}', \alpha')}$  that transforms in the  $\alpha'$  representation of  $\mathbf{G}$  and has  $\mathbf{g}'$ -symmetry-twisted boundary conditions by acting with a semi-infinite line operator  $\mathcal{Y}_{d'}$ .



$\mathcal{H}_d$  to obtain a locally isomorphic state in the sector  $\mathcal{H}_d$  (see Fig. 29). The Hilbert space  $\mathcal{H}_d$  can be spanned by the simultaneous eigenbasis of the operators  $B_{j,j+1}^\alpha$ , such that a given sector is constructed as

$$\mathcal{H}_d := \text{Span}_{\mathbb{C}} \left\{ |\underline{a}, d\rangle = W_d |\underline{a}, 0\rangle \right\}, \quad (\text{A.8})$$

where  $\underline{a} = (a_{1,2}, a_{2,3}, \dots, a_{L-1,L}, a_{L,1})$  where  $a_{j,j+1} \in \mathbf{G}$ . More formally  $\underline{a} \in C^1(M, \mathbf{G})$ , i.e. a  $\mathbf{G}$ -valued 1-cochain on the one dimensional pseudo-spin lattice denoted here as  $M$ . The eigenstates  $|\underline{a}, d\rangle$  are simultaneous eigenstates of  $B_{j,j+1}^\alpha$  and  $\Gamma_d$

$$B_{j,j+1}^\alpha |\underline{a}, d\rangle = R_\alpha(a_{j,j+1}) |\underline{a}, d\rangle, \quad \Gamma_{d'} |\underline{a}, d\rangle = e^{i\theta_{d,d'}} |\underline{a}, d\rangle. \quad (\text{A.9})$$

Meanwhile, the operators  $A_j^g$  act off-diagonally on the  $\{|\underline{a}, d\rangle\}$  basis as

$$\begin{aligned} \prod_j A_j^{\mathbf{g}_j} |\underline{a}, d\rangle &= |(a_{1,2} + \mathbf{g}_2 - \mathbf{g}_1, a_{2,3} + \mathbf{g}_3 - \mathbf{g}_2, \dots, a_{L,1} + \mathbf{g}_L - \mathbf{g}_1), d\rangle \\ &= |\underline{a} + \delta \underline{g}, d\rangle, \end{aligned} \quad (\text{A.10})$$

where  $\underline{\mathbf{g}} = (\mathbf{g}_1, \mathbf{g}_2, \dots, \mathbf{g}_L) \in C^0(M, \mathbf{G})$  a  $\mathbf{G}$ -values 0-cochain or simply a map from the vertices of the pseudo-spin chain lattice  $M$  to the group  $\mathbf{G}$ . From this construction one can see that the  $B^\alpha$  eigenbasis  $\{|\underline{a}, d\rangle\}$  is reminiscent of a  $\mathbf{G}$  gauge theory where the  $\underline{a}$  plays the role of the gauge field while the  $A^{\mathbf{g}}$  operators implement gauge transformations. This is ofcourse not entirely physically meaningful as in the present case, the “gauge transformations” are physical unlike in a gauge theory. In a particular sector,  $d = (\mathbf{g}, \alpha)$ , there is an additional constraint that the holonomy of the “gauge field”  $\prod_j a_{j,j+1} = \mathbf{g}$ . From a spin-chain perspective, the Hilbert space sector  $\mathcal{H}_d$  contains the states which have  $\mathbf{g}$  symmetry twisted boundary conditions and transform in the  $\alpha$  representation under global  $\mathbf{G}$  symmetry.

Next, let us focus on the local operators acting on the boundary pseudo-spin chain. Clearly the algebra of local operators is generated by  $\mathbb{A} := \{A_j^{\mathbf{g}}\}_{\mathbf{g},j}$  and  $\mathbb{B} := \{B_{j,j+1}^\alpha\}_{\alpha,j}$  operators. We refer to this algebra as the string operator algebra (SOA), denoted as  $\text{SOA}[\mathbf{G}]$ . Since every operator in  $\mathbb{A}$  and  $\mathbb{B}$  commutes with  $\Gamma_d$  for all  $d \in \mathcal{A}$ , we can further block decompose the SOA into eigenspaces of the  $\Gamma_d$  operators. Therefore, we get

$$\text{SOA}[\mathbf{G}] = \langle \mathbb{A}, \mathbb{B} \rangle = \bigoplus_d \text{SOA}_d[\mathbf{G}] = \bigoplus_d \langle \mathbb{A}_d, \mathbb{B}_d \rangle, \quad (\text{A.11})$$

where  $\text{SOA} \in \mathcal{L}(\mathcal{H}_d)$ , the space of linear operators acting on  $\mathcal{H}_d$ . In order to obtain a more explicit representation of the SOA, one requires a convenient basis of operators that span the algebra. In particular such a basis would play a crucial role in the construction of the space of  $\mathbf{G}$ -symmetric local Hamiltonians and consequently in systematizing the phase diagrams of  $\mathbf{G}$ -symmetric quantum systems. We would like to span the algebra  $\text{SOA}[\mathbf{G}]$  by operators that carry dyonic labels and have properties that encode topological correlations of the bulk dyonic line operators of  $\mathcal{T}_{\mathbf{G}}$ . Let us consider a general Abelian group  $\mathbf{G} = \prod_{j=a}^M \mathbb{Z}_{N_a}$  with a fixed (arbitrary) ordering on its generators  $(\mathbf{g}_1, \mathbf{g}_2, \dots, \mathbf{g}_M)$  such that  $\mathbf{g}_a > \mathbf{g}_b$  for  $a > b$ . Then an edge pseudo-spin chain operators  $\mathcal{O}_d$  can be constructed that



correspond to a general dyonic label  $d = (\mathbf{g}_1, \alpha_1; \mathbf{g}_2, \alpha_2; \dots; \mathbf{g}_M, \alpha_M) \in \mathcal{A}$ . We define a minimal length operator  $\mathcal{O}_d$  based at the site  $i_0$  as

$$\begin{aligned} \mathcal{O}_d[i_0] &= A_{i_0+\eta_d[1]}^{g_1} B_{i_0+\xi_d[1]; i_0+\xi_d[1]+1}^{\alpha_1} \cdots A_{i_0+\eta_d[M]}^{g_M} B_{i_0+\xi_d[M]; i_0+\xi_d[M]+1}^{\alpha_M} \\ &= \prod_{a=1}^M A_{i_0+\eta_d[a]}^{g_a} B_{i_0+\xi_d[a]; i_0+\xi_d[a]+1}^{\alpha_a}, \end{aligned} \quad (\text{A.12})$$

where the various operators in the product are located to the right of the site  $i_0$  where the sites are numbered in increasing order from left to right. A general dyonic operator takes the following form illustrated in Fig. 30. The precise location of each operator can be fixed by the following rules:

1. The first non-trivial element in  $d$  is located at  $i_0$ . That is:
  - (a) If  $g_{a_0} \neq 0$  and  $g_a = \alpha_b = 0$  for all  $a, b < a_0$ , then the operator string  $\mathcal{O}_d[i_0]$  starts with the operator  $A_{i_0}^{g_{a_0}}$ .
  - OR
  - (b) If  $\alpha_{a_0} \neq 0$  and  $g_a = \alpha_b = 0$  for all  $a \leq a_0$  and  $b < a_0$ , then the operator string  $\mathcal{O}_d[i_0]$  starts with the operator  $B_{i_0, i_0+1}^{\alpha_{a_0}}$ .
2. An  $A$ -operator is located at the site where the previous (non-vanishing)  $B$ -operator ends. The operators  $A^{\mathbf{g}_{a_0}}$  and  $A^{\mathbf{g}_{a_0+n}}$  are located at the same site iff  $\alpha_b = 0$  for all  $a_0 \leq b < a_0 + n$ .
3. A  $B$ -operator begins from the site where the previous non-vanishing  $A$ -operator is located. The operators  $B^{\alpha_{b_0}}$  and  $B^{\alpha_{b_0+n}}$  are located on the same link iff  $\mathbf{g}_a = 0$  for all  $b_0 < a \leq b_0 + n$ .

In order to express  $\eta_d$  and  $\xi_d$ , we need to define a function  $\Delta : \mathbf{G} \rightarrow \mathbb{Z}_2$  such that  $\Delta[*] = 1 - \delta_{*,0}$ .  $\Delta[\mathbf{g}] = 0$  if  $\mathbf{g}$  is identity element in  $\mathbf{G}$  and 1 otherwise. The function  $\eta(\mathbf{a})$  and  $\xi(\mathbf{a})$  can be expressed in terms of the following recursion relations

$$\begin{aligned} \eta_d[\mathbf{a}] &= \sum_{b=1}^{a-1} \Delta[\alpha_{a-b}] (\xi_d[\mathbf{a}-b] + 1) \prod_{c=2}^b \delta_{\alpha_{a-c+1}} \\ \xi_d[\mathbf{a}] &= \sum_{b=0}^{a-1} \Delta[\mathbf{g}_{a-b}] \eta_d[\mathbf{a}-b] \prod_{c=1}^b \delta_{\mathbf{g}_{a-c+1}}, \end{aligned} \quad (\text{A.13})$$

along with the conditions  $\eta_d[1] = \xi_d[1] = 0$ . The length of the operator  $\mathcal{O}_d[i_0]$  is denoted as  $\ell_d$  and is defined as the number of pseudo-spin sites on which  $\mathcal{O}_d[i_0]$  acts non-trivially. This is given by the number of sites between  $i_0$  and the end-point of the last  $B$  operator in the operator string in Eq. (A.12). In case, the operator string is only built from  $A$  operators, the length of the operator string is 1. We may express  $\ell_d$  as

$$\ell_d = \sum_{a=0}^{M-1} \Delta[\alpha_{M-a}] (\xi_d[M-a] + 1) \prod_{b=1}^a \delta_{\alpha_{M-a+b}} + \prod_{b=1}^M \delta_{\alpha_b}. \quad (\text{A.14})$$

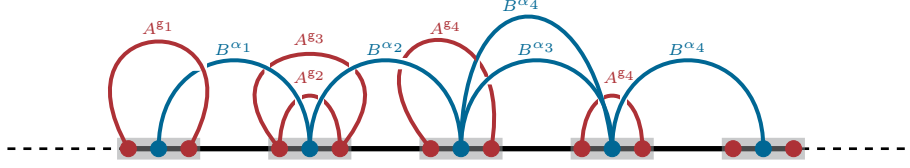


Figure 30: Representation of a dyonic operator (with  $\alpha_2 = \mathbf{g}_5 = 0$ ) on the edge quantum spin chain.

## B Computation of duality groups

Given a  $2 + 1d$  topological gauge theory with finite Abelian gauge group  $\mathbf{G}$  with anyons  $\mathcal{A} \simeq \mathbf{G} \times \mathbf{G}$ , the anyonic symmetry group (i.e. 0-form symmetries) is a subgroup  $\mathcal{G}[\mathbf{G}] \subset S_{|\mathcal{A}|}$  of the group of permutations  $S_{|\mathcal{A}|}$  of charges in  $\mathcal{A}$  satisfying

$$\mathcal{G}[\mathbf{G}] \equiv \{ \sigma \in S_{|\mathcal{A}|} \mid S_{\sigma(d), \sigma(d')} = S_{dd'} \text{ and } T_{\sigma(d), \sigma(d')} = T_{dd'} \}, \quad (\text{B.1})$$

where  $S$  and  $T$  are defined as in (3.7). In other words, these are all possible ways of permuting charges while leaving all topological properties like fusion rules and braiding statistics invariant. In the space of  $1 + 1d$   $\mathbf{G}$ -symmetric theories, these become the group of dualities. For any generic finite Abelian group  $\mathbf{G} = \prod_{i=1}^n \mathbb{Z}_{N_i}$ , the duality group is generated by three kinds of duality operations [151–153]

1. **Universal kinematical symmetries:** These are induced from the automorphisms of  $\mathbf{G}$ . For every automorphism  $\varphi : \mathbf{G} \rightarrow \mathbf{G}$ , one obtains a duality  $\sigma_\varphi : \mathcal{A} \rightarrow \mathcal{A}$  in  $\mathcal{G}[\mathbf{G}]$ , which acts on a dyon  $d = (\mathbf{g}, \alpha) \in \mathcal{A}$  as

$$\sigma_\varphi : (\mathbf{g}, \alpha) \rightarrow (\varphi(\mathbf{g}), (\varphi^{-1})^*(\alpha)), \quad (\text{B.2})$$

where  $\varphi^* : \text{Rep}(\mathbf{G}) \rightarrow \text{Rep}(\mathbf{G})$  defined as  $[\varphi^* \mathbf{R}_\alpha](\mathbf{g}) \equiv \mathbf{R}_\alpha(\varphi(\mathbf{g}))$ . This thus maps  $\alpha \in \text{Rep}(\mathbf{G})$  to some other  $\alpha' \in \text{Rep}(\mathbf{G})$ .

2. **Universal dynamical symmetries:** These correspond to elements in  $H^2(\mathbf{G}, \mathbf{U}(1))$ , where for  $\mathbf{G} = \prod_{i=1}^n \mathbb{Z}_{N_i}$  is

$$H^2(\mathbf{G}, \mathbf{U}(1)) = \prod_{i < j} \mathbb{Z}_{\text{gcd}(N_i, N_j)}. \quad (\text{B.3})$$

Given an element of  $H^2(\mathbf{G}, \mathbf{U}(1))$  labeled by  $\ell = \{\ell_{ij}\}$ , there is an associated alternating bicharacter  $\mathbf{c}_\ell$  given by

$$\mathbf{c}_\ell(\mathbf{g}, \mathbf{h}) = \exp \left\{ 2\pi i \sum_{i < j} \frac{\ell_{ij} \mathbf{g}_i \mathbf{h}_j}{\text{gcd}(N_i, N_j)} \right\}, \quad (\text{B.4})$$

where  $\mathbf{g} = (\mathbf{g}_1, \dots, \mathbf{g}_n)$ ,  $\mathbf{h} = (\mathbf{h}_1, \dots, \mathbf{h}_n)$ , and  $\ell_{ij} = -\ell_{ji}$ . An alternating bicharacter is a group homomorphism  $\mathbf{c} : \mathbf{G} \times \mathbf{G} \rightarrow \mathbb{C}^*$  in both arguments which satisfies the property  $\mathbf{c}(\mathbf{g}, \mathbf{g}) = 1$  for all  $\mathbf{g} \in \mathbf{G}$  [153]. Physically, such an alternating bicharacter

is furnished by the torus partition function of an SPT labelled by the corresponding cohomology class. Given such a bicharacter  $\mathbf{c}_\ell$ , one obtains a duality  $\sigma_\mathbf{c}$  which maps the dyon  $d = (\mathbf{g}, \alpha)$  as

$$\sigma_\mathbf{c} : (\mathbf{g}, \alpha) \mapsto (\mathbf{g}, \alpha_\mathbf{g}^\mathbf{c}), \quad (\text{B.5})$$

where the transformed representation  $\alpha_\mathbf{g}^\mathbf{c}$  has the form  $R_{\alpha_\mathbf{g}^\mathbf{c}}(\cdot) = R_\alpha(\cdot)\mathbf{c}_\ell(\mathbf{g}, \cdot)$ .

**3. Partial electric-magnetic dualities:** These correspond to performing an electric-magnetic duality on a given factor  $\mathbb{Z}_{N_j}$  in  $\mathbf{G}$

$$\sigma_j : \begin{aligned} (\mathbf{g}_1, \dots, \mathbf{g}_{j-1}, \mathbf{g}_j, \mathbf{g}_{j+1}, \dots, \mathbf{g}_n) &\mapsto (\mathbf{g}_1, \dots, \mathbf{g}_{j-1}, \alpha_j, \mathbf{g}_{j+1}, \dots, \mathbf{g}_n), \\ (\alpha_1, \dots, \alpha_{j-1}, \alpha_j, \alpha_{j+1}, \dots, \alpha_n) &\mapsto (\alpha_1, \dots, \alpha_{j-1}, \mathbf{g}_j, \alpha_{j+1}, \dots, \alpha_n). \end{aligned} \quad (\text{B.6})$$

The duality group  $\mathcal{G}[\mathbf{G}]$  is in general non-Abelian and often very large for even small Abelian groups  $\mathbf{G}$ . In this appendix, we will compute a few duality groups. Some concrete computations are done using the GAP System [190].

## B.1 $\mathbf{G} = \mathbb{Z}_2$

We first consider the simplest example which is  $\mathbf{G} = \mathbb{Z}_2$ . The fundamental dyonic excitations are the charge  $e = (0, 1)$  and flux  $m = (1, 0)$ . The fusion group is then

$$\mathcal{A}[\mathbb{Z}] = \{(0, 0), (1, 0), (0, 1), (1, 1)\} \equiv \{1, m, e, f\}. \quad (\text{B.7})$$

The modular  $T$ - and  $S$ -matrices are

$$T = \begin{pmatrix} 1 & 0 & 0 & 0 \\ 0 & 1 & 0 & 0 \\ 0 & 0 & 1 & 0 \\ 0 & 0 & 0 & -1 \end{pmatrix}, \quad S = \frac{1}{2} \begin{pmatrix} 1 & 1 & 1 & 1 \\ 1 & 1 & -1 & -1 \\ 1 & -1 & 1 & 1 \\ 1 & -1 & -1 & 1 \end{pmatrix}. \quad (\text{B.8})$$

A duality  $\sigma$  is a permutation of anyons that preserves these matrices

$$\mathcal{M}_\sigma T \mathcal{M}_\sigma^{-1} = T, \quad \mathcal{M}_\sigma S \mathcal{M}_\sigma^{-1} = S, \quad (\text{B.9})$$

here  $\mathcal{M}_\sigma$  is an invertible integer matrix permuting the set of anyons. Clearly, the only such permutation is the electric-magnetic duality transformation

$$e \longleftrightarrow m, \quad (\text{B.10})$$

whose matrix is given by

$$\mathcal{M}_\sigma = \begin{pmatrix} 1 & 0 & 0 & 0 \\ 0 & 0 & 1 & 0 \\ 0 & 1 & 0 & 0 \\ 0 & 0 & 0 & 1 \end{pmatrix}. \quad (\text{B.11})$$

Therefore, the group of anyonic symmetries is

$$\mathcal{G}[\mathbb{Z}_2] = \mathbb{Z}_2. \quad (\text{B.12})$$

## B.2 $G = \mathbb{Z}_2 \times \mathbb{Z}_2$

For  $G = \mathbb{Z}_2 \times \mathbb{Z}_2$ , there are 16 anyons and  $T$ - and  $S$ -matrices are given

$$T = \begin{pmatrix} 1 & 0 & 0 & 0 \\ 0 & 1 & 0 & 0 \\ 0 & 0 & 1 & 0 \\ 0 & 0 & 0 & -1 \end{pmatrix} \otimes \begin{pmatrix} 1 & 0 & 0 & 0 \\ 0 & 1 & 0 & 0 \\ 0 & 0 & 1 & 0 \\ 0 & 0 & 0 & -1 \end{pmatrix}, \quad (\text{B.13})$$

and

$$S = \frac{1}{4} \begin{pmatrix} 1 & 1 & 1 & 1 \\ 1 & 1 & -1 & -1 \\ 1 & -1 & 1 & -1 \\ 1 & -1 & -1 & 1 \end{pmatrix} \otimes \begin{pmatrix} 1 & 1 & 1 & 1 \\ 1 & 1 & -1 & -1 \\ 1 & -1 & 1 & -1 \\ 1 & -1 & -1 & 1 \end{pmatrix}, \quad (\text{B.14})$$

Dualities  $\mathcal{G}[\mathbb{Z}_2 \times \mathbb{Z}_2]$  is a subgroup of  $S_{16}$  such that

$$\mathcal{M}_\sigma T \mathcal{M}_\sigma^{-1} = T, \quad \mathcal{M}_\sigma S \mathcal{M}_\sigma^{-1} = S, \quad \forall \sigma \in \mathcal{G}[\mathbb{Z}_2 \times \mathbb{Z}_2], \quad (\text{B.15})$$

where  $\mathcal{M}_\sigma$  is a matrix representing the permutation associated to the duality  $\sigma$ . The duality group is

$$\mathcal{G}[\mathbb{Z}_2 \times \mathbb{Z}_2] = (S_3 \times S_3) \rtimes \mathbb{Z}_2. \quad (\text{B.16})$$

whose order is 72. For the details of the generators, see Section 5.3.

### B.2.1 Analysis of the outer automorphism group

We will here briefly describe the construction of the automorphism group of  $\mathcal{G}_2 \equiv \mathcal{G}[\mathbb{Z}_2 \times \mathbb{Z}_2] = (S_3 \times S_3) \rtimes \mathbb{Z}_2$  in terms of its generators. One can readily check that the following two maps are automorphisms

$$a : \begin{pmatrix} \sigma_L \\ h_1 \\ k_1 \\ h_2 h_3 \\ k_2 k_3 \end{pmatrix} \longrightarrow \begin{pmatrix} h_1 \\ \sigma_L (h_2 h_3)^2 (k_2 k_3) \\ \sigma_L k_1 h_1 (h_2 h_3) (k_2 k_3) \\ h_2 h_3 (k_2 k_3)^2 \\ (h_2 h_3)^2 (k_2 k_3)^2 \end{pmatrix} \quad x : \begin{pmatrix} \sigma_L \\ h_1 \\ k_1 \\ h_2 h_3 \\ k_2 k_3 \end{pmatrix} \longrightarrow \begin{pmatrix} \sigma_L k_1 h_1 (h_2 h_3) (k_2 k_3) \\ k_1 \\ h_1 (h_2 h_3)^2 \\ k_2 k_3 \\ (h_2 h_3)^2 \end{pmatrix}$$

and they satisfy the following properties

$$a^8 = x^2 = 1, \quad x a x^{-1} = a^3. \quad (\text{B.17})$$

It is clear that this group is a semidirect product  $\mathbb{Z}_8 \rtimes \mathbb{Z}_2$ , but it is distinct from the dihedral group  $D_8$  as the action of the  $\mathbb{Z}_2$  is different (dihedral group has  $x a x^{-1} = a^4 = a^{-1}$ ). It turns out that this group is called the quasi-dihedral group<sup>23</sup>

$$QD_{16} = \langle a, x \mid a^8 = x^2 = 1, x a x^{-1} = a^3 \rangle. \quad (\text{B.18})$$

<sup>23</sup>Sometimes called the semi-dihedral group  $SD_{16}$ . Please note that  $D_n$  is a group of  $2n$  elements and correspond to the symmetries of a regular polygon with  $n$  corners. This is a geometric notation. In abstract algebra this group is often notated as  $D_{2n}$ , to indicate the order of the group. The notation used for  $QD_{16}$  follows the abstract algebra notation, rather than the geometry one, as this group has no geometric origin.

Furthermore, we have to other automorphisms

$$b : \begin{pmatrix} \sigma_L \\ h_1 \\ k_1 \\ h_2 h_3 \\ k_2 k_3 \end{pmatrix} \longrightarrow \begin{pmatrix} \sigma_L \\ k_1 (k_2 k_3)^2 \\ h_1 (h_2 h_3)^2 \\ h_1 \\ h_2 h_3 \end{pmatrix}, \quad c : \begin{pmatrix} \sigma_L \\ h_1 \\ k_1 \\ h_2 h_3 \\ k_2 k_3 \end{pmatrix} \longrightarrow \begin{pmatrix} \sigma_L (h_2 h_3) (k_2 k_3)^2 \\ k_1 (k_2 k_3)^2 \\ h_1 (h_2 h_3) \\ k_2 k_3 \\ h_2 h_3 \end{pmatrix},$$

generating the product of two decoupled cyclic groups

$$\mathbb{Z}_3 \times \mathbb{Z}_3 = \langle b, c \mid b^3 = c^3 = 1, bc = cb \rangle. \quad (\text{B.19})$$

From the above four automorphisms, one can then check that  $QD_{16}$  has the following action on  $\mathbb{Z}_3 \times \mathbb{Z}_3$

$$\begin{aligned} xbx^{-1} &= c, & xcx^{-1} &= b, \\ aba^{-1} &= bc^2, & aca^{-1} &= bc. \end{aligned} \quad (\text{B.20})$$

In particular it can be seen that the orbit of the action of  $a$  on  $\mathbb{Z}_3 \times \mathbb{Z}_3$ , has period eight

$$b \longrightarrow bc^2 \longrightarrow c \longrightarrow bc \longrightarrow b^2 \longrightarrow b^2 c \longrightarrow c^2 \longrightarrow b^2 c^2 \longrightarrow b \quad (\text{B.21})$$

We therefore have the following automorphism group

$$\text{Aut}((S_3 \times S_3) \rtimes \mathbb{Z}_2) = (\mathbb{Z}_3 \times \mathbb{Z}_3) \rtimes QD_{16}, \quad (\text{B.22})$$

of order

$$|\text{Aut}(\mathcal{G}_2)| = 144, \quad (\text{B.23})$$

which is exactly twice the order of  $\mathcal{G}_2$ . Many of these automorphisms are however trivial, in the sense that they correspond to conjugation with group elements

$$\phi_h : \mathcal{G}_2 \rightarrow \mathcal{G}_2, \quad \phi(g) = hgh^{-1}. \quad (\text{B.24})$$

The set of such trivial automorphisms form the so-called inner automorphism group and is clearly isomorphic to the group itself

$$\text{Inn}(\mathcal{G}_2) = (S_3 \times S_3) \rtimes \mathbb{Z}_2. \quad (\text{B.25})$$

This is a normal subgroups of  $\text{Aut}(\mathcal{G}_2)$  and can be quotient out to get to the so-called outer automorphism group

$$\begin{aligned} \text{Out}(\mathcal{G}_2) &= \text{Aut}(\mathcal{G}_2) / \text{Inn}(\mathcal{G}_2), \\ &= \mathbb{Z}_2, \\ &= \{[1], [\phi]\}. \end{aligned} \quad (\text{B.26})$$

Note that these groups generally form a short exact sequence,

$$1 \longrightarrow \text{Inn}(\mathcal{G}_2) \longrightarrow \text{Aut}(\mathcal{G}_2) \longrightarrow \text{Out}(\mathcal{G}_2) \longrightarrow 1.$$

This group  $\text{Out}(\mathcal{G}_2)$  is clearly isomorphic to  $\mathbb{Z}_2$ , as the resulting group must be of order two of which there is only one (up to isomorphism). The automorphisms thus belong to two equivalence classes given by

$$[1] \approx (S_3 \times S_3) \rtimes \mathbb{Z}_2, \quad [\phi] = \phi \cdot [1], \quad (\text{B.27})$$

where  $\phi$  is a representative of the only non-trivial outer automorphism class

$$\phi : \begin{pmatrix} \sigma_L \\ h_1 \\ k_1 \\ h_2 h_3 \\ k_2 k_3 \end{pmatrix} \longrightarrow \begin{pmatrix} h_1 \\ \sigma_L \\ \sigma_L k_1 h_1 \\ (k_2 k_3)(h_2 h_3)^{-1} \\ (k_2 k_3)(h_2 h_3) \end{pmatrix}. \quad (\text{B.28})$$

The interpretation of this automorphism is clear: it rotates the  $S_3 \times S_3$  subgroup to a different one consisting of the diagonal and anti-diagonal  $S_3 \times S_3$ .<sup>24</sup>

### B.3 $\mathbf{G} = \mathbb{Z}_2 \times \cdots \times \mathbb{Z}_2$

The duality transformations discussed in the last section can easily be generalized to the case of  $k$ -layers of  $\mathbb{Z}_2$  symmetry. For example we have the following generators

$$\begin{aligned} \sigma_i &: \{e_i \mapsto m_i, m_i \mapsto e_i\}, \\ s_{ij} &: \{a_i \mapsto a_j, a_j \mapsto a_i \mid a = e, m\}, \\ c &: \{a_i \mapsto a_{i+1 \bmod k} \mid a = e, m\}, \end{aligned} \quad (\text{B.29})$$

where  $\sigma_i$  is the electromagnetic duality in the  $i^{\text{th}}$  layer,  $s_{ij}$  swaps layers  $i$  and  $j$ , and  $c$  is a cyclic permutation of the  $k$  layers. Note that we only need electromagnetic duality in one layer as the other layers can be gotten by

$$\sigma_i = s_{1i} \sigma_1 s_{1i}. \quad (\text{B.30})$$

Furthermore, only two generators are needed to generate the full group of permutations of  $k$  layers:  $S_k = \langle s_{12}, c \rangle$ . We also have a more non-trivial set of dualities

$$h_{ij} : \{e_i \mapsto e_i e_j, m_j \mapsto m_i m_j\}. \quad (\text{B.31})$$

Note that  $h_{ij}$  is not the same as  $h_{ji}$  but they are related as  $h_{ji} = s_{ij} h_{ij} s_{ij}$ . For any pairs of layers  $(i, j)$  we can generate the subgroup  $S_3 = \langle h_{ij}, h_{ji}, s_{ij} \rangle$ . These kind of subgroups are important when analyzing the phase-diagram of the system. We can also define

$$\begin{aligned} k_{ij} &: \{m_i \mapsto m_i e_j, m_j \mapsto e_i m_j\}, \\ \bar{k}_{ij} &: \{e_j \mapsto m_i e_j, e_i \mapsto e_i m_j\}. \end{aligned} \quad (\text{B.32})$$

Note that

$$k_{ij} = k_{ji}, \quad \bar{k}_{ij} = \bar{k}_{ji}, \quad \bar{k}_{ij} = \sigma_i \sigma_j k_{ij} \sigma_j \sigma_i. \quad (\text{B.33})$$

---

<sup>24</sup>If we write elements of  $S_3 \times S_3$  as  $(g_1, g_2)$ , then the left and right subgroups are  $(g, 1)$  and  $(1, g)$  corresponding to rotating two triangles independently. The diagonal subgroup is  $(g, g)$  where both triangles are rotated together, and the anti-diagonal is  $(g, g^{-1})$ , where the two triangles are rotated in opposite directions.

Again, for each pairs of layers  $(i, j)$  we have another  $S_3$  subgroup  $S_3 = \langle k_{ij}, \bar{k}_{ij}, \sigma_i \sigma_j s_{ij} \rangle$ , similar to the two-layer analysis. Another similarity to the two-layer analysis is the following relation

$$k_{ij} = \sigma_i h_{ij} \sigma_i. \quad (\text{B.34})$$

Therefore, for each pair of indices  $(i, j)$ , we have the subgroup

$$\langle h_{ij}, s_{ij}, k_{ij}, \sigma_i, \sigma_j \rangle \simeq (S_3 \times S_3) \rtimes \mathbb{Z}_2. \quad (\text{B.35})$$

In other words, the phase of diagram of  $(\mathbb{Z}_2)^{\times k}$ -symmetric theories contain many copies of the phase diagram of  $\mathbb{Z}_2 \times \mathbb{Z}_2$  symmetric theories, one for each pair of layers  $(i, j)$ . From the above discussion, we conclude that the full duality group is

$$\mathcal{G}_k = \langle \sigma_1, h_{12}, s_{12}, c \rangle, \quad (\text{B.36})$$

where we have defined the notation  $\mathcal{G}_k \equiv \mathcal{G}[(\mathbb{Z}_2)^{\times k}]$ . One can check that these generators leave the  $T$ - and  $S$ -matrices invariant. In the language discussed earlier,  $\sigma_i$  are partial electric-magnetic dualities,  $\{h_{ij}, s_{ij}, c\}$  are essentially universal kinematical symmetries related to automorphism group of  $(\mathbb{Z}_2)^{\times k}$  while  $k_{ij}$  are universal dynamical symmetries related to  $H^2((\mathbb{Z}_2)^{\times k}, \text{U}(1))$ . For small  $k$ , this group is isomorphic to the following groups

$$\mathcal{G}_k = \begin{cases} \mathbb{Z}_2 & k = 1 \\ (S_3 \times S_3) \rtimes \mathbb{Z}_2 & k = 2 \\ S_8 & k = 3 \\ O_8^+(2) \rtimes \mathbb{Z}_2 & k = 4 \end{cases}. \quad (\text{B.37})$$

Here  $O_8^+(2) = D_4(2)$  is a so-called Lie type group, more precisely an orthogonal Chevalley group of type D. The order of these groups are

$$|D_n(q)| = \frac{q^{n(n-1)} (q^n - 1)}{\gcd(4, q^n - 1)} \prod_{i=1}^{n-1} (q^{2i} - 1). \quad (\text{B.38})$$

In particular

$$|\mathcal{G}_4| = |O_8^+(2) \rtimes \mathbb{Z}_2| = 348\,364\,800. \quad (\text{B.39})$$

In other words, there are almost 350 million dualities for  $\mathbf{G} = (\mathbb{Z}_2)^4$  symmetry. It turns out that this is the same dimension as  $W^+(E_8)$ , the orientation preserving subgroup of the Weyl group of the exceptional Lie algebra  $E_8$ . It is known that  $W^+(E_8)$  is also a  $\mathbb{Z}_2$  extension of  $O_8^+(2)$ . Whether this connection has any significance will be studied elsewhere.

## B.4 $\mathbf{G} = \mathbb{Z}_p \times \mathbb{Z}_p$

Another interesting class of symmetries are  $\mathbf{G} = \mathbb{Z}_p \times \mathbb{Z}_p$  for prime numbers  $p$ . Here, the partial electric-magnetic dualities  $\sigma_i$  are again given in (B.6). The universal dynamical symmetries are given by elements of  $H^2(\mathbb{Z}_p \times \mathbb{Z}_p, \text{U}(1)) = \mathbb{Z}_p$ . The corresponding bicharacters are given by

$$\beta_\ell(\mathbf{g}, \mathbf{h}) = \exp \left[ \frac{2\pi i}{p} \ell(\mathbf{g}_2 \mathbf{h}_1 - \mathbf{g}_1 \mathbf{h}_2) \right], \quad (\text{B.40})$$

where  $\ell = 0, \dots, p-1$  labels different cohomology classes. Under these dualities, anyonic charges transform as

$$(\mathbf{g}_1, \mathbf{g}_2, \alpha_1, \alpha_2) \mapsto (\mathbf{g}_1, \mathbf{g}_2, \alpha_1 + \ell \mathbf{g}_2, \alpha_2 - \ell \mathbf{g}_1). \quad (\text{B.41})$$

Finally, the universal dynamical symmetries are related to the duality group of  $\mathbb{Z}_p \times \mathbb{Z}_p$ , which is

$$\text{Aut}(\mathbb{Z}_p \times \mathbb{Z}_p) = \text{GL}_2(\mathbb{F}_p). \quad (\text{B.42})$$

The action of these dualities on anyons is given in (B.2). Specifically, for  $p = 2$  we have  $\text{GL}_2(\mathbb{F}_2) = S_3$  and the full duality group becomes  $(S_3 \times S_3) \rtimes \mathbb{Z}_2$ , as shown earlier. For  $p = 3$ , we have  $\text{GL}_2(\mathbb{F}_3) = Q_8 \rtimes S_3$ , and they are generated by

$$\begin{aligned} h_1 : (\mathbf{g}_1, \mathbf{g}_2; \alpha_1, \alpha_2) &\mapsto (\mathbf{g}_2, \mathbf{g}_1; \alpha_2, \alpha_1), \\ h_2 : (\mathbf{g}_1, \mathbf{g}_2; \alpha_1, \alpha_2) &\mapsto (\mathbf{g}_1 + \mathbf{g}_2, \mathbf{g}_2; \alpha_1, 2\alpha_1 + \alpha_2). \end{aligned} \quad (\text{B.43})$$

The dynamical dualities are generated by

$$k : (\mathbf{g}_1, \mathbf{g}_2; \alpha_1, \alpha_2) \mapsto (\mathbf{g}_1, \mathbf{g}_2; \alpha_1 + \mathbf{g}_2, \alpha_2 - \mathbf{g}_1), \quad (\text{B.44})$$

with  $k^3 = 1$ . We have the relations

$$h_1 k h_1^{-1} = k^{-1}, \quad h_2 k h_2^{-1} = k. \quad (\text{B.45})$$

Thus  $\langle k, h_1, h_2 \rangle \simeq \mathbb{Z}_3 \rtimes \text{GL}_2(\mathbb{F}_3)$ . When adding electric-magnetic duality, the structure of the group becomes significantly more complicated and it is hard to write group in a simple way. One possible presentation of the full duality group is

$$\mathcal{G}[\mathbb{Z}_3 \times \mathbb{Z}_3] = \left\{ \left[ \left( (\mathbb{Z}_2 \times \mathbb{Z}_2 \times \mathbb{Z}_2) \rtimes (\mathbb{Z}_2 \times \mathbb{Z}_2) \right) \rtimes (\mathbb{Z}_3 \times \mathbb{Z}_3) \right] \rtimes \mathbb{Z}_2 \right\} \rtimes \mathbb{Z}_2, \quad (\text{B.46})$$

which is not very illuminating. The order of the group is  $|\mathcal{G}[\mathbb{Z}_3 \times \mathbb{Z}_3]| = 1152$  and one can check that this group is actually

$$\mathcal{G}[\mathbb{Z}_3 \times \mathbb{Z}_3] = W(F_4), \quad (\text{B.47})$$

the Weyl group of the exceptional Lie algebra  $F_4$ . Whether there is a deeper relation to the Lie algebra  $F_4$  will be investigated elsewhere.

## C From Wen plaquette model to $\mathbb{Z}_N$ -symmetric spin chains

In this section we exemplify our approach for the simple example of  $\mathbb{Z}_N$  topological order, using an exactly solvable model. We will show that this  $2 + 1d$  quantum model has a  $\mathcal{A} = \mathbb{Z}_N \times \mathbb{Z}_N$  1-form symmetry and a  $\mathcal{G} = \mathbb{Z}_2$  0-form symmetry related to electric-magnetic duality. We then show how a spin chain with  $\mathbb{Z}_N$  global symmetry naturally appears on the  $1 + 1d$  edge of the  $2 + 1d$  quantum model and elaborate on various global and topological issues of this bulk to edge correspondence. There are various equivalent formulations of the  $\mathbb{Z}_N$  topological gauge theory. Here we find it convenient to work with the so-called Wen plaquette formulation, since (0-form) anyonic symmetries appear as lattice translations.



**Bulk Hilbert space and Hamiltonian:** Consider a square lattice  $\Lambda$  with a  $N$ -state spin degree of freedom on each lattice site and the Hilbert space  $\mathcal{H}_\Lambda = \bigotimes_i \mathcal{H}_i$ , with the local Hilbert spaces  $\mathcal{H}_i \simeq \mathbb{C}^N$ . We define a basis  $|\sigma_i\rangle$  with  $\sigma_i = 0, \dots, N-1$  that spans  $\mathcal{H}_i$ . The  $\mathbb{Z}_N$  generalization of the Pauli matrices act on  $\mathcal{H}_i$  as

$$\begin{aligned} Z_i |\sigma_i\rangle &= \omega^{\sigma_i} |\sigma_i\rangle, \\ X_i |\sigma_i\rangle &= |\sigma_i - 1\rangle, \end{aligned}$$

where  $\omega = e^{\frac{2\pi i}{N}}$ . The operators satisfy the algebraic relations  $X_i^N = Z_i^N = 1$  and  $X_i Z_j = \omega^{\delta_{ij}} Z_j X_i$ . It will be convenient to use the following graphical notation

$$\begin{aligned} Z_i &= \text{diagram of } Z_i, & X_i &= \text{diagram of } X_i, \\ X_i^\dagger &= \text{diagram of } X_i^\dagger, & Z_i^\dagger &= \text{diagram of } Z_i^\dagger, \end{aligned} \tag{C.1}$$

in terms of which the algebraic relations take the form

$$\begin{aligned} \text{diagram of } Z_i Z_j &= \omega \text{diagram of } Z_j Z_i, & \text{diagram of } X_i X_j &= \omega^{-1} \text{diagram of } X_j X_i, \\ \text{diagram of } X_i X_j &= \omega^{-1} \text{diagram of } X_j X_i, & \text{diagram of } Z_i Z_j &= \omega \text{diagram of } Z_j Z_i. \end{aligned}$$

For each plaquette on the lattice, one can define the minimal closed string operator as

$$\mathcal{O}_p = \text{diagram of } \mathcal{O}_p = Z_1 X_2 Z_3^\dagger X_4^\dagger,$$

which again is unitary and satisfy  $\mathcal{O}_p^N = 1$  and satisfy  $[\mathcal{O}_p, \mathcal{O}_{p'}] = 0$  for all plaquettes  $p$  and  $p'$ . The  $\mathbb{Z}_N$  generalization of the Wen-plaquette model takes the form

$$H_{\mathbb{Z}_N}^{Wen} = -\frac{g}{2} \sum_p (\mathcal{O}_p + \mathcal{O}_p^\dagger) = -\frac{g}{2} \sum_p \left( \text{diagram of } \mathcal{O}_p + \text{diagram of } \mathcal{O}_p^\dagger \right). \tag{C.2}$$

Since all plaquettes commute, the eigenstates can be labelled by the  $\mathbb{Z}_N$  eigenvalues of the plaquette operators. The ground states subspace is given by

$$\mathcal{H}_{GS} = \{ |\psi\rangle \in \mathcal{H}_\Lambda \mid \mathcal{O}_p |\psi\rangle = |\psi\rangle, \forall p \} \subset \mathcal{H}_\Lambda. \tag{C.3}$$

The ground state degeneracy will depend on the global topology of the spatial manifold the theory lives on. For manifolds without boundary, this degeneracy is protected against any local perturbations that do not close the bulk gap while for manifolds with boundary only a subset of groundstates are protected while the rest correspond to edge states.

**String operators and anyonic excitations** The plaquettes of a square lattice admit a bipartitioning into ‘odd’ and ‘even’ plaquettes (see figure 31, where the ‘odd’ plaquettes are shaded gray). Now consider an oriented path on the square lattice that traverses diagonally between plaquettes such that it is fully contained in either the odd or even plaquettes. Any such path is in one-to-one correspondence with a line operator  $\mathcal{W}_\ell$  which acts non-trivially on the Hilbert spaces associated to the vertices contained in

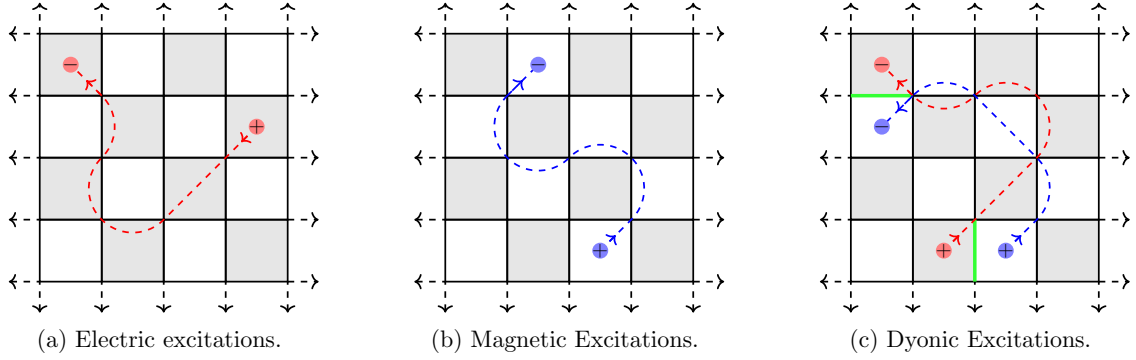


Figure 31

the path. The operator acting on any given vertex is determined by the orientation of the string using eq.(C.1). If the path is homologically trivial i.e. contractible, it can be expressed as a product of plaquette operators

$$\mathcal{W}_\ell = \prod_{p \in \partial^{-1}\ell} \mathcal{O}_p^{\mathfrak{o}(\ell)}, \quad (\text{C.4})$$

where  $\partial^{-1}\ell$  is the (non-unique) collection of plaquettes whose boundary is  $\ell$  and  $\mathfrak{o}(\ell)$  is the orientation of  $\ell$ , which we choose as  $\pm 1$  for clockwise and anti-clockwise paths respectively. From eq. (C.4), it follows that any closed contractible string operator commutes with the Wen-plaquette Hamiltonian.

Consider instead an open path  $\ell$  from plaquette  $a$  to plaquette  $b$  (see figure 31). Such an operator commutes with all the plaquette operators except those at  $a$  and  $b$ . More precisely

$$\mathcal{O}_p \mathcal{W}_\ell = \omega^{\delta_{p,a} - \delta_{p,b}} \mathcal{W}_\ell \mathcal{O}_p. \quad (\text{C.5})$$

Therefore, the operator  $\mathcal{S}_\ell$  acting on the ground state creates localized excitations at the plaquettes  $a$  and  $b$ . We may deform such a string operator by composing it with an arbitrary collection of plaquette operators which gives rise to modified string  $\ell'$  with the endpoints fixed at  $a$  and  $b$ . In this sense the operators defined on  $\ell$  and  $\ell'$  are equivalent and we may label them only by the end-points. Since the string operators are contained on either the even (white) or odd (shaded) plaquettes, there are two types of local excitations on plaquettes; magnetic charges  $m$  (even) and electric charges  $q$  (odd), while more generally we have dyons on both lattices and can they be thought of as living on the link separating them (see fig. 31). Thus the set of anyons is given by

$$\mathcal{A} = \{(q, m) \mid q, m = 0, \dots, N-1\}, \quad (\text{C.6})$$

with the anyon  $(0,0)$  corresponding to the trivial particle. For compact manifolds excitations can only be created pairwise while for non-compact manifolds we can have single particles since the other end of the string can either be stretched to infinity or onto a boundary. A single dyon with electric and magnetic charges  $q$  and  $m$ , respectively, cost the energy

$$\Delta E_{(q,m)} = g \left( 1 - \cos \left( \frac{2\pi}{N} q \right) \right) + g \left( 1 - \cos \left( \frac{2\pi}{N} m \right) \right). \quad (\text{C.7})$$

There are  $N^2$  different types of dyonic excitations labelled by  $(q, m)$ . These different excitations are topologically distinct in the sense that they cannot be turned into another excitation  $(\tilde{q}, \tilde{m}) \neq (q, m)$  by acting with any local operators.

**Global 1- and 0-form symmetries** As discussed in (C.4), homologically trivial (contractible) loops are given by products of  $\mathcal{O}_p$ . Such products can be used to topologically deform these curves, however there will always exist two different types of contractible loops that cannot be deformed into each other

$$\mathcal{W}_{\ell_{loop}}^e = \prod_p \text{[red loop around } p \text{]}, \quad \mathcal{W}_{\ell_{loop}}^m = \prod_p \text{[blue loop around } p \text{]}. \quad (\text{C.8})$$

Any such loop commutes with the Hamiltonian and corresponds to 1-form symmetries isomorphic to  $\mathcal{A} = \mathbb{Z}_N \times \mathbb{Z}_N$ . On Manifolds with non-trivial topology like a torus or genus- $g$  surfaces  $\Sigma_g$ , there will exist non-trivial homology cycles and we can therefore form non-contractible loops. These loops cannot be decomposed into  $\mathcal{O}_p$ , but will still commute with the Hamiltonian. Their algebra will lead to non-trivial ground-state degeneracies that only depend on (1) the kind of topological order ( $\mathbb{Z}_N$  in this case) and (2) topology of the manifold (in particular, first homology group). This degeneracy is protected against local perturbations, because they are not coming from a 0-form symmetry but rather from 1-form symmetries.

Now note that a lattice translation acts on 1-form symmetries

$$\mathcal{W}_\ell^e \longleftrightarrow \mathcal{W}_\ell^m. \quad (\text{C.9})$$

It exchanges anything electric and magnetic (lines and excitations), and therefore called electric-magnetic duality. Thus symmetry acts everywhere in space and is therefore a 0-form symmetry (see figure (4b)). Such symmetry exists in any description of a  $\mathbb{Z}_N$  topological order, the fact that it is generated by lattice translations is a special feature of the Wen plaquette model. If we wanted to put the 0-form symmetry along time to create a domain wall as in figure 6b, we would have to create lattice dislocation (see [191, 192]). But note that this object is really a surface in spacetime and not just a line, as it might naively appear in much of the literature on twist defects.

**Semi-infinite cylinder:** We will now consider the model (C.2) defined on a semi-infinite cylinder, where the periodic direction is along the  $y$ -axis with  $L_y$  lattice sites (see fig. 32). For now, we will assume that  $L_y$  is even and we will label the even plaquettes by  $p$  while the odd ones are labelled by  $\tilde{p}$ .

Besides the bulk plaquette operators  $\text{[red loop around } p \text{]}$  and  $\text{[blue loop around } \tilde{p} \text{]}$ , for this geometry we can consider several other string operators. First we have a set of operators acting near the boundary defined as (see also fig. 32)

$$S_p = \text{[red string through } p \text{]}, \quad S_{\tilde{p}} = \text{[blue string through } \tilde{p} \text{]}.$$

These are nothing but the bulk plaquette operators, cut in half. It is easy to see that both  $S_p$  and  $S_{\tilde{p}}$  commute with any  $\mathcal{O}_{p'}$  and  $\mathcal{O}_{\tilde{p}'}$ , but for nearest neighbour  $p$  and  $\tilde{p}$  on the

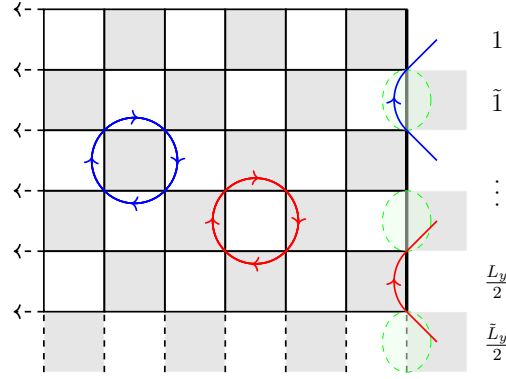


Figure 32: Semi-infinite along  $x$ -direction, but periodic along  $y$ . The boundary operators (BO) can be thought of as half of the small loop operators in the bulk. The green ellipses on the edge correspond to the pseudo-spin degree spin of freedom. The blue BO act on a single pseudo-spin, while the red BO act on a pair of nearest-neighbour pseudo-spins.

boundary we have

$$S_p S_{\tilde{p}} = \begin{cases} \omega S_{\tilde{p}} S_p & \text{if } \begin{array}{c} \vdots \\ \tilde{p} \\ p \\ \vdots \end{array}, \\ \omega^{-1} S_{\tilde{p}} S_p & \text{if } \begin{array}{c} \vdots \\ p \\ \tilde{p} \\ \vdots \end{array}, \end{cases} \quad \text{or graphically} \quad \begin{array}{c} \text{blue BO} = \omega \text{ red BO}, \\ \text{red BO} = \omega^{-1} \text{ blue BO}. \end{array} \quad (\text{C.10})$$

Next we have two types of non-contractable string operators along the periodic direction defined as

$$\Gamma = \text{red wavy line}, \quad \tilde{\Gamma} = \text{blue wavy line}. \quad (\text{C.11})$$

These operators both commute among each other and with all bulk plaquette operators and boundary operators. Finally we have two operators along the other cycle, stretching from infinity and ending on the boundary defined as

$$W = \text{red wavy line with boundary}, \quad \tilde{W} = \text{blue wavy line with boundary}. \quad (\text{C.12})$$

Note that if we had a finite cylinder, by gluing it into a torus the above two operators would become non-contractable and contribute to the GSD. While these commute among themselves and with all bulk plaquette operators, we have the following relations

$$\begin{aligned} \tilde{\Gamma} W &= \omega W \tilde{\Gamma}, & \Gamma \tilde{W} &= \omega \tilde{W} \Gamma, \\ \Gamma W &= W \Gamma, & \tilde{\Gamma} \tilde{W} &= \tilde{W} \tilde{\Gamma}. \end{aligned} \quad (\text{C.13})$$

A choice of maximal set of commuting and independent operators is

$$\{\mathcal{O}_p, \mathcal{O}_{\tilde{p}}, S_{\tilde{p}}, \Gamma\} = \left\{ \text{red circle } p, \text{ blue circle } \tilde{p}, \text{ green ellipse } \tilde{p}, \text{ red wavy line} \right\}. \quad (\text{C.14})$$

Note that the operators  $\tilde{\Gamma}$  is also included in this set of operators, as it can be generated from the boundary operators  $S_{\tilde{p}}$ . Since the above set commute and is maximal, the corresponding eigenbasis will span the full Hilbert space and is labelled by their eigenvalues. This basis is convenient, since all these states will automatically be eigenstates of the Hamiltonian (C.2). Given one state in (C.3), we can construct all other ground-states by projecting into eigenstates of  $S_{\tilde{p}}$  and  $\Gamma$ . Since there is one  $\Gamma$  and  $L_y/2$   $S_{\tilde{p}}$ , we have  $N^{\frac{L_y}{2}+1}$  ground states. However, only  $N^2$  of these (from  $\Gamma$  and  $\tilde{\Gamma} = \prod_{\tilde{p}} S_{\tilde{p}}$ ) are topologically robust against perturbations, while the rest correspond to edge states and the degeneracy is lifted once we add local perturbations. Since there are roughly  $N^{\frac{L_y}{2}}$  degrees of freedom on the edge, there is  $\sqrt{N}$  degrees of freedom per site. From this we might conclude that the edge contains **parafermions** (Majorana fermions for  $N = 2$ ).

In order to see the emergence of Kramers-Wannier duality and its subtle global effects, it is useful to parametrize the subspace corresponding to edge degrees of freedom carefully and study how boundary operators act on this subspace. Thus we will construct the  $N^{\frac{L_y}{2}+1}$  states explicitly. First note that the eigenstates of  $\Gamma$  and  $\tilde{\Gamma}$  cannot be connected to each other using any local operator, since they are only connected through the infinite line operators  $\tilde{W}$  and  $W$ . We can thus decompose the full Hilbert space into  $N^2$  distinct **superselection sectors** or **topological sectors**

$$\mathcal{H}_{full} = \bigoplus_{\Gamma, \tilde{\Gamma}=0}^{N-1} \mathcal{H}_{\Gamma, \tilde{\Gamma}}, \quad (\text{C.15})$$

corresponding to the eigenspaces of  $\Gamma$  and  $\tilde{\Gamma}$ . The projection operators projecting onto the ground state subspace are given by

$$P_p = \frac{1}{|\mathbb{Z}_N|} \sum_{n=0}^{N-1} \mathcal{O}_p^n, \quad P_{\tilde{p}} = \frac{1}{|\mathbb{Z}_N|} \sum_{n=0}^{N-1} \mathcal{O}_{\tilde{p}}^n, \quad (\text{C.16})$$

and a ground state is thus given by

$$|\Gamma = 0, \tilde{\Gamma} = 0\rangle = \mathcal{N} P_{\Gamma} P_{\tilde{\Gamma}} \prod_p P_p \prod_{\tilde{p}} P_{\tilde{p}} |\psi\rangle, \quad (\text{C.17})$$

for a choice of reference state  $|\psi\rangle$ . We have further projected into the  $\Gamma = 0$  and  $\tilde{\Gamma} = 0$  sectors using

$$P_{\Gamma} = \frac{1}{|\mathbb{Z}_N|} \sum_{n=0}^{N-1} \Gamma^n \quad \text{and} \quad P_{\tilde{\Gamma}} = \frac{1}{|\mathbb{Z}_N|} \sum_{n=0}^{N-1} \tilde{\Gamma}^n. \quad (\text{C.18})$$

All  $N^2$  topological sectors are now given by

$$|\Gamma = a, \tilde{\Gamma} = b\rangle = \tilde{W}^a W^b |\Gamma = 0, \tilde{\Gamma} = 0\rangle, \quad (\text{C.19})$$

with the eigenvalues

$$\Gamma |\Gamma = a, \tilde{\Gamma} = b\rangle = \omega^a |\Gamma = a, \tilde{\Gamma} = b\rangle, \quad \tilde{\Gamma} |\Gamma = a, \tilde{\Gamma} = b\rangle = \omega^b |\Gamma = a, \tilde{\Gamma} = b\rangle. \quad (\text{C.20})$$

The states are all locally indistinguishable, differ only globally, thus cannot be mixed under local perturbations. To construct the  $N^{\frac{L_y}{2}-1}$  locally distinguishable edge states within each superselection sector, we can use the following set of projectors

$$Q_{\tilde{p}}(\alpha) = \frac{1}{|\mathbb{Z}_N|} \sum_{n=0}^{N-1} \omega^{-\alpha n} S_{\tilde{p}}^n \quad (\text{C.21})$$

satisfying

$$Q_{\tilde{p}}(\alpha)^\dagger = Q_{\tilde{p}}(\alpha), \quad Q_{\tilde{p}}(\alpha)Q_{\tilde{p}}(\beta) = \delta_{\alpha,\beta}Q_{\tilde{p}}(\alpha), \quad S_{\tilde{p}}Q_{\tilde{p}}(\alpha) = \omega^\alpha Q_{\tilde{p}}(\alpha).$$

Here we have  $\alpha = 0, \dots, N-1$ . As can be seen, the operator  $Q_{\tilde{p}}(\alpha)$  projects a state down to the  $\omega^\alpha$  eigenstate of  $S_{\tilde{p}}$ . This implies that we can think of the  $\tilde{p}$  plaquettes on the boundary as a pseudo spin-chain with  $L_y/2$  sites (while the  $p$  plaquettes is the dual lattice). For later use, we note the following commutation relations (using equation (C.10))

$$S_p Q_{\tilde{p}}(\alpha) = \begin{cases} Q_{\tilde{p}}(\alpha-1)S_p & \text{if } \begin{array}{c} \vdots \\ \tilde{p} \\ p \\ \vdots \end{array}, \\ Q_{\tilde{p}}(\alpha+1)S_p & \text{if } \begin{array}{c} \vdots \\ p \\ \tilde{p} \\ \vdots \end{array}, \end{cases} \quad (\text{C.22})$$

While they commute for any  $p$  and  $\tilde{p}$  that are not nearest neighbours. A complete basis of  $\mathcal{H}_{\text{ground}}$  is thus given by

$$|\Gamma = a, \tilde{\Gamma} = b; S_{\tilde{1}} = \alpha_{\tilde{1}}, \dots, S_{\frac{\tilde{L}_y}{2}} = \alpha_{\frac{\tilde{L}_y}{2}}\rangle_1 = \prod_{\tilde{p}} Q_{\tilde{p}}(\alpha_{\tilde{p}}) \tilde{W}^a W^b |\Gamma = 0, \tilde{\Gamma} = 0\rangle.$$

Each of these states correspond to a boundary state with pseudospin configuration  $(\alpha_{\tilde{1}}, \alpha_{\tilde{2}}, \dots, \alpha_{\tilde{L}/2})$ .

The structure of (C.3) is thus  $\mathcal{H}_{\text{ground}} = \bigoplus_{a,b=0}^{N-1} \mathcal{H}_{a,b}$ , with  $\dim \mathcal{H}_{\text{ground}} = N^{\frac{L_y}{2}+1}$  and  $\dim \mathcal{H}_{a,b} = N^{\frac{L_y}{2}-1}$ . We see therefore that this basis is eigenbasis for the  $S_{\tilde{p}}$  operators, while  $S_p$  flip two nearest neighbour spins.

Alternatively, we could use a slightly different basis where  $S_p$  are diagonal and  $\tilde{S}_{\tilde{p}}$  flip spins. For convenience, we will make the following choice of reference state

$$|\psi\rangle = \left| \begin{array}{cc} |0\rangle_z & |0\rangle_x \\ |0\rangle_x & |0\rangle_z \end{array} \right\rangle, \quad (\text{C.23})$$

making the action of  $P_p$  and  $P_{\Gamma}$  trivial. The new set of states are now given by

$$|\Gamma = a, \tilde{\Gamma} = b; \alpha_{\tilde{1}}, \dots, \alpha_{\frac{\tilde{L}_y}{2}}\rangle_2 \equiv |a, b; \{\alpha_{\tilde{p}}\}\rangle = \mathcal{N} \prod_{\tilde{p}} S_{\tilde{p}}^{\alpha_{\tilde{p}}} |\Gamma = a, \tilde{\Gamma} = b\rangle. \quad (\text{C.24})$$

In this basis, it is clear that  $S_{\tilde{p}}$  changes only one spin  $\alpha_{\tilde{p}} \rightarrow \alpha_{\tilde{p}} + 1$ , while leaving the rest invariant. The action of the other boundary operators are

$$S_p |a, b; \{\alpha_{\tilde{p}}\}\rangle = \omega^{\alpha_{\tilde{p}} - \alpha_{\tilde{p}+1}} \omega^{\delta_{p, L_y/2} a} |a, b; \{\alpha_{\tilde{p}}\}\rangle,$$

where the  $\omega^{\delta_p, L_y/2 \cdot a}$  factor is due to  $\tilde{W} = \text{[diagram: a blue wavy line with a vertical line through its center, labeled with a tilde W]}. Whether we are using basis  $|\dots\rangle_1$  or  $|\dots\rangle_2$ , it is clear that the boundary degrees of freedom can be interpreted as a  $\mathbb{Z}_N$  spin chain with twisted boundary conditions. This pseudospin chain lives on the  $\tilde{p}$  sites in figure 32, of which there are  $\tilde{L}_y/2$  sites (where each pseudospin consists of a pair of physical spin). On these boundary pseudo-spins we can make the following identifications of operators$

$$\begin{aligned} S_{\tilde{p}} &= \text{[diagram: a blue wavy line with a vertical line through its center, labeled with a tilde p]} \rightarrow \tau_{\tilde{p}}^{x\dagger}, & \tilde{\Gamma} &= \text{[diagram: a blue wavy line with a vertical line through its center, labeled with a tilde Gamma]} \rightarrow \mathcal{S} = \prod_{\tilde{p}} \tau_{\tilde{p}}^{x\dagger}, \\ S_p &= \text{[diagram: a red wavy line with a vertical line through its center, labeled with a p]} \rightarrow \tau_p^z \tau_{p+1}^{z\dagger}, & \Gamma &= \text{[diagram: a red wavy line with a vertical line through its center, labeled with a Gamma]} \rightarrow \mathcal{T} = \omega^a \mathbb{I}, \end{aligned} \quad (\text{C.25})$$

with the following twisted boundary condition

$$\text{BC:} \quad \tau_{\frac{L_y}{2}+1}^z = \omega^{-a} \tau_1^z. \quad (\text{C.26})$$

In other words,  $\tau_{\tilde{L}_y/2}^z \tau_{\tilde{L}_y/2+1}^{z\dagger} = \omega^a \tau_{\tilde{L}_y/2}^z \tau_1^{z\dagger}$ . So each topological sector  $\Gamma = a$  can be mapped into a  $\mathbb{Z}_N$  spin chain language with boundary condition (C.26), the  $\Gamma = 0$  sector corresponds to the usual periodic boundary condition. In this language, the ground states  $|\Gamma = a; \{\alpha_{\tilde{p}}\}\rangle$  correspond to boundary pseudo-spin configurations.

**Boundary Conditions and Emergence of Kramer-Wannier Duality** Now with a clear understanding of the structure of the Hilbert space and the operators that act on it, let us consider the following boundary conditions of the model on a semi-infinite cylinder

$$H_{\partial} = -J/2 \sum_p \text{[diagram: a red wavy line with a vertical line through its center, labeled with a p]} - h/2 \sum_{\tilde{p}} \text{[diagram: a blue wavy line with a vertical line through its center, labeled with a tilde p]} + h.c. \quad (\text{C.27})$$

We see that the model (bulk + boundary) is exactly solvable when  $J = 0$  or when  $h = 0$ , which correspond to the gapped boundaries  $L_m$  and  $L_e$ . However when both  $J$  and  $h$  are non-zero, the boundary terms do not commute anymore and at some point a phase-transition will happen between these two phases.

Note that the boundary Hamiltonian only changes dynamics of the boundary modes, which are separated from bulk excitations with a large energy. In other words, the boundary Hamiltonian is the low-energy effective Hamiltonian in this case. Decomposing this into the  $N^2$  superselection sectors we get

$$H_{eff} = \bigoplus_{a,b=0}^{N-1} H_{eff}^{S=a, \mathcal{T}=b}, \quad (\text{C.28})$$

where in each superselection sector we have the Hamiltonians

$$H_{eff}^{S=a, \mathcal{T}=b} = P_S(a) H_{eff}^{\mathcal{T}=b} P_S(a), \quad (\text{C.29})$$

where  $H_{eff}^{\mathcal{T}=a}$  is the Hamiltonian in the  $\Gamma = \mathcal{T} = a$  superselection sector (but all  $\tilde{\Gamma} = \mathcal{S}$

sectors) and is given by

$$H_{eff}^{\mathcal{T}=b} = -J/2 \sum_{\tilde{p}=0}^{\tilde{L}/2-1} \left( \tau_{\tilde{p}}^z \tau_{\tilde{p}+1}^{z\dagger} + \tau_{\tilde{p}+1}^z \tau_{\tilde{p}}^{z\dagger} \right) - h/2 \sum_{\tilde{p}=0}^{\tilde{L}/2} \left( \tau_{\tilde{p}}^{x\dagger} + \tau_{\tilde{p}}^x \right) - J/2 \left( \omega^b \tau_{\tilde{L}/2}^z \tau_1^{z\dagger} + \omega^{-b} \tau_1^z \tau_{\tilde{L}/2}^{z\dagger} \right) \quad (\text{C.30})$$

and

$$P_S(a) = \frac{1}{|\mathbb{Z}_N|} \sum_{n=0}^{N-1} \omega^{-bn} \mathcal{S}^n. \quad (\text{C.31})$$

is the projector to the  $\Gamma = \mathcal{S} = a$  symmetry sector (where eigenvalue of  $\mathcal{S}$  is  $\omega^a$ ). Therefore the low-energy effective Hamiltonian in each superselection sector is nothing but a  $\mathbb{Z}_N$  generalization of the Ising model (Potts model?) with a particular symmetry twisted boundary conditions  $\mathcal{T} = b$  and symmetry sector  $\mathcal{S} = a$ . These superselection are sectors naturally inherited from the Bulk topological order and are one-to-one with states created on top of each minimally entangled ground state (MES).

Note that instead of (C.14), we could have chosen a different set of maximal commuting set of independent operators. In particular, we could have replaced  $S_{\tilde{p}}$  and  $\Gamma$  with  $S_p$  and  $\tilde{\Gamma}$ . Had we done that, the whole discussion above would have been the same, except the pseudospins would instead live on dual lattice ( $p$  instead of  $\tilde{p}$ ). And this would have changed the map (C.25) to

$$\begin{aligned} S_{\tilde{p}} &= \boxed{\text{blue wavy line}}_{\tilde{p}} \rightarrow \tau_{\tilde{p}}^z \tau_{\tilde{p}+1}^{z\dagger}, & \tilde{\Gamma} &= \boxed{\text{blue wavy line}} \rightarrow \mathcal{T} = \omega^a \mathbb{I}, \\ S_p &= \boxed{\text{red wavy line}}_p \rightarrow \tau_p^{x\dagger}, & \Gamma &= \boxed{\text{red wavy line}} \rightarrow \mathcal{S} = \prod_p \tau_p^{x\dagger}. \end{aligned} \quad (\text{C.32})$$

This means that when writting the boundary Hamiltonian (C.27) in the pseudospin language we would have to make the following changes

## D Symmetry-twisted boundary conditions

Symmetry-twisted boundary conditions (STBC) play an important role in dualities that act on the space of  $\mathbf{G}$ -symmetric Hamiltonians. Let us consider a 1+1 dimensional  $\mathbf{G}$ -symmetric quantum system to be compact in the spatial direction (quantum model on a circle). From a space-time point of view, a symmetry-twisted boundary condition corresponds to inserting the topological line defect  $\mathcal{U}_{\mathbf{g}}$  along a line in the time-direction (fixed space point) in a partition function (see Figure 33). Any local operator moving along the circle in the spatial direction will eventually cross the  $\mathcal{U}_{\mathbf{g}}$  line and transform according to the corresponding symmetry  $\mathbf{g} \in \mathbf{G}$ . This amounts to coupling the quantum system to a background  $\mathbf{G}$  gauge field that has a holonomy  $\mathbf{g} \in \mathbf{G}$  around the non-contractible spatial cycle. As is familiar in the context of, say,  $\text{U}(1)$  gauge theories, coupling to a background gauge field requires extending the derivatives to covariant derivatives. In order to do this on the lattice, consider



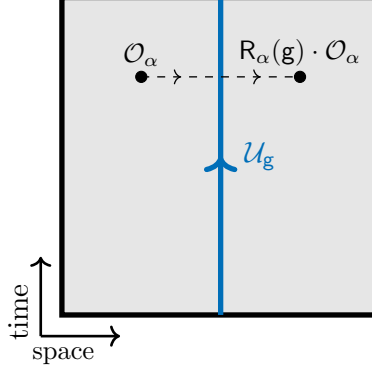


Figure 33: The insertion of  $\mathcal{U}_g$  line defects along time direction. Any charged local operator  $\mathcal{O}_\alpha$  crossing the symmetry defect will transform under the symmetry.

G-symmetric spin chains where G can possibly be non-abelian (or even a Lie group). For simplicity, consider the G-symmetric Hamiltonian

$$\begin{aligned}
H &= \sum_{i=1}^L \left[ \sum_{\alpha \in \text{Rep}(\mathbf{G})} J_\alpha \mathcal{O}_{\alpha,i}^\dagger \cdot \mathcal{O}_{\alpha,i+1} + \sum_{\mathbf{g}' \in \mathbf{G}} h_{\mathbf{g}'} \mathcal{O}_{\mathbf{g}',i} \right] + \text{h.c.}, \\
&= \sum_{i=1}^L \left[ \sum_{\alpha \in \text{Rep}(\mathbf{G})} J_\alpha \mathcal{O}_{\alpha,i}^\dagger \cdot \mathbb{T} \mathcal{O}_{\alpha,i} \mathbb{T}^{-1} + \sum_{\mathbf{g}' \in \mathbf{G}} h_{\mathbf{g}'} \mathcal{O}_{\mathbf{g}',i} \right] + \text{h.c.},
\end{aligned} \tag{D.1}$$

where  $\mathcal{O}_{\alpha,i}^I$  is a local field transforming under some finite-dimensional unitary representation of G (see (2.11) and (2.12)) and  $\mathcal{O}_{\alpha,i}^\dagger \cdot \mathcal{O}_{\alpha,i+1} = \sum_{I=1}^{\dim \alpha} (\mathcal{O}_{\alpha,i}^I)^\dagger \mathcal{O}_{\alpha,i+1}^I$ . In the last equation, we have written the Hamiltonian in terms of the translation operator (see section 2.2 for notation)

$$\mathbb{T} : \begin{cases} \mathcal{O}_{\mathbf{g},i} \mapsto \mathcal{O}_{\mathbf{g},i+1}, \\ \mathcal{O}_{\alpha,i} \mapsto \mathcal{O}_{\alpha,i+1}, \end{cases} \tag{D.2}$$

In order to twist the boundary condition with a symmetry  $\mathbf{g} \in \mathbf{G}$ , we can couple the theory to a background G gauge field  $\mathbf{g}$  with holonomy  $\mathbf{g}$  in the spatial direction corresponding to the insertion of  $\mathcal{U}_g$  along time. We can think of the background gauge field as distributing group elements on the links of the lattice,  $\mathbf{g} = (\mathbf{g}_{1,2}, \dots, \mathbf{g}_{L,1})$ , where  $\mathbf{g}_{i,i+1} \in \mathbf{G}$  is the value of the gauge field on the link  $(i, i+1)$ . The holonomy is defined as

$$\text{hol}(\mathbf{g}) \equiv \prod_i \mathbf{g}_{i-1,i} = \mathbf{g}. \tag{D.3}$$

One way to couple the theory to this gauge field is to introduce the modified symmetry-twisted translation operator

$$\mathbb{T}_{\mathbf{g}} \equiv \left( \prod_{i=1}^L \mathcal{O}_{\mathbf{g}_{i-1,i},i} \right) \mathbb{T}. \tag{D.4}$$

Replacing the translation operator in equation (D.1) we find

$$\begin{aligned} H(\mathbf{g}) &= \sum_{i=1}^L \left[ \sum_{\alpha \in \text{Rep}(\mathbf{G})} J_{\alpha} \mathcal{O}_{\alpha,i}^{\dagger} \cdot \mathbb{T}_{\mathbf{g}} \mathcal{O}_{\alpha,i} \mathbb{T}_{\mathbf{g}}^{-1} + \sum_{\mathbf{g}' \in \mathbf{G}} h_{\mathbf{g}'} \mathcal{O}_{\mathbf{g}',i} \right] + \text{h.c.}, \\ &= \sum_{i=1}^L \left[ \sum_{\alpha \in \text{Rep}(\mathbf{G})} J_{\alpha} \mathcal{O}_{\alpha,i}^{\dagger} \cdot \mathbf{R}_{\alpha}(\mathbf{g}_{i,i+1}) \cdot \mathcal{O}_{\alpha,i+1} + \sum_{\mathbf{g}' \in \mathbf{G}} h_{\mathbf{g}'} \mathcal{O}_{\mathbf{g}',i} \right] + \text{h.c.}, \end{aligned} \quad (\text{D.5})$$

where again  $\cdot$  corresponds to matrix product. The appearance of  $\mathbf{R}_{\alpha}(\mathbf{g}_{i,i+1})$  in the Hamiltonian above is essentially a Peierls substitution.

Note that the above construction has an ambiguity, the choice of  $\mathbf{g}$  such that (D.3) holds is not unique. However, any other choice is gauge equivalent and corresponds to a topological deformation of the symmetry operator  $\mathcal{U}_{\mathbf{g}}$  along time. In particular, consider the redefinition of charged operators

$$\mathcal{O}_{\alpha,i} \mapsto \mathbf{R}_{\alpha}(\lambda_i) \cdot \mathcal{O}_{\alpha,i}, \quad \lambda_i \in \mathbf{G}. \quad (\text{D.6})$$

This is essentially a local gauge transformation corresponding to  $\boldsymbol{\lambda} = (\lambda_1, \dots, \lambda_L)$ . Under this redefinition, the Hamiltonian changes as

$$H(\mathbf{g}) \mapsto H(\boldsymbol{\lambda}^{-1} \mathbf{g} \boldsymbol{\lambda}) = \sum_{i,\alpha} \mathcal{O}_{\alpha,i}^{\dagger} \cdot \mathbf{R}_{\alpha}(\lambda_i^{-1} g_{i,i+1} \lambda_{i+1}) \cdot \mathcal{O}_{\alpha,i+1} + \text{h.c.}, \quad (\text{D.7})$$

where  $\boldsymbol{\lambda}^{-1} \mathbf{g} \boldsymbol{\lambda} = (\lambda_1^{-1} g_{1,2} \lambda_2, \dots, \lambda_L^{-1} g_{L,1} \lambda_1)$ . Clearly, the new transformed background gauge field has the same holonomy

$$\text{hol}(\boldsymbol{\lambda}^{-1} \mathbf{g} \boldsymbol{\lambda}) = \text{hol}(\mathbf{g}) = \mathbf{g}. \quad (\text{D.8})$$

Therefore, different choices of  $\mathbf{g}$  correspond to redefinition of local operators and give rise to unitary-equivalent Hamiltonians

$$U_{\boldsymbol{\lambda}}^{\dagger} H(\mathbf{g}) U_{\boldsymbol{\lambda}} = H(\boldsymbol{\lambda}^{-1} \mathbf{g} \boldsymbol{\lambda}), \quad (\text{D.9})$$

where the unitary transformation is given by

$$U_{\boldsymbol{\lambda}} \equiv \prod_i \mathcal{O}_{\lambda_i,i}. \quad (\text{D.10})$$

By construction, the Hamiltonian  $H(\mathbf{g})$  commutes with the symmetry-twisted translation operator, which satisfies

$$\mathbb{T}_{\mathbf{g}}^L = \mathcal{U}_{\mathbf{g}}. \quad (\text{D.11})$$

If  $\mathcal{U}_{\mathbf{g}}$  generates an order- $n$  subgroup of  $\mathbf{G}$ , i.e.  $\mathcal{U}_{\mathbf{g}}^n = 1$ , such a symmetry-twist mathematically corresponds to extending the group  $\mathbb{Z}_L$  of translations (generated by  $\mathbb{T}$ ) by the finite group  $\mathbb{Z}_n$  generated by  $\mathcal{U}_{\mathbf{g}}$ . Practically, this has the implication that the momentum eigenvalues are quantized as  $nL^{\text{th}}$  roots of unity. It can be immediately checked that local operators satisfy symmetry-twisted conditions

$$\begin{aligned} \mathcal{O}_{\alpha,i+L} &= \mathbb{T}_{\mathbf{g}}^L \mathcal{O}_{\alpha,i} \mathbb{T}_{\mathbf{g}}^{-L} = \mathbf{R}_{\alpha}(\mathbf{g}) \cdot \mathcal{O}_{\alpha,i}, \\ \mathcal{O}_{\mathbf{h},i+L} &= \mathbb{T}_{\mathbf{g}}^L \mathcal{O}_{\mathbf{h},i} \mathbb{T}_{\mathbf{g}}^{-L} = \mathcal{O}_{\mathbf{h},i}, \end{aligned} \quad (\text{D.12})$$

In summary, coupling a spin Hamiltonian with global symmetry  $\mathbf{G}$  to a background  $\mathbf{G}$  gauge field  $\mathbf{g}$  with holonomy  $\text{hol}(\mathbf{g}) = \mathbf{g}$  in the spatial direction corresponds to the insertion of the symmetry operator  $\mathcal{U}_{\mathbf{g}}$  along the time direction. The ambiguity in the choice of background field  $\mathbf{g} \mapsto \boldsymbol{\lambda}^{-1} \mathbf{g} \boldsymbol{\lambda}$  corresponds to topological deformations of the symmetry operator and has no physical effect. Moving a local operator a full cycle along the spatial direction, it will inevitably cross the symmetry operator and transform as in (D.12). Therefore, this procedure will give rise to the symmetry-twisted Hamiltonian  $H_{\mathbf{g}}$ .

## E Simplicial calculus

In this work, we often encountered expressions of the form

$$\int_M A \cup A^\vee, \quad (\text{E.1})$$

for some gauge fields  $A$  and  $A^\vee$ , some space  $M$  and  $\cup$  denotes the so-called cup product. We would like to compute these expressions explicitly. We thus need an analog of the theory of integration of differential forms on a differentiable manifold. For triangulated spaces, whose definition we explain below, there is a simplicial analog of the theory of differential forms. In this appendix, we briefly review this simplicial calculus. Standard references are [193, 194].

### E.1 Simplicial complexes

Let  $\{v_0, \dots, v_n\}$  be a set of geometrically-independent points in  $\mathbb{R}^N$ . This means that if there exists a set of real scalars  $\{t_a\}$  such that

$$\sum_{a=0}^n t_a = 0, \quad \sum_{a=0}^n t_a v_a = 0, \quad (\text{E.2})$$

imply  $t_0 = \dots = t_n = 0$ . The  $n$ -simplex  $\Delta$  defined by  $\{v_0, \dots, v_n\}$  is the set of all points  $x \in \mathbb{R}^N$  such that

$$x = \sum_{a=0}^n t_a v_a, \quad \sum_{a=0}^n t_a = 1, \quad \forall t_a \geq 0. \quad (\text{E.3})$$

The points  $v_0, \dots, v_n$  are called the vertices of  $\Delta$  and  $n$  is its dimension. For a simplex  $\Delta$  defined by vertices  $\{v_0, \dots, v_n\}$ , we can define an ordering of its vertices. Two orderings are equivalent if they are different by an even number of permutation of vertices. An oriented simplex is denoted as  $[v_0, \dots, v_n]$ . We use the convention that the orientation of a given  $n$ -simplex is given by the orientation of its edges in increasing order. An example of simplices in  $\mathbb{R}^3$  and their orientations are shown in Figure 34. We sometimes denote an  $n$ -simplex by  $\Delta^n$ , i.e.

$$\Delta^n \equiv [v_0, \dots, v_n]. \quad (\text{E.4})$$

Simplices generated by all proper subsets<sup>25</sup> of vertices in  $\{v_0, \dots, v_n\}$  are collectively called subsimplices. Any simplex spanned by a subset of  $\{v_0, \dots, v_n\}$  obtained by removing only

---

<sup>25</sup>A proper subset of a set is any subset which is not the set itself.

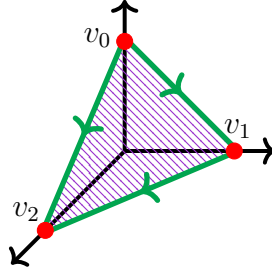


Figure 34: An example of a 2-simplex in  $\mathbb{R}^3$ . The vertices (in red), i.e. 0-simplices, are denoted as  $[v_0] = v_0$ ,  $[v_1] = v_1$ , and  $[v_2] = v_2$ . The 1-simplices (in green) are  $[v_0, v_1] = v_0 - v_1$ ,  $[v_1, v_2] = v_1 - v_2$ , and  $[v_0, v_2] = v_0 - v_2$ . Finally, the only 2-simplex (in velvet) is  $[v_0, v_1, v_2]$ .

one of the vertices is called a face of  $\Delta$ . The union of all faces is called the boundary of  $\Delta$  and it is denoted as  $\partial\Delta$ . Accordingly, one can define the interior of an  $n$ -simplex by  $\text{Int}(\Delta) = \Delta - \partial\Delta$ .

A simplicial complex  $\mathcal{S}$  in  $\mathbb{R}^N$  is a collection of simplices in  $\mathbb{R}^N$  with two properties: 1) every subsimplex of a simplex  $\Delta \in \mathcal{S}$  also belongs to  $\mathcal{S}$ ; and 2) every intersection of two simplices  $\Delta, \Delta' \in \mathcal{S}$  is a face of each of them. An example of a simplicial complex (35a) and an example which is not a simplicial complex (35b) is shown in Figure 35. The dimension of a simplicial complex  $\mathcal{S}$  is simply the maximum dimension of the simplices in  $\mathcal{S}$ .

An important result<sup>26</sup> is that any (reasonably-nice-behaved) space  $M$  can be built from  $n$ -simplices inductively by starting from vertices, and attach edges to them to make a graph, and then attach 2-simplices, and so on. To make this more precise, let  $\mathcal{S}$  be a simplicial complex in  $\mathbb{R}^N$  and let  $|\mathcal{S}|$  denote the subset of  $\mathbb{R}^N$  consists of the union of simplices in  $\mathcal{S}$ . This subset admits a natural topology: a subset  $S \subset |\mathcal{S}|$  is closed if and only if  $S \cap \Delta$  is closed for all simplices  $\Delta \in \mathcal{S}$ . Such sets are closed under finite union and arbitrary intersections, and hence define a topology on  $|\mathcal{S}|$ . The subset  $|\mathcal{S}|$  endowed with this topology is called the *underlying space* of  $\mathcal{S}$  or its *polytope*. A map  $\phi : |\mathcal{S}| \rightarrow M$  from  $|\mathcal{S}|$  to a topological space  $M$  is continuous if its restriction  $f|_{\Delta}$  to each  $\Delta \in \mathcal{S}$  is continuous. Equipped with these definition, we see that the polytope of a simplicial complex can be homeomorphic<sup>27</sup> to a topological space. Finally, notice that there might be many simplicial complexes which are homeomorphic to a given topological space  $M$ . Alternatively, one can choose different homeomorphisms from a given polytope to a homeomorphic topological space. A choice of such homeomorphism is called a *triangulation* of  $M$ . After choosing such a homeomorphism,  $M$  is called a triangulated space. The study of simplicial aspects of  $M$  (simplicial homology and cohomology groups and cup product, etc) can thus be reduced to the study of the simplicial complex underlying its triangulation. We use this correspondence in the following, and often use the simplicial complex  $\mathcal{S}$  and the space  $M$  for which  $\mathcal{S}$  provides a triangulation interchangeably. For example, the simplicial homology and cohomology groups of a simplicial complex are actually the simplicial homology and

<sup>26</sup>To make this precise, one has to introduce the notion of cell-complex structure on a space and identify the space as a quotient of disjoint simplices in this cell-complex structure by certain equivalence relation. Here, and to avoid the mathematical details, we will just state the final result.

<sup>27</sup>A homeomorphism between two topological spaces is a continuous bijective map with a continuous inverse.

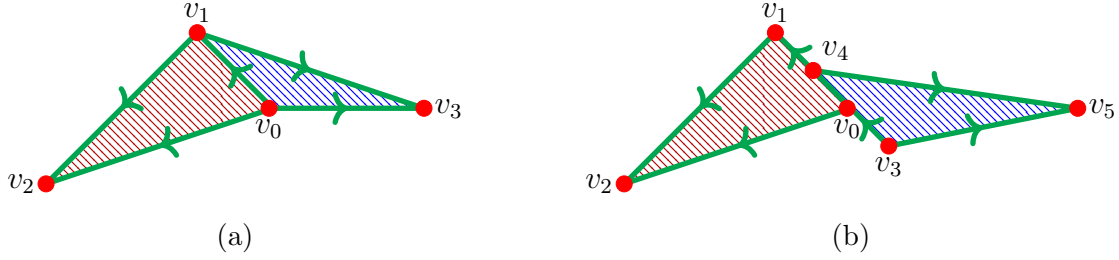


Figure 35: (a) This shows a proper simplicial complex consists of two 2-simplices (filled in red and blue), their edges (in green) and their vertices (in red). The intersection of these 2-simplices is the edge of either of them and hence belong to the simplicial complex; (b) This shows two 2-simplices that do not form a simplicial complex. The intersection of them is a subset of the edge of either of them. Hence, the union of the two triangles do not define a simplicial complex.

cohomology of its underlying space, which is homeomorphic to some topological space. As an example, consider the simplicial complex in Figure 36 whose underlying space is a cylinder.

## E.2 Simplicial homology groups

For a simplicial complex  $\mathcal{S}$ , a  $p$ -chain is a function  $c$  from the set of oriented simplices in  $\mathcal{S}$  into integers (or more generally any Abelian group  $G$ ) satisfying 1) for two oppositely-oriented simplices  $\Delta$  and  $\Delta'$ , we have  $c(\Delta) = -c(\Delta')$ ; 2)  $c(\Delta) = 0$  for all but finitely-many oriented  $p$ -simplices  $\Delta$ . The set of all  $p$ -chains naturally forms an Abelian group under addition, which will be denoted as  $C_p(\mathcal{S}, G)$ , which is a free Abelian group. For  $p < 0$  and  $p > \dim(K)$ , this is a trivial group. One can define the boundary operator  $\partial_p$  as the following homomorphism  $\partial_p : C_p(\mathcal{S}, G) \rightarrow C_{p-1}(\mathcal{S}, G)$ , which for an oriented  $n$ -simplex  $\Delta = [v_0, \dots, v_n]$  is defined as

$$\partial_p \Delta \equiv \sum_{a=0}^p (-1)^a [v_0, \dots, \widehat{v}_a, \dots, v_n], \quad (\text{E.5})$$

and  $[v_0, \dots, \widehat{v}_a, \dots, v_n]$  means that the vertex  $v_a$  is removed from the set of vertices. The boundary operator has two important properties: 1) For the oppositely-oriented simplex  $-\Delta$  of a simplicial complex  $\Delta$ , we have  $\partial_p(-\Delta) = -\partial_p(\Delta)$ ; 2) it satisfies

$$\partial_{p-1} \circ \partial_p = 0. \quad (\text{E.6})$$

As an example, consider a 2-simplex  $[v_0, v_1, v_2]$  for which we have  $\partial_2[v_0, v_1, v_2] = [v_1, v_2] - [v_0, v_2] + [v_0, v_1]$ . The boundary operation defined here is the analog of the boundary operation in the singular homology theory in the context of integration of differential forms on Riemannian manifolds.

(E.6) makes it clear how to define homology group of a simplicial complex. They can be defined by considering the boundary operators  $\partial_p : C_p(\mathcal{S}, G) \rightarrow C_{p-1}(\mathcal{S}, G)$  and  $\partial_{p+1} : C_{p+1}(\mathcal{S}, G) \rightarrow C_p(\mathcal{S}, G)$ . The kernel of the first is called the group of  $p$ -cycles  $Z_p(\mathcal{S}, G)$ , and

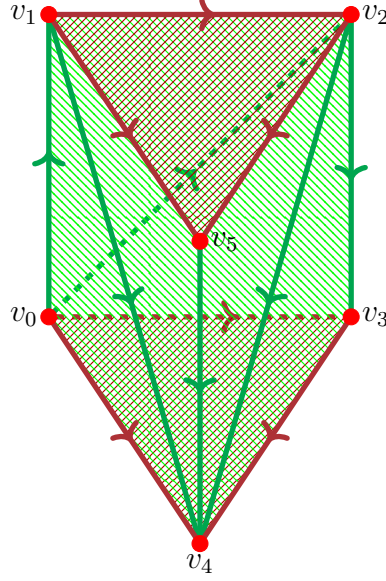


Figure 36: A simplicial complex consisting of six 2-simplices, their faces (edges) and vertices. The underlying space of the top and bottom triangles are circles and the underlying space of the whole simplicial complex is (homeomorphic to) a cylinder. To study simplicial aspects of cylinder, one can instead study similar aspects of this simplicial complex.

the image of the second is called the group of  $p$ -boundaries  $B_p(\mathcal{S}, G)$ . The second property above guarantees that  $B_p(\mathcal{S}, G) \subset Z_p(\mathcal{S}, G)$ . One can then define the  $p^{\text{th}}$  homology group of  $\mathcal{S}$  by

$$H_p(\mathcal{S}, G) \equiv Z_p(\mathcal{S}, G)/B_p(\mathcal{S}, G). \quad (\text{E.7})$$

As we have explained above, these are the homology groups of a topological space  $M$  which is isomorphic to the underlying space  $|\mathcal{S}|$  of  $\mathcal{S}$ . In the following, we thus use the notations  $C_p(M, G)$  and  $C_p(\mathcal{S}, G)$ ,  $Z_p(M, G)$  and  $Z_p(\mathcal{S}, G)$ ,  $B_p(M, G)$  and  $B_p(\mathcal{S}, G)$ , and  $H_p(M, G)$  and  $H_p(\mathcal{S}, G)$  interchangeably.

**Example (homology groups of a point with integer coefficients):** Let us consider the simplest possible example, i.e. when  $M$  is just a point and  $G \simeq \mathbb{Z}$ . It is clear that  $H_p(M, \mathbb{Z}) = 0, \forall p \geq 1$  since there are not  $p$ -chains with  $p \geq 1$  in  $M$ . On the other hand,  $H_0(M, \mathbb{Z})$  is the free Abelian group generated by the single point of  $M$  and hence  $H_0(M, \mathbb{Z}) \simeq \mathbb{Z}$ .

### E.3 Simplicial cohomology groups

In this section, we define the cohomology groups of simplicial complexes. As it will become clear, these are dual, in some precise sense, to the homology groups. They are the analog of de Rham cohomology groups in the context of differential forms.

To this end, we consider functions on set of simplicial complexes. For a simplicial complex  $\mathcal{S}$  the group  $C^p(\mathcal{S}, G)$  of  $p$ -cochains of  $\mathcal{S}$  with coefficients in an Abelian group  $G$  is defined

to be

$$C^p(\mathcal{S}, G) \equiv \text{Hom}(C_p(\mathcal{S}, G), G), \quad (\text{E.8})$$

where  $\text{Hom}(C_p(\mathcal{S}, G), G)$  denotes the Abelian group of all homomorphism of  $C_p(\mathcal{S}, G)$  into  $G$ <sup>28</sup>. The value of a  $p$ -cochain  $\varphi^p \in C^p(\mathcal{S}, G)$  on an oriented  $p$ -chain  $[v_0, \dots, v_p] \in C_p(\mathcal{S}, G)$  is denoted by a pairing notation  $\langle \cdot, \cdot \rangle : C^p(\mathcal{S}, G) \times C_p(\mathcal{S}, G) \rightarrow G$  as

$$\langle \varphi^p, [v_0, \dots, v_p] \rangle \in G. \quad (\text{E.9})$$

To be able to define cohomology groups, one needs to have a notion of a differential on complexes of cochains. In the context of simplicial calculus, this is called the coboundary operator. It is a map  $\delta_p : C^p(\mathcal{S}, G) \rightarrow C^{p+1}(\mathcal{S}, G)$  and it is defined as being the dual of the boundary operator in the following sense

$$\langle \delta_p \varphi^p, [v_0, \dots, v_{p+1}] \rangle \equiv \langle \varphi^p, \partial_p [v_0, \dots, v_{p+1}] \rangle. \quad (\text{E.10})$$

Using (E.5) for the boundary operator  $\partial_p$ , we have

$$\langle \delta_p \varphi^p, [v_0, \dots, v_{p+1}] \rangle = \sum_{a=0}^{p+1} (-1)^a \langle \varphi^p, [v_0, \dots, \widehat{v}_a, \dots, v_{p+1}] \rangle. \quad (\text{E.11})$$

Using this formula, one can show the important property

$$\delta_{p+1} \circ \delta_p = 0. \quad (\text{E.12})$$

This property, which is the dual version of (E.6), then makes it clear how to define the cohomology group of simplicial complexes. The kernel of  $\delta_p : C^p(\mathcal{S}, G) \rightarrow C^{p+1}(\mathcal{S}, G)$  is the Abelian group of  $p$ -cocycles  $Z^p(\mathcal{S}, G)$  and the image of  $\delta_p : C^p(\mathcal{S}, G) \rightarrow C^{p+1}(\mathcal{S}, G)$  is the Abelian group of  $p$ -coboundaries  $B^p(\mathcal{S}, G)$ . The  $p^{\text{th}}$  simplicial cohomology group of a simplicial complex  $\mathcal{S}$  is defined as

$$H^p(\mathcal{S}, G) \equiv Z^p(\mathcal{S}, G) / B^p(\mathcal{S}, G). \quad (\text{E.13})$$

The coefficients of all these groups are in  $G$ , as the notation implies. Since boundary operation  $\partial$  and coboundary operation  $\delta$  are dual in the sense of (E.10), the simplicial homology and cohomology groups are dual to each other. Finally, as we have explained above, notice that these cohomology groups are the cohomology groups of a topological space  $M$  which is isomorphic to the underlying space  $|\mathcal{S}|$  of  $\mathcal{S}$ , i.e. we have  $H^p(M, G) \simeq H^p(\mathcal{S}, G)$ . In the following, we thus use the notations  $C^p(M, G)$  and  $C^p(\mathcal{S}, G)$ ,  $Z^p(M, G)$  and  $Z^p(\mathcal{S}, G)$ ,  $B^p(M, G)$  and  $B^p(\mathcal{S}, G)$ , and  $H^p(M, G)$  and  $H^p(\mathcal{S}, G)$  interchangeably.

**Example (cohomology groups of a point with integer coefficient):** Let us continue our simple example, i.e. when  $M$  is a point and  $G \simeq \mathbb{Z}$ . As we have explained in the previous section,  $H_p(M, \mathbb{Z})$  vanishes for  $p \geq 1$  and  $H_0(M, \mathbb{Z}) \simeq \mathbb{Z}$ . On the other hand, (E.8) and the fact that all homology groups are free Abelian tell us that

$$H^p(M, \mathbb{Z}) \simeq \text{Hom}(H_p(M, \mathbb{Z}), \mathbb{Z}) = \begin{cases} \text{Hom}(\mathbb{Z}, \mathbb{Z}) \simeq \mathbb{Z}, & p = 0, \\ \text{Hom}(\mathbb{Z}, 0) \simeq 0, & p \neq 0. \end{cases} \quad (\text{E.14})$$

---

<sup>28</sup>Note that  $C_p(\mathcal{S}, G)$  are Abelian groups and hence one can define the Abelian group  $\text{Hom}(C_p(\mathcal{S}, G))$  as the group of all homomorphisms between two Abelian groups. The addition in  $\text{Hom}(C_p(\mathcal{S}, G))$  is defined as follows: the addition of two homomorphisms  $f_1, f_2 \in \text{Hom}(C_p(\mathcal{S}, G))$  is defined by the addition of their values in  $G$ .

## E.4 Cup product

As we have seen in previous section, the theory of simplicial complexes is in direct analogy with the theory of singular complexes, which is used for a rigorous treatment of the theory of differential forms on a manifold culminated in The de Rham Theorem. Therefore, we expect that there should be an analog of wedge product. We will now explain what this operation is. One of the main differences between homology and cohomology is that the latter can be endowed with a natural product. The analog of the wedge product in the simplicial context is called *cup product* which turns  $H^\bullet \equiv \bigoplus_p H^p(M, R)$  into a ring called the cohomology ring of  $M$ .

The cup product is defined by considering cohomology with coefficients in a commutative ring  $R$ . We are mostly interested in the case that  $R = \prod_a \mathbb{Z}_{N_a}$ . For cochains  $\varphi^p \in C^p(\mathcal{S}, R)$  and  $\varphi^q \in C^q(\mathcal{S}, R)$ , the cup product  $\varphi^p \cup \varphi^q$  defines an element of  $C^{p+q}(\mathcal{S}, R)$  such that whose value on a  $(p+q)$ -simplex  $\Delta = [v_0, \dots, v_{p+q}]$  is given by

$$\langle \varphi^p \cup \varphi^q, \Delta \rangle \equiv \langle \varphi^p, [v_0, \dots, v_p] \rangle \bullet \langle \varphi^q, [v_p, \dots, v_{p+q}] \rangle, \quad (\text{E.15})$$

where  $\bullet$  denotes the product operation on the ring  $R$ . The cup product has some important properties; It is associative, i.e. for  $\varphi^{p_i} \in C^{p_i}(\mathcal{S}, G)$ ,  $i = 1, 2, 3$ , we have

$$(\varphi^{p_1} \cup \varphi^{p_1}) \cup \varphi^{p_3} = \varphi^{p_1} \cup (\varphi^{p_1} \cup \varphi^{p_3}), \quad (\text{E.16})$$

which can be easily verified using (E.15). Furthermore, it is distributive with respect to the addition in the ring  $R$ . We also have

$$\delta(\varphi^{p_1} \cup \varphi^{p_2}) = \delta\varphi^{p_1} \cup \varphi^{p_2} + (-1)^{p_1} \varphi^{p_1} \cup \delta\varphi^{p_2}. \quad (\text{E.17})$$

Note that the operator  $\delta$  reduces to  $\delta_{p_i}$  defined in (E.10) when acting on  $C^{p_i}(\mathcal{S}, R)$ .

Up to now, we have define the cup product for  $p$ -cochains. However, it can be seen that this cup product induces one at the level of cohomologies. This can be seen by noting that  $p$ -cocycles are in particular  $p$ -cochains so one can consider the cup product of cocycles. On the other hand, the cup product of a cocycle and a coboundary is a coboundary, which can be easily seen by noting that  $\varphi \cup \delta\varphi' = \delta(\varphi \cup \varphi')$  for  $\delta\varphi = 0$ . We thus see that cup product is a well-defined operation at the level of cohomology, i.e.

$$\cup : H^{p_1}(\mathcal{S}, R) \times H^{p_2}(\mathcal{S}, R) \longrightarrow H^{p_1+p_2}(\mathcal{S}, R). \quad (\text{E.18})$$

Taking into its properties stated above (associativity, distributive with respect to addition in  $R$ ), we see that it indeed endows  $\bigoplus_p H^p(M, R)$  with a ring<sup>29</sup> structure.

**Example (cohomology ring of a point with integer coefficients):** To complete our very basic example, i.e. the case of that  $M$  is a point and  $G \simeq \mathbb{Z}$ , let us compute the cohomology ring of this space. We have seen that the cohomology groups of a point vanishes except for  $p = 0$ , which is isomorphic to  $\mathbb{Z}$ . Due to (E.18), we thus see that  $H^{p_1+p_2}$  vanishes except for  $p_1 + p_2 = 0$ , which implies  $p_1 = p_2 = 0$ . Consider  $\varphi_1^0, \varphi_2^0 \in H^0(M, \mathbb{Z})$ . They satisfy

$$\delta\varphi_1^0 = \delta\varphi_2^0 = 0, \quad (\text{E.19})$$

---

<sup>29</sup>Actually cup product endows  $H^\bullet$  with the structure of an  $R$ -algebra and hence an  $R$ -module.



They are thus both constant functions. The value of their cup product  $\varphi_1^0 \cup \varphi_2^0$  is the product of their values. This is the complete description of the cohomology ring of a point.

In many situation, we are interested in integrating a cup product over a triangulated space  $M$ . For this purpose, it is enough to know how to compute the integral on the cohomology-ring  $H^\bullet(\mathcal{S}, R)$  of a simplicial complex  $\mathcal{S}$ , as follows. Let  $\varphi^{p_i} \in C^{p_i}(\mathcal{S}, R)$ ,  $i = 1, \dots, N$  be a set of  $p_i$ -cochains. The integral of their cup product over a simplex

$$\Delta^p \equiv \Delta^{p_1+\dots+p_N} = [v_0, \dots, v_{p_1+\dots+p_N}], \quad (\text{E.20})$$

is defined by

$$\int_{\Delta^p} \varphi^{p_1} \cup \dots \cup \varphi^{p_N} = \langle \varphi^{p_1} \cup \dots \cup \varphi^{p_N}, \Delta^p \rangle. \quad (\text{E.21})$$

Using (E.15), we have

$$\int_{\Delta^p} \varphi^{p_1} \cup \dots \cup \varphi^{p_N} = \prod_{a=1}^N \langle \varphi^{p_a}, [v_{p_1+\dots+p_{a-1}}, \dots, v_{p_1+\dots+p_a}] \rangle, \quad p_0 \equiv 0, \quad (\text{E.22})$$

where the product is taken in the ring  $R$ . Using this result, we can define the cup products of cochains on a given space  $M$  which is homeomorphic to the underlying space of a simplicial complex  $\mathcal{S}$ . The integral of such cochains are defined by

$$\int_M \varphi^{p_1} \cup \dots \cup \varphi^{p_N} \equiv \sum_{\Delta^p \in \mathcal{S}} \int_{\Delta^p} \varphi^{p_1} \cup \dots \cup \varphi^{p_N} \quad (\text{E.23})$$

where the sum is taken over all oriented  $p$ -simplices.

Let us now get back to the question we posed in the beginning of this appendix, i.e. the explicit computation of expressions of the form

$$\int_M A \cup A^\vee, \quad (\text{E.24})$$

for some gauge fields  $A$  and  $A^\vee$  and some space  $M$ . This expression can be calculated by what we have explained so far. Since gauge fields are 1-cochains (and indeed 1-cocycles) with values  $\mathbb{Z}_N$  (or product of such Abelian groups),  $A \cup A^\vee$  is a 2-cochain. Therefore, it has to be computed on a 2-chain. Using the 2-simplex in Figure 34 and denoting it as  $\Delta^2$ , we have

$$\begin{aligned} \int_{\Delta^2} A \cup A^\vee &= \langle A \cup A^\vee, [v_0, v_1, v_2] \rangle \\ &= \langle A, [v_0, v_1] \rangle \langle A^\vee, [v_1, v_2] \rangle, \end{aligned} \quad (\text{E.25})$$

where  $\langle A, [v_0, v_1] \rangle$  is just the  $\mathbb{Z}_N$ -value of the gauge field on the oriented edge  $[v_0, v_1]$  (also denotes as  $A_{v_0 v_1}$  in the main text) and the same for  $\langle A^\vee, [v_1, v_2] \rangle$ . Using this basic result, we can now compute the integral of  $A \cup A^\vee$  over a triangulated space  $M$  using (E.23).

## F Group structure of the web of dualities

In this appendix, we collect the computations that verify the group structure at the level of transformation of twisted partition functions for the duality group of  $\mathbf{G}$ -symmetric systems when  $\mathbf{G}$  is  $\mathbb{Z}_2 \times \mathbb{Z}_2$ .

We first consider the case of  $\mathbb{Z}_2 \times \mathbb{Z}_2$ . Recall, that the duality group as described in Sec. 5.3 is

$$\mathcal{G}[\mathbb{Z}_2 \times \mathbb{Z}_2] = \langle \sigma_L, k_1, k_2, k_3 \rangle = (S_3 \times S_3) \rtimes \mathbb{Z}_2. \quad (\text{F.1})$$

Concretely,  $k_2$  and  $k_1 k_3$  generate one of the  $S_3$  groups such that  $k_2^2 = \text{id}$ ,  $(k_1 k_3)^3 = \text{id}$  and  $k_2(k_1 k_3)k_2^{-1} = (k_1 k_3)^{-1}$ . which  $\sigma_L$  acts on by conjugation to give the other  $S_3$  group, which is generated by  $h_2$  and  $h_1 h_3$ , where

$$\begin{aligned} \sigma_L(m_L, m_R; e_L, e_R) &= (e_L, m_R; m_L, e_R), \\ \sigma_R(m_L, m_R; e_L, e_R) &= (m_L, e_R; e_L, m_R), \\ h_1(m_L, m_R; e_L, e_R) &= (m_L, m_L m_R; e_L e_R, e_R), \\ h_2(m_L, m_R; e_L, e_R) &= (m_L m_R, m_R; e_L, e_L e_R), \\ h_3(m_L, m_R; e_L, e_R) &= (m_R, m_L; e_R, e_L), \\ k_1(m_L, m_R; e_L, e_R) &= (m_L e_R, m_R e_L; e_L, e_R), \\ k_2(m_L, m_R; e_L, e_R) &= (m_L, m_R; e_L m_R, e_R m_L), \\ k_3(m_L, m_R; e_L, e_R) &= (e_R, e_L; m_R, m_L). \end{aligned} \quad (\text{F.2})$$

At the level of twisted partition functions, these transformations take the form

$$\begin{aligned} k_1 : \mathcal{Z}[A_L, A_R] &\mapsto \mathcal{Z}[A_L, A_R] e^{i\pi \int_{\Sigma} A_L \cup A_R}, \\ k_2 : \mathcal{Z}[A_L, A_R] &\mapsto \mathcal{Z}^{\vee}[A_L^{\vee}, A_R^{\vee}] = \frac{1}{\sqrt{|H^1(\Sigma, \mathbb{Z}_2^2)|}} \sum_{A_L, A_R} \mathcal{Z}[A_L, A_R] e^{i\pi \int_{\Sigma} (A_L^{\vee} - A_L) \cup (A_R^{\vee} - A_R)}, \\ k_3 : \mathcal{Z}[A_L, A_R] &\mapsto \mathcal{Z}^{\vee}[A_L^{\vee}, A_R^{\vee}] = \frac{1}{\sqrt{|H^1(\Sigma, \mathbb{Z}_2^2)|}} \sum_{A_L, A_R} \mathcal{Z}[A_L, A_R] e^{i\pi \int_{\Sigma} A_L \cup A_R^{\vee} + A_R \cup A_L^{\vee}}, \\ \sigma_L : \mathcal{Z}[A_L, A_R] &\mapsto \mathcal{Z}^{\vee}[A_L^{\vee}, A_R] = \frac{1}{\sqrt{|H^1(\Sigma, \mathbb{Z}_2)|}} \sum_{A_L} \mathcal{Z}[A_L, A_R] e^{i\pi \int_{\Sigma} A_L \cup A_L^{\vee}}. \end{aligned} \quad (\text{F.3})$$

These can for example be computed using the anyonic symmetries with the formulas (4.25) and (4.26). Here, we demonstrate that these transformations satisfy the group composition rules in  $\mathcal{G}[\mathbb{Z}_2 \times \mathbb{Z}_2]$ . In particular we verify the following relations (1)  $k_1^2 = \text{id}$ , (2)  $k_2^2 = \text{id}$ , (3)  $k_3^2 = \text{id}$ , (4)  $\sigma_L^2 = \text{id}$ , (5)  $(k_1 k_3)^3 = \text{id}$  and (6)  $k_2(k_1 k_3)k_2^{-1} = (k_1 k_3)^{-1}$ . For simplicity we consider  $\Sigma = T^2$  in the formulas below such that  $|H^1(\Sigma, \mathbf{G})| = |\mathbf{G}|^2$ .

1.  $k_1^2 = \text{id}$ : From (F.3), twisted partition transform as follows under  $k_1^2$

$$k_1^2 : \mathcal{Z}[A_L, A_R] \mapsto \mathcal{Z}^{\vee}[A_L, A_R] = \mathcal{Z}[A_L, A_R] (-1)^{\int_{\Sigma} 2A_L \cup A_R} = \mathcal{Z}[A_L, A_R]. \quad (\text{F.4})$$

Which verifies  $k_1^2 = \text{id}$ . Physically,  $k_1$  corresponds to pasting a  $\mathbb{Z}_2 \times \mathbb{Z}_2$  SPT, and therefore  $k_1^2$  corresponds to pasting two copies of the  $\mathbb{Z}_2 \times \mathbb{Z}_2$  SPT. Since  $\mathbb{Z}_2 \times \mathbb{Z}_2$  SPTs

are classified by  $\mathbb{Z}_2$ , this process is adiabatically connected to not pasting anything at all.

2.  $k_2^2 = \text{id}$ : Implementing the  $k_2$  transformation in (F.3) twice successively,

$$k_2^2 : \mathcal{Z}[A_L, A_R] \mapsto \mathcal{Z}^{\vee\vee}[A_L^{\vee\vee}, A_R^{\vee\vee}], \quad (\text{F.5})$$

where

$$\begin{aligned} \mathcal{Z}^{\vee\vee}[A_L^{\vee\vee}, A_R^{\vee\vee}] &= \frac{1}{|\mathbf{G}|^2} \sum_{A_L, R, A_{L,R}^{\vee}} \mathcal{Z}[A_L, A_R] (-1)^{\int_{\Sigma} [(A_L^{\vee} - A_L) \cup (A_R^{\vee} - A_R) + (A_L^{\vee\vee} - A_L^{\vee}) \cup (A_R^{\vee\vee} - A_R^{\vee})]} \\ &= \sum_{A_L, A_R} \mathcal{Z}[A_L, A_R] (-1)^{\int_{\Sigma} [A_L \cup A_R + A_L^{\vee\vee} \cup A_R^{\vee\vee}]} \delta_{A_L, A_L^{\vee\vee}} \delta_{A_R, A_R^{\vee\vee}} \\ &= \mathcal{Z}[A_L^{\vee\vee}, A_R^{\vee\vee}]. \end{aligned} \quad (\text{F.6})$$

In going to the second line, we have summed over  $A_L^{\vee}$  and  $A_R^{\vee}$ <sup>30</sup>

3.  $k_3^2 = \text{id}$ : Implementing the  $k_3$  transformation in (F.3) twice successively,

$$k_3^2 : \mathcal{Z}[A_L, A_R] \mapsto \mathcal{Z}^{\vee\vee}[A_L^{\vee\vee}, A_R^{\vee\vee}], \quad (\text{F.8})$$

where

$$\mathcal{Z}^{\vee\vee}[A_L^{\vee\vee}, A_R^{\vee\vee}] = \frac{1}{|\mathbf{G}|^2} \sum_{A_L, R, A_{L,R}^{\vee}} \mathcal{Z}[A_L, A_R] (-1)^{\int_{\Sigma} [A_L \cup A_R^{\vee} + A_R \cup A_L^{\vee} + A_L^{\vee} \cup A_R^{\vee\vee} + A_R^{\vee} \cup A_L^{\vee\vee}]}. \quad (\text{F.9})$$

Summing over  $A_L^{\vee}$  and  $A_R^{\vee}$ , imposes  $A_L = -A_L^{\vee\vee}$  and  $A_R = -A_R^{\vee\vee}$ , which implies

$$\mathcal{Z}^{\vee\vee}[A_L^{\vee\vee}, A_R^{\vee\vee}] = \mathcal{Z}[A_L^{\vee\vee}, A_R^{\vee\vee}], \quad (\text{F.10})$$

i.e.,  $k_3^2 = \text{id}$ .

4.  $\sigma_L^2 = \text{id}$ : The duality operation  $\sigma_L$ , corresponds to Kramer's Wannier duality, i.e., gauging the global symmetry corresponding to the background  $A_L$ . Performing this operation twice furnishes

$$\sigma_L^2 : \mathcal{Z}[A_L, A_R] \mapsto \mathcal{Z}^{\vee\vee}[A_L^{\vee\vee}, A_R], \quad (\text{F.11})$$

where

$$\begin{aligned} \mathcal{Z}^{\vee\vee}[A_L^{\vee\vee}, A_R] &= \frac{1}{|\mathbf{G}|} \sum_{A_L, A_L^{\vee}} \mathcal{Z}[A_L, A_R] (-1)^{\int_{\Sigma} [A_L \cup A_L^{\vee} + A_L^{\vee} \cup A_L^{\vee\vee}]} \\ &= \sum_{A_L} \mathcal{Z}[A_L^{\vee\vee}, A_R] \delta_{A_L, A_L^{\vee\vee}} \\ &= \mathcal{Z}[A_L^{\vee\vee}, A_R]. \end{aligned} \quad (\text{F.12})$$

---

<sup>30</sup>We use the equation

$$\frac{1}{|\mathbf{G}|} \sum_{A_R^{\vee}} (-1)^{\int_{\Sigma} A_R^{\vee} \cup (A + \dots)} = \delta(A + \dots). \quad (\text{F.7})$$

5.  $(k_1 k_3)^3 = \text{id}$ : Acting with the  $k_1 k_3$  duality, transforms the twisted partition function as

$$\mathcal{Z}[A_L, A_R] \xrightarrow{k_1 k_3} \mathcal{Z}^\vee[A_L^\vee, A_R^\vee] = \frac{1}{|\mathbf{G}|} \sum_{A_L, A_R} \mathcal{Z}[A_L, A_R] (-1)^{f_\Sigma[A_L \cup A_R^\vee + A_R \cup A_L^\vee + A_L^\vee \cup A_R^\vee]}.$$
(F.13)

Acting with  $k_1 k_3$  again produces the partition function

$$\begin{aligned} \mathcal{Z}^{\vee\vee}[A_L^{\vee\vee}, A_R^{\vee\vee}] &= \frac{1}{|\mathbf{G}|^2} \sum_{A_L, R, A_{L,R}^\vee} \mathcal{Z}[A_L, A_R] \\ &\times (-1)^{f_\Sigma[A_L \cup A_R^\vee + A_R \cup A_L^\vee + A_L^\vee \cup A_R^\vee + A_L^\vee \cup A_R^{\vee\vee} + A_R^\vee \cup A_L^{\vee\vee} + A_L^{\vee\vee} \cup A_R^{\vee\vee}]}. \end{aligned}$$
(F.14)

This expression can be simplified by summing over  $A_L^\vee$  and  $A_R^\vee$ . Doing so, we obtain

$$\mathcal{Z}^{\vee\vee}[A_L^{\vee\vee}, A_R^{\vee\vee}] = \frac{1}{|\mathbf{G}|} \sum_{A_L, A_R} \mathcal{Z}[A_L, A_R] (-1)^{f_\Sigma[A_R \cup A_L^{\vee\vee} - A_R \cup A_L - A_L \cup A_R^{\vee\vee}]}.$$
(F.15)

Finally acting with the  $k_1 k_3$  duality a third time gives

$$\begin{aligned} \mathcal{Z}^{\vee\vee\vee}[A_L^{\vee\vee\vee}, A_R^{\vee\vee\vee}] &= \frac{1}{|\mathbf{G}|^2} \sum_{A_L, R, A_{L,R}^\vee} \mathcal{Z}[A_L, A_R] \\ &\times (-1)^{f_\Sigma[A_R \cup A_L^{\vee\vee} - A_R \cup A_L - A_L \cup A_R^{\vee\vee} + A_L^{\vee\vee} \cup A_R^{\vee\vee\vee} + A_R^{\vee\vee} \cup A_L^{\vee\vee\vee} + A_L^{\vee\vee\vee} \cup A_R^{\vee\vee\vee}]}. \end{aligned}$$
(F.16)

summing over  $A_L^{\vee\vee}$  and  $A_R^{\vee\vee}$  impose the constraints  $A_R = A_R^{\vee\vee\vee}$  and  $A_L = A_L^{\vee\vee\vee}$  respectively, therefore we get.

$$\begin{aligned} \mathcal{Z}^{\vee\vee\vee}[A_L^{\vee\vee\vee}, A_R^{\vee\vee\vee}] &= \sum_{A_L, A_R} \mathcal{Z}[A_L, A_R] \delta_{A_R, A_R^{\vee\vee\vee}} \delta_{A_L, A_L^{\vee\vee\vee}} (-1)^{f_\Sigma[-A_R \cup A_L + A_L^{\vee\vee\vee} \cup A_R^{\vee\vee\vee}]} \\ &= \mathcal{Z}[A_L^{\vee\vee\vee}, A_R^{\vee\vee\vee}]. \end{aligned}$$
(F.17)

Thus establishing that  $(k_1 k_3)^3 = \text{id}$ .

6.  $k_2(k_1 k_3)^2 k_2^{-1} = (k_1 k_3)^{-2}$ : This equation translates to

$$k_2(k_1 k_3)^2 k_2(k_1 k_3)^2 = \text{id},$$
(F.18)

As a first step, we need to obtain how the twisted partition functions transform under  $k_2(k_1 k_3)^2$ . Using (F.15) and (F.3), following the same steps as above, it can be shown that

$$k_2(k_1 k_3)^2 : \mathcal{Z}[A_L, A_R] \mapsto \mathcal{Z}^\vee[A_L^\vee, A_R^\vee] = \frac{1}{|\mathbf{G}|} \sum_{A_L, A_R} \mathcal{Z}[A_L, A_R] (-1)^{f_\Sigma[A_L \cup A_R^\vee + A_L^\vee \cup A_R]}.$$
(F.19)

Acting with the  $k_2(k_1 k_3)^2$  duality again gives

$$\begin{aligned}\mathcal{Z}^{\vee\vee}[A_L^{\vee\vee}, A_R^{\vee\vee}] &= \frac{1}{|\mathbb{G}|^2} \sum_{A_{L,R}, A_{L,R}^{\vee}} \mathcal{Z}[A_L, A_R] (-1)^{\int_{\Sigma} [A_L \cup A_R^{\vee} + A_L^{\vee} \cup A_R + A_L^{\vee} \cup A_R^{\vee\vee} + A_L^{\vee\vee} \cup A_R^{\vee}]} \\ &= \mathcal{Z}[A_L^{\vee\vee}, A_R^{\vee\vee}].\end{aligned}\tag{F.20}$$

We have thus established that the transformation (F.3), form a representation of  $\mathcal{G}[\mathbb{Z}_2 \times \mathbb{Z}_2]$ .

## G Conformal spectra of various phase transitions

In this appendix, we collect conformal spectra of various critical points for some of the quantum spin chains studied in Section 5.

### G.1 Brief recap of $\mathbb{Z}_N$ parafermion CFT

Let us briefly recap some of the main features of the CFT describing the critical point between ferromagnetic (fully-broken) and paramagnetic (unbroken) phases of  $N$ -state Potts model, i.e. the  $\mathbb{Z}_N$  parafermion CFT [174]. This is a diagonal RCFT described by the coset model  $\mathfrak{su}(2)_N/\mathfrak{u}(1)_{2N}$  with central charge

$$c = \frac{2(N-1)}{N+2}.\tag{G.1}$$

The primary states of the theory are labeled by a pair of integers  $(l, m)$  whose range is as follows:  $l = 0, \dots, N$  labels  $\mathfrak{su}(2)_N$  primary fields and  $-l+2 \leq m \leq l$  labels the primaries of  $\mathfrak{u}(1)_{2N}$ . Furthermore, these integers must satisfy the constraint  $l = m \pmod{2}$ . From this, one can conclude that there are  $N(N+1)/2$  primary fields, which we denote as  $\varphi_{l,m}$ . The conformal dimensions of these fields are given by

$$h_{lm} = \bar{h}_{lm} = \frac{l(l+2)}{4(N+2)} - \frac{m^2}{4N}.\tag{G.2}$$

We also have the following identification of primary fields

$$\varphi_{l,m} = \varphi_{N-l, m-N} = \varphi_{N-l, m+N}.\tag{G.3}$$

The components of modular  $T$ -matrix of the theory are given

$$T_{lm}{}^{l'm'} = e^{2\pi i h_{lm}} \delta_l^{l'} \delta_m^{m'},\tag{G.4}$$

while those of the modular  $S$ -matrix are

$$S_{lm}{}^{l'm'} = \frac{2}{\sqrt{N(N+2)}} \sin \left[ \frac{\pi(l+1)(l'+1)}{N+2} \right] e^{\pi i m m' / N}.\tag{G.5}$$

We are often interested in knowing twisted partition functions for  $\mathbb{Z}_N$  parafermion CFT in various symmetry sectors and with twisted boundary conditions (see (4.15)) in terms

of Virasoro characters. The twisted partition functions in the sector  $(\mathbf{g}, \mathbf{h})$  in terms of Virasoro characters  $\chi_{l,m}(\tau)$  is given by [174]

$$\mathcal{Z}_{\mathbf{g}, \mathbf{h}} = \sum_{l,m} e^{2\pi i \frac{\mathbf{h}(m-\mathbf{g})}{N}} \chi_{l,m} \bar{\chi}_{l,m}. \quad (\text{G.6})$$

The modular group  $\Gamma \simeq \text{PSL}(2, \mathbb{Z})$  is generated by  $T : \tau \mapsto \tau + 1$  and  $S : \tau \mapsto -\frac{1}{\tau}$ . Under a modular transformation

$$\tau \mapsto \frac{a\tau + b}{c\tau + d}, \quad \begin{pmatrix} a & b \\ c & d \end{pmatrix} \in \Gamma, \quad (\text{G.7})$$

partition functions (G.6) transform as

$$\mathcal{Z}(\mathbf{g}, \mathbf{h}) \mapsto \mathcal{Z}(a\mathbf{g} + b\mathbf{h}, c\mathbf{g} + d\mathbf{h}). \quad (\text{G.8})$$

## G.2 Some Results for $\mathbf{G} = \mathbb{Z}_2 \times \mathbb{Z}_2$ transitions

In this section, we collect numerical data showing the agreement between theoretically predicted conformal spectrum and numerical data for several quantum phase transitions realized in  $\mathbb{Z}_2 \times \mathbb{Z}_2$  symmetric quantum spin chains.

### G.2.1 Some basic facts about Ising CFT

To compute the spectra analytically, let us first write down the modular  $T$ - and  $S$ -matrices for Ising CFT. Using (G.4) and (G.5) and ordering the three primary fields of the model as  $\{\varphi_{0,0} \equiv \mathbb{I}, \varphi_{1,1} \equiv \sigma, \varphi_{2,0} \equiv \psi\}$ , whose conformal dimension are  $(h_{lm}, \bar{h}_{lm}) = \{(0,0), (\frac{1}{16}, \frac{1}{16}), (\frac{1}{2}, \frac{1}{2})\}$ , we see that these matrices are given by

$$T^{\text{Ising}} = \begin{pmatrix} 1 & 0 & 0 \\ 0 & e^{\frac{\pi i}{8}} & 0 \\ 0 & 0 & 1 \end{pmatrix}, \quad S^{\text{Ising}} = \frac{1}{2} \begin{pmatrix} 1 & \sqrt{2} & 1 \\ \sqrt{2} & 0 & -\sqrt{2} \\ 1 & -\sqrt{2} & 1 \end{pmatrix}, \quad (\text{G.9})$$

The spectrum of CFT is tabulated in Table 7.

Primary fields	$\mathbb{I}$	$\epsilon$	$\sigma$
$(h, \bar{h})$	$(0, 0)$	$(\frac{1}{2}, \frac{1}{2})$	$(\frac{1}{16}, \frac{1}{16})$

Table 7: Primary fields of the Ising CFT describing the phase transition between ferromagnet and paramagnetic phases of Ising chain.

### G.2.2 Analytical and numerical results

The theoretical predictions are made using a known transition and various duality mappings. The known transition is in the Ising <sup>2</sup> universality class and is realized between the minimal realizations of either the fully symmetric paramagnet ( $\mathcal{L}_6$ ) and the symmetry

Symmetry sector $(\mathbf{g}, \alpha)$	Conformal spectrum
$1 = (0, 0; 0, 0)$	$( \chi_0 ^2 +  \chi_{1/2} ^2)^2$
$m_L = (1, 0; 0, 0)$	$( \chi_{1/16} ^2)^2$
$m_R = (0, 1; 0, 0)$	$( \chi_{1/16} ^2)^2$
$m_L m_R = (1, 1; 0, 0)$	$(\chi_0 \bar{\chi}_{1/2} + \bar{\chi}_0 \chi_{1/2})^2$
$e_L = (0, 0; 1, 0)$	$( \chi_0 ^2 +  \chi_{1/2} ^2)  \chi_{1/16} ^2$
$m_L e_L = (1, 0; 1, 0)$	$(\chi_0 \bar{\chi}_{1/2} + \bar{\chi}_0 \chi_{1/2})  \chi_{1/16} ^2$
$m_R e_L = (0, 1; 1, 0)$	$( \chi_0 ^2 +  \chi_{1/2} ^2)  \chi_{1/16} ^2$
$m_R m_L e_L = (0, 1; 1, 0)$	$(\chi_0 \bar{\chi}_{1/2} + \bar{\chi}_0 \chi_{1/2})  \chi_{1/16} ^2$
$e_R = (0, 0; 0, 1)$	$( \chi_0 ^2 +  \chi_{1/2} ^2)  \chi_{1/16} ^2$
$m_L e_R = (1, 0; 0, 1)$	$( \chi_0 ^2 +  \chi_{1/2} ^2)  \chi_{1/16} ^2$
$m_R e_R = (1, 0; 0, 1)$	$(\chi_0 \bar{\chi}_{1/2} + \bar{\chi}_0 \chi_{1/2})  \chi_{1/16} ^2$
$m_L m_R e_R = (1, 1; 0, 1)$	$(\chi_0 \bar{\chi}_{1/2} + \bar{\chi}_0 \chi_{1/2})  \chi_{1/16} ^2$
$e_L e_R = (0, 0; 1, 1)$	$( \chi_{1/16} ^2)^2$
$m_L e_L e_R = (1, 0; 1, 1)$	$(\chi_0 \bar{\chi}_{1/2} + \bar{\chi}_0 \chi_{1/2}) ( \chi_0 ^2 +  \chi_{1/2} ^2)$
$m_R e_L e_R = (0, 1; 1, 1)$	$(\chi_0 \bar{\chi}_{1/2} + \bar{\chi}_0 \chi_{1/2}) ( \chi_0 ^2 +  \chi_{1/2} ^2)$
$m_L m_R e_L e_R = (1, 1; 1, 1)$	$( \chi_{1/16} ^2)^2$

Table 8: Conformal spectrum for the critical point  $\mathcal{C}_{15}$  realized as the minimal transition between the spontaneous symmetry breaking phase (labelled by  $\mathcal{L}_1$ ) and the symmetry protected topological phase (labelled by  $\mathcal{L}_5$ ).

broken phase ( $\mathcal{L}_1$ ) or between two partial symmetry broken phases ( $\mathcal{L}_2$  and  $\mathcal{L}_3$ ). More precisely in the Hamiltonians  $H_{16}$  and  $H_{23}$  as described in (5.89) which realize the transitions  $\mathcal{C}_{16}$  and  $\mathcal{C}_{23}$ .

1. The transition  $\mathcal{C}_{15}$  between the symmetry broken phase and the the SPT described by the Lagrangian subgroups  $\mathcal{L}_1$  and  $\mathcal{L}_5$  respectively can be obtained from the the transition  $\mathcal{C}_{16}$  using the duality transformation  $k_1$ . The conformal spectrum in the different symmetry eigensectors  $\alpha \in \text{Rep}(\mathbb{Z}_2 \times \mathbb{Z}_2)$  and with different symmetry twisted boundary conditions  $\mathbf{g} \in \mathbb{Z}_2 \times \mathbb{Z}_2$  are given in Table. 8. The comparison between the numerically obtained spectrum and the analytically predicted conformal spectrum can be found in Figure 37.

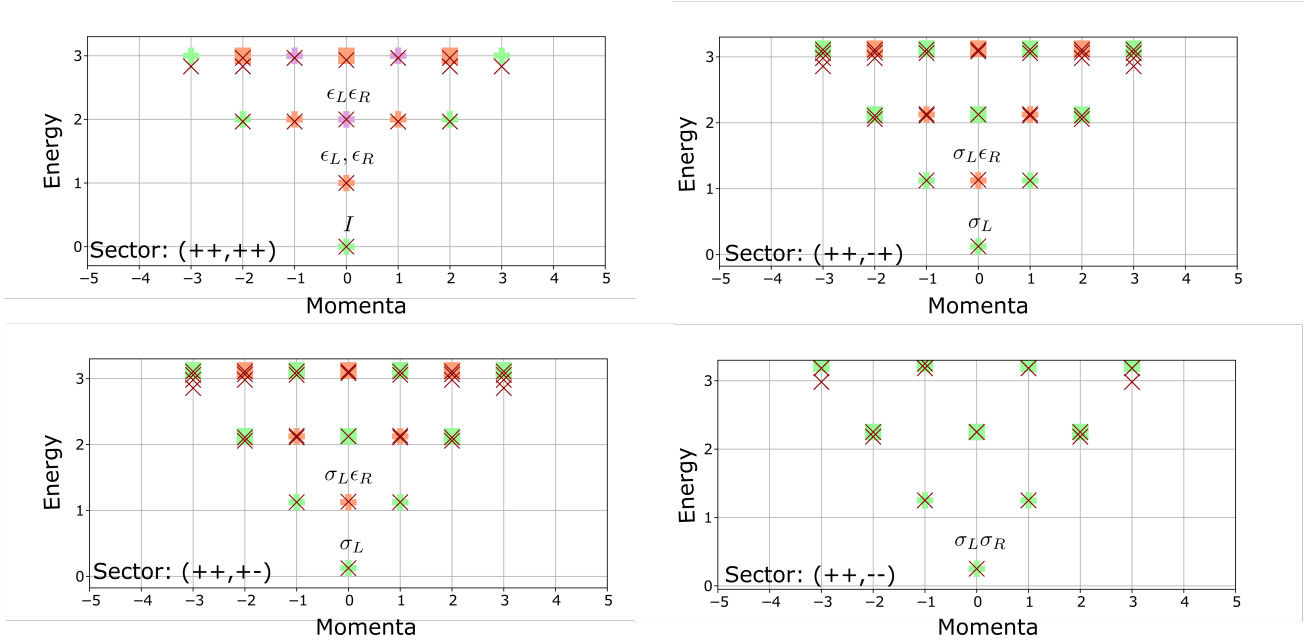


Figure 37: The figure shows a comparison between the analytically computed conformal spectrum of the transition  $\mathcal{C}_{15}$  and the numerically obtained spectrum for the Hamiltonian  $H_{15}$  in (5.89) using exact diagonalization (depicted with crosses). All the numerics have been performed for spin chains of length  $L = 12$ , i.e., spin-chains containing 24  $\mathbb{Z}_2$ -spins. The subplots (a)-(d) correspond to  $\times \mathbb{Z}_2$  eigensectors  $(++)$ ,  $(-+)$ ,  $(+-)$  and  $(--)$  and with periodic boundary conditions.

2. The transition  $\mathcal{C}_{34}$  between the partial symmetry symmetry broken phases labelled by the Lagrangian subgroups  $\mathcal{L}_3$  and  $\mathcal{L}_4$  respectively can be obtained from the the transition  $\mathcal{C}_{23}$  using the duality transformation  $h_2$ . The conformal spectrum in the different symmetry eigensectors  $\alpha \in \text{Rep}(\mathbb{Z}_2 \times \mathbb{Z}_2)$  and with different symmetry twisted boundary conditions  $\mathbf{g} \in \mathbb{Z}_2 \times \mathbb{Z}_2$  are given in Table. 9. The comparison between the numerically obtained spectrum and the analytically predicted conformal spectrum can be found in Figure 38.



Symmetry sector $(\mathbf{g}, \alpha)$	Conformal spectrum
$1 = (0, 0; 0, 0)$	$( \chi_0 ^2 +  \chi_{1/2} ^2)^2$
$m_L = (1, 0; 0, 0)$	$( \chi_{1/16} ^2)^2$
$m_R = (0, 1; 0, 0)$	$( \chi_0 ^2 +  \chi_{1/2} ^2) \chi_{1/16} ^2$
$m_L m_R = (1, 1; 0, 0)$	$( \chi_0 ^2 +  \chi_{1/2} ^2) \chi_{1/16} ^2$
$e_L = (0, 0; 1, 0)$	$( \chi_0 ^2 +  \chi_{1/2} ^2) \chi_{1/16} ^2$
$m_L e_L = (1, 0; 1, 0)$	$(\chi_0 \bar{\chi}_{1/2} + \bar{\chi}_0 \chi_{1/2}) \chi_{1/16} ^2$
$m_R e_L = (0, 1; 1, 0)$	$( \chi_{1/16} ^2)^2$
$m_R m_L e_L = (0, 1; 1, 0)$	$(\chi_0 \bar{\chi}_{1/2} + \bar{\chi}_0 \chi_{1/2})( \chi_0 ^2 +  \chi_{1/2} ^2)$
$e_R = (0, 0; 0, 1)$	$( \chi_{1/16} ^2)^2$
$m_L e_R = (1, 0; 0, 1)$	$(\chi_0 \bar{\chi}_{1/2} + \bar{\chi}_0 \chi_{1/2})^2$
$m_R e_R = (1, 0; 0, 1)$	$(\chi_0 \bar{\chi}_{1/2} + \bar{\chi}_0 \chi_{1/2}) \chi_{1/16} ^2$
$m_L m_R e_R = (1, 1; 0, 1)$	$(\chi_0 \bar{\chi}_{1/2} + \bar{\chi}_0 \chi_{1/2}) \chi_{1/16} ^2$
$e_L e_R = (0, 0; 1, 1)$	$( \chi_0 ^2 +  \chi_{1/2} ^2) \chi_{1/16} ^2$
$m_L e_L e_R = (1, 0; 1, 1)$	$(\chi_0 \bar{\chi}_{1/2} + \bar{\chi}_0 \chi_{1/2}) \chi_{1/16} ^2$
$m_R e_L e_R = (0, 1; 1, 1)$	$(\chi_0 \bar{\chi}_{1/2} + \bar{\chi}_0 \chi_{1/2})( \chi_0 ^2 +  \chi_{1/2} ^2)$
$m_L m_R e_L e_R = (1, 1; 1, 1)$	$( \chi_{1/16} ^2)^2$

Table 9: Conformal spectrum for the critical point  $\mathcal{C}_{34}$  realized as the minimal transition between the two partial symmetry breaking gapped phases labelled by  $\mathcal{L}_3$  and  $\mathcal{L}_4$ .

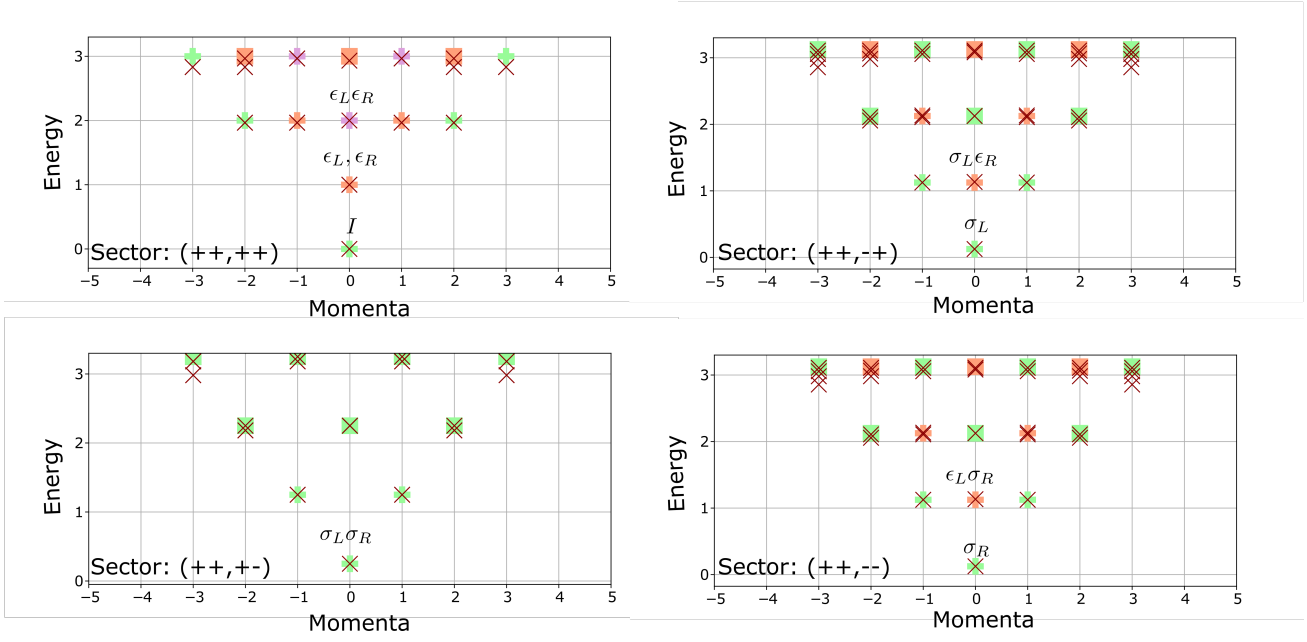


Figure 38: The figure shows a comparison between the analytically computed conformal spectrum of the transition  $\mathcal{C}_{34}$  and the numerically obtained spectrum for the Hamiltonian  $H_{34}$  in (5.89) using exact diagonalization (depicted with crosses). All the numerics have been performed for spin chains of length  $L = 12$ . The subplots (a)-(d) correspond to  $\times \mathbb{Z}_2$  eigensectors  $(++)$ ,  $(-+)$ ,  $(+-)$  and  $(--)$  and with periodic boundary conditions.

3. The transition  $\mathcal{C}_{24}$  between the partial symmetry symmetry broken phases labelled by the Lagrangian subgroups  $\mathcal{L}_2$  and  $\mathcal{L}_4$  respectively can be obtained from the transition  $\mathcal{C}_{23}$  using the duality transformation  $h_1$ . The conformal spectrum in the different symmetry eigensectors  $\alpha \in \text{Rep}(\mathbb{Z}_2 \times \mathbb{Z}_2)$  and with different symmetry twisted boundary conditions  $\mathbf{g} \in \mathbb{Z}_2 \times \mathbb{Z}_2$  are given in Table. 10. The comparison between the numerically obtained spectrum and the analytically predicted conformal spectrum can be found in Figure 39.

Symmetry sector $(\mathbf{g}, \alpha)$	Conformal spectrum
$1 = (0, 0; 0, 0)$	$( \chi_0 ^2 +  \chi_{1/2} ^2)^2$
$m_L = (1, 0; 0, 0)$	$( \chi_0 ^2 +  \chi_{1/2} ^2) \chi_{1/16} ^2$
$m_R = (0, 1; 0, 0)$	$( \chi_{1/16} ^2)^2$
$m_L m_R = (1, 1; 0, 0)$	$( \chi_0 ^2 +  \chi_{1/2} ^2) \chi_{1/16} ^2$
$e_L = (0, 0; 1, 0)$	$( \chi_{1/16} ^2)^2$
$m_L e_L = (1, 0; 1, 0)$	$(\chi_0 \bar{\chi}_{1/2} + \bar{\chi}_0 \chi_{1/2}) \chi_{1/16} ^2$
$m_R e_L = (0, 1; 1, 0)$	$(\chi_0 \bar{\chi}_{1/2} + \bar{\chi}_0 \chi_{1/2})^2$
$m_R m_L e_L = (0, 1; 1, 0)$	$(\chi_0 \bar{\chi}_{1/2} + \bar{\chi}_0 \chi_{1/2}) \chi_{1/16} ^2$
$e_R = (0, 0; 0, 1)$	$( \chi_0 ^2 +  \chi_{1/2} ^2) \chi_{1/16} ^2$
$m_L e_R = (1, 0; 0, 1)$	$( \chi_{1/16} ^2)^2$
$m_R e_R = (1, 0; 0, 1)$	$(\chi_0 \bar{\chi}_{1/2} + \bar{\chi}_0 \chi_{1/2}) \chi_{1/16} ^2$
$m_L m_R e_R = (1, 1; 0, 1)$	$(\chi_0 \bar{\chi}_{1/2} + \bar{\chi}_0 \chi_{1/2})( \chi_0 ^2 +  \chi_{1/2} ^2)$
$e_L e_R = (0, 0; 1, 1)$	$( \chi_0 ^2 +  \chi_{1/2} ^2) \chi_{1/16} ^2$
$m_L e_L e_R = (1, 0; 1, 1)$	$(\chi_0 \bar{\chi}_{1/2} + \bar{\chi}_0 \chi_{1/2})( \chi_0 ^2 +  \chi_{1/2} ^2)$
$m_R e_L e_R = (0, 1; 1, 1)$	$(\chi_0 \bar{\chi}_{1/2} + \bar{\chi}_0 \chi_{1/2}) \chi_{1/16} ^2$
$m_L m_R e_L e_R = (1, 1; 1, 1)$	$( \chi_{1/16} ^2)^2$

Table 10: Conformal spectrum for the critical point  $\mathcal{C}_{24}$  realized as the minimal transition between the two partial symmetry breaking gapped phases labelled by  $\mathcal{L}_2$  and  $\mathcal{L}_4$ .

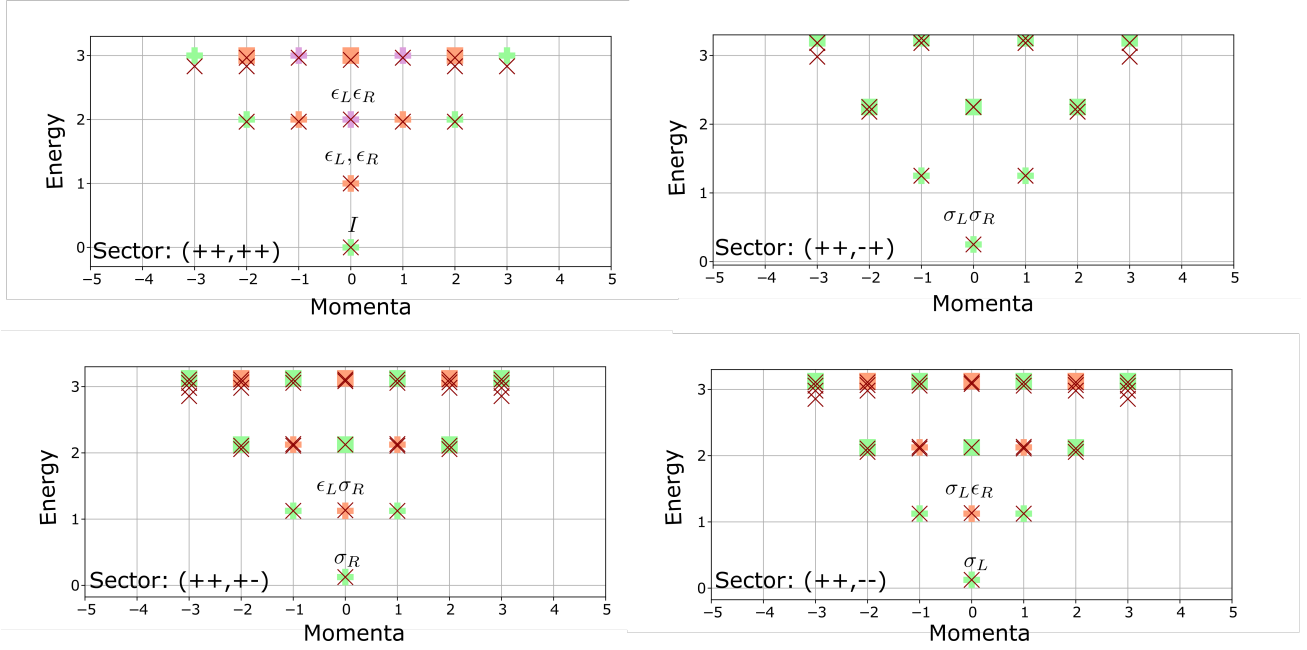


Figure 39: The figure shows a comparison between the analytically computed conformal spectrum of the transition  $\mathcal{C}_{24}$  and the numerically obtained spectrum for the Hamiltonian  $H_{24}$  in (5.89) using exact diagonalization (depicted with crosses). All the numerics have been performed for spin chains of length  $L = 12$ , i.e., spin-chains containing 24  $\mathbb{Z}_2$ -spins. The subplots (a)-(d) correspond to  $\times \mathbb{Z}_2$  eigensectors  $(++)$ ,  $(-+)$ ,  $(+-)$  and  $(--)$  and with periodic boundary conditions.

Using (4.19), we can compute the CFT partition functions in various twisted sectors. First consider the criticality  $\mathcal{C}_{15}$  (the phase transition between fully symmetry-broken phase  $\mathcal{L}_1$  and  $\text{SPT}_1$  phase  $\mathcal{L}_5$ ). We have

$$\begin{aligned}
\mathcal{Z}_{(1,0),(0,1)}(\mathcal{C}_{15}) &= |\chi_{\frac{1}{16}}|^4 - |\chi_0|^2 |\chi_{\frac{1}{16}}|^2 - |\chi_{\frac{1}{2}}|^2 |\chi_{\frac{1}{16}}|^2 \\
&\quad + \left( |\chi_0|^2 + |\chi_{\frac{1}{16}}|^2 - |\chi_{\frac{1}{2}}|^2 \right) \chi_0 \bar{\chi}_{\frac{1}{2}} + \left( |\chi_0|^2 + |\chi_{\frac{1}{16}}|^2 - |\chi_{\frac{1}{2}}|^2 \right) \bar{\chi}_0 \chi_{\frac{1}{2}}, \\
\mathcal{Z}_{(0,1),(0,1)}(\mathcal{C}_{15}) &= |\chi_{\frac{1}{16}}|^4 + |\chi_0|^2 |\chi_{\frac{1}{16}}|^2 + |\chi_{\frac{1}{2}}|^2 |\chi_{\frac{1}{16}}|^2 \\
&\quad + \left( |\chi_0|^2 - |\chi_{\frac{1}{16}}|^2 - |\chi_{\frac{1}{2}}|^2 \right) \chi_0 \bar{\chi}_{\frac{1}{2}} + \left( |\chi_0|^2 - |\chi_{\frac{1}{16}}|^2 - |\chi_{\frac{1}{2}}|^2 \right) \bar{\chi}_0 \chi_{\frac{1}{2}}, \\
\mathcal{Z}_{(1,1),(1,0)}(\mathcal{C}_{15}) &= 2|\chi_0|^2 |\chi_{\frac{1}{2}}|^2 + \bar{\chi}_0^2 \chi_{\frac{1}{2}}^2 + \chi_0^2 \bar{\chi}_{\frac{1}{2}}^2 - |\chi_{\frac{1}{16}}|^4. \\
\mathcal{Z}_{(1,1),(1,0)}(\mathcal{C}_{15}) &= |\chi_{\frac{1}{16}}|^4 - 2|\chi_{\frac{1}{16}}|^2 \left( \bar{\chi}_0 \chi_{\frac{1}{2}} + \chi_0 \bar{\chi}_{\frac{1}{2}} \right) + \chi_0^2 \bar{\chi}_{\frac{1}{2}}^2 + 2|\chi_0|^2 |\chi_{\frac{1}{2}}|^2 + \bar{\chi}_0^2 \chi_{\frac{1}{2}}^2
\end{aligned} \tag{G.10}$$

Similarly, for the  $\mathcal{C}_{56}$  criticality between  $\text{SPT}_0$  and  $\text{SPT}_1$ , we have

$$\begin{aligned}
\mathcal{Z}_{(1,0),(0,0)}(\mathcal{C}_{56}) &= 2 \left( |\chi_0|^2 + |\chi_{\frac{1}{2}}|^2 + \chi_0 \bar{\chi}_{\frac{1}{2}} + \bar{\chi}_0 \chi_{\frac{1}{2}} \right) |\chi_{\frac{1}{16}}|^2, \\
\mathcal{Z}_{(1,0),(1,0)}(\mathcal{C}_{56}) &= 2|\chi_0|^2 |\chi_{\frac{1}{16}}|^2 - 2\chi_0 \bar{\chi}_{\frac{1}{2}} |\chi_{\frac{1}{16}}|^2 - 2\bar{\chi}_0 \chi_{\frac{1}{2}} |\chi_{\frac{1}{16}}|^2 + 2|\chi_{\frac{1}{2}}|^2 |\chi_{\frac{1}{16}}|^2, \\
\mathcal{Z}_{(0,0),(1,0)}(\mathcal{C}_{56}) &= |\chi_0|^4 - \chi_0^2 \bar{\chi}_{\frac{1}{2}}^2 - \bar{\chi}_0^2 \chi_{\frac{1}{2}}^2 + |\chi_{\frac{1}{2}}|^2, \\
\mathcal{Z}_{(1,1),(1,1)}(\mathcal{C}_{56}) &= 2|\chi_{\frac{1}{16}}|^4 - 2|\chi_0|^2 \left( \chi_0 \bar{\chi}_{\frac{1}{2}} + \bar{\chi}_0 \chi_{\frac{1}{2}} \right) - 2|\chi_{\frac{1}{2}}|^2 \left( \chi_0 \bar{\chi}_{\frac{1}{2}} + \bar{\chi}_0 \chi_{\frac{1}{2}} \right)
\end{aligned}$$

### G.3 Some results for $G = \mathbb{Z}_3 \times \mathbb{Z}_3$ transitions

The primary states of the  $\mathbb{Z}_3$  parafermion CFT are tabulated in Table 11.

Primary fields	$\mathbb{I}$	$\psi\bar{\psi}$	$\psi^\dagger\bar{\psi}^\dagger$	$E = \epsilon\bar{\epsilon}$	$S = \sigma\bar{\sigma}$	$S^\dagger = \sigma^\dagger\bar{\sigma}^\dagger$
$(h, \bar{h})$	$(0, 0)$	$(\frac{2}{3}, \frac{2}{3})$	$(\frac{2}{3}, \frac{2}{3})$	$(\frac{2}{5}, \frac{2}{5})$	$(\frac{1}{15}, \frac{1}{15})$	$(\frac{1}{15}, \frac{1}{15})$

Table 11: Primary fields of the  $\mathbb{Z}_3$  parafermion CFT describing the phase transition between ferromagnet and paramagnetic phases of 3-state Potts model

The modular  $T$ - and  $S$ -matrices are given by

$$T^{\mathbb{Z}_3} = \begin{pmatrix} 1 & 0 & 0 & 0 & 0 & 0 \\ 0 & e^{\frac{-2\pi i}{3}} & 0 & 0 & 0 & 0 \\ 0 & 0 & e^{\frac{-2\pi i}{3}} & 0 & 0 & 0 \\ 0 & 0 & 0 & e^{\frac{4\pi i}{5}} & 0 & 0 \\ 0 & 0 & 0 & 0 & e^{\frac{2\pi i}{15}} & 0 \\ 0 & 0 & 0 & 0 & 0 & e^{\frac{2\pi i}{15}} \end{pmatrix}, \quad (\text{G.11})$$

and  $(\phi = \frac{1+\sqrt{5}}{2}$  and  $\omega = \exp(\frac{2\pi i}{3}))$

$$S^{\mathbb{Z}_3} = \frac{1}{\sqrt{6+2\phi}} \begin{pmatrix} 1 & 1 & 1 & \phi & \phi & \phi \\ 1 & \omega^2 & \omega & \phi & \omega^2\phi & \omega\phi \\ 1 & \omega & \omega^2 & \phi & \omega\phi & \omega^2\phi \\ \phi & \phi & \phi & -1 & -1 & -1 \\ \phi & \omega^2\phi & \omega\phi & -1 & -\omega^2 & -\omega \\ \phi & \omega\phi & \omega^2\phi & -1 & -\omega & -\omega^2 \end{pmatrix} \quad (\text{G.12})$$

A typical twisted partition functions for the  $\text{SPT}_0$  and  $\text{SPT}_1$  phases is

$$\begin{aligned} \mathcal{Z}_{(0,1),(0,0)}(\mathcal{C}_{67}) = & +|\chi_{\frac{1}{15}}|^4 + |\chi_{\frac{2}{3}}|^4 + \chi_0^2\bar{\chi}_{\frac{2}{3}}^2 + \bar{\chi}_0^2\chi_{\frac{2}{3}}^2 + \chi_{\frac{2}{5}}^2\bar{\chi}_{\frac{1}{15}}^2 + \bar{\chi}_{\frac{2}{5}}^2\chi_{\frac{1}{15}}^2 \\ & + 2\left(\chi_0\bar{\chi}_{\frac{2}{3}} + \bar{\chi}_0\chi_{\frac{2}{3}} + |\chi_{\frac{2}{3}}|^2 + |\chi_{\frac{2}{5}}|^2 + \chi_{\frac{2}{5}}\bar{\chi}_{\frac{1}{15}} + \bar{\chi}_{\frac{2}{5}}\chi_{\frac{1}{15}}\right)|\chi_{\frac{1}{15}}|^2 \\ & + 2\left(\chi_0\bar{\chi}_{\frac{2}{3}} + \bar{\chi}_0\chi_{\frac{2}{3}} + \chi_{\frac{1}{15}}\bar{\chi}_{\frac{2}{5}} + \bar{\chi}_{\frac{1}{15}}\chi_{\frac{2}{5}} + |\chi_{\frac{2}{5}}|^2\right)|\chi_{\frac{2}{3}}|^2 \\ & + 2\left(|\chi_{\frac{1}{15}}|^2 + |\chi_{\frac{2}{3}}|^2\right)|\chi_0|^2 + 2\chi_0\bar{\chi}_{\frac{2}{3}}\chi_{\frac{2}{5}}\bar{\chi}_{\frac{1}{15}} + 2\bar{\chi}_0\chi_{\frac{2}{3}}\bar{\chi}_{\frac{2}{5}}\chi_{\frac{1}{15}}. \end{aligned} \quad (\text{G.13})$$

Here, we have demonstrated the method for few simple example. Similarly, one can obtain the twisted partition functions in any sector for any finite Abelian group of the form (2.8) using (4.24).

## References

- [1] L. D. Landau, *On the Theory of Phase Transitions. I.*, *Phys. Z. Sowjet.* **11** (1937) 26.
- [2] V. L. Ginzburg and L. D. Landau, *On the Theory of Superconductivity*, pp. 113–137. Springer Berlin Heidelberg, Berlin, Heidelberg, 2009. 10.1007/978-3-540-68008-6.
- [3] L. Landau and E. M. Lifschitz, *Statistical Physics*, 1958.
- [4] S. Sachdev, *Quantum Phase Transitions*. Cambridge University Press, 2 ed., 2011, 10.1017/CBO9780511973765.
- [5] B. Zeng and X.-G. Wen, *Gapped Quantum Liquids and Topological Order, Stochastic Local Transformations and Emergence of Unitarity*, *Phys. Rev. B* **91** (2015) 125121 [[1406.5090](#)].
- [6] D. C. Tsui, H. L. Stormer and A. C. Gossard, *Two-dimensional magnetotransport in the extreme quantum limit*, *Phys. Rev. Lett.* **48** (1982) 1559.
- [7] R. B. Laughlin, *Anomalous quantum hall effect: An incompressible quantum fluid with fractionally charged excitations*, *Phys. Rev. Lett.* **50** (1983) 1395.
- [8] V. Kalmeyer and R. B. Laughlin, *Equivalence of the resonating-valence-bond and fractional quantum hall states*, *Phys. Rev. Lett.* **59** (1987) 2095.
- [9] A. Kitaev and J. Preskill, *Topological entanglement entropy*, *Phys. Rev. Lett.* **96** (2006) 110404.
- [10] M. Levin and X.-G. Wen, *Detecting topological order in a ground state wave function*, *Phys. Rev. Lett.* **96** (2006) 110405.
- [11] S. Dong, E. Fradkin, R. G. Leigh and S. Nowling, *Topological entanglement entropy in chern-simons theories and quantum hall fluids*, *J. High Energy Phys.* **2008** (2008) 016.
- [12] X. Wen, H. He, A. Tiwari, Y. Zheng and P. Ye, *Entanglement entropy for (3+1)-dimensional topological order with excitations*, *Phys. Rev. B* **97** (2018) 085147.
- [13] X. G. Wen and A. Zee, *Classification of abelian quantum hall states and matrix formulation of topological fluids*, *Phys. Rev. B* **46** (1992) 2290.
- [14] M. A. Levin and X.-G. Wen, *String-net condensation: A physical mechanism for topological phases*, *Phys. Rev. B* **71** (2005) 045110.
- [15] A. Tiwari, X. Chen and S. Ryu, *Wilson operator algebras and ground states of coupled BF theories*, *Phys. Rev. B* **95** (2017) 245124.
- [16] P. Putrov, J. Wang and S.-T. Yau, *Braiding Statistics and Link Invariants of Bosonic/Fermionic Topological Quantum Matter in 2+1 and 3+1 dimensions*, *Annals Phys.* **384** (2017) 254 [[1612.09298](#)].
- [17] X. G. Wen, *Topological Order in Rigid States*, *Int. J. Mod. Phys. B* **4** (1990) 239.
- [18] X. G. Wen, *Vacuum Degeneracy of Chiral Spin States in Compactified Space*, *Phys. Rev. B* **40** (1989) 7387.

- [19] X. G. Wen and A. Zee, *Topological degeneracy of quantum Hall fluids*, *Phys. Rev. B* **58** (1998) 15717 [[cond-mat/9711223](#)].
- [20] E. Keski-Vakkuri and X.-G. Wen, *The Ground state structure and modular transformations of fractional quantum Hall states on a torus*, *Int. J. Mod. Phys. B* **7** (1993) 4227 [[hep-th/9303155](#)].
- [21] Y. Zhang, T. Grover, A. Turner, M. Oshikawa and A. Vishwanath, *Quasiparticle statistics and braiding from ground-state entanglement*, *Physical Review B* **85** (2012) 235151 [[1111.2342](#)].
- [22] H. Moradi and X.-G. Wen, *Universal Wave-Function Overlap and Universal Topological Data from Generic Gapped Ground States*, *Phys. Rev. Lett.* **115** (2015) 036802 [[1401.0518](#)].
- [23] H. He, H. Moradi and X.-G. Wen, *Modular matrices as topological order parameter by a gauge-symmetry-preserved tensor renormalization approach*, *Phys. Rev. B* **90** (2014) 205114.
- [24] F. J. Wegner, *Duality in Generalized Ising Models and Phase Transitions Without Local Order Parameters*, *J. Math. Phys.* **12** (1971) 2259.
- [25] E. Fradkin and S. H. Shenker, *Phase diagrams of lattice gauge theories with higgs fields*, *Phys. Rev. D* **19** (1979) 3682.
- [26] J. B. Kogut, *An introduction to lattice gauge theory and spin systems*, *Rev. Mod. Phys.* **51** (1979) 659.
- [27] A. Y. Kitaev, *Fault Tolerant Quantum Computation by Anyons*, *Annals Phys.* **303** (2003) 2 [[quant-ph/9707021](#)].
- [28] N. Read and S. Sachdev, *Large-n expansion for frustrated quantum antiferromagnets*, *Phys. Rev. Lett.* **66** (1991) 1773.
- [29] X. G. Wen, *Mean-field theory of spin-liquid states with finite energy gap and topological orders*, *Phys. Rev. B* **44** (1991) 2664.
- [30] S. Sachdev, *Kagome'- and triangular-lattice heisenberg antiferromagnets: Ordering from quantum fluctuations and quantum-disordered ground states with unconfined bosonic spinons*, *Phys. Rev. B* **45** (1992) 12377.
- [31] L. Savary and L. Balents, *Quantum spin liquids: a review*, *Reports on Progress in Physics* **80** (2016) 016502.
- [32] P. W. Anderson, *The resonating valence bond state in  $la_2cuo_4$  and superconductivity*, *Science* **235** (1987) 1196.
- [33] S. A. Kivelson, D. S. Rokhsar and J. P. Sethna, *Topology of the resonating valence-bond state: Solitons and high- $T_c$  superconductivity*, *Phys. Rev. B* **35** (1987) 8865.
- [34] G. Baskaran and P. W. Anderson, *Gauge theory of high-temperature superconductors and strongly correlated Fermi systems*, *Phys. Rev. B* **37** (1988) 580.
- [35] D. S. Rokhsar and S. A. Kivelson, *Superconductivity and the quantum hard-core dimer gas*, *Phys. Rev. Lett.* **61** (1988) 2376.

- [36] N. Read and B. Chakraborty, *Statistics of the excitations of the resonating-valence-bond state*, *Phys. Rev. B* **40** (1989) 7133.
- [37] T. Senthil and M. P. A. Fisher,  *$Z_2$  gauge theory of electron fractionalization in strongly correlated systems*, *Phys. Rev. B* **62** (2000) 7850.
- [38] R. Dijkgraaf and E. Witten, *Topological Gauge Theories and Group Cohomology*, *Commun. Math. Phys.* **129** (1990) 393.
- [39] M. D. F. de Wild Propitius, *Topological interactions in broken gauge theories*, Ph.D. thesis, Amsterdam U., 1995. [hep-th/9511195](#).
- [40] Y. Hu, Y. Wan and Y.-S. Wu, *Twisted quantum double model of topological phases in two dimensions*, *Phys. Rev. B* **87** (2013) 125114.
- [41] C.-K. Chiu, J. C. Y. Teo, A. P. Schnyder and S. Ryu, *Classification of topological quantum matter with symmetries*, *Rev. Mod. Phys.* **88** (2016) 035005.
- [42] X. Chen, Z.-C. Gu, Z.-X. Liu and X.-G. Wen, *Symmetry-Protected Topological Orders and the Group Cohomology of their Symmetry Group*, *Phys. Rev. B* **87** (2013) 155114.
- [43] S. Ryu, J. E. Moore and A. W. W. Ludwig, *Electromagnetic and gravitational responses and anomalies in topological insulators and superconductors*, *Phys. Rev. B* **85** (2012) 045104.
- [44] M. Levin and Z.-C. Gu, *Braiding statistics approach to symmetry-protected topological phases*, *Phys. Rev. B* **86** (2012) 115109.
- [45] O. M. Sule, X. Chen and S. Ryu, *Symmetry-protected topological phases and orbifolds: Generalized Laughlin's argument*, *Phys. Rev. B* **88** (2013) 075125.
- [46] C.-T. Hsieh, G. Y. Cho and S. Ryu, *Global anomalies on the surface of fermionic symmetry-protected topological phases in (3+1) dimensions*, *Phys. Rev. B* **93** (2016) 075135.
- [47] B. Han, A. Tiwari, C.-T. Hsieh and S. Ryu, *Boundary conformal field theory and symmetry-protected topological phases in 2 + 1 dimensions*, *Phys. Rev. B* **96** (2017) 125105.
- [48] A. Tiwari, X. Chen, K. Shiozaki and S. Ryu, *Bosonic topological phases of matter: Bulk-boundary correspondence, symmetry protected topological invariants, and gauging*, *Phys. Rev. B* **97** (2018) 245133.
- [49] E. Witten, *Fermion path integrals and topological phases*, *Rev. Mod. Phys.* **88** (2016) 035001.
- [50] C. L. Kane and E. J. Mele, *Quantum spin hall effect in graphene*, *Phys. Rev. Lett.* **95** (2005) 226801.
- [51] C. L. Kane and E. J. Mele,  *$Z_2$  topological order and the quantum spin hall effect*, *Phys. Rev. Lett.* **95** (2005) 146802.
- [52] B. A. Bernevig, T. L. Hughes and S.-C. Zhang, *Quantum spin hall effect and topological phase transition in HgTe quantum wells*, *Science* **314** (2006) 1757.
- [53] L. Fu and C. L. Kane, *Topological insulators with inversion symmetry*, *Phys. Rev. B* **76** (2007) 045302.



- [54] A. Kitaev, *Periodic table for topological insulators and superconductors*, *AIP Conf. Proc.* **1134** (2009) 22.
- [55] A. P. Schnyder, S. Ryu, A. Furusaki and A. W. W. Ludwig, *Classification of topological insulators and superconductors in three spatial dimensions*, *Phys. Rev. B* **78** (2008) 195125.
- [56] S. Ryu, A. P. Schnyder, A. Furusaki and A. W. W. Ludwig, *Topological insulators and superconductors: tenfold way and dimensional hierarchy*, *New Journal of Physics* **12** (2010) 065010.
- [57] L. Fidkowski and A. Kitaev, *Topological Phases of Fermions in One-Dimension*, *Phys. Rev. B* **83** (2011) 075103.
- [58] L. Fidkowski and A. Kitaev, *Effects of interactions on the topological classification of free fermion systems*, *Phys. Rev. B* **81** (2010) 134509.
- [59] C. Wang and T. Senthil, *Interacting fermionic topological insulators/superconductors in three dimensions*, *Phys. Rev. B* **89** (2014) 195124.
- [60] T. Morimoto, A. Furusaki and C. Mudry, *Breakdown of the topological classification  $\mathbb{Z}$  for gapped phases of noninteracting fermions by quartic interactions*, *Phys. Rev. B* **92** (2015) 125104.
- [61] Z.-C. Gu and X.-G. Wen, *Symmetry-protected topological orders for interacting fermions: Fermionic topological nonlinear  $\sigma$  models and a special group supercohomology theory*, *Phys. Rev. B* **90** (2014) 115141.
- [62] L. Bhardwaj, D. Gaiotto and A. Kapustin, *State sum constructions of spin-tfts and string net constructions of fermionic phases of matter*, *JHEP* **2017** (2017) 96.
- [63] A. Kapustin, *Symmetry Protected Topological Phases, Anomalies, and Cobordisms: Beyond Group Cohomology*, **1403.1467**.
- [64] A. Kapustin, R. Thorngren, A. Turzillo and Z. Wang, *Fermionic Symmetry Protected Topological Phases and Cobordisms*, *JHEP* **12** (2015) 052.
- [65] F. Pollmann, E. Berg, A. M. Turner and M. Oshikawa, *Symmetry protection of topological phases in one-dimensional quantum spin systems*, *Phys. Rev. B* **85** (2012) 075125 [0909.4059].
- [66] X. Chen, Z.-C. Gu, Z.-X. Liu and X.-G. Wen, *Symmetry-protected topological orders in interacting bosonic systems*, *Science* **338** (2012) 1604.
- [67] X. Chen, Z. C. Gu and X. G. Wen, *Local Unitary Transformation, Long-Range Quantum Entanglement, Wave Function Renormalization, and Topological Order*, *Phys. Rev. B* **82** (2010) 155138 [1004.3835].
- [68] J. Slingerland and F. Bais, *Quantum groups and non-abelian braiding in quantum hall systems*, *Nuclear Physics B* **612** (2001) 229.
- [69] F. Bais and J. Slingerland, *Condensate-induced transitions between topologically ordered phases*, *Physical Review B* **79** (2009) 045316.
- [70] L. Tsui, H.-C. Jiang, Y.-M. Lu and D.-H. Lee, *Quantum phase transitions between a class of symmetry protected topological states*, *Nuclear Physics B* **896** (2015) 330 .

- [71] X. Chen, F. Wang, Y.-M. Lu and D.-H. Lee, *Critical Theories of Phase Transition Between Symmetry Protected Topological States and their Relation to the Gapless Boundary Theories*, *Nucl. Phys.* **B873** (2013) 248 [[1302.3121](#)].
- [72] T. Senthil, A. Vishwanath, L. Balents, S. Sachdev and M. P. A. Fisher, *Deconfined quantum critical points*, *Science* **303** (2004) 1490.
- [73] T. Senthil, L. Balents, S. Sachdev, A. Vishwanath and M. P. A. Fisher, *Quantum criticality beyond the landau-ginzburg-wilson paradigm*, *Phys. Rev. B* **70** (2004) 144407.
- [74] M. Levin and T. Senthil, *Deconfined quantum criticality and néel order via dimer disorder*, *Phys. Rev. B* **70** (2004) 220403.
- [75] E. Lieb, T. Schultz and D. Mattis, *Two soluble models of an antiferromagnetic chain*, *Annals of Physics* **16** (1961) 407.
- [76] M. Oshikawa, *Commensurability, excitation gap, and topology in quantum many-particle systems on a periodic lattice*, *Phys. Rev. Lett.* **84** (2000) 1535.
- [77] M. B. Hastings, *Lieb-schultz-mattis in higher dimensions*, *Phys. Rev. B* **69** (2004) 104431.
- [78] G. Y. Cho, C.-T. Hsieh and S. Ryu, *Anomaly manifestation of lieb-schultz-mattis theorem and topological phases*, *Phys. Rev. B* **96** (2017) 195105.
- [79] H. Watanabe, H. C. Po, A. Vishwanath and M. Zaletel, *Filling constraints for spin-orbit coupled insulators in symmorphic and nonsymmorphic crystals*, *PNAS* **112** (2015) 14551.
- [80] O. M. Aksoy, A. Tiwari and C. Mudry, *Lieb-Schultz-Mattis type theorems for Majorana models with discrete symmetries*, *Phys. Rev. B* **104** (2021) 075146 [[2102.08389](#)].
- [81] D. Gaiotto, A. Kapustin, N. Seiberg and B. Willett, *Generalized Global Symmetries*, *JHEP* **02** (2015) 172 [[1412.5148](#)].
- [82] A. Kapustin and R. Thorngren, *Higher symmetry and gapped phases of gauge theories*, [1309.4721](#).
- [83] R. Thorngren and Y. Wang, *Fusion Category Symmetry I: Anomaly In-Flow and Gapped Phases*, [1912.02817](#).
- [84] C. Córdova, T. T. Dumitrescu and K. Intriligator, *Exploring 2-group global symmetries*, *JHEP* **2019** (2019) 184 [[1802.04790](#)].
- [85] F. Benini, C. Córdova and P.-S. Hsin, *On 2-group global symmetries and their anomalies*, *JHEP* **2019** (2019) 118 [[1803.09336](#)].
- [86] C. Delcamp and A. Tiwari, *From gauge to higher gauge models of topological phases*, *JHEP* **10** (2018) 049 [[1802.10104](#)].
- [87] C. Delcamp and A. Tiwari, *On 2-form gauge models of topological phases*, *JHEP* **05** (2019) 064 [[1901.02249](#)].
- [88] V. B. Petkova and J. B. Zuber, *Generalised twisted partition functions*, *Phys. Lett. B* **504** (2001) 157 [[hep-th/0011021](#)].

- [89] J. Fuchs, I. Runkel and C. Schweigert, *TFT construction of RCFT correlators 1. Partition functions*, *Nucl. Phys. B* **646** (2002) 353 [[hep-th/0204148](#)].
- [90] J. Fuchs, M. R. Gaberdiel, I. Runkel and C. Schweigert, *Topological defects for the free boson CFT*, *J. Phys. A* **40** (2007) 11403 [[0705.3129](#)].
- [91] L. Bhardwaj and Y. Tachikawa, *On Finite Symmetries and their Gauging in two Dimensions*, *JHEP* **03** (2018) 189 [[1704.02330](#)].
- [92] L. Kong, T. Lan, X.-G. Wen, Z.-H. Zhang and H. Zheng, *Algebraic higher symmetry and categorical symmetry: A holographic and entanglement view of symmetry*, *Phys. Rev. Research* **2** (2020) 043086.
- [93] C.-M. Chang, Y.-H. Lin, S.-H. Shao, Y. Wang and X. Yin, *Topological Defect Lines and Renormalization Group Flows in Two Dimensions*, *JHEP* **01** (2019) 026 [[1802.04445](#)].
- [94] T. Lichtman, R. Thorngren, N. H. Lindner, A. Stern and E. Berg, *Bulk anyons as edge symmetries: Boundary phase diagrams of topologically ordered states*, *Phys. Rev. B* **104** (2021) 075141.
- [95] J. Kaidi, K. Ohmori and Y. Zheng, *Kramers-Wannier-like Duality Defects in (3+1)D Gauge Theories*, *Phys. Rev. Lett.* **128** (2022) 111601 [[2111.01141](#)].
- [96] Y. Choi, C. Cordova, P.-S. Hsin, H. T. Lam and S.-H. Shao, *Non-Invertible Duality Defects in 3+1 Dimensions*, [2111.01139](#).
- [97] M. J. S. Yang, *Diagonal reflection symmetries, four-zero texture, and trimaximal mixing with predicted  $\theta_{13}$  in an  $A_4$  symmetric model*, *PTEP* **2022** (2022) 013B12 [[2104.12063](#)].
- [98] B. Heidenreich, J. McNamara, M. Montero, M. Reece, T. Rudelius and I. Valenzuela, *Non-invertible global symmetries and completeness of the spectrum*, *JHEP* **09** (2021) 203 [[2104.07036](#)].
- [99] K. Roumpedakis, S. Seifnashri and S.-H. Shao, *Higher Gauging and Non-invertible Condensation Defects*, [2204.02407](#).
- [100] L. Bhardwaj, L. Bottini, S. Schafer-Nameki and A. Tiwari, *Non-Invertible Higher-Categorical Symmetries*, [2204.06564](#).
- [101] Y. Choi, C. Cordova, P.-S. Hsin, H. T. Lam and S.-H. Shao, *Non-invertible Condensation, Duality, and Triality Defects in 3+1 Dimensions*, [2204.09025](#).
- [102] E. Lake, *Higher-Form Symmetries and Spontaneous-Symmetry Breaking*, [1802.07747](#).
- [103] J. McGreevy, *Generalized Symmetries in Condensed Matter*, [2204.03045](#).
- [104] P.-S. Hsin, H. T. Lam and N. Seiberg, *Comments on One-Form Global Symmetries and Their Gauging in 3d and 4d*, *SciPost Phys.* **6** (2019) 39.
- [105] D. S. Freed and C. Teleman, *Topological dualities in the Ising model*, [1806.00008](#).
- [106] D. Gaiotto and J. Kulp, *Orbifold Groupoids*, *J. High Energy Phys* **02** (2021) 132 [[2008.05960](#)].
- [107] F. Apruzzi, F. Bonetti, I. n. G. Etxebarria, S. S. Hosseini and S. Schafer-Nameki, *Symmetry TFTs from String Theory*, [2112.02092](#).

- [108] L. Bhardwaj, Y. Lee and Y. Tachikawa,  *$SL(2, \mathbb{Z})$  action on QFTs with  $\mathbb{Z}_2$  symmetry and the Brown-Kervaire invariants*, *JHEP* **11** (2020) 141 [[2009.10099](#)].
- [109] F. Apruzzi, *Higher Form Symmetries TFT in 6d*, [2203.10063](#).
- [110] D. Freed, *Finite Symmetry in QFT - Lectures at Perimeter Institute*, 2022.
- [111] E. Witten, *AdS / CFT Correspondence and Topological Field Theory*, *JHEP* **12** (1998) 012 [[hep-th/9812012](#)].
- [112] W. Ji and X.-G. Wen, *Categorical symmetry and noninvertible anomaly in symmetry-breaking and topological phase transitions*, *Phys. Rev. Research* **2** (2020) 033417.
- [113] W. Ji, S.-H. Shao and X.-G. Wen, *Topological Transition on the Conformal Manifold*, *Phys. Rev. Res.* **2** (2020) 033317 [[1909.01425](#)].
- [114] A. Chatterjee and X.-G. Wen, *Algebra of local symmetric operators and braided fusion  $n$ -category – symmetry is a shadow of topological order*, [2203.03596](#).
- [115] A. Chatterjee and X.-G. Wen, *Holographic theory for the emergence and the symmetry protection of gaplessness and for continuous phase transitions*, [2205.06244](#).
- [116] L. Lootens, C. Delcamp, G. Ortiz and F. Verstraete, *Dualities in one-dimensional quantum lattice models: symmetric Hamiltonians and matrix product operator intertwiners*, [2112.09091](#).
- [117] D. Aasen, R. S. K. Mong and P. Fendley, *Topological defects on the lattice: I. the ising model*, *Journ. Phys. A: Math and Theor* **49** (2016) 354001.
- [118] D. Aasen, P. Fendley and R. S. K. Mong, *Topological Defects on the Lattice: Dualities and Degeneracies*, [2008.08598](#).
- [119] R. Verresen, R. Thorngren, N. G. Jones and F. Pollmann, *Gapless Topological Phases and Symmetry-Enriched Quantum Criticality*, *Phys. Rev. X* **11** (2021) 041059 [[1905.06969](#)].
- [120] W. W. Ho, L. Cincio, H. Moradi, D. Gaiotto and G. Vidal, *Edge-entanglement spectrum correspondence in a nonchiral topological phase and Kramers-Wannier duality*, *Phys. Rev. B* **91** (2015) 125119 [[1411.6932](#)].
- [121] H. Moradi and W. W. Ho, “Fermionic gapped edges in bosonic abelian topological states via fermion condensation.” 2014.
- [122] H. Moradi, *Topological Order and Universal Properties of Gapped Quantum Systems*, Ph.D. thesis, Perimeter Institute for Theoretical Physics, 2018.
- [123] P. Gorantla, H. T. Lam, N. Seiberg and S.-H. Shao, *Low-Energy Limit of Some Exotic Lattice Theories and UV/IR Mixing*, *Phys. Rev. B* **104** (2021) 235116 [[2108.00020](#)].
- [124] G. 't Hooft, *Naturalness, Chiral Symmetry, and Spontaneous Chiral Symmetry Breaking*, *NATO Sci. Ser. B* **59** (1980) 135.
- [125] C.-T. Hsieh, G. Y. Cho and S. Ryu, *Global anomalies on the surface of fermionic symmetry-protected topological phases in  $(3+1)$  dimensions*, *Phys. Rev. B* **93** (2016) 075135.

- [126] D. V. Else and R. Thorngren, *Topological theory of lieb-schultz-mattis theorems in quantum spin systems*, *Phys. Rev. B* **101** (2020) 224437.
- [127] H. Kurzweil and B. Stellmacher, *The Theory of Finite Groups: An Introduction*. Springer New York, 2004.
- [128] D. Harlow and H. Ooguri, *Constraints on Symmetries from Holography*, *Phys. Rev. Lett.* **122** (2019) 191601 [[1810.05337](#)].
- [129] D. Harlow and H. Ooguri, *Symmetries in Quantum Field Theory and Quantum Gravity*, *Commun. Math. Phys.* **383** (2021) 1669 [[1810.05338](#)].
- [130] E. Witten, *Anti-de Sitter Space and Holography*, *Adv. Theor. Math. Phys.* **2** (1998) 253 [[hep-th/9802150](#)].
- [131] K. Costello and S. Li, *Twisted Supergravity and its Quantization*, [1606.00365](#).
- [132] K. Costello, *M-Theory in the Omega-Background and 5-Dimensional Non-Commutative Gauge Theory*, [1610.04144](#).
- [133] K. Costello, *Holography and Koszul Duality: The Example of the M2-Brane*, [1705.02500](#).
- [134] N. Ishtiaque, S. F. Moosavian and Y. Zhou, *Topological Holography: The Example of the D2-D4 Brane System*, *SciPost Phys.* **9** (2020) 017 [[1809.00372](#)].
- [135] K. Costello and D. Gaiotto, *Twisted Holography*, [1812.09257](#).
- [136] H. Bombin, *Topological order with a twist: Ising anyons from an abelian model*, *Phys. Rev. Lett.* **105** (2010) 030403.
- [137] M. Barkeshli, C.-M. Jian and X.-L. Qi, *Twist defects and projective non-abelian braiding statistics*, *Phys. Rev. B* **87** (2013) 045130.
- [138] M. Barkeshli, C.-M. Jian and X.-L. Qi, *Theory of defects in abelian topological states*, *Phys. Rev. B* **88** (2013) 235103.
- [139] J. C. Teo, T. L. Hughes and E. Fradkin, *Theory of twist liquids: Gauging an anyonic symmetry*, *Annals of Physics* **360** (2015) 349.
- [140] M. Barkeshli, P. Bonderson, M. Cheng and Z. Wang, *Symmetry fractionalization, defects, and gauging of topological phases*, *Phys. Rev. B* **100** (2019) 115147.
- [141] A. Kapustin and N. Saulina, *Topological boundary conditions in abelian Chern-Simons theory*, *Nucl. Phys. B* **845** (2011) 393 [[1008.0654](#)].
- [142] M. Levin, *Protected Edge Modes without Symmetry*, *Phys. Rev. X* **3** (2013) 021009 [[1301.7355](#)].
- [143] M. Barkeshli, C.-M. Jian and X.-L. Qi, *Classification of topological defects in Abelian topological states*, *Phys. Rev. B* **88** (2013) 241103 [[1304.7579](#)].
- [144] J. Kaidi, Z. Komargodski, K. Ohmori, S. Seifnashri and S.-H. Shao, *Higher Central Charges and Topological Boundaries in 2+1-Dimensional TQFTs*, [2107.13091](#).
- [145] V. Ostrik, *Module Categories over the Drinfeld Double of a Finite Group*, *Int. Math. Res. Not* **2003** (2003) 1507 [[arXiv:math/0202130](#)].
- [146] V. Ostrik, *Module categories, weak Hopf algebras and modular invariants*, *arXiv Mathematics e-prints* (2001) math/0111139 [[math/0111139](#)].



- [147] X. Chen, Z.-C. Gu and X.-G. Wen, *Classification of Gapped Symmetric Phases in One-Dimensional Spin Systems*, *Phys. Rev. B* **83** (2011) 035107 [[1008.3745](#)].
- [148] L. Fidkowski and A. Kitaev, *Topological phases of fermions in one dimension*, *Phys. Rev. B* **83** (2011) 075103 [[1008.4138](#)].
- [149] N. Schuch, D. Pérez-García and I. Cirac, *Classifying quantum phases using matrix product states and projected entangled pair states*, *Phys. Rev. B* **84** (2011) 165139 [[1010.3732](#)].
- [150] R. Verresen, R. Moessner and F. Pollmann, *One-dimensional symmetry protected topological phases and their transitions*, *Phys. Rev. B* **96** (2017) 165124.
- [151] Etingof, Pavel and Nikshych, Dmitri and Ostrik, Viktor , *Fusion Categories and Homotopy Theory*, *Quantum Topol.* (2010) 209 [[arXiv:0909.3140](#)].
- [152] D. Nikshych and B. Riepel, *Categorical Lagrangian Grassmannians and Brauer-Picard Groups of Pointed Fusion Categories*, *J. Algebra* **411** (2014) 191 [[arXiv:1309.5026](#)].
- [153] J. Fuchs, J. Priel, C. Schweigert and A. Valentino, *On the Brauer Groups of Symmetries of Abelian Dijkgraaf-Witten Theories*, *Commun. Math. Phys.* **339** (2015) 385 [[1404.6646](#)].
- [154] A. Kitaev and L. Kong, *Models for Gapped Boundaries and Domain Walls*, *Communications in Mathematical Physics* **313** (2012) 351 [[1104.5047](#)].
- [155] C. Cordova, D. S. Freed, H. T. Lam and N. Seiberg, *Anomalies in the Space of Coupling Constants and Their Dynamical Applications I*, *SciPost Phys.* **8** (2020) 1.
- [156] E. Cobanera, G. Ortiz and Z. Nussinov, *The Bond-Algebraic Approach to Dualities*, *Advances in Physics* **60** (2011) 679 [[1103.2776](#)].
- [157] J. Frohlich, J. Fuchs, I. Runkel and C. Schweigert, *Kramers-Wannier Duality from Conformal Defects*, *Phys. Rev. Lett.* **93** (2004) 070601 [[cond-mat/0404051](#)].
- [158] J. Frohlich, J. Fuchs, I. Runkel and C. Schweigert, *Defect Lines, Dualities, and Generalised Orbifolds*, in *16th International Congress on Mathematical Physics*, 9, 2009, [0909.5013](#), DOI.
- [159] D. Tambara and S. Yamagami, *Tensor categories with fusion rules of self-duality for finite abelian groups*, *Journal of Algebra* **209** (1998) 692.
- [160] S. F. Moosavian, H. Moradi and A. Tiwari, “*From Generalized Spin Chains to Non-invertible Symmetry Structures.*” in preparation, 2022.
- [161] U. Grimm, *Spectrum of a duality-twisted ising quantum chain*, *Journal of Physics A: Mathematical and General* **35** (2002) L25.
- [162] A. Kapustin and R. Thorngren, *Fermionic spt phases in higher dimensions and bosonization*, *Journal of High Energy Physics* **2017** (2017) 80.
- [163] C. Vafa, *Modular Invariance and Discrete Torsion on Orbifolds*, *Nucl. Phys. B* **273** (1986) 592.
- [164] C. Vafa and E. Witten, *On orbifolds with discrete torsion*, *J. Geom. Phys.* **15** (1995) 189 [[hep-th/9409188](#)].

- [165] P. D. Francesco, P. Mathieu and D. Sénéchal, *Conformal Field Theory*. Springer New York, 1997.
- [166] W. Selke, *The annni model — theoretical analysis and experimental application*, *Phys. Rep.* **170** (1988) 213.
- [167] A. Rahmani, X. Zhu, M. Franz and I. Affleck, *Phase diagram of the interacting majorana chain model*, *Phys. Rev. B* **92** (2015) 235123.
- [168] Y. Zou, A. Milsted and G. Vidal, *Conformal data and renormalization group flow in critical quantum spin chains using periodic uniform matrix product states*, *Phys. Rev. Lett.* **121** (2018) 230402.
- [169] E. O’Brien and P. Fendley, *Lattice supersymmetry and order-disorder coexistence in the tricritical ising model*, *Phys. Rev. Lett.* **120** (2018) 206403.
- [170] M. Lässig, G. Mussardo and J. L. Cardy, *The scaling region of the tricritical ising model in two dimensions*, *Nuclear Physics B* **348** (1991) 591.
- [171] Y. Zou and G. Vidal, *Emergence of conformal symmetry in quantum spin chains: Antiperiodic boundary conditions and supersymmetry*, *Phys. Rev. B* **101** (2020) 045132.
- [172] M. Levin and X.-G. Wen, *Fermions, strings, and gauge fields in lattice spin models*, *Physical Review B* **67** (2003) 245316 [[cond-mat/0302460](#)].
- [173] A. Zamolodchikov and V. Fateev, *Nonlocal (Parafermion) Currents in Two-Dimensional Conformal Quantum Field Theory and Self-Dual Critical Points in  $\mathbb{Z}_N$ -Symmetric Statistical Systems*, *Zh. Eksp. Teor. Fiz* **89** (1985) 399.
- [174] D. Gepner and Z.-a. Qiu, *Modular Invariant Partition Functions for Parafermionic Field Theories*, *Nucl. Phys.* **B285** (1987) 423.
- [175] P. Di Francesco, H. Saleur and J. B. Zuber, *Generalized Coulomb Gas Formalism for Two-dimensional Critical Models Based on  $SU(2)$  Coset Construction*, *Nucl. Phys.* **B300** (1988) 393.
- [176] D. Pérez-García, M. M. Wolf, M. Sanz, F. Verstraete and J. I. Cirac, *String order and symmetries in quantum spin lattices*, *Phys. Rev. Lett.* **100** (2008) 167202.
- [177] F. Pollmann, E. Berg, A. M. Turner and M. Oshikawa, *Symmetry protection of topological phases in one-dimensional quantum spin systems*, *Phys. Rev. B* **85** (2012) 075125.
- [178] L. Tsui, F. Wang and D.-H. Lee, *Topological versus Landau-Like Phase Transitions*, *arXiv e-prints* (2015) [[1511.07460](#)].
- [179] L. Tsui, Y.-T. Huang, H.-C. Jiang and D.-H. Lee, *The phase Transitions Between  $\mathbb{Z}_n \times \mathbb{Z}_n$  Bosonic Topological Phases in  $1+1D$ , and a Constraint on the Central Charge for the Critical Points Between Bosonic Symmetry-Protected Topological Phases*, *Nucl. Phys.* **B919** (2017) 470 [[1701.00834](#)].
- [180] P. H. Ginsparg, *Applied Conformal Field Theory*, in *Les Houches Summer School in Theoretical Physics: Fields, Strings, Critical Phenomena*, 9, 1988, [hep-th/9108028](#).
- [181] M. Fishman, S. R. White and E. M. Stoudenmire, *The ITensor Software Library for Tensor Network Calculations*, 2020.

- [182] P. Calabrese and J. L. Cardy, *Entanglement Entropy and Quantum Field Theory*, *J. Stat. Mech.* **0406** (2004) P06002 [[hep-th/0405152](#)].
- [183] P. Weinberg and M. Bukov, *QuSpin: a Python Package for Dynamics and Exact Diagonalisation of Quantum Many-Body Systems Part I: Spin Chains*, *SciPost Phys.* **2** (2017) 003 [[arXiv:1610.03042](#)].
- [184] R. Samajdar, S. Choi, H. Pichler, M. D. Lukin and S. Sachdev, *Numerical study of the chiral  $F_3$  quantum phase transition in one spatial dimension*, *Phys. Rev. A* **98** (2018) 023614.
- [185] V. G. Turaev and O. Y. Viro, *State sum invariants of 3 manifolds and quantum 6j symbols*, *Topology* **31** (1992) 865.
- [186] J. W. Barrett and B. W. Westbury, *Invariants of piecewise linear three manifolds*, *Trans. Am. Math. Soc.* **348** (1996) 3997 [[hep-th/9311155](#)].
- [187] D. Gaiotto and A. Kapustin, *Spin TQFTs and fermionic phases of matter*, *Int. J. Mod. Phys. A* **31** (2016) 1645044 [[1505.05856](#)].
- [188] X. Chen, A. Roy, J. C. Y. Teo and S. Ryu, *From orbifolding conformal field theories to gauging topological phases*, *Phys. Rev. B* **96** (2017) 115447 [[1706.00557](#)].
- [189] X. Chen, A. Tiwari, C. Nayak and S. Ryu, *Gauging (3+1)-dimensional topological phases: an approach from surface theories*, *Phys. Rev. B* **96** (2017) 165112 [[1706.00560](#)].
- [190] The GAP Group, *GAP – Groups, Algorithms, and Programming, Version 4.11.1*, 2021.
- [191] H. Bombin, *Topological Order with a Twist: Ising Anyons from an Abelian Model*, *Phys. Rev. Lett.* **105** (2010) 030403 [[1004.1838](#)].
- [192] Y.-Z. You and X.-G. Wen, *Projective non-Abelian statistics of dislocation defects in a  $Z_N$  rotor model*, *Phys. Rev. B.* **86** (2012) 161107 [[1204.0113](#)].
- [193] J. R. Munkres, *Elements of Algebraic Topology*. CRC Press, Mar, 2018.
- [194] A. Hatcher, *Algebraic Topology*. Cambridge University Press, Feb, 2002.